Beta cell differentiation status in Type 2 Diabetes

Nicola Jeffery

Submitted by Nicola Mary Jeffery of the University of Exeter Medical School as a thesis for the degree of Doctor of Philosophy in Medical Studies, 27 September 2018

I certify that all the material in this thesis is my own work and that no unchanged or unacknowledged material has previously been submitted and approved for the award of degree by this or any other University.

Abstract

Type 2 Diabetes (T2D) affects over 415 million people globally and is characterised by cellular stresses including: poor glucose homeostasis, dyslipidaemia, inflammation, hypoxia and ER stress. Studies in mice have shown that exposure to these stresses influences beta cell differentiation status as well as cell survival and may explain the extent of beta cell mass loss that is seen in the disease. To date, studies of altered beta cell differentiation have largely been confined to murine models. I used the EndoC-βH1 human beta cell line, along with human pancreatic tissue sections, to better characterise this mechanism in human disease.

To elucidate these mechanisms, I firstly established a humanised version of cell culture techniques for the EndoC βH1 cell model and assessed the influence on cell function. Secondly, I evaluated the effects of the diabetic microenvironment on beta cell differentiation and gene expression patterns. Finally, I investigated whether a diabetomimetic microenvironment induced differences in microRNA regulation in the cells.

I found that the humanised EndoC-βH1 culture techniques improved glucose sensitive insulin release in the cell model. EndoC-βH1 cells exposed to a Diabetic microenvironment showed some degree of transdifferentiation and this may be due to dysregulation of splicing factor expression. These effects may be compounded by altered microRNA regulation in response to these cell stresses. These data suggest that altered gene regulation caused by a diabetic

microenvironment may alter gene regulation to produce a reversible delta-like phenotype in human beta cells.

List of Contents

List of tables

List of figures

List of supplementary information

Abbreviations

Ago2	Argonaute 2
ARNT	Aryl hydrocarbon receptor nuclear translocator
ARX	Aristaless related homeobox
BCL2L11	BCL2 like family 11
cDNA	Complementary DNA
CDK2	Cyclin dependent kinase 2
DAG	Diacylglycerol
DDIT3	DNA damage inducible transcript 3
DLG2	Discs Large MAGUK Scaffold protein 2
DNMT1	DNA methyltransferase 1
DNMT3A	DNA methyltransferase 3 alpha
ELISA	Enzyme linked immunosorbent assay
ER	Endoplasmic reticulum
ESE	Exonic splicing enhancer
ESRP1	Epithelial splicing regulatory protein 1
ESRP2	Epithelial splicing regulatory protein 2
ESS	Exonic splicing silencer
FOXO1	Forkhead box protein O1
FFAs	Free fatty acids
GCG	Glucagon
GCK	Glucokinase
GRG3	Transducin like enhancer of split 3 groucho 3
GSEA	Gene set enrichment analysis
GSIS	Glucose sensitive insulin secretion

GUSB	Beta-glucorinidase
H3K4me3	Trimethylation of histone 3 at lysine 4
HDAC1	Histone deacetylase 1
HES1	Hes family BHLH Transcription factor 1
HESCs	Human embryonic stem cells
HHEX	Haematopoietically expressed homeobox protein
HIF1A	Hypoxia inducible factor 1 subunit alpha
hnRNPs	Heterogenous nuclear ribonuclear proteins
HPRT1	Hypoxanthine phosphoribosyltransferase 1
HNF1α	Hepatic nuclear factor 1 alpha
IF	Immunofluorescence
IL-6	Interleukin 6
IL-1β	Interleukin 1 beta
IL-IR1	Interleukin type 1 receptor
lNFγ	Interferon gamma
INS	Insulin
iPSCs	Induced pluripotent stem cells
IRS-1	Insulin receptor substrate 1
ISE	Intronic splicing enhancer
ISS	Intronic splicing silencer
JNK	Jun N terminal kinase
KMT2C	Lysine methyltransferase 2C
LDHA	Lactate dehydrogenase A
lncRNA	Long non-coding RNA
MAFA	MAF BZIP transcription factor A
MAFB	MAF BZIP transcription factor B

MAPK1	Mitogen-activated protein kinase 1
miRNA	MicroRNA
MOB1A	MOB kinase activator 1A
MODY	Mature onset Diabetes of the Young
MYCL	MYCL proto-oncogene BHLH transcription factor
NANOG	Nanog homeobox
NEUROD1	Neuronal differentiation 1
NEUROG3 (NGN3)	Neurogenin 3
NFκB1	Nuclear factor kappa B
NKX2-2	NKX homeobox 2
NKX6-1	NKX homeobox 1
NMD	Nonsense mediated decay
PAX4	Paired box 4
PAX6	Paired box protein pax-6
PCR	Polymerase chain reaction
PDK1	Pyruvate dehydrogenase Kinase 1
PDX1 (IPF1)	Insulin promoter factor 1
PKC	Protein kinase C
POU5F1	POU Class 5 homeobox 1
PPIA	Peptidylprolyl isomerase A
PTPN1	Protein tyrosine phosphatase no receptor type 1
qPCR	Quantitative PCR
qRT PCR	Quantitative real time polymerase chain reaction
RISC	RNA induced silencing complexes
RRMs	RNA recognition motifs
RT	Reverse transcription

SCL16A1	Solute carrier family 16 member 1
SERPINE 1	Serpin family E Member 1
SF	Splicing factor
siRNA	Silencer RNA
SLC2A2 (GLUT2)	Solute carrier family 2 member 2
SNP	single nucleotide polymorphism
snRNPs	Small nuclear ribonuclear proteins
SOCS	Cytokine signalling proteins
SOD	superoxide dismutase 1
SOX9	SRY-Box 9
SP1	SP1 transcription factor
SRSF	Serine/ arginine rich splicing factor
SST	Somatostatin
STK11 (LKB1)	Serine threonine kinase 11
SYP	Synaptophysin
T1D	Type 1 Diabetes
T2D	Type 2 Diabetes
TEAD1	Integrin subunit alpha M
TF	Transcription factor
TLDA	Taqman low density array
TNFα	Tumour necrosis factor alpha
UPR	Unfolded protein response
VEGF-A	Vascular endothelial growth factor A

Acknowledgements

I'd like to thank my supervisors, Professor Lorna Harries and Dr Sarah Richardson, who have provided continued support during the 3 years of my PhD. Professor Lorna Harries deserves special mention for inspiring me to do a PhD in the first place. She thought I'd like it, and she was right, as she always is. I owe her a great deal for her confidence in me.

My colleagues in Team RNA have been extremely helpful throughout. I would particularly like to thank Ben Lee for his unwavering patience and sound advice during the last 3 years. Dr Eva Latorre has been inspirational, her work ethic is a thing of wonder. Also, thanks to Shanaz Haque and Cyrielle Tonneau for their friendship and support. Thank you all for being so lovely, I owe everyone chocolate and/ or beer.

Very special thanks go to my family. My husband was long suffering before I started my PhD and he definitely deserves a medal now. My beautiful grown up girls, Isobel and Katie are my inspiration. If it wasn't for them, I wouldn't have discovered my passion for medical science in the first place. Finally, thanks to my parents who are always proud of me whatever I get up to and who have given me a solid foundation of love throughout my life.

Chapter 1:

Introduction

1.1 Background to Type 2 Diabetes

Type 2 Diabetes (T2D) affects over 415 million people globally. In the UK, 90% of the people diagnosed with diabetic disease have T2D. (https://www.diabetes.org.uk/diabetes-the-basics/what-is-type-2-diabetes). T2D is a polygenic disease associated with obesity and a sedentary lifestyle and is characterised by chronic high blood sugar, dyslipidaemia, hypoxia and chronic inflammation, as a result of insulin resistance and impaired beta cell function[(1)]. It occurs when the cells that utilise insulin become less able to respond to it, further reducing the ability to remove excess glucose from the circulation. This state is referred to as insulin resistance. As the disease progresses, chronic high blood glucose results in a state of hyperinsuliaemia, where the insulin producing beta cells have to produce abnormal quantities of insulin to try and re-establish glucose homeostasis. Over time this impairs beta cell function and they are no longer capable of producing sufficient insulin, a state referred to as insulin deficiency.

This combination of impaired insulin release and resistance mean that patients may require insulin therapy. Poor glucose control also increases risks of cardiovascular disease, stroke, vascular dementia, diabetic nephropathy, diabetic retinopathy and peripheral neuropathy[(2-5)]. As a result, the disease can be very disabling and, in the UK alone, accounts for over £20 billion of the overall NHS spend each annually and over 10% of UK health expenditure[(6-9)]. Globally the costs are over £825 billion per year, predicted to rise to trillions of dollars by 2030[(10)].

1.2 Mechanisms of type 2 Diabetes: features of the diabetic microenvironment

1.2.1 Insulin synthesis

Insulin is an anabolic hormone that comprises two chains joined by disulphide bonds. It has a highly conserved amino acid sequence, which has enabled insulin replacement therapy using animal forms of insulin. The translated insulin mRNA transcript has only one chain, termed preproinsulin. On insertion into the endoplasmic reticulum (ER) for processing the signal peptide is cleaved and this action forms proinsulin. At this stage the structure has an amino terminal B chain and a carboxyl terminal A chain which are connected by the C peptide. Endopeptidases within the ER excise the C peptide and generate the mature form of insulin. It is then packaged into secretory vesicles in the golgi which accumulate in the cytoplasm. Dysregulation of this process is a feature of T2D, as improper ER processing can occur during hyperinsulinaemia leading to the accumulation of misfolded proteins which trigger the unfold protein response (UPR) leading to ER stress[11, 12].

1.2.2 Insulin secretion

Insulin is secreted from beta cells that sit within the islets of Langerhans in the pancreas. The role of islet cells is maintenance of glucose homeostasis and beta cells achieve this by secreting insulin, which can be used by cells such as skeletal myocytes, lipocytes and hepatocytes to remove glucose from the blood stream. Insulin is secreted by beta cells in response to increased concentrations of glucose in their immediate cellular microenvironment. Glucose is transported into

beta cells via facilitated diffusion through glucose transporter channels. The glucose molecules enter glycolysis leading to an increase in the ratio of intracellular ATP/ ADP. Increased ATP levels allow the ATP sensitive potassium (K^+) channels to close, preventing the positively charged ions from leaving. This change in membrane potential opens voltage gated calcium ion channels in the cell membrane allowing calcium ions to passively diffuse into the cell. Calcium ions are required for insulin containing vesicle fusion with the cell membrane and subsequent exocytosis.

1.2.3 Insulin method of activity

Insulin acts via insulin receptors on the cell membrane of target cells. In hepatocytes it facilitates storage of glycogen and suppresses gluconeogenesis. In skeletal myocytes and lipocytes insulin facilitates glucose transport through the insertion of GLUT4 glucose transporter channels in the cell membrane. As well as these activities it has pleiotropic effects in many other cell types and recent studies suggest that it has regulatory roles in beta cell survival and gene expression[13].

1.2.4 Glucose sensing in beta cells

There are two main types of glucose transporter: sodium-glucose linked (SGLTs) and facilitated diffusion glucose (GLUT) transporters, which have three sub-classes incorporating fourteen isoforms that vary in their tissue specificity and affinity for glucose[14, 15]. Class one GLUT transporters, include isoforms GLUT1, GLUT2, GLUT3 and GLUT4, of which GLUT1 is the primary variant in human beta cells[16]. GLUT2 is also expressed in beta cells and a loss of expression is

known to be associated with failure of glucose sensitive insulin secretion. However, the principal glucose sensor in beta cells is glucokinase[17], rather than GLUT1 and GLUT2, both of which have a low affinity for glucose[16, 18].

1.2.5 Islet architecture

Pancreatic endocrine cells are clustered to form the Islets of Langerhans with the principal role of regulating glucose homeostasis. Islets consist of 5 cell types incorporating: beta cells, alpha cells, delta cells, epsilon cells and pancreatic polypeptide (PP) cells[19-22]. As described above, beta cells are glucose sensing, releasing insulin in response to a glucose stimulus. Alpha cells release glucagon in response to low blood glucose concentrations which acts on hepatocytes and myocytes to convert glycogen stores into glucose in a process termed gluconeogenesis[20-22]. Islet delta cells secrete somatostatin in response to Urocortin3 and ghrelin, secreted from epsilon cells, which in turn regulates insulin and glucagon secretion. Pancreatic polypeptide cells secret pancreatic polypeptide which is required for regulating pancreatic secretions, gut motility and metabolism. Islet architecture varies significantly between species[19, 22]. In mouse, beta cells are generally situated centrally within the islets with alpha cells located around the periphery, while in human alpha cells can also be located centrally[19, 20, 23].

1.2.6 Mechanism of peripheral insulin resistance

Insulin resistance arises from a complex series of interactions initiated by chronically high blood glucose, dyslipidaemia, innate immune responses, activation of the unfold protein response, and hyperinsulinaemia[24]. It is caused

by a number of lifestyle factors including: obesity, inactivity, heredity, ageing and certain medications. As previously described, chronic hyperglycaemia causes beta cells to increase insulin secretion resulting in hyperinsulinaemia. Insulin receptors on the surface of target cells respond by either increasing the translocation of GLUT4 transporters to the cell membrane or increasing glycogen storage to remove glucose from the circulation. However, both of these processes rely upon appropriate myocyte, lipocyte and hepatocyte cellular responses.

In the pathogenesis of T2D these functions are impaired due to dyslipidaemia arising from increased adiposity. This results in the circulation of free fatty acids (FFAs) and ectopic lipid accumulation within muscle, adipose and hepatic tissues. This has been shown to impair insulin signalling and GLUT4 translocation. Studies in rodents and humans have shown that accumulations of diacylglycerol (DAG) in myocytes impaired insulin signalling[25, 26]. DAG is a signalling intermediary that activates protein kinase C (PKC). Increased accumulation of DAG impaired insulin signalling via generation of novel PKC isoforms. Similarly, ectopic lipid accumulations in hepatocytes have also been identified as a cause of lipid related insulin resistance[27]. In hepatocytes it is thought that lipid accumulations disrupt PKC isoforms, which sequester Akt2, impairing FOXO1 inactivation thereby increasing gluconeogenesis and decreasing glycogen synthesis[24]. Excess lipid storage in hepatocytes also causes increased release and circulation of FFAs, including toxic FFAs that have cytotoxic effects. Beta cells have been shown to be sensitive to toxic fatty acids such as palmitic acid, which is associated with increased rates of cell death[28, 29].

The interaction of dyslipidaemia and hyperinsulinaemia is also thought to contribute to insulin resistance through the UPR. As discussed, in beta cells, increased rates of insulin translation lead to the accumulation of mis-folded proteins which trigger ER stress[1, 11, 24]. In myocytes, lipocytes and hepatocytes, lipogenesis has been shown to trigger the UPR through a variety of mechanisms which function to regulate cellular metabolic responses via lipogenesis, lipid droplet formation, lipid storage and regulation of glucose metabolism[11, 30-33]. Through a combination of these mechanisms the UPR is believed to play an indirect, but contributory, role in insulin resistance.

Along with dyslipidaemia, increased adiposity can induce oxidative and ER stress[26, 33, 34]. This activates cellular pathways, such as JNK, IKKβ and NFκB, via ligand binding of proinflammatory molecules including TNFα, IL-6, INFγ and IL1β, in a positive feedback loop that increases the transcription of proinflammatory factors[35, 36]. IL1β induces insulin resistance by binding the interleukin 1 type 1 receptor (IL-IR1) which in turn inhibits insulin receptor substrate 1 (*IRS-1*) expression[3, 37]. It regulates the production of IL-6, increasing its production via IL-IR1 activation, which compounds ectopic lipid accumulation due to the suppression of lipase[3, 37]. This then feeds into the lipid associated mechanisms of insulin resistance. IL-6 is also known to impair insulin signalling by activation of cytokine signalling proteins (SOCS) which in turn block insulin receptor activation[3, 37]. Similarly, TNFα activates JNK and NFκB pathways which again inhibit IRS1 activity, leading to impaired insulin signalling and subsequent insulin resistance[3, 37]. Fatty acid mediated activation of IL1β and INFγ pathways has also been shown to induce ER stress, impacting maintenance of beta cell fate and survival[38-40]. All of these mechanisms act in a synergistic,

interdependent manner that reduces sensitivity to insulin leading to insulin resistance. The long-term effects of insulin resistance are poor glucose homeostasis and, over time, this can lead to beta cell failure.

1.2.7 Physiological cellular stresses associated with type 2 Diabetes

The impact of an obesogenic environment on beta cell differentiation and transcription factor expression has been the subject of a number of studies[41-46]. Chronic hyperglycaemia is known to be toxic and the effects of obesity on the cellular environment include hypoxia, lipotoxicity and increased inflammation. In primates given a high fat/ high sugar diet, decreased expression of *FOXO1, NKX6.1, NKX2.2* and *PDX1* was observed. This resulted in a switch from beta to alpha expression profile, characterised by increased expression of the alpha cell specific markers *ARX, GCG* and *DNMT1*, which was then rescued by treatment with resveratrol[44].Studies have also shown a highly selective decrease in the expression of transcription factors *FOXO1, MAFA, MAFB, NKX6-1* and *PDX1* in beta cells exposed to oxidative stress resulting from hyperglycaemia[42, 47-49]. *FOXO1* under-expression precedes downregulation of *MAFA*, but both are early indicators of beta cell stress[42, 47]. In the context of T2D this has relevance relating to prediabetes or metabolic syndrome where postprandial hyperglycaemia may impact *FOXO1* and *MAFA* expression, with subsequent disruption to insulin secretion[42]. It has recently been proposed that beta cells transition between two states to balance high rates of insulin biosynthesis, with accompanying risk of pro-insulin misfolding, and UPR recovery of ER stress[50]. In this model, hyperglycaemia overwhelms the unfolded protein response

resulting in uncontrolled ER stress, impaired beta cell function and increased rates of apoptosis[11, 38].

Beta cells are also highly sensitive to hypoxia, which also acts to induce the ER stress pathway, leading to the accumulation of unfolded pro-insulin and compromised beta cell function[51]. Hypoxia can occur as a result of hyperinsulinaemia where the cells energy output exceeds its oxygen supply[52, 53]. A study investigating the effects of hypoxia in MIN6 cells showed it induced beta cell dysfunction and caused downregulation of *Mafa, Pdx1, Slc2a2, Kcnj11* and *Neurod1*, resulting in abnormal insulin secretion[45]. This study also indicated that *Mafa* expression increased on *Hif1a* knockdown, which suggests Hif1 is involved in regulation of its expression[45].

Not all FFAs are toxic to beta cells and some have protective activity[28], however lipotoxicity is an important feature of T2D[1, 29, 34, 54]. Historically, it was thought that lipotoxicity in beta cells arose from altered PKC signalling leading to reduced glucose sensitivity[54]. Many studies now suggest that exposure to FFAs activate cell stress responses, such as oxidative stress, ER stress, and autophagy[1, 29, 31, 34, 54]. One of the proposed mechanisms for beta cell dysfunction is that disrupted lipoprotein lipase signals may contribute to reduction of the lipid component of glucose stimulated insulin secretion (GSIS)[55]. Palmitate is also known to impair glucose transport, calcium signalling and insulin secretion also resulting in reduced GSIS[54]. It is also associated with increased rates of beta cell apoptosis.

Inflammation has been well studied in relation to insulin resistance and beta cell failure in T2D[2, 36, 39, 48, 56]. It is known that immune cell filtration of islets is a feature of the disease. An emerging field of study is the role of proinflammatory cytokines on beta cell differentiation status[2]. Studies have shown that IL1β, IL-6 and TNFα repress the expression of genes that maintain mature beta cell differentiation status, including *Ins2, Slc2a2* and *Pdx1*[2, 36]. Loss of *Pdx1* expression is associated with changes in beta cell fate[57, 58]. Cytokines IL1β, INFγ,TNFα and IL-6 are also associated with increased rates of apoptosis[2, 56]. However, to date, the exact mechanism by which proinflammatory factors may be driving changes in beta cell fate remains to be elucidated.

It has also been shown that cellular ageing is an important feature of T2D and it has been identified that it leads to the upregulation of *Pdx1* and *Neurod1*[59], genes that have roles in the maintenance of beta cell function and mass. A recent study using single cell mass cytometry in human islets has clearly shown that beta cell proliferation declines with age and suggests that different classes of beta cell subset predominate throughout the ageing process, with cells switching from a proliferative to a quiescent state[60]. A study in mice found a global methylation drift in ageing beta cells and decreased proliferations but no associated decrease in function[59]. This is corroborated by other studies which show that beta cell replication declines with age but function is unaffected[61-63]. Given the potential association of decreased cell density with increased cell plasticity, ageing is another potential driver for changes in beta cell differentiation status[59]. Rodent models of T2D have also shown that increased incidence of de-differentiation and

trans-differentiation are observed in aged mice with *Foxo1* knockout, suggesting that ageing increases likelihood of changes to cell fate[43, 64].

Beta cell mass loss exerts its own stresses and several studies have considered the importance of cell density in beta cell mass via proliferation and changes to beta cell differentiation status[47, 65-69]. A mathematical model looking at the crosstalk between two signalling mechanisms, lateral inhibition and lateral stabilization, which exert environmental control over cell fate stability and the transdifferentiation of pancreatic cells, noted that cell density affects efficiency of conversion from one cell type to another[70]. *NGN3*, crucial for endocrine differentiation, is regulated in this way, influencing beta cell replication rate[71]. Contact inhibition acts via the Wnt signalling pathway and in vitro studies have shown that β-catenin is recruited to the plasma membrane only in confluent cells[66]. Interestingly, an *in vitro* study of stem cell differentiation showed that initial seeding density influenced the pancreatic endocrine progenitor commitment, with high densities resulting in cells co-secreting insulin and glucagon[68]. This suggests that paracrine environmental conditions affecting cell density may be of significant importance in determining cell fate, and with this, cell mass. Further, Brissova et al.[72] used a model of inducible and reversible beta cell specific *VEGF-A* overexpression to investigate how VEGF-A signalling modulates intra-islet vasculature, islet microenvironment and beta cell mass. The study showed that increased vasculature created a local microenvironment, which resulted in beta cell proliferation and the restoration of beta cell mass.

1.3 Beta cell differentiation status and Type 2 Diabetes

1.3.1 Beta cell mass loss in T2D

Until recently, the loss of beta cell mass seen in T2D was considered to be the result of increased rates of apoptosis[73]. Global data from autopsy results of patients with T2D show significantly reduced numbers of pancreatic beta cells compared with those of non-diabetic control subjects. These findings are supported by studies reporting increased rates of apoptosis in the islets of patients with T2D, and there is also evidence of a beta cell deficit in people with prediabetes and impaired fasting glucose levels.[74-76] Such studies do not, however, address whether the observed incidence of reduced beta cell mass is a result of the disease process or is attributable to a lower starting point in these individuals that may have conferred increased T2D risk[77, 78]. It is also worth noting that there is some overlap between the extent of beta cell mass loss seen between people with and without diabetes. More recently it has been proposed that apoptosis alone does not account for the extent of beta cell mass loss seen in T2D, and loss of beta cell function is an important feature of the disease[75].

1.3.2 Beta cell differentiation status

One of the possible mechanisms, distinct from inadequate glucose sensing, that drives loss of beta cell function involves changes in the differentiation status of mature beta cells. Trans-differentiation into alpha cells and dedifferentiation of beta cells to progenitor cell types have been studied, particularly in mouse models, and the mechanisms instigating changes in cell fate are beginning to be characterized[61].

A recent study by Johnston et al[79] presents the intriguing possibility that beta cells have the potential to convert into other pancreatic endocrine cell types in response to loss of function, a phenomenon referred to as cellular plasticity. Increased beta cell plasticity may occur via the expression of immature beta cell markers in islet hubs and appears to be linked to the capacity for beta cell hubs to coordinate islet function, including increased glucose responsivity[79]. It is possible that the expression of immature beta cell markers, and consequent increased plasticity, causes the hubs to be more sensitive to the effects of a diabetic microenvironment, losing beta cell function and insulin positivity. Understanding how the diabetic milieu effects the transcriptional profile of genes involved in beta cell fate is therefore an important next step in this field of research.

Dedifferentiation can be defined as the loss in expression of mature beta cell markers with accompanying loss of function so that the cells lose their insulin positivity. Trans-differentiation refers to the process of a change in cell type, commonly from mature beta cells into alpha cells, with accompanying gain of glucagon positivity and expression of alpha cell markers[80]. Similarly, knockout studies of alpha cell regulators Arx and Dnmt1 have shown a loss of mature alpha cell status with gain of beta cell-like electrophysiology and glucose sensitive insulin secretion[81]. Some studies have suggested that, in non-human mammalian models, the change in differentiation status is rapid rather than gradual[58]. This has been shown in studies using lineage tracers where trans-differentiation has occurred within 2 days of the loss of expression of mature beta cell markers[58]. There are two proposed pathways for trans-differentiation: de-differentiation to progenitor cell followed by re-differentiation into an alternative

islet cell type, or dual hormone positivity, such as where individual cells express insulin and glucagon at the same time[82].

To date, much of the work on changes to differentiation status in the literature has been carried out using murine models, which, while providing valuable insights into the role of inducible stress triggers in cell fate, are not without problems. Studies on human tissues are few, but early results from recent studies suggest similar phenomena may also occur in humans[80]. A study looking at transdifferentiation in human pancreatic tissues found expression of mesenchymal and beta cell markers in insulin-positive islet beta cells and also reported co-expression of glucagon and insulin[80]. These results do have to be considered cautiously, as the study was based on a very small sample size and so further study is required to corroborate their findings.

The significant differences between murine and human islet structure, however, make definite comparison difficult. Mouse islets are mainly arranged with alpha cells around the outside of the islet, with beta and delta cells within the centre. This is described as a mantle of alpha cells surrounding a core of beta and delta cells[19]. Conversely, in humans and monkeys, alpha cells are not exclusive to the periphery or mantle and instead are dispersed throughout the islet (Figure 1).

Figure 1 Differences in Islet architecture between Rodents (part A) and Human (part B)

Red = alpha cells. Blue = beta cells. Green = delta cells. Yellow = PP cells. Pink = epsilon cells. In rodents alpha cells tend to be arranged around the periphery of the islet. In beta cells they can also be located centrally within the islet.

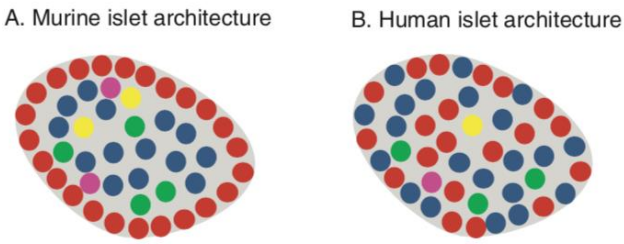

These differences in architecture are considered to influence sensitivity for glucose sensing, with human islets being more efficient at detecting low glucose concentrations[22, 83]. It has also been shown that there are mechanistic differences in terms of gene expression between species and their responsiveness to the stress conditions associated with T2D, as seen with *NGN3, NANOG, POU5F1* (*Oct4*) and *MYCL1* expression[58]. The problems of comparison between murine and human models are also illustrated in differences in the expression levels of Pax4, which has been shown to be highly expressed in mouse models, favouring the beta cell fate; however, in human cells *PAX4* expression has been shown to be poorly expressed in fully mature beta cells, suggesting it may not be a good marker of active transcription factors with specific roles in beta cell fate[84]. Other differences in gene expression include *MAFB* expression, which persists in human adult beta cells but not in mouse[85].

1.3.3 Factors important to beta cell differentiation status

Understanding the factors involved in beta cell development is key to appreciating the close relationship between alpha and beta cell maturation and, therefore, the potential for changes in mature endocrine cell differentiation status that allow trans-differentiation to occur[58]. It is also apparent that subpopulations of alpha and beta cells exist. It has been suggested that beta cell plasticity may confer protection against cell stress caused by hyperglycaemia, also allowing the cell to re-differentiate should the paracrine environmental condition improve[86]. *NGN3* is critical for endocrine differentiation and is activated by *ONECUT* (Hnf6) and *FOXA2*. It is absolutely required for induction of *PAX4*, and also has *PAX6, ISL1* and *NEUROD1* expression as its immediate down-stream targets[87]. Beta cell progenitors also express *NKX2.2* and *NKX6.1*, and as they continue to mature, *ISL1* and *PAX6* (Figure 2).

Figure 2 Differences in Expression of Beta cell development[88, 89].

Schematic showing gene expression during pancreatic development and beta cell differentiation. NGN3 is activated by ONECUT (Hnf6) and FOXA2 and is critical for endocrine differentiation. Downstream targets for NGN3 are: PAX4, PAX6, ISL1 and NEUROD1. Beta cell progenitors express NKX2.2 and NKX6.1, PDX1 and PAX6

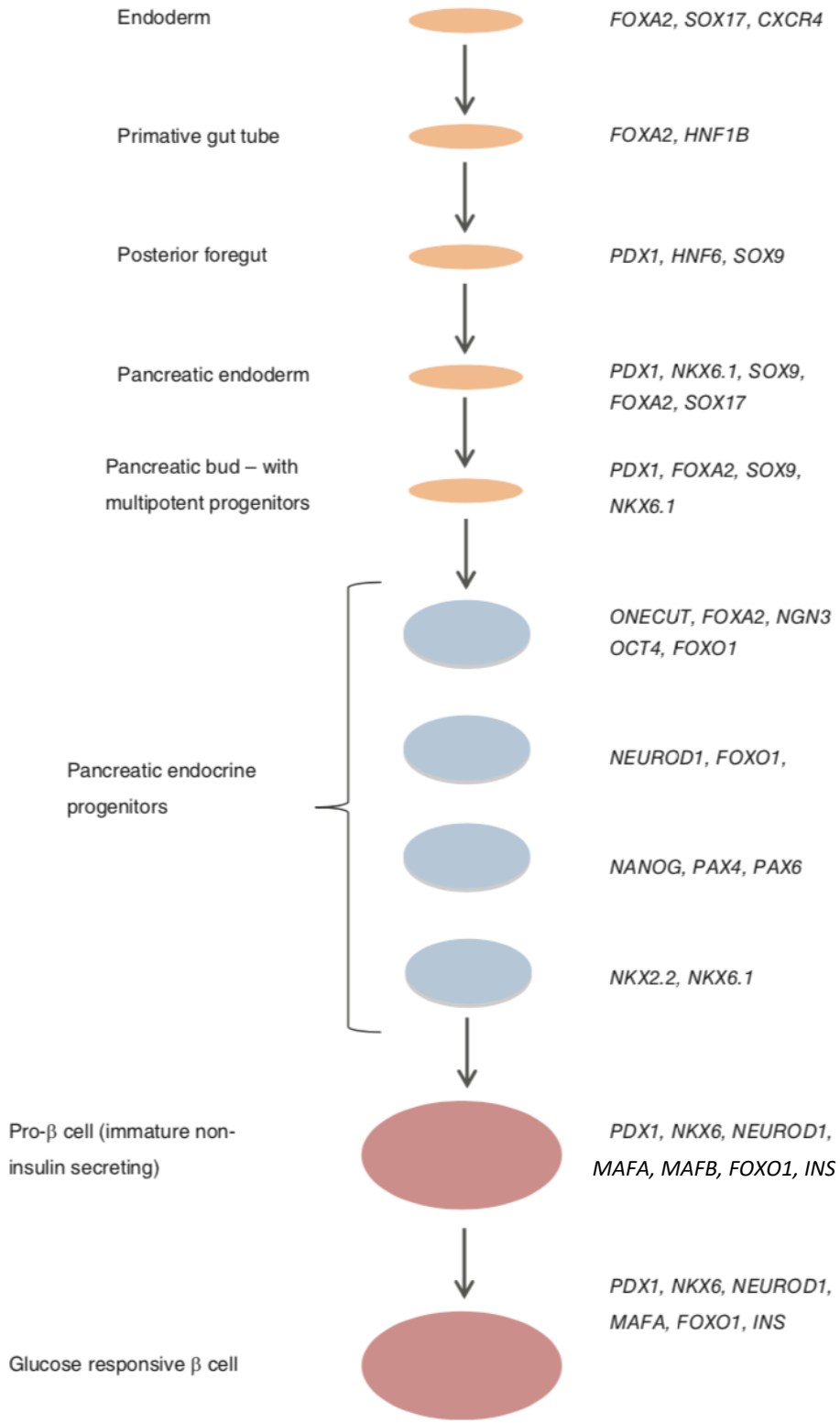

The importance of *NGN3,* as a regulator of differentiation status, can be seen by its own tight regulation, with the number of *NGN3*-positive differentiating cells limited by lateral inhibition via notch signalling[71, 90]. *PAX4* and *NKX2.2* act in parallel to continue the process of beta cell differentiation, with a resulting increase in the expression of *PDX1*, along with concomitant induction of *HB9* expression and, ultimately, insulin synthesis.

Many of the genes important to the maturation of beta cells are also expressed in progenitor alpha cells, with the exception of specific markers such as *ARX* in alpha cells and the mature beta cell markers *NKX6.1* and *PDX1*. It is therefore the tight regulation of these cell fate-specific transcription factors that ensures maintenance of cell fate. In beta cells the transcription factors *PDX1, FOXO1, MAFA* and *NKX2.2* are critical to maintaining the function of beta cells. There are also increases in the expression of “disallowed” beta cell genes, such as *SLC16A1* and *LDHA* in T2D[91]. These genes are “disallowed” to ensure that pyruvate and lactate generated during exercise do not stimulate insulin release, and are typically inactivated by histone modifications and micro-RNA mediated silencing[91]. Expression of such genes could therefore considerably exacerbate the effects of oxidative stress responses in beta cells, further driving changes in differentiation status.

1.3.3 Transcription factors with roles in regulation of cell fate

1.3.3.1 PAX4

Given the importance of cell-specific transcription factors in the maintenance of cell fate, it is helpful to consider the role of these key genes in turn. In mouse models, Pax4 is a beta cell-specific transcription factor; however, as discussed, there are some species differences. In a study of human islet cells, *PAX4* was detected in 43% of human alpha cells and 39% of beta cells, with much lower levels of expression than those seen in mouse islet cells. This is consistent with reports of weak *PAX4* mRNA expression in human cells. In studies of *PAX4* expression, in which cells were subjected to an obesogenic environment, there was no significant change in expression. This suggests that *PAX4* may not be affected by T2D, although there was a decrease in *PAX4*-positive alpha cells in T2D patient samples, where there was no change in beta cell *PAX4* expression[41]. Murine models have also characterized the *PAX4*/ *ARX* regulatory negative feedback axis, whereby *PAX4* favours the beta cell fate and *ARX* favours alpha cells[92, 93]. *PAX4* regulates the balance between alpha and beta cells by antagonizing *ARX* in endocrine progenitors[65, 93]. In a study of *PAX4* and *NKX2.2*, it was seen that these transcription factors regulate parallel pathways and are both necessary to initiate the beta cell differentiation programme and act in parallel to increase *PDX1* expression; however, it is still unclear how this role is accomplished[84].

1.3.3.2 PDX1 (IPF1)

PDX1 (IPF1) is the first transcription factor produced in the developing pancreas but becomes confined to beta cells during development[57, 90]. Given the close developmental relationship between alpha and beta cells, several studies have looked at forced changes to expression of *Pdx1*, to observe its effects on endocrine cell fate[58, 94, 95]. In a study of the conversion of adult alpha cells to beta cells after extreme beta cell loss, *Pdx1* expression was shown to have an important role in alpha cell conversion. Here it was also shown that the extent of beta cell loss determines whether there is any regeneration[65]. This was corroborated by another study by Gao et al.[58] which used lineage tracing to follow the fate of adult beta cells after *Pdx1* deletion, and which also observed that many of the cells became alpha cells, and similarly found that isolated beta cells differentiated into alpha cells. This offers up the intriguing possibility that a key driver of beta cell fate is possibly cell density, which has significant connotations in the context of T2D, with its associated loss of beta cell mass. Interestingly, these studies showed that the reprogrammed alpha cells crucially lack the alpha specific transcription factor *Arx*[94, 96].

Studies have also investigated the role of alpha to beta cell reprogramming by considering upregulation of *Pdx1* expression. Yang et al.[94] forced *Pdx1* expression in cells from the *Ngn3* commitment point onward and saw two periods of reprogramming. The first occurred during early organogenesis and resulted in fewer alpha cells, while the second forced reprogramming at the peri-postnatal stage, resulting in redirection of alpha cells into a beta cell lineage. All studies of IPF1 (Pdx1) conclude that it is a master regulator of beta cell fate and has roles

in repressing genes that are associated with alpha cell identity, most notably *Mafb*, where a transcriptional shift showed de-repression of the gene[84, 94, 96]. Pdx1 normally binds within *Mafb* and glucagon promoters in beta cells competitively inhibiting them so they are not expressed[41, 42]. These studies suggest that *Pdx1* is not required for beta cell survival but is associated with a loss of beta cell identity.

1.3.3.3 ARX

As described above, *ARX* is a specific transcription factor for the alpha cell fate. It is expressed in endocrine progenitors and then restricted to glucagon-producing alpha cells[97]. Deletion of *Arx* in mice leads to the loss of alpha cell identity, resulting in alpha to beta cell-like conversion with the cells expressing *Pdx1, Mafa* and *Glut2*[98]. A study by Wilcox et al.[98] showed that ablation of *Arx* in neonatal glucagon positive cells resulted in the loss of alpha cell identity but in adult animals there was no such reduction and no increase in beta cells. This suggests that *Arx* is important for the early maintenance of alpha cell fate but is no longer required in adult animals for alpha cell fate maintenance. It has a similar role, therefore, to the beta cell-specific transcription factor *PAX4* and these findings indicate that in both alpha and beta cells, plasticity decreases as cells mature[98].

Specific mature endocrine cell transcription factors such as *PAX4* and *ARX* are tightly regulated to ensure maintenance of cell fate[92, 93, 99]. This is demonstrated by the mechanism of the *NKX2.2* repressor complex which regulates beta cell fate and prevents beta to alpha cell reprogramming. The repressor complex includes *DNMT3A, GRG3* and *HDAC1*, and works by blocking

the *ARX* promoter to prevent transcription[97]. Antagonistic expression of specific beta or alpha cell transcription factors is an important determinant of endocrine cell fate.

1.3.3.4 MAFA and MAFB

The transcription factor *MAFA* is an important regulator of the insulin gene and is not typically expressed in alpha cells[42]. *MAFB* is another transcription factor whose expression precedes an increase in *Pdx1* expression and marks the start of insulin transcription[58]. It persists in human mature beta cells but importantly is not seen in the adult beta cells of mice[41, 42, 85], and a recent study has shown that MAFA compensates for the absence of MAFB in mice as it is functionally similar[100]. In a study of human islets looking at the effects of obesogenic environment on cell fate it was noted that *MAFA* and *MAFB* were expressed in both alpha and beta cells, which is consistent with the results of the 2015 Bramswig study[41, 101]. *MAFA* expression in both alpha and beta cells was shown to be altered in a significant proportion of patients with T2D, which suggests a greater degree of plasticity in human islets than has been previously observed in murine models[41].

1.3.3.5 FOXO1

FOXO1 has roles in gluconeogenesis and beta cell differentiation and is most abundant in beta cells. It effectively integrates beta cell proliferation with adaptive function and, in human embryonic stem cells, is an important regulator pluripotency via *OCT4, NANOG* and *SOX2*[47, 64]. It also suppresses beta cell neogenesis in pancreatic duct cells. Studies have shown that in beta cells under

metabolic stress, it is protective, enabling the maintenance of insulin secretion via *MAFA*[43, 90, 102]. In this way it is protective against beta cell failure via the transcription factors *MAFA* and *NEUROD1*, regulating their transcription and maintaining insulin secretion[43, 47]. In studies where expression of the *FOXO1* gene was ablated there was a resultant de-differentiation of beta cells in stress conditions[64]. Knockout of *Foxo1* in mice and loss of beta cell mass was also attributable to de-differentiation rather than cell death[61]. Here beta cells reverted to progenitor-like cells, whereas some beta cells trans-differentiated into alpha cells. The knockout caused hyperglycaemia in the mice and was compounded by additional stresses such as age or pregnancy[61].

FOXO1 is phosphorylated by *AKT* as well as the *JNK* kinases *NFkB* and *CDK2*[39, 47, 103]. When AKT phosphorylates FOXO1 it causes it to leave the nucleus and go to the cytoplasm, inactivating its transcription factor capability. This shows that AKT signalling is important in pancreatic cell plasticity because of its regulation of FOXO1 activity. Overexpression of the *AKT* gene has been shown to induce expansion of ductal structures and is implicated in acinar to ductal, as well as beta cell to acinar/ductal trans-differentiation. In this way AKT plays a critical role in maintaining cell fate, as well as beta cell function, given the role of *FOXO1* in the stress response[104].

1.3.3.6 *NKX6* genes

Nkx6 genes have been shown to be important to both alpha and beta cell differentiation in mice, as well as other animal models[105]. Decreased expression of the beta cell-specific transcription factor *NKX6.1* is seen in T2D and leads to

loss of beta cell function[106]. Reduced expression is also associated with *Ngn3* induction in mouse models of the disease, with cells acquiring a delta-like expression profile. Nkx6.1 has also been shown to have as its target the alpha cell-specific *Arx*, and acts to repress its expression, which preserves beta cell identity[107, 108]. *Nkx6.1* acts antagonistically with Isl1 to regulate alpha vs beta cell identity, again highlighting the close relationship and crosstalk between these islet cell types[96, 106, 108, 109].

Nkx6.2, is known to be expressed during embryonic development, from E10.5[110]. In a study by Nelson et al.[110] it was observed that, while *Nkx6.2*-deficient mice did not exhibit a distinct phenotype, the double knockout *Nkx6.1/Nkx6.2* mice showed decreased numbers of insulin-positive beta cells. They point to a divergent spatial temporal relationship between the expression of *Nkx6* genes, which is key to understanding their role in the maintenance of beta or alpha cell lineages[111].

1.3.3.7 NGN3

As indicated earlier, *NGN3* plays a pivotal role in endocrine development, including the induction of *PAX4* as well as the downstream targets *PAX6, ISL1* and *NEUROD1*[87]. In a 2002 study by Gu et al.[112] the progeny of *NGN3*-positive cells was followed and it was determined that cells derived from those expressing *NGN3* coalesced to form mature islets. *NGN3* was therefore shown to be a progenitor for the endocrine lineage and not a ductal progenitor. Further, this study indicated that *NGN3* expression is required for all types of pancreatic endocrine islet cell and exists in the mature pancreas, facilitating maintenance of

endocrine islet cell fate. Wang et al.[113] examined the effect of a diabetic state in mouse cells and islets and noted that beta cells lost mature beta cell markers, de-differentiating into insulin negative progenitors expressing *Ngn3*. When blood glucose was lowered using insulin therapy, lineage-tracing experiments revealed a restoration of insulin positivity, and *Ngn3* expression was lost. Control islets showed negligible *Ngn3* positivity[113]; however, Guo et al.[42] observed no similar increases in *NGN3* expression in a recent study of human islets from patients with T2D. *NGN3* has been reported in the islets of adult mice with such studies suggesting a role for *NGN3* in maintenance of islet cell function[114]. However, this finding is complicated by data from other studies which show that NGN3 expression in adult islets is linked to islet cell injury and exposure to ER stress, which reactivates *NGN3* expression, suggesting that expression may be associated with cell stress[115, 116]. Such discrepancies may be the result of differences in antibody specificity but more work needs to be done to elucidate the mechanism of altered *NGN3* expression in mature islet cells. This again also highlights the differences between murine and human islet cell transcription factor expression and the importance for such findings to be corroborated using human model systems.

1.3.3.8 NKX2.2

In mice, *Nkx2.2* is expressed in endocrine progenitors but, as part of the secondary transition, it is restricted to mature beta cells as well as a subset of alpha and PP cells[117]. During development of the pancreas, *Nkx2.2*, along with *Arx*, specifies distinct islet cell subtypes. Kordowich et al.[118] note that *Arx* null mice fail to develop alpha cells, with a concomitant increase in beta and delta cell number. *Nkx2.2* mutants exhibit impaired alpha and beta cell development as

well as markedly increased *Arx* expression. These data suggest that *Nkx2.2* is necessary to maintenance of beta cell function, maintenance of beta cell fate and suppression of alpha cell identity[119, 120].

As indicated above, *Nkx2.2* forms a repressor complex which regulates beta cell fate. It acts to support transcriptional networks induced by *Pax4* and *Arx*, as part of an axis to counteract *Arx* expression in pre-beta cells that are committed to a beta cell identity[118]. The repressor complex works via the methyltransferase Dnmt3a, and the histone deacetylase Hdac1, to methylate CG dinucloetides. Together, the complex competitively binds the *Arx* promoter region, thereby inhibiting *Arx* transcription.[71, 97] *Nkx2.2* is therefore required for endocrine differentiation, maintenance of beta cell fate and prevention of trans-differentiation to an alpha cell phenotype.

1.4 Gene expression

1.4.1 Control and regulation of gene expression

Gene regulation occurs throughout multiple and interlinked processes of modifications to chromatin structure, transcription, post transcriptional regulation, translation, protein modification, and mRNA and protein degradation. It allows a range of mechanisms to regulate initiation of transcription, nonsense mediated decay (NMD) for aberrant or deleterious mRNA synthesis, alternative splicing, miRNA targeting of transcripts, post translational modifications including protein folding and ubiquitination. Tight regulation of gene expression is essential to stability of the cellular environment and allows an adaptive response to changes in the cellular microenvironment.

The nucleosome is the fundamental unit for chromatin, comprising 145-7 base pairs of DNA wound around a histone octomer[121, 122]. Regulation of chromatin structure can determine gene expression in a dynamic process termed nucleosome positioning, which affects transcription factor binding[123, 124]. A range of epigenetic modifications including DNA methylation, histone marks, long non-coding RNA (lncRNA) mediated imprinting and chromosome coordination via Lamin A, also influence initiation of transcription[125, 126]. In eukaryotic cells, the pre-mRNA molecule is synthesized from a DNA template and processed into a mature mRNA molecule by splicing, which removes introns and ligates exons, 5' end capping and polyadenylation, the addition of a poly A tail[127], please refer to Figure 3.

Figure 3 mRNA processing.

Figure shows removal of introns by splicing, the addition of 5' cap, consisting of 5' to 5' triphosphate bridge and 7-methylguanosine, and 3' polyadenylation. During mRNA processing constitutive splicing/ alternative splicing typically removes introns and ligates the exons. The 5' cap is added at the same time, along with the polyadenylation at the 3' end of the transcript.

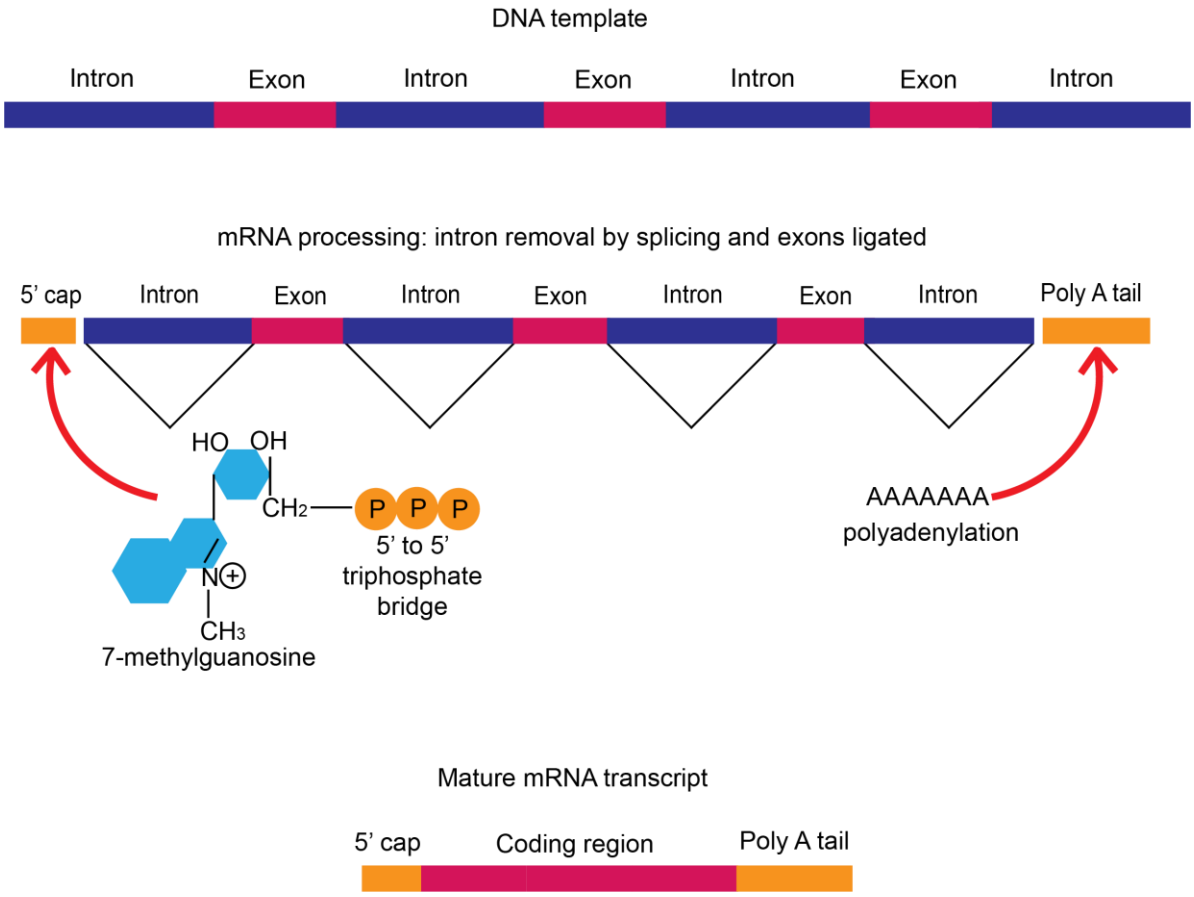

The process of alternative splicing allows one gene to code for more than one protein isoform, often with tissue specific and functionally distinct cellular roles[36]. Once processed, expression of the mature mRNA transcript can be regulated by small non-coding RNAs, including microRNAs, which can affect translational efficiency and allow for transcript degradation[128]. MicroRNA expression is itself regulated, via changes to transcription or promotor hypermethylation and changes to microRNA processing and degradation, thereby adding a further level of regulation of gene expression[129]. Following translation, the protein product is also subject to post translational modifications, including degradation via the

ubiquitination pathway, protein folding and phosphorylation which controls the activity of the product[130].

1.4.2 Constitutive and alternative Splicing

Constitutive splicing, where the mRNA molecule is spliced in exactly the same way each time, occurs as part of mRNA processing and is the mechanism by which introns are excised and exons ligated to form the mature mRNA molecule, as shown in Figure 3[131, 132]. Splice sites are defined by the GU residue splice donor sequences, the AG residue splice acceptor sequences, the A residue branch sites and the polypyrimidine tract. Splice site selection is also regulated by *cis* acting elements and *trans* acting factors, which variously act upon auxiliary splice site elements to enhance or inhibit splice events. These are termed exonic splicing enhancers (ESEs), exonic splicing silencers (ESSs), intronic splicing enhancers (ISEs) and intronic splicing silencers (ISSs). Typically, though not absolutely, serine/ arginine rich SR proteins bind to enhancers, either ESSs or ISSs to promote splice site usage. Conversely, heterogenous nuclear ribonucleoproteins (hnRNPS) bind to silencers, either ESSs or ISSs, to inhibit splice site usage[131, 132].

Following splice site recognition, the spliceosome complex is assembled and recruited, which is facilitated by completion of the consensus sequence from sequence residues surrounding the splice site[131]. The spliceosome comprises five uridine rich small nuclear ribonucleoproteins (snRNPs), called U1, U2, U4, U5 and U6 and ~100 splicing factor proteins[132, 133]. Of these, U1, U2 and U5 contain RNA recognition motifs (RRMs) which recognise specific sequences at

the intron-exon boundary. The splicing process then involves a two-step transesterification reaction where the first step cleaves the 5’ splice site forming a lariat structure known as the C complex. The second part of the reaction cleaves the 3’ end and ligates the two exons to form the mRNA molecule[131, 133].

This process is achieved by the U1 snRNP being recruited to the 5’ splice site. Simultaneously, SF1 is recruited to the branch site, U2AF 65 to the polypyrimidine tract and U2AF 35 to the 3’ splice site, where it forms the E complex[133]. SF1 forms the A complex at the branch site with U2 and two U2AF subunits. U5 forms a trimer and is recruited to the 3’ splice site while U6 trimer replaces U1 at the 5’ splice site forming the B complex[131, 133]. The subsequent dissociation of U4 facilitates a reaction between U6 and U2 snRNPs which draws the 5’ splice site and branch site together. This allows formation of the lariat and the two exon coding regions to be ligated in the second step of the reaction[131, 132]. U2, U5 and U6 snRNPs cleave the 3’ splice site to join the exons, after which the mature mRNA molecule is released, and the lariat degraded[131, 133], please refer to figure 4, splicing and the spliceosome.

Figure 4 Splicing and the spliceosome.

A. *Formation of the E complex (commitment complex) and the A complex. This is formed by the association of the U1 snRNP with the 5' splice site*
B*. Formation of the B complex. An intermediary complex that is inactive until it undergoes conformational changes resulting from dissociation of U1 and U4*
C. *Formation of the C complex and release of U4 and the lariat, this catalyses the second step of the splicing reaction.*
D. *Spliced mRNA transcript.*

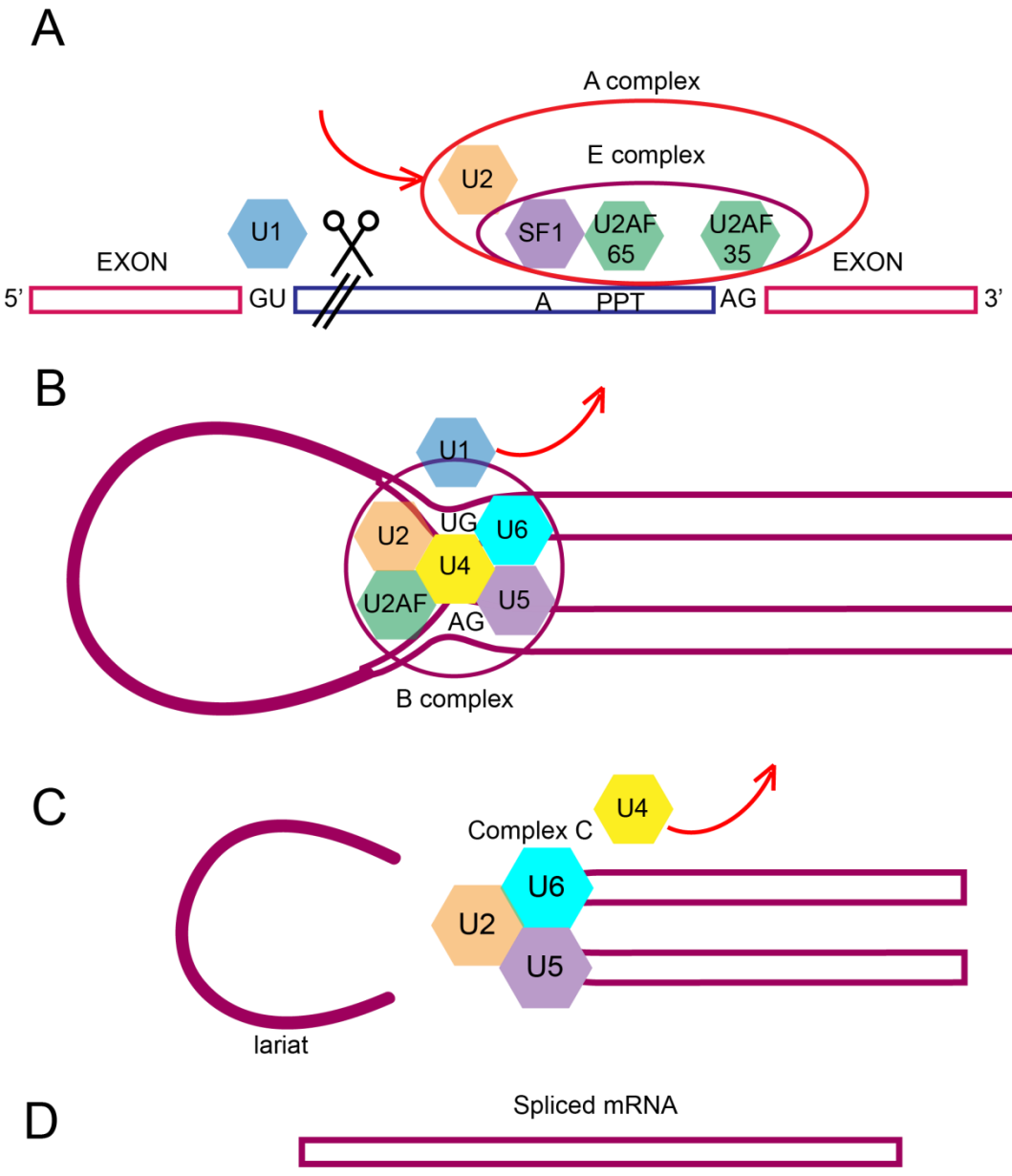

1.4.3 Alternative Splicing

As previously described, alternative splicing is the mechanism by which one gene can code for more than one protein isoform, please refer to figure 5[134, 135]. In humans ~95% of genes are alternatively spliced allowing for protein isoform specificity in tissues and development, as well as functionally distinct protein isoforms in the same cell[134, 135]. Alternative splicing typically involves the various inclusion or exclusion of exons, termed cassette exons, however, figure 6 shows the various types of alternative splicing. Exons can also be mutually exclusive, where one or the other must be excised[135-137]. This form of splicing can allow for the inclusion of intron sequence, alternative splice sites, promoter sequences, alternative first exons and termination sites[137]. It may also include non-coding sequence that has a regulatory role, such as regulation of translational efficiency or introduction of a premature stop codon to initiate nonsense mediated decay[138, 139]. Multiple splice events can occur at the same time and the process is dependent upon splice site recognition by the spliceosome[133]. This activity is itself regulated by the competing actions of splice enhancers and silencers. In this way, alternative splicing acts as both a form of gene regulation as well as allowing for translation specific, development specific or functionally distinct protein isoforms[134, 136].

Figure 5 Schematic of constitutive and alternative splicing.

Constitutive splicing refers to the excision of introns and inclusion of exons as part of mRNA processing. Alternative splicing allows for the excision or inclusion of cassette exons, as well as intronic, splice site, codon and promoter sequence inclusion. Such inclusions may include coding sequence or confer a regulatory role for the mRNA transcript.

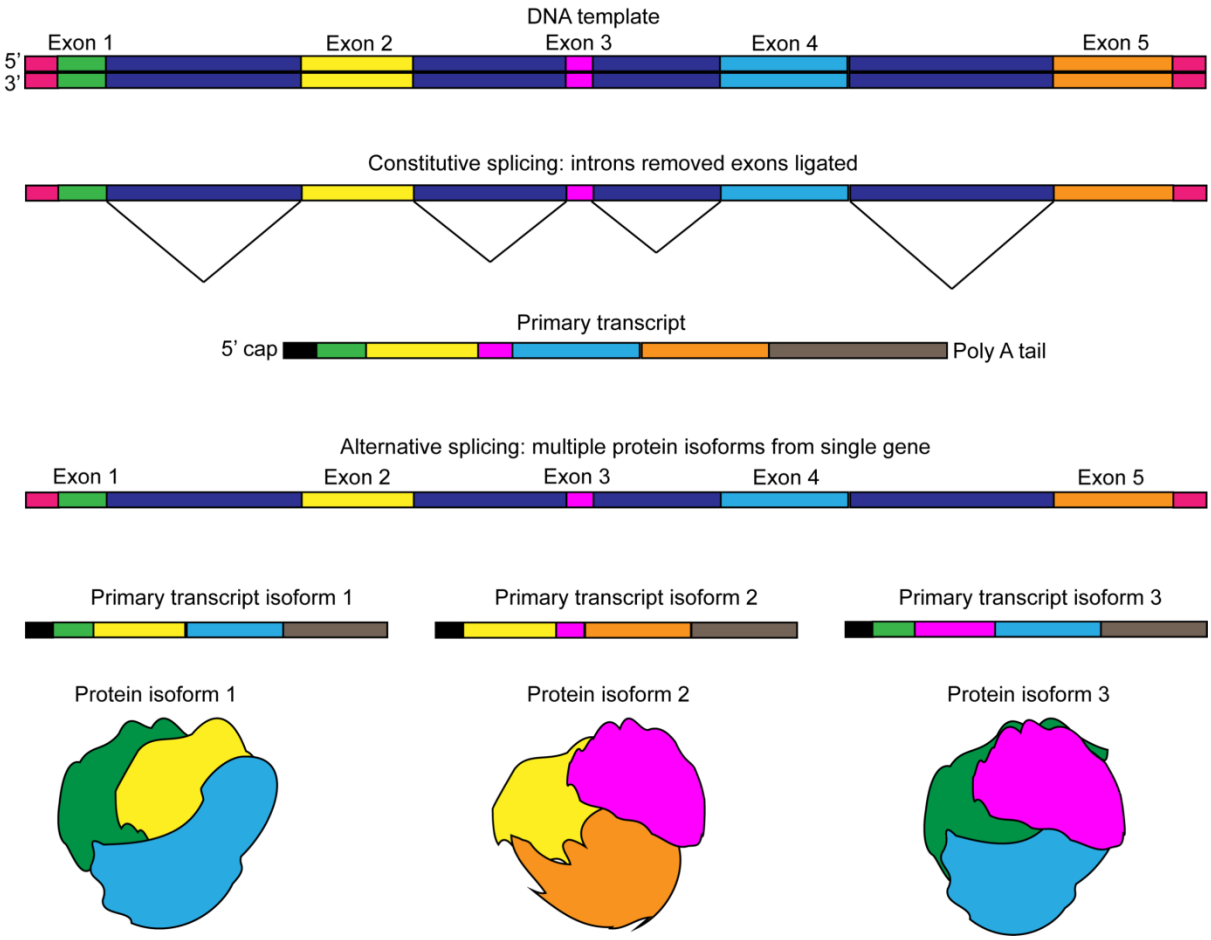

Figure 6 Types of alternative splicing.

Figure shows different types of alternative splicing: cassette exons, mutually exclusive exons, intron retention, alternative 5' or 3' splice sites, alternative promoters and alternative splicing and polyadenylation.

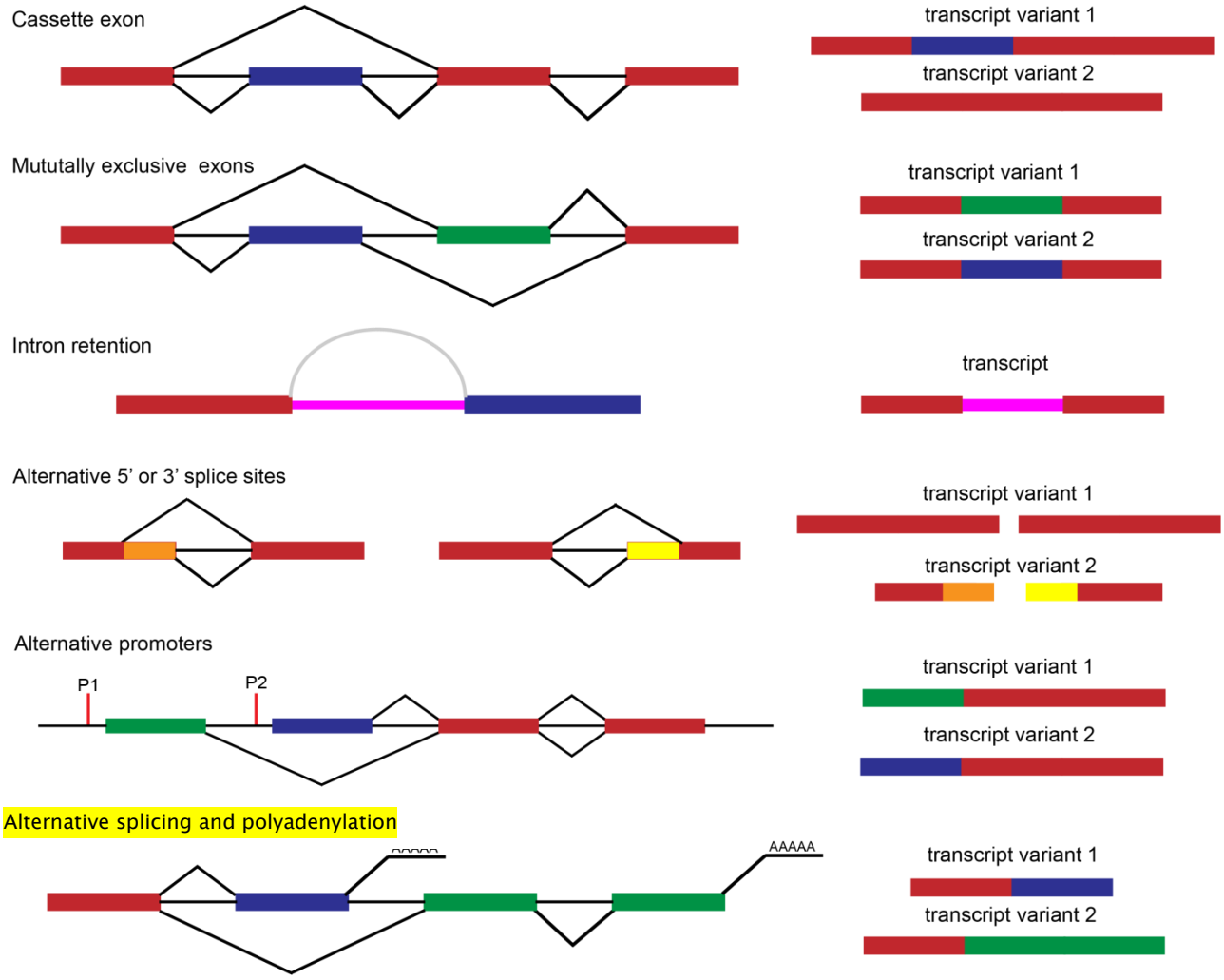

1.4.4 Alternative splicing and Type 2 Diabetes

Alternative splicing is particularly important in response to cell stresses caused by the physiological changes associated with T2D. Different isoforms are expressed at varying points in endocrine cell development and in response to environmental conditions[134, 140]. It has been shown that hepatic nuclear factor 1 alpha (*HNF1α*), which regulates the insulin gene, can produce 3 transcript variants and specific mutations in these isoforms is associated with lower insulin production and development of diabetes[140, 141]. The insulin gene (*INS*) itself is alternatively spliced with an intronic inclusion which confers increased translational efficiency of variants that have increased glucose responsiveness[142]. Studies using monkey models of diabetes have also identified that impaired insulin sensitivity is associated with increased expression of the insulin receptor A isoform (*IR A*)[143]. Protein tyrosine phosphatase non-receptor type 1 (*PTPN1*) is a gene that is associated with beta cell function, insulin secretion and regulation of insulin signalling and has two functionally distinct isoforms. The long isoform has been shown to correlate with body fat percentage and is a biomarker for hyperinsulinaemia[144, 145]. *Oct4* has three isoforms, of which one, *Oct4b*, is important to stress response, while the other isoforms are linked to plasticity and the activation or repression of differentiation[134]. It can also cause miRNA mediated degradation as a result of exon skipping, demonstrating a regulatory hierarchy from miRNAs to splicing networks. Further, alternative splicing is important to cell plasticity and stem cell pluripotency. Differentially expressed isoforms of *OCT4, NANOG* and *SOX2* produce functionally different protein counterparts at specific stages of beta cell differentiation[134]. Downregulation of RNA binding proteins Epithelial Splicing

Proteins 1 and 2 (*ESRP1* and *ESRP2*) is also important for epithelial to mesenchymal splicing changes inferring plasticity[134]. Of note, it has also been shown that the splicing factor protein SRSF3 regulates insulin receptor exon 11 skipping, which contains sequence that modulates insulin binding[146, 147]. The neuron specific splicing factor *NOVA1* has been shown to be highly expressed in human islets and at protein level in beta and alpha cells. In a study by Eizirik et al, knockdown of *Nova1* has been shown to modify splicing in beta cells[40]. Such examples highlight the importance of proper regulation of alternative splicing in T2D and diabetic disease. Regulation of splicing is therefore potentially critical to endocrine cell fate, particularly in the context of T2D. Intervening in this process via the use of small molecules, antisense oligonucleotides and morpholinos to regulate splicing events is already being explored in other diseases, such as Duchenne's muscular dystrophy (DMD)[148]. Stage 3 clinical trials are in process for pharmacological modulation of alternative splicing in DMD[148] and therefore characterising aberrant splicing events which contribute to T2D may also offer similar opportunities for small molecule splicing modifications in diabetes therapeutics.

1.4.5 MicroRNAs

MicroRNAs (miRNAs) are short non-coding RNA molecules of ~22 nucleotides (nts) which have roles in post-transcriptional gene regulation[128]. Their main function is to act as a guide sequence that targets transcripts for degradation or repression via RNA-induced silencing complexes (RISC)[149]. They have well defined roles in disease and are useful biomarkers as well as therapeutic treatment targets[150, 151]. Single miRNAs are known to target multiple genes and

conversely, genes may be targeted by multiple miRNAs allowing many levels of regulation of gene expression[128, 152]. The synthesis and transcription of miRNAs is itself tightly regulated[152, 153], as shown in figure 7. Pri-miRNA are transcribed in the nucleus from DNA template by RNA polymerase II (pol II)[149]. This molecule is cleaved by the drosha enzyme into the step-loop pre-miRNA structure which undergoes nuclear export via the exportin-5, Ran and GTP complex[149, 153]. In the cytosol dicer cleaves the pre-miRNA into two short strands that are incorporated into the RISC complex, which includes argonaute 2 (Ago2) proteins[149, 153, 154]. Target mRNA transcripts are recognised by their sequence complementarity to the first 6-8 nts of the miRNA known as the seed region. Through complementary base pairing the miRNA is able to bind to mRNA 3' regions[149].

Figure 7 microRNA synthesis.

Schematic shows synthesis of pri-miRNA from DNA template by RNA polymerase II, cleavage by drosha to form the pre-miRNA molecule and nuclear export by exportin 5. In the cytoplasm pre-miRNA is cleaved by Dicer to form the mature miRNA and degradation of transcripts by the RISC complex.

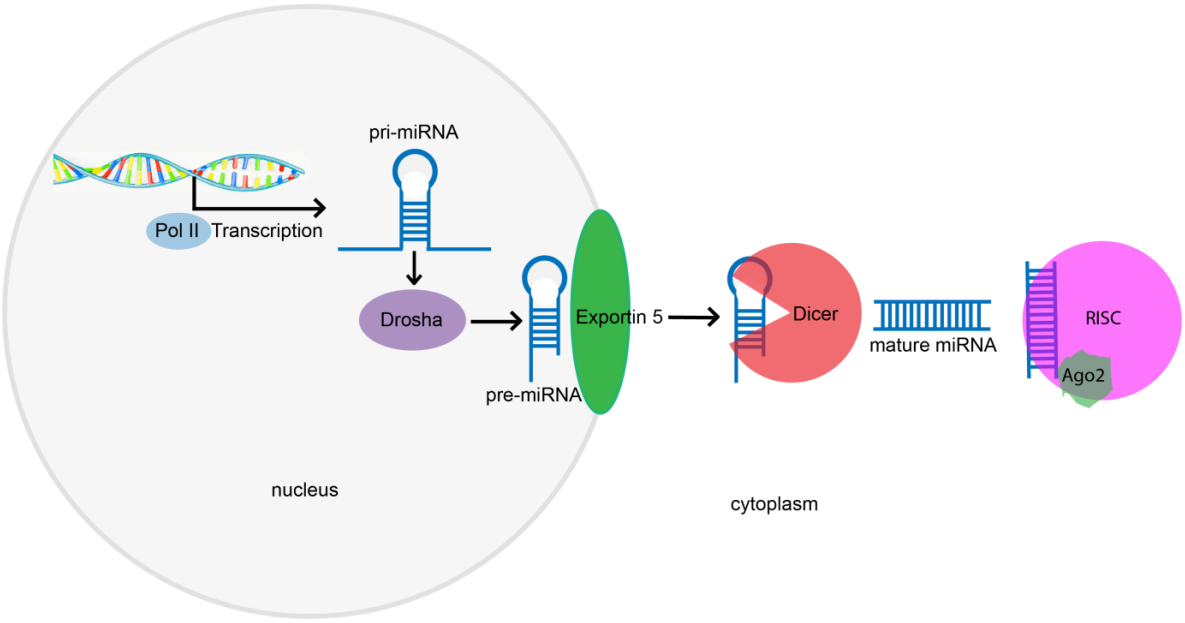

1.4.6 MicroRNAs and Type 2 Diabetes

A number of miRNAs are implicated in the pathogenesis of T2D in relation to glucose homeostasis, beta cell differentiation and survival and response to cell stress, please refer to table 1[155]. Studies on miR-375 in rodent models show that it is implicated in impaired glucose sensitive insulin secretion (GSIS)[155, 156]. Similarly, increased miR-187 expression in human islets correlates with reduced GSIS[156]. Dysregulation of miRNA expression has also been linked with impaired insulin secretion[157]. In particular, reduced expression of miR-185 is seen in T2D, which in turn correlates with blood glucose concentration and impaired insulin secretion[158, 159]. Beta cell microRNAs directly target components of the insulin secretory machinery[160] in response to hyperglycaemia. Poor glucose homeostasis leading to ER stress induces stress induced miR-708 expression, which is again linked to impaired GSIS[161].

There are also well-established roles for miRNAs in relation to beta cell differentiation. Notably, miR-375 is absolutely required for both pancreatic development and mature beta cell differentiation[162, 163]. Regulation of beta cell mass by miR-375 during beta cell differentiation is conserved between species and the location of binding sites for beta cell differentiation genes *PDX1, NGN3,* and *NEUROD1* have been identified in enhancer regions that are required for full miR-375 gene activity[164, 165]. Studies of the role of microRNAs during pancreatic development in rodents and humans have identified that Dicer is required for pancreatic lineage differentiation[155, 166, 167]. Dicer1 null mice show a significant reduction in Ngn3 positive progenitor cells along with decreases in endocrine cell mass[166, 168]. Expression of a number of miRNAs are known to be altered during

beta cell differentiation[169], however, microRNA expression patterns differ significantly between species, highlighting the importance of using human model systems when studying T2D in man[164, 169, 170].

MicroRNAs are also required for the maintenance of mature beta cell differentiation status by repressing the expression of disallowed beta cell genes as well as by mediating beta cell responses[171]. Studies in rodents and human islets have shown that microRNAs are essential for beta cell response to the obesity related stresses hyperglycaemia, dyslipidaemia, ER stress, inflammation and hypoxia[156, 172-175]. The cellular stress response is intimately connected with miRNA expression, with stress granules linked to miRNA regulation[176] and increased expression of Dicer complex proteins associated with increased stress tolerance[177, 178]. The miR-200 family is known to regulate beta cell apoptosis[160] and miRNA regulation of beta cell responses to inflammatory factors have also been shown to induce apoptosis[151]. miR-7 and mir-708 are known to regulate beta cell proliferation[161, 169] and miR-708 is associated with increased rates of apoptosis[161].

Table 1 MicroRNAs implicated in T2D [160, 164, 179]

Table shows microRNAs that have been experimentally validated to have well established roles in beta cell function and are known to target genes with known roles in beta cell differentiation and function.

MicroRNA ID	Role in beta cell function
miR-7	Inhibition of insulin signalling and beta cell proliferation
let-7a	Beta cell insulin signalling, pancreas development
miR-9	Inhibition of insulin signalling
miR-15a	Increased insulin biosynthesis
miR-21	Beta cell apoptosis and survival
miR-29	Inhibition of GSIS. Overexpression causes apoptosis
miR-30a	Targets *NEUROD1* – role in glucotoxicity
miR-30-d	Increases insulin expression by increasing *MAFA*
miR-34a	Beta cell differentiation and beta cell apoptosis
miR-124	Beta cell differentiation, proliferation and insulin secretion
miR-148	Targets *ABCA1*, decreases insulin mRNA
miR-152	Negatively affects insulin secretion
miR-199a	Targets mTOR signalling: insulin secretion
miR-375	Decreases GSIS via Mtpn, decreases insulin gene via *PDK1*, increases beta cell proliferation

1.4.7 Epigenetic modifications

Alongside these mechanistic changes, inheritance of epigenetic information from environmental stimuli can regulate pancreatic endocrine cell identity [59, 101, 180]. An example of this is seen where ARX is bound by the protein MeCP2, thereby linking two epigenetic processes: methylation and histone modification. In a study looking at the effects of activating and repressing epigenetic histone modifications in alpha, beta and exocrine cells, *PDX1* was shown to have a gene-activating H3K4me3 modification in beta cells[62, 101]; however, in alpha cells, there is bivalent marking of both activating and repressing modifications[101]. Further, in beta cells *ARX* expression is downregulated via the presence of the repression histone mark H3K27me3. This suggests that the presence of bivalent epigenetic modifications relates directly to increased plasticity[181]. Studies have identified the *ARX* gene as methylated and repressed in beta cells, whereas it is

hypomethylated and highly expressed in alpha cells. In a study by Dhawan et al.[62] the *ARX* locus in beta cells was bound by MeCP2 protein, which methylates the histone H3R2, thereby linking methylation and histone modification. *DNMT1* propagates methylation of *ARX* during cell division, and by doing so, preserves beta cell identity, effectively stopping them from becoming alpha cells[62]. In *Dnmt1* ablated cells there was a gradual switch in cell identity from beta cell to alpha cell. Insulin and glucagon staining also revealed dual secreting cells[62]. In mice it is considered that the switch is gradual because Dnmt1 propagates methylation during cell division and so effects are only seen in the progeny[62]. It is thought that *Dnmt1* knockout causes passive demethylations linked to rates of beta cell replication and newly divided cells are not able to re-enter the cell cycle after cell division[62].

1.5 Developments in human model systems

1.5.1 Human beta cell lines

The recent development of the EndoC human beta lines by Scharfmann et al.[182, 183] has offered a practical alternative to the use of rodent-derived cell lines in the study of diabetes. This cell line was created by transduction of foetal pancreatic buds using an SV40LT lentiviral vector controlled by the insulin promoter and grafted into SCID mice to develop into pancreatic tissue[182]. This allowed beta cell differentiation and proliferation of insulinomas which were subsequently transduced with human telomerase reverse transcriptase (hTERT) and re-grafted into SCID mice to amplify beta cell proliferation[182]. To culture the cell line, the transplanted grafts were removed and cells dissociated to expand in culture[183]. Physiological characterization of the targeted oncogene-derived cell lines has

shown that EndoC-βH1 cells contain and secrete insulin in response to glucose stimulation and are stable at least for 80 passages, although it is worth noting that the EndoCBH1 cell line contains only 10% of the insulin seen in normal beta cells[184]. Characterization of physiological changes across passages is also yet to be realized and requires investigation. Despite these compromises, however, gene expression profiling has shown that they express all key beta cell markers at both gene and protein level. Further, they exhibit characteristics that more closely mimic human beta cells than other permanent murine cell lines, with higher levels of glucose-sensitive insulin secretion and no response to pyruvate and lactate, when compared with rodent cell line equivalents[185]. A recent study from Gloyn and Rorsman et al showed that they share many of the same electrophysiological characteristics as primary human beta cells and from this perspective make an effective model[186].

Given the differences in levels of gene expression in key transcription factors between mice and humans, as described above, the EndoC cell lines are more appropriate to studies involving the genetic characterization of the physiological effects of diabetes on beta cell function as they carry the human genome. This facilitates a deeper understanding of the transcriptomic changes associated with T2D on mRNA processing and epigenetics. In comparison to the use of isolated human pancreatic islets, human beta cell lines are less affected by admixtures of other islet cell types. The EndoC βH2 and βH3 cell lines that have since been developed also offer the potential for excision of the immortalizing trans-gene, and early physiological characterization suggests they are closer to human beta cells[185]. Although the EndoC βH1 cell line has many characteristics which make it a good model for studying human disease, there

are nevertheless a number of issues that need to be considered relating to their use. This is an immortalised cell line and so it is not possible to use this model to investigate the effects of ageing on beta cell function. Similarly, they are not, in isolation, a good model to study lifestyle factors like BMI, gender and activity level, which would be better studied by incorporating other model systems into the study, such as *ex vivo* islets. As a beta cell-only monolayer culture the model is also an imperfect model for investigating effects of cell-cell interactions and, again, it would be preferable to include the use of human islets. Despite these considerations, the EndoC βH1 cell line is a significant advancement in the study of diabetes using human models.

1.5.2 Islets

The use of isolated human islets in research has been vital to research into T2D, enabling greater understanding of the behaviour of beta cells in response to a diabetic microenvironment within the context of native islet biology[187]; however, there are a number of difficulties around their usage for research, not the least of which is that of supply and demand. Islets are a precious resource that is difficult to obtain, which stands at odds with the requirement for high-volume availability in order to satisfy repeated experimentation[187]. Alongside these issues, it is well documented in the literature that lack of standardization in pancreas and islet processing can result in impure or compromised samples. This can result in hypoxia, contamination from other pancreatic cell types and a high incidence of beta cell death[96, 187, 188]. Despite these challenges, the significant differences between murine and human islet architecture mean that the use of isolated

human islets, in conjunction with human beta cell lines, is the most robust approach for researching human disease.

1.5.3 Stem cells

Human embryonic stem cells (HESCs) are derived from undifferentiated cells taken from the embryonic blastocyst which have been donated to research. As such, there are a number of ethical considerations surrounding their use. In contrast, induced pluripotent stem cells (iPSCs) result from fully differentiated adult cells, from human donors, that have been transfected to temporarily express transcription factors involved in the determination of cell fate. As such, there are fewer ethical considerations[189].

Both HESCs and iPSCs have been used to generate pancreatic beta cells, with varying success. Some of the difficulties encountered have included observations that stem cell-derived beta cells had a fetal, rather than adult beta cell phenotype, as well as some important differences in gene expression profiles[190-193]. More recently, there has been progress using step-wise differentiation protocols, which has overcome many of these issues, and trials are currently being conducted for the use of stem cell-derived beta cells in the treatment of type 1 diabetes[189, 192, 194]. Disagreements remain, however, over the status, characterization and assessment of maturing versus mature stem cell-generated beta cells. Currently, as indicated above, combined use of isolated human islets and human beta cell lines remains the most practical method for research into T2D.

1.6 Conclusion

As discussed, apoptosis may not account for the extent of beta cell mass loss seen in T2D, and loss of beta cell function relates to changes in beta cell differentiation status along with disruption to beta cell function genes. Most of the work in this field has been carried out using murine models, but differences between murine and human islet structure make definite comparison difficult. This, coupled with mechanistic differences in gene expression between species, means that these studies need to be corroborated in human models. Understanding these processes in newly available human beta cell lines will elucidate whether changes to beta cell differentiation status account for some of the beta cell mass loss that is seen in T2D in humans. This would be an important step in characterizing the mechanisms that lead to beta cell failure and could inform potential future therapies. The studies within this thesis have been performed under the auspices of Animal Free Research UK policies which state that animal products could not be used.

1.7 Research hypothesis

We believe that altered RNA processing or gene regulation, caused by cellular stresses associated with T2D, can affect mature beta cell differentiation status. The beta cell mass loss that is seen in T2D is due, in part, to loss of beta cell function as a result of changes in beta cell differentiation status.

1.8 Aims and objectives of thesis

It has been shown in mouse models that changes in mature beta cell differentiation status occur in response to cellular stresses seen in T2D[61]. The objective of this thesis is to investigate whether cellular stresses, associated with T2D, alter mature beta cell differentiation status in humans. Such a finding would be important because changes in beta cell differentiation may be identified as an important feature of the disease in humans. This may also offer potential treatment targets in the management of the disease.

I have assessed this by investigating the importance of species origin on the cellular microenvironment for the EndoC βH1 human cell line. This established physiologically relevant culture conditions in which to assess the effect of cell stresses associated with T2D including: altered glycaemia, hypoxia, dyslipidaemia, inflammation and the ER stress inducer tunicamycin. I have used this model to identify changes in the expression of relevant beta cell genes, altered splicing factor expression and dysregulated expression of specific alternatively spliced genes. This led to development of a hypothesis, where dysregulated splicing may be an important feature of altered mature beta cell

status. To support these data, I have investigated changes in protein expression in both the EndoC βH1 model and *in situ* islets from patients with long duration T1D and T2D. Having identified important changes in protein expression, I investigated the hypothesis that removal of cell stresses may allow 'rescue' of a mature beta cell phenotype.

I have then gone on to assess the fine control of gene regulation by investigating altered microRNA expression in response to these cell stresses. This included gene enrichment analysis of the most altered microRNAs to identify the pathways implicated in stress response, along with subsequent validation of these target genes. I will describe in more detail the specific aims of this thesis within each data chapter.

1.8.1 Chapter 3: Determining the effect of species origin of the cellular microenvironment

Summary

The aim of chapter 3 was to investigate the importance of the species origin of the cellular microenvironment. This allowed the development of an optimised, physiologically relevant, set of culture conditions from which to assess the effects of cell stresses in a human beta cell model system. The aim was for work from this chapter to form the basis for ongoing investigation of the effects of cell stresses associated with T2D on beta cell differentiation status. To investigate the effects of species origin, I aimed to culture cells using non-human reagents and compare this to cells cultured in human derived reagents. This incorporated

assessment of altered gene expression for a panel of relevant beta cell genes. I aimed to investigate beta cell function by assessing changes in glucose sensitive insulin secretion between non-human and human culture reagents. To assess the effects of species origin, I aimed to use immunofluorescence microscopy to investigate the expression of markers of mature beta cell status.

1.8.2 Chapter 4: Determining the effect of cellular stressors on beta cell differentiation status

Summary

The aim of chapter 4 was to investigate the effects of the cell stresses hyperglycaemia, hypoglycaemia, hypoxia, dyslipidaemia, inflammation and ER stress inducer tunicamycin, on beta cell differentiation status in man. This utilised the optimised EndoC βH1 cell line, demonstrated in chapter 3, along with *in situ* pancreatic islets from patients with T1D and T2D. We hypothesized that these cell stresses would dysregulate the expression of relevant beta cells genes, chosen for roles in beta cell fate and function, markers of cell stress and markers for other pancreatic endocrine islet cell types. I aimed to use this targeted transcriptomic profiling to analyse altered splicing factor expression and changes in the isoform expression of specific alternatively spliced genes. I further aimed to investigate changes in hormone expression in response to the cell stresses using immunofluorescence microscopy in both the cell model and cases from patients with long duration T1D and T2D. Having identified changes in protein expression I aimed to investigate whether the removal of cellular stresses allowed rescue of a mature beta cell phenotype.

Following on from this work, we hypothesized that beta cell differentiation status may be influenced by dysregulated splicing. To investigate this, I designed an siRNA knock down to determine the effects of alternative splicing of *PAX6* on beta cell stress response. This gene was selected due to the earlier work which showed it's splicing was dysregulated in response to the cell stresses and its importance in the maintenance of mature beta cell differentiation status[195-197]. Our group were also aware that the AKT pathway, and its downstream effector *FOXO1*, have been implicated in regulation of splicing and is also important to pancreatic plasticity[104, 198]. We hypothesized that altered *FOXO1* expression may influence regulation of splicing and investigated this using SH6 small molecule inhibition of the AKT pathway.

1.8.3 Chapter 5: Cellular stress responses may be coordinated by microRNAs

Summary

In Chapter 5 I aimed to investigate the fine control of gene regulation by assessing altered microRNA expression in response to the cell stresses. To identify targets for further investigation, I performed a global high throughput assay of the expression of 757 microRNAs using the EndoC βH1 cell model. From this, I aimed to validate the altered expression of selected microRNAs known to target relevant beta cell genes and compared this to changes in the expression of their targets. Along with this, I aimed to select the most altered microRNAs from the global screen for validation and use these results for gene enrichment analysis. Having identified the pathways and gene targets implicated

in EndoC βH1 responses to these cellular stresses, I aimed to validate these targets to determine whether they showed changes in expression in response to the cell stresses.

Chapter 2:

Methods

2.1 Tissue culture

2.1.1 General Culture conditions for EndoC-βH1 cells

Throughout this study EndoC-βH1 cells were used, obtained from EndoCells, INSERM in France. They are a human beta cell line developed by transducing human pancreatic foetal buds with a lentivirus that is then grafted into severe combined immune-deficient mice (SCID)[199]. As a result, the cells express the Simian Virus 40 large T antigen (SV40LT) oncogene[199]. Following this, they were then expanded in culture to create cell lines[199]. The cells are stable for up to 80 passages[183], however, in this study all of the cell treatment assays were carried out <P25. Here, the cells were cultured for 7 days between passages in T25 flasks and were fed once per week by removing half of the old culture media and replacing it with fresh media. Coating medium was prepared in, as described below, and the flasks were incubated for minimum of 5 hours prior to passage. The coating medium was then removed and immediately replaced with culture medium to prevent the matrix from drying out. The cells were passaged and seeded into the prepared T25 flasks at a density of 1.75 x 10^6/ µL and showed mean population doubling times of 19hrs.

2.1.2 Standard culture conditions for EndoC-βH1 cell microenvironment using animal derived reagents

EndoC βH1 cells (Endo Cells, INSERM, France) were cultured in accordance with the published guidelines[182, 183, 199]. Cells were seeded onto an ECM coat consisting of DMEM 4.5 g/ L (Thermo Fisher, Waltham, MA USA), matrigel (100 µg/ mL) fibronectin from bovine plasma 2 µg/ mL coat (both from Sigma-

Aldrich, Steinheim, Germany), and cultured in DMEM 1 g/ L glucose (Thermo Fisher, Waltham, MA, USA) 2% BSA fraction V (Merck Chemicals, Darmstadt, Germany), 10 mM nicotinamide (Sigma-Aldrich, Steinheim, Germany) 50 µM β-2-Mercaptoethanol, 5.5 µg/ mL transferrin, 6.7 ng/mL sodium selenite, and 100 U/ mL penicillin and 100 µg/ mL streptomycin (Sigma Aldrich, Steinheim, Germany)

2.1.3 Modified culture conditions for EndoC βH1 cell microenvironment using human derived reagents

EndoC-βH1 cells were cultured on Maxgel ECM mixture liquid (Sigma Aldritch, Steinheim, Germany) containing fibronectin from human plasma (Sigma-Aldritch, Steinheim, Germany). Culture medium (DMEM 1 g/ L glucose, Thermo Fisher Waltham, MA USA) contained 2% human serum albumin fraction V (Merck Chemicals, Darmstadt, Germany), 100 U/ mL Penicillin and 100 µg/ mL streptomycin, 50 µM β-2-Mercaptoethanol (Sigma-Aldrich, Steinheim, Germany), 10 mM nicotinamide (Sigma Aldritch Steinheim, Germany), 5.5 µg/ mL human transferrin (Sigma Aldritch, Steinheim, Germany) and 6.7 ng/ mL of sodium selenite (Sigma Aldritch, Steinheim, Germany). Cells were passaged using TRYPLE 1x (Thermo Fisher, Waltham, MA, USA) and neutralised with heat inactivated human serum from human male AB plasma (Sigma Aldritch, Steinheim, Germany).

2.1.4 Glucose-stimulated insulin secretion

The insulin enzyme linked immunoassay (ELISA) kit used in the study was a sandwich ELISA for insulin which utilizes an antibody that is immobilized onto the microplate wells along with a horse radish peroxidase (HRP) enzyme. Sandwich ELISAs have sample bound between two primary antibodies, one of which is a reporter and are considered to be the most sensitive assays for quantitatively determining the amount of analyte in samples[200]. In this instance, the sample was incubated in the ELISA microplate along with the HRP labelled reported antibody and then washed after the 2 hr incubation period to remove the unbound antibody. The substrate solution was then added and incubated for 15 minutes before the reaction was stopped.

To ensure parity of cell number, cell counts were used to ensure equal numbers of cells were plated in each well, with. EndoC-βH1 cells seeded onto 24 well plates at 4×10^5 per well and cultured for 72 hrs in separate cultures. Cells were then transferred to a culture medium containing 2.8 mM glucose as a starvation medium and cultured overnight, before being incubated for 1 hr in a starvation medium containing 0.5 mM glucose in HEPES Krebs Ringer Buffer (KRB) at pH 7.4 containing: 116 mM/ L NaCl, 5 mM/ L KCl, 1 mM/ L $CaCl_2$, 1 mM/ L $MgCl_2$, 1.2 mM/ L KH_2PO_4, 24 mM/ L $NaHCO_3$, 10 mM/ L HEPEs, 0.2% Human Serum Albumin (HSA). After 1 hr, the 0.5 mM glucose starvation HEPES KRB starvation buffer was removed and replaced with HEPES KRB containing 20 mM glucose and cells incubated for 1 hr. Media was removed from each sample, spun at 1000 g for 5 min to

remove protein debris and supernatant harvested for comparison with controls using the ELISA against fully processed human insulin. (Human Insulin ELISA, Crystal Chem, Downers Grove, IL, USA, assay range 0.9 - 220 mU/ L, analytical sensitivity 0.25 mU/ L, precision CV < 10%, 1.2% cross reactivity with pro insulin). Absorbance was measured using a plate reader and measured A_{450} values, subtracting A_{630} values. Insulin levels were normalized to total protein.

2.1.5 EndoC-βH1 insult assays to mimic diabetic microenvironment

2.1.5.1 Hyperglycaemia and Hypoglycaemia

For all assays the cells were seeded at 1.00 x 10^6/ µL in 6 well plates and cultured for 72 hours prior to treatment. In line with published hyperglycaemia methodologies, media containing 25 mM glucose was used to mimic hyperglycaemia across 24 hr, 36 hr and 48 hr time points in three separate cultures (n=3 for each time period)[46, 201]. This method was duplicated for hypoglycaemia but cells were treated with media containing 2.5 mM glucose across the same time periods (n=3 for each time period). Controls were cultured in media containing 1g/ L glucose across the same time periods (n=3 for each time period).

2.1.5.2 Hypoxia

Cells were seeded at 1.00 x 10^6/ µL in 6 well plates and cultured for 72 hrs prior to treatment. To investigate the effects of hypoxia, separate cell cultures were placed in New Brunswick Galaxy 170R nitrogen fed, oxygen controlled, hypoxia incubators and exposed to 3% and 1% oxygen respectively across 4 hr, 12 hr and 24 hr time points (n=3 for each condition and each time point)[51, 202]. Controls were maintained at usual cell culture protocols of 19% oxygen[203].

2.1.5.3 Lipotoxicity

Cells were seeded as previously described and cultured for 72 hrs prior to treatment. The effects of lipotoxicity were assessed by treatment with 0.5 mM Palmitic Acid conjugated to BSA as an ethanol carrier over 12 hrs, 24 hrs and 48 hrs (n=3 for each time point)[29, 54, 204]. Controls and BSA only controls were cultured in standard culture media with the addition of ethanol to account for its use as a carrier in treated cells (n=3 for each time point).

2.1.5.4 Inflammatory cytokines

Cells were seeded as previously described and cultured for 72 hrs prior to treatment. Inflammation was induced using the pro-inflammatory cytokines TNFα at 1000 U/ mL, INFγ at 750 U/ mL and IL1β at 75 U/ mL over 12hrs, 24hrs and 36hrs (n=3 for each time point)[39, 56, 205]. Controls were cultured in standard culture media for the same time periods (n=3 for each time point).

2.1.5.5 Induced Endoplasmic Reticulum stress

Endoplasmic Reticulum (ER) stress was induced using 0.5 mM Tunicamycin.[38, 206] Cells were seeded as previously described and cultured for 72 hrs prior to treatment with Tunicamycin for 24hrs. For rescue from ER stress, after 24 hrs treatment cells were restored to normal culture media for a further 72 hrs (n=3 for each condition including controls).

2.1.5.6 Palmitate and oleate test of metabolic response

Metabolic response to cell treatments was tested via administration of 0.5 mM palmitic acid versus 0.5 mM oleic acid, as oleic acid is known to not cause beta cell stress[207]. Cells were seeded as previously described and initially cultured for 72 hrs prior to treatment with either palmitic acid or oleic acid. A further treatment combining both 0.5 mM palmitic acid with 0.5 mM oleic acid was carried out for the same time points (n=3 for all conditions and controls) Controls were treated with the empty EtOH carrier.

2.1.5.7 Phenotype rescue

As previously, cells were seeded at 1.00 $x10^6$ / µL in 6 well plates. Determination of phenotype ‘rescue’ was investigated by culturing cells for 48 hours prior to treatment with 25 mM glucose for 24 hrs. It was not possible to culture the cells for 72 hrs prior to treatment as this would not have allowed sufficient time to ‘rescue’ in 5 mM glucose, euglycaemic, media before the cells became overly confluent. After 24hrs of exposure to 25 mM glucose cells were restored to normal culture media containing 5 mM glucose for a further 72hr (n=3 for each condition including controls).

2.2 Immunofluorescent cytochemistry.

Immunofluorescence staining was used to determine the expression of mature beta cell markers, as well as islet cell hormones, in EndoC-βH1 cells grown in conditions mimicking a diabetic microenvironment. Cells were fixed with 4% paraformaldehyde for 15 minutes at 4^{o}C. Primary antibodies for PDX1 (Abcam Ab47267, rabbit polyclonal, 1/400), NEUROD1 (Abcam Ab60704, mouse monoclonal, 1/400), PAX6 (Abcam Ab195045, rabbit monoclonal, 1/350), Somatostatin (SST) (Abcam Ab30788, rat monoclonal, 1/200) and Glucagon (GCG) (Abcam Ab10988, mouse monoclonal, 1/2000) were diluted in phosphate buffered saline (PBS) with 0.1M Lysine, 10% donor calf serum, 0.02% sodium azide and 0.02% Triton (ADST), to permeabilise the cell membranes and incubated overnight. Primary antibodies were visualised using highly cross-absorbed secondary antibodies (Life Technologies) diluted in ADST at 1/400: goat anti-rabbit Alexa Fluor 555 for PDX1 and PAX6 at 1/400, goat anti-mouse Alex Fluor 555 for NEUROD1 at 1/400, goat anti-rat Alex Fluor 488 for SST at 1/400 and goat anti-mouse Alexa Fluor 488 for GCG at 1/400 and incubated for 1 hour. Coverslips were then sequentially stained with insulin antisera (80564, LN10088287 Dako) and diluted in ADST at a concentration of 1/400 and incubated for 1 hour. Coverslips were then incubated with an appropriate secondary goat anti guinea-pig Alex Fluor (dependent on the Alexa Fluor utilised to recognise the first antisera) along with DAPI (Sigma-Aldritch D9542), were diluted in ADST at respective concentrations of 1/400 and 1µg/ ml. Slides were visualised using a LEICA DM4000 B-LED fluorescence microscope using LAS X image software. For fluophore filters details please refer to table 2. Due to

constraints on the use of animals, antibodies were not validated in knock out tissue.

2.2.1 Image analysis

Quantification of the proportion of somatostatin positive cells within the culture was achieved by cell count from images taken blinded to the somatostatin 488 nm wavelength. Ten randomly selected images from 3 treated and 3 controls were taken for each assay. Images were visualised and analysed using Image J software and were normalised to the same settings for brightness and contrast[208].

Table 2 Fluophore filter excitation and emission details

Fluophore	Colour	Excitation/ Emission	Excitation filter	Emission Filter
Platinum bright 405	Dark Blue	410/455	405/10	460/36
Platinum bright 495	Green	495/517	495/25	537/29
Platinum bright 550	Red	550/580	546/22	590/23
Platinum bright 647	Far red	587/612	580/25	625/30

2.3 Immunofluorescent characterisation of pancreatic tissue sections from patients with T1D and T2D

Immunofluorescence staining was used to determine the expression of islet cell hormones in pancreatic sections from individuals with no diabetes (n=7), patients with Type 1 Diabetes (T1D) (n=7) and also patients with T2D (n=7). Tissue

sections were utilised from two pancreatic biobanks, the Exeter Archival Diabetes Biobank (EADB, UK) and the JDRF network of Pancreatic Organ Donors with Diabetes (nPOD, USA) that contain both organ donor and post mortem tissue, please refer to supplementary table S2 for patient data. Tissue sections were soaked for 2 x 5 minute washes in Histoclear to remove the $HgCl_2$ or BF fixation and rehydrated using 1 min incubations in 100% EtOH, 90% EtOH, 70% EtOH, 100%MeOH, with a final 5 minutes incubation in ddH_2O. Heat induced epitope retrieval (HIER) using a citrate pH6 buffer was carried out for 20 minutes. Following a block in 5% normal goat serum tissue sections were incubated with the following primary antibodies against SST (Abcam Ab30788, rat monoclonal, 1/200) and GCG (Abcam Ab10988, mouse monoclonal, 1/2000) were diluted in DAKO antibody diluent (Dako SO809) and incubated for 1 hour. The primary antibodies were visualised using highly cross-absorbed secondary antibodies (Life Technologies) diluted in Dako antibody at 1/400: goat anti-rat Alexa Fluor 488 for SST and goat anti-mouse Alexa Fluor 555 for GCG and incubated for 1 hour. This was followed by sequential staining with insulin antisera (80564, LN10088287 Dako) diluted in Dako antibody diluent at a concentration of 1/360 and incubated for 1 hour. This was visualised using a secondary goat anti guinea-pig Alexa Fluor 647 along with DAPI (Sigma-Aldritch D9542), that were diluted in Dako antibody diluent at respective concentrations of 1/400 and 1 µg/ µL and incubated for 1 hour. Slides were visualised using a LEICA DM4000 B-LED fluorescence microscope using LAS X image software. For fluophore filters details please refer to table 2

2.3.1 Image analysis

Quantification of pancreatic endocrine cells types within the islet was achieved by assessing the comparative number of cells as a percentage of total islet area between T1D/ T2D patients and controls. Images from 10 randomly selected islets from 7 cases and controls were taken. Areas of somatostatin, insulin and glucagon staining were selected and measured using Image J[208].

2.4 Candidate genes for expression analysis

Target genes were selected for their roles in beta cell fate, maturity and function. Transcription factors with roles in the regulation of beta cell fate were also selected, including: *PAX4, PAX6, PDX1, NEUROD1, FOXO1, NKX6.1,* and *NKX2.2* as well as the tumour suppressor *STK11 (LKB1)*[42, 43, 57, 90, 94, 107, 196, 197]. Key genes to beta cell function genes were also chosen, including: *INS, GCK, MAFA, MAFB, PTPN1, SLC2A2, SLC2A4* and *SYP*[58, 85, 107, 144, 209-211]. To investigate cellular plasticity, genes with roles in beta cell differentiation were selected, including: *NGN3, SOX9, NANOG, POU5F1 and HES1*[61, 86, 103, 212-215]. Selection also included *SLC16A1* and *LDHA,* genes that are typically disallowed in beta cells due to their roles in inappropriate insulin release as a result of lactate and pyruvate metabolism in response to exercise [91, 171, 216]. Alongside these, the target panel included genes associated with cell stress and apoptosis, including *MYC, ARNT, HIF1a and DDIT3*[39, 45, 51, 103, 217-219]. Finally, genes that are markers for other endocrine pancreatic islet cell identity were selected, *ARX* and *GCG* as alpha cell markers, as well as *SST* and *HHEX*, the delta cell associated gene for

the hormone Somatostatin[62, 92, 96, 99, 113, 220]. For gene names, roles and assay IDs please refer to table 3.

Table 3 Gene assay IDs.

Target panel of genes selected for their roles in beta cell fate and function, markers for increased plasticity and cell stress and markers for other pancreatic endocrine cell types.

Gene Symbol	**Assay ID**	**Role in beta cells**
GUSB	Hs00939627_m1	Housekeeper
PPIA	Hs04194521_s1	Housekeeper
HPRT1	Hs02800695_m1	Housekeeper
STK11	Hs00176092_m1	Beta cell function
FOXO1	Hs01054576_m1	Beta cell differentiation and beta cell function
PAX6	Hs00240871_m1	Beta cell differentiation and beta cell function
GCK	Hs01564555_m1	Beta cell function
MAFA	Hs01651425_s1	Beta cell function
NKX6-1	Hs00232355_m1	Beta cell differentiation and beta cell function
NEUROD1	Hs01922995_s1	Beta cell differentiation and beta cell function
NKX2-2	Hs00159616_m1	Beta cell differentiation and beta cell function
INS	Hs00355773_m1	Beta cell function
PDX1	Hs00236830_m1	Beta cell differentiation and beta cell function
PTPN1	Hs00942477_m1	Beta cell function
SLC16A1	Hs01560299_m1	Lactate/ pyruvate solute carrier – disallowed in beta cells
SYP	Hs00300531_m1	Beta cell function
LDHA	Hs01378790_g1	Lactate/ pyruvate solute carrier – disallowed in beta cells
PAX4	Hs00173014_m1	Beta cell differentiation and beta cell function

Gene Symbol	Assay ID	Role in beta cells
MAFB	Hs00271378_s1	Beta cell function
SLC2A2	Hs01096908_m1	Beta cell function
ARX	Hs00292465_m1	Alpha cell differentiation and function
GCG	Hs01031536_m1	Alpha cell function
SST	Hs00356144_m1	Delta cell function
HHEX	Hs00242160_m1	Delta cell marker
SOX9	Hs01001343_g1	Beta cell progenitor marker
NEUROG3	Hs01875204_s1	Beta cell progenitor marker
HES1	Hs00172878_m1	Beta cell progenitor marker
POU5F1	Hs04260367_gH	Beta cell progenitor marker
NANOG	Hs04399610_g1	Beta cell progenitor marker
HIF1A	Hs00153153_m1	Hypoxia marker
ARNT	Hs01121918_m1	Cellular stress and hypoxia marker
MYCL	Hs00420495_m1	Cellular stress and proliferation marker
DDIT3	Hs00358796_g1	Cellular stress and apoptosis marker

2.5 Alternatively spliced genes candidate selection

Five genes were investigated for the effects of microenvironment on alternative splicing. The genes were selected from the existing target panel based on three criteria: it was possible to design probes that differentiate between the isoforms, there are known functional differences between the isoforms, and isoform differences are relevant to the pancreas. Please refer to table 4 for assay IDs.

2.5.1 Insulin

Human Insulin (*INS*) contains 3 exons. Exon 1, intron 1 and the first section of exon 2 contain the 5' untranslated region (UTR) and so are likely to be regulatory[142, 221]. Exon 2 encodes the signal peptide, the B chain and part of the c-peptide. Exon 3 encodes the rest of the C-peptide and the A chain. Both of the 2 introns are flanked by canonical splice sites and encode the consensus sequences of GT(U)-AG introns[142, 221]. Despite the small number of exons, there are two functionally distinct isoforms: the canonical variant excises intron 1. However, there is also a 5' cryptic splice site which creates an isoform that retains the first 26bp of the first intron. This isoform is known to make up about 10% of all insulin transcripts and is highly regulated by glucose, conferring increased translational efficiency[142, 221]. Glucose enhances translational efficiency by inducing binding of the polypyrimidine tract binding protein (PTB) to its 3' UTR. Here, Taqman® custom assays (Thermo Fisher, Waltham, MA, USA) were designed to distinguish between the isoform containing the 26bp intron inclusion and the other variants. *In-silico* splicing was used to be able to identify exon boundaries that contained the target sequence

GTGGGCTCAGGATTCCAGGGTGGCTG for the 26bp intron inclusion, termed variant 1, that detects human gene *INS* refseq NM_001185098, from Human genome assembly December 2013 (GRCh38/hg38). The same process was used to detect exon boundary sequences that would only distinguish the other variants, termed variant 2. The resulting sequences were used to design custom Taqman gene assays that detect human gene *INS* refseq NM_001185097 and NM_000207, from the same genome assembly.

2.5.2 Paired box protein 6 (PAX6)

Alternative splicing generates two *PAX6* isoforms, referred to as *PAX6* and *PAX6(5a)*, which differ by the inclusion of 14 amino acids (aa) encoded by the additional exon 5a[222-224]. The 14-aa insertion profoundly alters the DNA-binding activity of the Pax6 paired domain[225]. The paired domain of Pax6 depends on both subdomains for DNA sequence recognition, similar to all members of the Pax2/5/8 family[223, 225]. As these insertions severely restrict the sequence recognition of the paired domain, they may almost entirely switch the DNA-binding mode of certain Pax proteins [such as Pax6(5a)] from the paired domain to the homeodomain. The transcriptional function of the two isoforms is influenced by the ratio of *PAX6:PAX6(5a)*; depending on cell type and developmental stage[197, 226]. In this way it has been suggested that exon 5a functions as a molecular switch which specifies target genes[227].

Studies have also shown that the *PAX6(5a)* isoform is associated with pancreatic cancer[197, 226, 228]. Pax6 is known to regulate the expression, via binding of the promoters, of *INS*, *PDX1*,*MAFA, NKX6-1 and SLC2A2 (GLUT2)*, indicating it's critical role in beta cellfunction[197, 226]. Studies have also shown that it is important for glucagon synthesis in alpha cells via regulation of the glucagon gene *GCG*. In alpha cells it also regulates *MAFB* and *NEUROD1,* which are also critical for GCG expression and maintenance of alpha cell fate.

Taqman® custom assays (Thermo Fisher, Waltham, MA, USA) were designed to distinguish between canonical *PAX6* and *PAX6(5a)*. *In-silico* splicing was used to be able to identify exon boundaries that contained the target sequence for the

14aa exon 5 inclusion which detects human gene *PAX6* refseqs NM_001258462.1, NM_001258463.1, NM_001310158.1, NM_ 001310160.1, NM_001310161.1 and NM_001604.5 from Human genome assembly December 2013 (GRCh38/hg38). The same process was used to detect exon boundary sequences that would only distinguish the canonical variants. The resulting sequences were used to design custom Taqman gene assays that detects human gene *PAX6* refseqs NM_001258463.1, NM_001258464, NM_001258465, NM_000280 from the same genome assembly.

2.5.3 POU class 5 homeobox 1 (POU5F1 (OCT4))

There are three main isoforms of human POU5F1, also known as OCT4, which are categorised as OCT 4A, OCT4B and OCT4B1. Previous studies have established that OCT4A is associated with stemness properties, where as OCT4B and OCT4B1 appear to be responsive to cellular stress[229]. The cellular localisation of the OCT4 isoforms has also been previously characterised, with OCT4A exclusively localised to the nucleus where it acts as a transcription factor[229, 230]. However, OCT4B and OCT4B1 are localised to both the cytoplasm and the nucleus[229]. Localisation changes are known to be associated with response to cellular stress. Here, Taqman® custom assays (Thermo Fisher, Waltham, MA, USA) were designed to differentiate between the *OCT4A* and *OCT4B/ B1* isoforms. Again, *in-silico* splicing was used to identify sequence differences across the exon 2 and 3 boundary for the *OCT4A* isoform refseqs NM_002701 from Human genome assembly December 2013 (GRCh38/hg38). The same process was used to detect exon boundary sequences that would only distinguish the *OCT4B/B1* variants and these were used to design custom

Taqman® gene assays to detect refseqs NM_001285987, NM_001285986.1 and NM_203289.5 from the same genome assembly.

2.5.4 Nanog homeobox (NANOG)

NANOG has two isoforms resulting from alternative splicing[231, 232]. The long variant is known to be more highly expressed in ES cells than the shorter isoform. However, in multipotent adult progenitor cells the shorter isoform shows much higher expression than is seen in ES cells, hence expression level is considered an important determining factor for pluripotency[231, 232]. It has been suggested that the increase in ratio of short to long form variants is indicative of a role in the regulation and control of differentiation[233]. To differentiate between the long and short form *NANOG* variants, Taqman® custom assays (Thermo Fisher, Waltham, MA, USA) were designed. The technique of in-silico splicing was again used to identify sequence differences in exon 4 between the long and short isoforms. Termed *NANOG* exon 4 long, this assays identified the refseq variant NM_024865.3 from Human genome assembly December 2013 (GRCh38/hg38). The other assay, called exon 4 truncated, detected the NM_001298698.1 from the same genome assembly.

2.5.5 Protein tyrosine phosphate PTPN1

PTPN1 (PTP1B) is known to negatively regulate insulin and leptin signalling via dephosphorylation of the activating phosphor-tyrosines on the insulin receptor[234, 235]. There are two variants resulting from alternative splicing: a long transcript which includes intron 9 and a shorter form where intron 9 is excised. Studies have

shown that the long isoform is associated with body fat percentage and fasting insulin scores and has been suggested as a biomarker for hyperinsulinaemia in Diabetes[145, 234, 235]. To distinguish between the long and short form *PTPN1* variants, Taqman® custom assays (Thermo Fisher, Waltham, MA, USA) were designed by *in-silico* splicing to identify sequence differences in exon 2. *PTPN1* 'long' detected the refseq variant NM_002827.3 from Human genome assembly December 2013 (GRCh38/hg38). The other assay, *PTPN1* 'short', identified refseq NM_001278618.1 from the same genome assembly.

Table 4 Alternatively spliced gene assay IDs.

Custom assays were designed using in silico splicing to distinguish between isoforms.

Assay Name	Forward Primer Seq.	Reverse Primer Seq.	Reporter 1 Sequence
INS_EX1	CCATCAAGCAGGTCTGTTCCAA	GGGCCATGGCAGAAGGA	CCTTTGCGTCAGATCACT
PTPN1_EX2DEL	AGTTCGAGCAGATCGACAAGTC	GCGTTGATATAGTCATTATCTTCTTGATGTAGT	CTATGGTCAACTGGTAAATG
INS_EX1DEL	GGCTTCTTCTACACACCCAAGAC	CCTCCAGGGCCAAGGG	CTGCAGGGCAGCCTG
NANOG1_EX4LNG	TGGCCGAAGAATAGCAATGGT	CATCCCTGGTGGTAGGAAGAGTA	ACGCAGAAGGCCTCAGC
PAX6_EX5DEL	CGTGCGACATTTCCCGAATT	GTCTCGTAATACCTGCCCAGAATTT	ATCCGTTGGACACCTGC
NANOG_EX4TRU	TGGCCGAAGAATAGCAATGGT	GGTTCCCAGTCGGGTTCAC	ACGCAGGGATGCCTG
INS_EX1LNG	GGACAGGCTGCATCAGAAGAG	GGGCCATGGCAGAAGGA	CCATCAAGCAGATCACTG
POU5F1_EX3	GAAGAGGATCACCCTGGGATATACA	TGGCTGAATACCTTCCCAAATAGAAC	CAGGCCGATGTGGCTC

2.6 RNA extraction

RNA was extracted from EndoC βH1 cells for each of the cell assays using the TRI®reagent/ chloroform method. TRI®reagent, or TRIzol, is a solution of phenol and guanidium isothiocyanate which lyses the cells, denatures protein and has the advantage of eradicating RNases which would otherwise degrade the sample. The addition of chloroform causes phase separation, where RNA

remains in the aqueous phase, DNA is at the interface and protein is in the organic phase. This method is useful in that it allows the isolation of RNA, DNA and protein from the same sample[236-238]. The addition of $MgCl_2$ was used to protect against the loss of miRNAs during the extraction process. It has been shown that TRI®reagent can lead to the loss of small RNAs with a low GC content[239]. $MgCL_2$ is thought to stabilise the phosphate backbone of small RNAs, allowing them to survive this method of extraction[239].

For the extraction, cells were washed in Dulbecco's phosphate buffered saline (D-PBS). TRI® reagent (Sigma-Aldrich, Steinheim, Germany), was used to harvest RNA, 10 µL of $MgCl_2$ to stabilise short RNAs, such as microRNAs with low GC content (Thermo Fisher, Waltham, MA, USA) and 200 µL of Chloroform (Thermo Fisher, Waltham, MA, USA)added[239]. Samples were centrifuged at 14800 rpm, 4 ^{o}C for 20 mins, the clear aqueous layer removed and 500 µL of isopropanol (Thermo Fisher, Waltham, MA, USA) added for overnight precipitation. Samples were centrifuged at 14800 rpm, 4 ^{o}C for 45 minutes to form RNA pellet. The pellet was then repeatedly washed using 75% molecular grade ethanol (Thermo Fisher, Waltham, MA, USA), air dried and then re-suspended in 20 µL RNase-free water.

2.7 Reverse transcription

Reverse transcription is the process by which single stranded complementary (cDNA) is synthesized. It uses RNA as the template and a reverse transcriptase enzyme to synthesise the cDNA molecule. The reaction amplifies the product for use in quantitative polymerase chain reaction (qPCR) studies. Here we used three different methods for reverse transcription, using RNA extracted from

EndoC βH1 cells from each of the cell treatment assays. Superscript® VILO™ was used for all of the gene expression assays in Chapter's 3 and 4. However, for the siRNA gene modification and SH6 AKT pathway inhibition assays EvoScript Universal cDNA synthesis kits were used. Taqman® Advanced miRNA cDNA kits were used for the microRNA expression assays in Chapter 5. Finally, we again used EvoScript Universal cDNA synthesis kits for the target gene expression assays in Chapter 5.

2.7.1 Superscript™ VILO™ cDNA synthesis.

For the total gene expression, alternative splicing, splicing factor expression, rescue of phenotype and ER stress assays, cDNA synthesis was carried out using Superscript® VILO™ cDNA synthesis kit (Thermo Fisher, Waltham, MA USA). Samples were normalised to 100 ng/ µL RNA prior to reverse transcription. This enzyme mix has good thermostability which is required since the reaction includes a high temperature denaturing step. It also contains an inhibitor which eliminates RNase H activity and increases the yield of cDNA. The reaction mix contains random primers, dNTPs and $MgCL_2$ for phosphodiester bond formation. Cycling conditions were incubation at room temperature (25 ^{o}C) for 10 minutes, 42 ^{o}C for 60 minutes and 85 ^{o}C for 5 minutes.

2.7.2 Taqman™ Advanced microRNA cDNA synthesis.

For the microRNA (miRNA) open array and miRNA expression assays, cDNA synthesis was carried out using the Taqman® Advanced miRNA Assay kit (Thermo Fisher, Waltham, MA USA). Samples were normalised to 10 ng/ µL prior

to reverse transcription. The first stage of the reaction adds a polyA tail to the 3' end, cycling at 37 ^{o}C for 45 minutes and then a 10 minute cycle at 65 ^{o}C to stop the reaction. The second step is 5' adapter ligation to extend the mature miRNAs present in the sample, at 16 ^{o}C for 60 minutes. Following these preliminary reactions, the reverse transcription reaction is performed using universal primers that recognize the universal sequences on the 5' and 3' ends of the miRNAs. The cycling conditions for this reaction are 42 ^{o}C for 15 minutes and the reaction is stopped by a 5 minute cycle at 85 ^{o}C. To increase detection of lowly expressed miRNA targets, the product of the reverse transcription reaction is then amplified in the miR-Amp reaction, with enzyme activation and denaturing at 95 ^{o}C for 5 minutes, and 14 cycles of annealing at 60 ^{o}C before the reaction is stopped by a 10 minute cycle at 99 ^{o}C for 10 minutes. The resulting product is then ready for qPCR reactions.

2.7.3 EvoScript Universal cDNA Master cDNA synthesis.

For the siRNA *PAX6*(5a) knockdown, SH6 AKT pathway inhibition and miRNA pathway target gene validation assays, cDNA synthesis was performed using EvoScript Universal cDNA master (Roche life science, Burgess Hill, UK). Samples were normalised to 100 ng/ µL RNA prior to reverse transcription. Similarly to the VILO kit, this enzyme mix is also thermostable during the high temperature denaturing step. However, the enzyme mix does have RNase activity and therefore the enzyme is added last to avoid digestion of the sample. Cycling conditions were 42 ^{o}C for 30 minutes, 85 ^{o}C for 5 minutes and 65 ^{o}C for 15 minutes.

2.8 Quantitative real-time Polymerase Chain reaction (qRT PCR) assessment of gene expression

The polymerase chain reaction (PCR) is a method for amplifying regions of DNA and utilises a reaction where DNA polymerase copies a DNA template to generate a new DNA strand. To detect gene expression, RNA is extracted from samples and reverse transcription is used to synthesize cDNA. An oligonucleotide probe, designed against the region of interest, hybridises to the cDNA and initiates a reaction that allows the DNA polymerase enzyme to add nucleotides. Reaction mixtures incorporate dNTPs, a buffer solution and $MgCl_2$, which acts as a cofactor for the Taq polymerase enzyme. It is necessary for the removal of the phosphate from dNTPs, breaking them down to dNMPs and the formation of a phosphodiester bond between the 3' OH of the adjacent nucleotide and the 5' phosphate of the next nucleotide. Adjusting the concentration of $MgCl_2$ is therefore important to primer annealing as increased concentrations improve annealing but at the risk of reducing specificity.

Cycling temperature changes facilitate the exponential reaction and amplification of the cDNA. High temperatures at the beginning of the reaction denature the double stranded cDNA molecule before reducing temperature to allow the oligonucleotide probe to anneal to the template and extension of the primer sequence. At each cycle the PCR reaction increases the number of template copies exponentially until there are either insufficient reagents and template or accumulation of phosphates and primer-dimerisation, which causes the reaction to enter the stationary phase. Quantitative PCR (qPCR) allows for the determination of the amount of starting template during the exponential phase.

Real time q-PCR (RT-PCR) allows quantification to be determined at each cycle of the reaction.

Taqman chemistry uses an oligonucleotide probe which contains a fluorescent fluorophore reporter, FAM™, at the 5' end and a quencher fluorophore at the 3' end. In this state the quencher fluorophore is sufficiently close to the FAM™ fluorophore that no fluorescence can be detected. Once the reaction is initiated, the Taq polymerase, which has 5' activity, digests the oligonucleotide probe and, at completion of the cDNA replication, it cleaves the quencher from the 3' end. This allows fluorescence from the FAM™ reporter to be emitted so that it can be detected. This chemistry allows calculation of the cycle at which fluorescence exceeds the baseline threshold, which will be discussed in more detail below.

Here, we measured gene expression levels by quantitative real-time PCR. Endogenous control genes were *PPIA, UBC, HPRT1, GUSB, B2M* and *IDH3B.* Reaction mix included 2.5 µL Taqman® Universal PCR mastermix II (no AmpErase® UNG) (Thermo Fisher, Waltham, MA, USA), 1.75 µL dH_2O, 0.5 µL cDNA and 0.25 µL Taqman® gene assay (Thermo Fisher, Waltham, MA, USA) in a 5 µL reaction volume. The reaction mixes were spun, vortexed and re-spun at 3000 rpm to ensure reagents were well mixed before being added to a 384 well qRT-PCR plate. Cycling conditions were: 50 °C for 2 min, 95 °C for 10 min and 50 cycles of 15 seconds at 95°C for 30 s and 1 minute at 60°C. Reactions were carried out in 3 biological replicates and 3 technical replicates. Expression levels were normalised to the median level of expression seen in unstimulated EndoC-βH1 cell controls. Using the $\Delta\Delta Ct$ method for relative quantification, described below, differences in gene expression levels between EndoC-βH1 cells subjected

to each separate diabetogenic stimulus were compared to the same time point controls for each assay and investigated by student independent t-test carried out using SPSS version 23 (IBM, North Castle, NY, USA). Data were presented as means ± S.E.M.

2.8.1 Relative Quantification

There are a number of different approaches to determining gene expression. Of these, relative quantification[240, 241], which is expressed as fold change, can be performed either by the $\Delta\Delta Ct$ method, the Pfaffl method or the sigmoidal curve fitting method[240]. The Pfaffl approach is particularly useful for when primer sets have different efficiencies as this uses standard curves and corrects for differences in efficiencies[242]. Relative expression is calculated from the amplification efficiencies and the crossing point of an unknown sample versus a control[242]. The sigmoidal curve fitting approach also precludes the need to know amplification efficiencies and is therefore useful for analysing high throughput data. It uses mathematical modelling of amplification reactions to assess relative quantification[243, 244]. For all of the gene expression and miRNA expression assays in this study, the relative expression of each test transcript was calculated by the $\Delta\Delta Ct$ comparative Ct method[240, 241]. This method uses the Ct value, which is the PCR cycle at which fluorescence goes above the background threshold. Although this approach is easy to use, it assumes that the transcript amplification efficiency is 100%. To address this issue, Taqman and IDT gene expression assays were used in this study as they have been validated at essentially 100% efficiency. For determination of threshold, background fluorescence threshold values are set at 10 standard deviations above the baseline fluorescence.

Replication is exponential and lower Ct values equate to higher levels of cDNA. Expression was assessed relative to global mean of each test transcript, or miRNA, and normalized back to the median level of expression of each individual transcript.

2.8.3 Other Statistical approaches

Data was log transformed to ensure normal distribution. and was analysed using SPSS version 23 (IBM, North Castle, NY, USA). However normality tests, such as Kolmogorov-Smirnov and Shapiro-Wilks which compare the sample values to a set of normally distributed values, were not applied due to the unreliable nature of such tests in small sample sizes or where there is large variation[245]. Data were presented as *p* value and mean difference. ANOVA tests were used for analysis. This compares the means between two independent groups against the same dependent variable to see if there is a statistically significant difference between the two groups. It can be used to determine the difference in means between treatments and controls and was selected for this purpose by this study. A Bonferroni correction was applied to take into account multiple testing to ensure no reporting of false positives, or type one errors. The Bonferroni correction accounts for the problem of high numbers of tests increasing the likelihood that the *p* value might be due to pure chance. It divides the standard $p = 0.05$ value by the number of tests applied. However, as this correction can increase the risk of a type two error, failing to reject the null hypothesis, standard $p = 0.05$ values have been reported. It has been clearly stated throughout where a Bonferroni correction has been applied and the number of multiple tests that have been considered.

2.9 Splicing factor expression

Splicing factor expression was quantified using using Taqman® Low Density Array (TLDA). This method allows the quantification of gene expression for multiple genes on one array. TLDA plates comprise 384 wells that are connected by microfluidic channels and which contain the gene expression assays and each plate accommodates 8 samples. The reaction mixes included 50 µL Taqman® Fast Universal PCR Mastermix (Life Technologies, Foster City, USA), 30 µL dH2O and 20 µL cDNA template. The 100 µL reaction mixture was dispensed into the TLDA card chamber and centrifuged twice, for 1 min, at 1000 rpm to ensure correct distribution of solution to each well and removal of bubbles. Cycling conditions were 1 cycle each of 50 °C for 2 min, 94.5 °C for 10 min and then 40 cycles of 97 °C for 30 s and 57.9 °C for 1 min. Expression was again assessed by the Comparative Ct approach, relative to the *IDH3B*, *GUSB* and *PPIA* endogenous control genes, selected on the basis of empirical evidence for stability in beta cells. Changes in expression were expressed relative to the level of splicing factor expression in the control cells.

2.10 Modification of gene expression using and siRNA to knock down the expression of *PAX6* isoform, *PAX6(5a)*.

To investigate whether the *PAX6(5a)* isoform of the *PAX6* gene was important for changes in beta cell differentiation status during cell stress, a custom select siRNA was designed (assay ID 1THO, Thermo Fisher, Waltham, MA, USA). Effective candidate sequences were selected using siDIRECT2. Cells were cultured in 1 mL penicillin and streptomycin free culture media with 250 µL from

a master mix of siRNA containing 300 µL Optim-MEM® (Life Technologies, Foster City, USA) , 9 µL Lipofectamine® (Life Technologies, Foster City, USA) and 3 µL siRNA at 10 µM, made up according to the manufacturer's instructions. Cells were cultured for 72 hrs prior to the administration of siRNA and were then incubated for a further 48 hours. At this point RNA was harvested using the protocol previously described. Reverse transcription and qPCR was performed to ascertain whether the *PAX6(5a)* knock down was successful. Following siRNA validation, cells were cultured in 24 well plates for 72 hrs before the addition of the siRNA mastermix at the concentration specified in the manufacturer's protocol. The siRNA was incubated for 48 hrs, before treating relevant wells with 25 mM glucose for 24 hrs. After treatment cells were fixed with 4% paraformaldehyde for 15 minutes at 4ºC.

2.11 High throughput global microRNA screen by open array

The Taqman® open arrays have 3072 reactions on each plate and up to 4 plates can be run at once, allowing for high throughput expression profiling. Each plate contains 48 subarrays with 64 x 300 µM holes. The holes are 300 µM deep and are treated with hydrophilic and hydrophobic coatings. which retain the reaction mix due to surface tension. The reaction mix is loaded into the plates by robot and the plate immediately sealed with a mineral oil-like material to prevent evaporation of the very small volumes. Here we used inventoried Taqman® Advanced microRNA (miRNAs) open arrays, containing 757 miRNA targets, to investigate all diabetic microenvironment treatment conditions and selection of miRNAs for further study, please refer to supplementary table S11 for assay IDs.

The resulting data was analysed using Thermo Fisher cloud software to identify the ten most altered miRNAs, across all assays, for pathways analysis.

2.11.1 miRNA enrichment analysis

To assess what the likely pathway and gene targets were for miRNAs found to be dysregulated in response to the cellular stress assays, we used the DNA intelligent analysis (DIANA) mirPath v3.0 database and the DIANA-micro-T-CDS v 5.0 algorithm[246, 247]. The DIANA mirPath database focuses on the identification of miRNA targeted cell pathways and operates by allowing the selection of single or multiple miRNAs[246, 247]. The algorithm then performs gene set enrichment analysis (GSEA) using a Fisher's exact test to determine the statistical significance of microRNA gene targets in KEGG pathways[246, 247]. Following identification of the significant pathways from the multiple miRNA effect analysis, it is then possible to access DIANA microT-CDS entries to determine which target genes within those pathways are predicted by this pattern of altered miRNA expression[248]. Each gene has an MITG score which predicts the probability of the microRNA targeting that gene[248]. Here, we used this platform to carry out GSEA using miRNAs differentially regulated across several treatment regimes to determine whether any were overrepresented in gene ontology or functional category pathways derived from KEGG. The *p* value was set to 0.050 and MicroT threshold to 0.8.

2.11.2 Validation of dysregulated miRNAs

miRs selected from the large-scale analysis were validated by qRT PCR using Taqman® advanced miRNA assays (Thermo Fisher, Waltham, MA USA). Three miRNAs (miRNA 106b-3p, miR-191-3p and miR103-3p) were empirically selected from the large dataset for stability in response to treatment for use as endogenous control genes. qRT PCR reaction mixes included 2.5 µL Taqman® Universal PCR mastermix II (no AmpErase® UNG) (Thermo Fisher, Waltham, MA, USA), 1.75 µL dH_2O, 0.5 µL cDNA and 0.25 µL Taqman® gene assay (Thermo Fisher, Foster City USA) in a 5 µL reaction volume. Cycling conditions were: 50 °C for 2 min, 95 °C for 10 min and 50 cycles of 15 seconds at 95 °C for 30 s and 1 minute at 60 °C. Reactions were carried out in 3 biological replicates and 3 technical replicates. MicroRNA assay Identifiers are given in table 5. The relative expression of each was determined by the comparative Ct approach. Expression levels were calculated relative to the geometric mean of the empirically-determined endogenous control genes, but also to the global mean of expression across all transcripts tested which provided a robust baseline. Expression levels were then normalised to the median level of expression seen in untreated EndoC-βH1 cell controls. Differences in gene expression levels between mock-treated and treated EndoC-βH1 cells were compared to the same time point controls for each condition and investigated for statistical significance by student independent t-test carried out using SPSS version 23 (IBM, North Castle, NY, USA). Data were presented as means ± S.E.M.

Table 5 MicroRNA assay IDs for most altered miRs selected from large global screen.

Assay name	Assay ID	Assay name	Assay ID
hsa-miR-576-5p	478165_mir	hsa-miR-148b-5p	478719_mir
hsa-miR-376a-3p	478240_mir	hsa-miR-454-5p	478919_mir
hsa-miR-9-5p	478214_mir	hsa-miR-30c-2-3p	479401_mir
hsa-miR-101-3p	477863_mir	hsa-miR-27b-3p	478270_mir
hsa-miR-365a-3p	478065_mir	hsa-miR-186-3p	479544_mir
hsa-miR-202-5p	478755_mir	hsa-miR-34a-5p	478048_mir
hsa-miR-34a-5p	478048_mir	hsa-miR-195-3p	478744_mir
hsa-miR-93-5p	478210_mir	hsa-miR-593-5p	479077_mir
hsa-miR-23a-3p	478532_mir	hsa-miR-106b-3p	477866_mir
hsa-miR-34b-3p	478049_mir	hsa-miR-577	479057_mir
hsa-miR-34c-5p	478052_mir	hsa-miR-299-5p	478793_mir
hsa-miR-30c-1-3p	479412_mir	hsa-miR-199a-3p	477961_mir
hsa-miR-27a-3p	478384_mir	hsa-miR-99a-3p	479224_mir
hsa-miR-92b-5p	479207_mir	hsa-miR-124-3p	477879_mir
hsa-miR-30a-5p	479448_mir	hsa-miR-29a-3p	478587_mir
hsa-miR-185-3p	478732_mir	hsa-miR-136-5p	478307_mir
hsa-miR-885-5p	478207_mir	hsa-miR-152-3p	477921_mir
hsa-miR-374b-3p	479421_mir	hsa-miR-21-3p	477973_mir

2.11.3 Validation of miRNA target gene mRNA levels

Target genes for validation were based on the MITG scores from the DIANA-microT-CDS v5.0 algorithm, table 6. A panel of 10 miRNAs were selected on the basis of highest MITG score, most statistically significant *p* value, number of genes predicted and number of miRNAs targeting the top 5 pathways; Lysine degradation, FOXO signalling pathway, HIPPO signalling pathway, TGFβ - estrogen signalling and Pathways in Cancer. MITG score is the predictive score, where the higher the score the higher the target probability[248].

The expression levels of predicted target genes was measured using quantitative RT-PCR performed using IDT mini primetime™ gene expression assays (Integrated DNA Technologies, Skokie, Illinois, USA) as detailed in table 6. Reactions were run in triplicate on 384 well plates, using one assay per plate containing all samples. Each reaction included 2.5 µL Taqman® Universal PCR mastermix II (no AmpErase® UNG) (Thermo Fisher, Waltham, MA, USA), 1.75 µL dH_2O, 0.5 µL cDNA and 0.25 µL Taqman® gene assay (Thermo Fisher, Foster City USA) in a 5 µL reaction volume. Cycling conditions were: 50 °C for 2 min, 95 °C for 10 min and 50 cycles of 15 seconds at 95 °C for 30 s and 1 minute at 60 °C. Associations between miRNA and mRNA target expression were assessed using independent t-tests carried out using SPSS v23 (IBM, North Castle, NY, USA).

Table 6 Targets from DIANA pathways analysis.

Genes selected from DIANA-microT-CDS v5.0 algorithm based on highest MITG scores, most statistically significant p value, the numbers of genes predicted and number of microRNAs targeting the top 5 pathways.

GENE	**Pathway**	**Pathway *p*-value**	**MITG score**	**ASSAYS**
KMT2C	Lysine degradation	3.00×10^{-3}	0.97/0.92/0.80	All assays
BCL2L11	FOXO	0.02	0.99/ 0.89	Glycaemia and Palmitic acid
DLG2	Hippo	5.84×10^{-5}	0.92/0.81	Glycaemia, Palmitic acid and pro-inflammatory cytokines
SP1	TGFβ and Estrogen	0.02	0.99	Glycaemia and Hypoxia
SOD	FOXO	0.02	0.98	Glycaemia and Palmitic acid
MAPK1	FOXO	0.02	0.9	Glycaemia and Palmitic acid
TEAD1	Hippo	5.84×10^{-5}	0.85	Glycaemia and Hypoxia
SERPINE1	Hippo	5.84×10^{-5}	0.82	Glycaemia
MOB1A	Hippo	5.84×10^{-5}	0.82	Glycaemia
PDK1	Central carbon cancer	3.00×10^{-3}	0.82	Glycaemia and Hypoxia

Chapter 3:

Data chapter.

The species origin of the cellular microenvironment influences markers of beta cell fate and function in EndoC-βH1 cells

3.1 Introduction

Communication between pancreatic beta cells and other endocrine cell types is important for the maintenance of beta cell fate and function[249-251]. Within islets, beta cells interact intimately with the micro-environment, critical for glucose sensing and the regulation of islet cell function[249-251]. The cellular microenvironment of beta cells is also known to influence cell behaviour and survival[65, 66, 68] and can influence aspects of growth morphology, such as cell density, which is vital to beta cell survival as well as influencing differentiation, cell-cell signalling and function[69, 70]. Differences in pancreatic islet architecture, between humans and other species such as rodents, have also been shown to have implications for cell-to-cell crosstalk and beta cell function[19, 20, 199].

Accordingly, several features of beta cell function and behaviour also differ between species. Glucose sensitivity and transport are different between human and rodent beta cells, with the major glucose transporter being GLUT2 (encoded by the solute carrier family 2 member 2 (slc2a2) gene) in rodents and GLUT1 and GLUT3 (encoded by the *SLC2A1* and *SLC2A3* genes) in humans[20, 22, 83, 199]. Proliferation rate and expression of cyclin dependent kinases also vary between rodents and man, as do responses to cellular stress, pancreatic beta cell injury and inflammation[20, 39, 48, 58, 199, 252, 253]. There are also important transcriptomic distinctions between species, with insulin being coded for by one gene (*INS*) in humans but two genes (Ins1 and Ins2) in rodents[84, 85, 182, 183, 199]. Gene expression differences, especially in relation to stress response, are also seen in human beta cells compared with rodent cells, most notably in neurogenin3

(NGN3), NANOG homeobox (*NANOG*), POU class 5 homeobox 1 (*POU5F1* (Oct4)), L-Myc-1 proto oncogene (*MYCL1*), paired box 4 (*PAX4*) and MAF BZIP transcription factor B (*MAFB*) expression[58].

Given the importance of cellular microenvironment to beta cell fate and function, it follows that the nature of the microenvironment may influence these features in *in vitro* culture systems. Model systems to investigate the effect of a non-human cellular microenvironment have been difficult to source until recently since fully functional human beta cell lines have been few and far between. The creation of EndoC-βH1, a human cell line derived from fetal pancreata, has provided a new and physiologically-relevant model system for the investigation of beta cell function *in vitro.*[182, 199, 252] These cells demonstrate stable insulin gene expression across multiple passages and are responsive to glucose[182, 183, 199, 252]. Like many other differentiated cell lines, EndoC-βH1 cells require an extracellular matrix (ECM) coat containing fibronectin and other components such as Fraction V for culture[183]. This requirement allows investigation of the effects of different components of the cellular microenvironment on aspects of beta cell behaviour.

In this work, we have compared the effects of a non-human culture microenvironment with those of a culture system containing only human components on aspects of cell morphology and culture dynamics, beta cell function (insulin content, insulin processing and glucose-stimulated insulin secretion), and on the transcriptional output of genes involved in beta cell differentiation status and beta cell identity. Cells cultured according to these modified protocols grow reliably in pseudo islet-like structures, and can be

propagated for long periods of time without compromise to beta cell survival, function or phenotype. Cells also show evidence of a more consolidated beta cell phenotype at the transcriptional level, with increased expression of mature beta cell markers and decreased expression of markers associated with other islet subtypes. These data highlight the potential advantages of propagating human beta cell lines in a microenvironment more reminiscent of human physiology, when considering aspects of islet biology in experimental systems.

3.2 Methods

3.2.1 Standard culture protocol: non-human microenvironment

Cells were cultured in accordance with the guidelines for EndoC βH1 cells from the manufacturers Endo Cells, INSERM, France. Flasks or plates were coated, at least 6 hours in advance of seeding, with an ECM consisting of DMEM 4.5 g/ L (Thermo Fisher, Waltham, MA USA), matrigel (100 µg/ mL) fibronectin from bovine plasma 2 µg/ mL coat (both from Sigma-Aldrich, Steinheim, Germany). At seeding the ECM coat was replaced with culture medium containing: DMEM 1 g/ L glucose (Thermo Fisher, Waltham, MA, USA) 2% BSA fraction V (Merck Chemicals, Darmstadt, Germany), 10 mM nicotinamide (Sigma-Aldrich, Steinheim, Germany) 50 µM β-2-Mercaptoethanol, 5.5 µg/ mL transferrin, 6.7 ng/ mL sodium selenite, and 100 U/mL penicillin and 100 µg/ mL streptomycin (Sigma Aldrich, Steinheim, Germany).

3.2.2 Human microenvironment

Culture reagents were replaced with human equivalents. Here, flasks were again coated at least 6 hours prior to seeding with coating medium consisting of: Maxgel ECM mixture liquid (Sigma Aldritch, Steinheim, Germany) and fibronectin from human plasma (Sigma-Aldritch, Steinheim, Germany). The ECM was replaced at seeding with a modified culture medium consisting of: DMEM 1 g/ L glucose, (Thermo Fisher Waltham, MA USA), 2% human serum albumin fraction V (Merck Chemicals, Darmstadt, Germany), 100 U/ mL Penicillin and 100 µg/ mL streptomycin, 50 µM β-2-Mercaptoethanol (Sigma- Aldrich, Steinheim, Germany), 10 mM nicotinamide (Sigma Aldritch Steinheim, Germany), 5.5 µg/ mL human transferrin (Sigma Aldritch, Steinheim, Germany) and 6.7 ng/ mL of sodium selenite (Sigma Aldritch, Steinheim, Germany). Cells were passaged using TRYPLE 1x (Thermo Fisher, Waltham, MA, USA) and neutralised with heat inactivated human serum from human male AB plasma (Sigma Aldritch, Steinheim, Germany).

3.2.3 Immunofluorescence characterisation of EndoC-βH1 cells cultured in human microenvironment

Immunofluorescence staining was used to determine expression of mature beta cell markers in EndoC-βH1 cells grown in conditions to mimic a more human microenvironment, compared with cells grown using the standard non-human culture reagent protocol. EndoC-βH1 cells were cultured on coverslips for 72 hrs before fixing with 4% paraformaldehyde for 15 min at 4 °C. Primary antibodies for PDX1 (Abcam Ab47267, rabbit polyclonal) and NEUROD1 (Abcam Ab60704,

mouse monoclonal) were diluted in phosphate buffered saline (PBS) with .1 M Lysine, 10% donor calf serum, .02% sodium azide and .02% Triton (ADST), to permeabilise the cell membranes, at concentrations of 1/500 and 1/400 respectively and incubated overnight. Primary antibodies were visualised using highly cross-absorbed secondary antibodies (Life Technologies) also diluted in ADST at 1/400: goat anti-rabbit for PDX1 at 1/400 (555 nm) and goat anti-mouse for NEUROD1 at 1/400 (555 nm) and incubated for 1 hr. Insulin antibody (80564, LN10088287 Dako) was diluted in ADST at a concentration of 1/700 and incubated for 1 hr. Secondary goat anti guinea-pig insulin along with DAPI (Sigma- Aldritch D9542), were diluted in ADST at respective concentrations of 1/400 and 1 µg/ mL. Slides (n= 3 separate cultures) were visualised using a LEICA DM4000 B-LED fluorescence microscope using LAS X image software.

3.2.4 Assessment of glucose-stimulated insulin secretion

EndoC-βH1 cells were seeded onto 24 well plates at 4 x 10^5 per well and cultured for 72 hrs in separate cultures. Cells were then transferred to a culture medium containing 2.8 mM glucose as a starvation medium and cultured overnight, before being incubated for 1 hr in a starvation medium containing 0.5 mM glucose in HEPES Krebs Ringer Buffer (KRB) at pH 7.4 containing: 116 mM/L NaCl, 5 mM/L KCl, 1 mM/L CaCl2, 1 mM/L MgCl2, 1.2 mM/L KH2PO4, 24 mM/L NaHCO3, 10 mM/L HEPEs, 0.2% Human Serum Albumin (HSA). After 1 hr the 0.5 mM glucose starvation HEPES KRB starvation buffer was removed and replaced with HEPES KRB containing 20 mM glucose and cells incubated for 1 hr. This concentration of glucose was selected as representative of a high glucose environment and from previous documented studies in the literature, including those on EndoC

βH1 cells[182]. Media was removed from each sample (n=10), spun at 1000 g for 5 min to remove protein debris and supernatant harvested for comparison with controls using an ELISA against fully processed human insulin. (Human Insulin ELISA, Crystal Chem, Downers Grove, IL, USA, assay range 0.9 - 220 mU/ L, analytical sensitivity 0.25 mU/ L, precision CV < 10%, 1.2% cross reactivity with pro insulin). Absorbance was measured using a plate reader and measured A450 values, subtracting A630 values.

3.2.5 Candidate genes for expression analysis

As previously described, the panel of target genes were selected for their roles in beta cell fate, maturity and function. Markers of other pancreatic endocrine cell types and also genes associated with cell stress were also included.

3.2.6 Quantitative real-time polymerase chain reaction (qRT PCR) assessment of gene expression

RNA was extracted using the TRI®reagent (Sigma-Aldrich, Steinheim, Germany), chloroform (Thermo Fisher, Waltham, MA, USA) method. Cells were washed in Dulbecco's phosphate buffered saline (D-PBS). TRI® reagent was used to harvest RNA, 10 µL of $MgCl_2$ (Thermo Fisher, Waltham, MA, USA) and 200 µL of Chloroform added. Samples were centrifuged at 14,800 rpm, 4 °C for 20 mins, the clear aqueous layer removed and 500 µL of isopropanol (Thermo Fisher, Waltham, MA, USA) added for overnight precipitation. Samples were centrifuged at 14,800 rpm, 4 °C for 45 min to form RNA pellet. The pellet was then repeatedly washed using 75% molecular grade ethanol (Thermo Fisher,

Waltham, MA, USA), air dried and then re-suspended in 20 µL RNase- free water. cDNA synthesis was carried out using Superscript® VILO™ cDNA synthesis kit (Thermo Fisher, Waltham, MA USA). Samples were normalised to 100 ng/ µL RNA prior to reverse transcription.

We measured the expression levels of 31 target genes by quantitative real-time PCR. Endogenous control genes were *PPIA, UBC, HPRT1, GUSB, B2M* and *IDH3B* Reaction mix included 2.5 µL Taqman® Universal PCR mastermix II (no AmpErase® UNG) (Thermo Fisher, Waltham, MA, USA), 1.75 µL dH2O, 0.5 µL cDNA and 0.25 µL Taqman® gene assay (Thermo Fisher, Waltham, MA, USA) in a 5 µL reaction volume. The reaction mixes were spun, vortexed and re-spun at 3000 rpm to ensure reagents were well mixed before being added to a 384 well qRT-PCR plate. Cycling conditions were: 50 °C for 2 min, 95 °C for 10 min and 50 cycles of 15 s at 95 °C for 30 s and 1 min at 60 °C.

Reactions were carried out in 3 biological replicates and 3 technical replicates. The relative expression of each test transcript was calculated by the comparative Ct technique which was used to calculate the expression of each test transcript. Expression was assessed relative to the global mean of expression across all transcripts which was empirically determined not to vary across test conditions. Expression levels were normalised to expression levels as seen in unstimulated EndoC-βH1 cells cultured in a non-human microenvironment. The data were log transformed to ensure normal distribution and differences in gene expression levels were then investigated by student independent t-test carried out using SPSS version 23 (IBM, North Castle, NY, USA). Data were presented as means ± S.E.M.

3.3 Results

3.3.1 EndoC-βH1 cells show morphological changes when cultured in a more 'human-like' microenvironment

EndoC-βH1 cells cultured in a cellular microenvironment containing only human components showed no observational change in replication rate compared with cultures grown according to standard protocols, and this remained stable over eight passages. Population doubling (PD) showed no differences between culture methodologies (p = 0.975, mean difference 0.023). Culture in human reagents showed population doubling values of (mean PD = 18.98 hrs, n = 3) while those cultured using non-human reagents had values of (mean PD = 19.0 hrs, n = 3). The cells showed an increased tendency to form three-dimensional structures resembling pseudo-islets under human culture conditions, which were visible under fluorescence microscopy, whereas cells cultured in a non-human microenvironment, grew as a flat confluent monolayer (Figure. 8, images C and D). EndoC-βH1 cells grown in the 'human' microenvironment, analysed and quantified, appeared smaller and more rounded compared with cells grown in a non-human microenvironment; the median area in μM for cells cultured in non-human reagents was 81.2 μM compared with 77.6 μM for cells in human reagents, although this was not quite statistically significant (p = .070). However, despite this difference in area, there was no increased evidence of nuclear blebbing when cells were visualised using a nuclear dye (Figure 8). Nuclear size is considered to be linked to cell function and integrity[254], with cell cycle progression potentially dependent upon changes in the ratio between cytoplasmic and nuclear volume[255]. Levels of transcription also correlate with

increased nuclear size and larger nuclei can also indicate the loss of nuclear lamina structural integrity[254]. Such findings may therefore be an indication of altered cell function.

Figure 8 Culture morphology and pseudo islet structure of EndoC-βH1 cells grown in different species microenvironments.

1) *Morphological differences between EndoC-βH1 cells grown in a human microenvironment compared with the same cells grown in a non-human microenvironment. A. Cells cultured in human derived culture reagents. B. Cells cultured in non-human derived culture reagents. C. DAPI nuclear stain in blue cells cultured in human derived reagents. No increase in nuclear blebbing. D. DAPI nuclear stain. Cells cultured in non-human derived reagents. No increase in nuclear blebbing.*

2) *Bar graph showing number of pseudoislet structures. Cells cultured in human reagents showed significantly increased tendency to form three dimensional structures resembling beta cell only pseudo islets (p = 0.0005). Those cultured in non-human reagents form a confluent monolayer (p=0.004).*

1

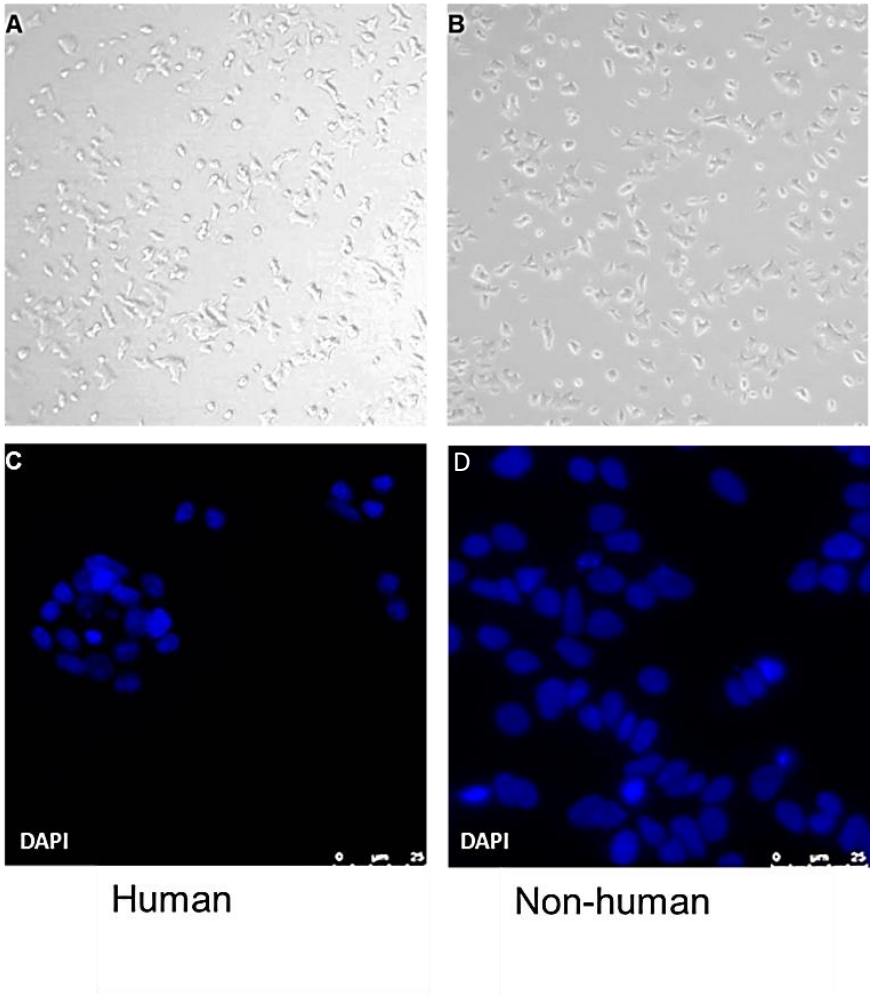

2

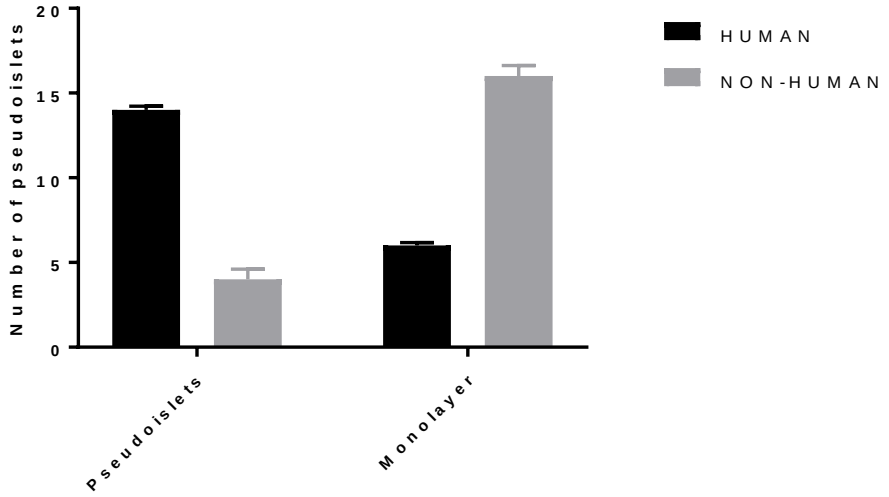

3.3.2 EndoC-βH1 cells cultured in a more human microenvironment demonstrate no alteration in insulin secretion, insulin processing or protein expression of mature beta cell markers

We measured insulin secretion, insulin processing and expression of the mature beta cell proteins Pdx-1 and NeuroD1 in EndoC-βH1 cells cultured in a human-like microenvironment by immunofluorescence (IF). EndoC-βH1 cells stained positively with antibodies against both insulin and pro-insulin, suggesting that they contain both pro-insulin and processed 'free' insulin, and there was no discernible difference in localisation or intensity of the insulin or pro-insulin staining between the two conditions (Figure 9). However, no area measurement was taken for proinsulin and therefore ratios have been based solely upon cell positivity. EndoC-βH1 cells cultured in both systems were also assessed for expression of the mature beta cell markers NeuroD1 (p = 0.335; mean difference − 2.72, standard error 2.79; Figure 10) and Pdx-1 (p = .164, mean difference 3.91, standard error 2.76; Figure 10). No difference in the level of protein

expression of either marker was identified in EndoC-βH1 cells cultured using either methodology.

Figure 9 Proinsulin and insulin expression in EndoC-βH1 cells grown in human vs non-human microenvironments.

1A–1D: *EndoC-βH1 cells cultured in human reagents (n = 6). 1A. DAPI stain. 1B. Proinsulin stain. 1C. Insulin Stain. 1D. Overlay image of 1A-C showing co-localisation of proinsulin with insulin as well as 'free' processed insulin indicating proper insulin processing in the cells cultured in human derived reagents.*

2A-D: *EndoC-βH1 cells cultured in non-human reagents (n = 6) 2A. DAPI stain. 2B. Pro-insulin stain. 2C. Insulin stain. 2D Overlay image of 2A-C showing co-localisation of proinsulin with insulin as well as 'free' processed insulin indicating proper insulin processing in the cells cultured in non-human reagents. This experiment was carried out in 6 replicates.*

3 *Bar graph showing number of cells expressing proinsulin, free insulin and colocalised proinsulin and insulin compared to total cell counts from 5 representative images.*

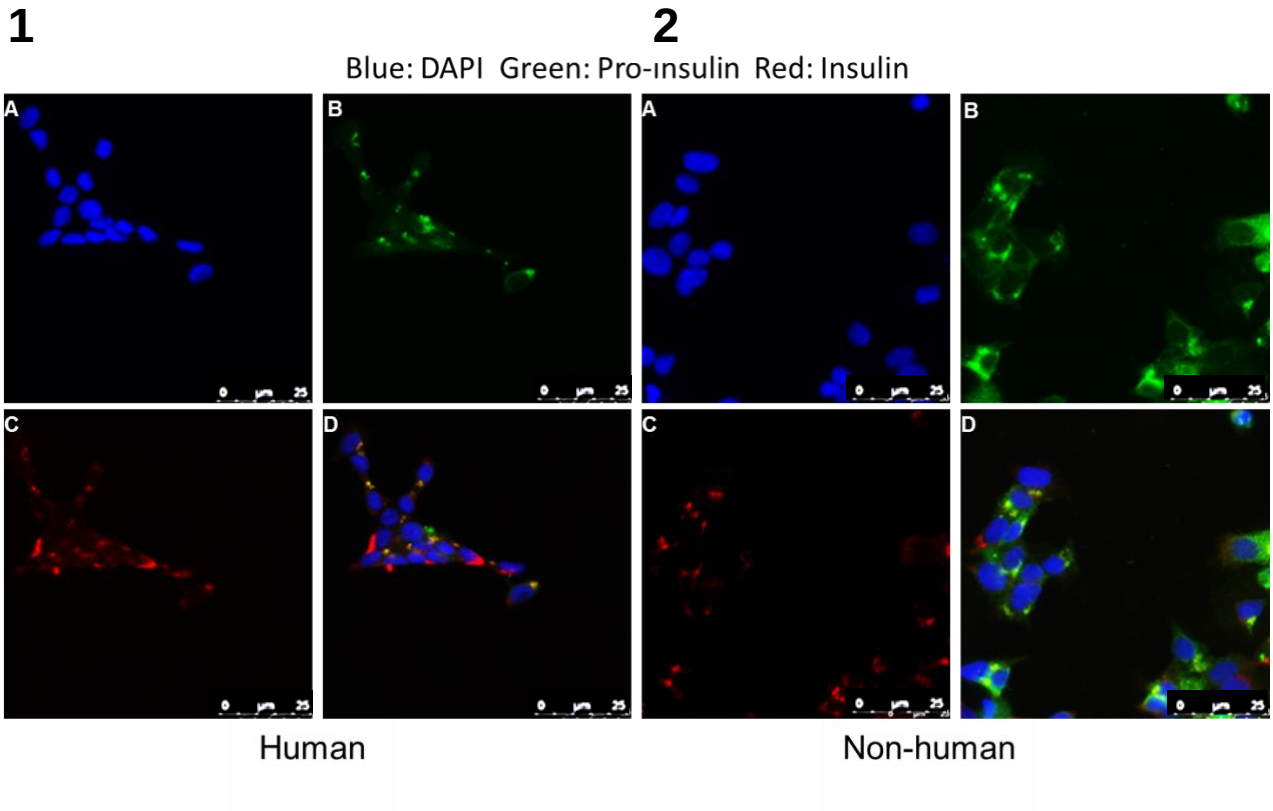

3

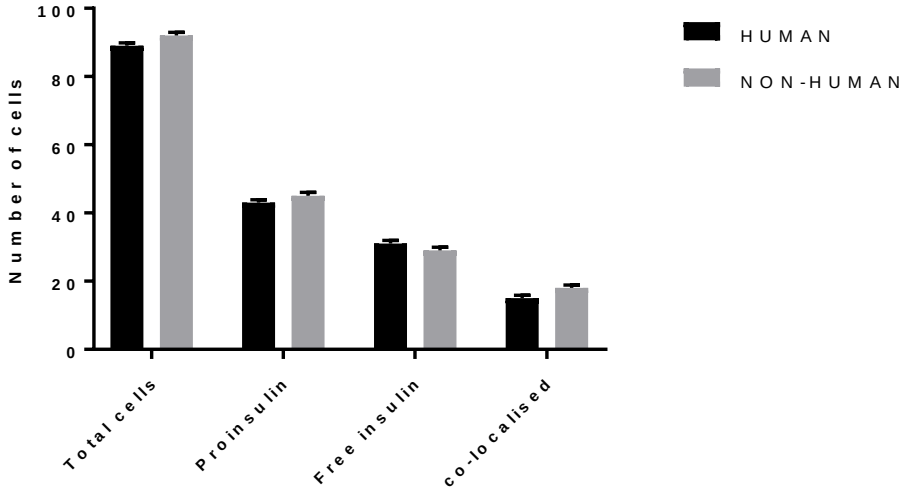

Figure 10 NEUROD1 and PDX1 expression in EndoC-βH1 cells grown in different species microenvironments.

1 A-D: *EndoC-βH1 cells cultured in human reagents (n = 6). 1A. DAPI stain. 1B NEUROD1 stain. 1C. Insulin Stain. 1D. Overlay image of 1A-C showing co-localisation of NEUROD1 with DAPI.* ***2 A-D****. EndoC-βH1 cells cultured in non-human reagents (n = 6). 2A. DAPI stain. 2B. NEUROD1 stain. 2C. Insulin stain. 2D Overlay image of 2A-C showing co-localisation of NEUROD1 with DAPI.*

3 E-H*: EndoC-βH1 cells cultured in human reagents (n = 6). 1E. DAPI stain. 1F PDX1 stain. 1G. Insulin Stain. 1H. Overlay image of 1E-G showing co-localisation of PDX1 with DAPI.****4 E-H****. EndoC-βH1 cells cultured in non-human reagents (n= 6). 2E. DAPI stain. 2F. PDX1 stain. 2G. Insulin stain. 2H Overlay image of 2E-G showing co-localisation of PDX1 with DAPI.*

5 *Bar graph showing the number of NEUROD1 and PDX1 positive cells from cells cultured in both human and non-human culture conditions.*

Blue: DAPI Green A-D: NEUROD1 Green E-H: PDX1 Red: Insulin

1 **HUMAN A-D: NEUROD1**

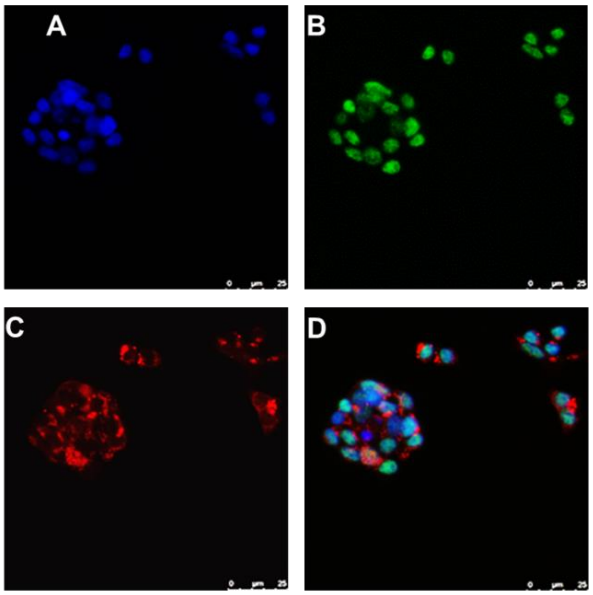

2 **NON-HUMAN A-D: NEUROD1**

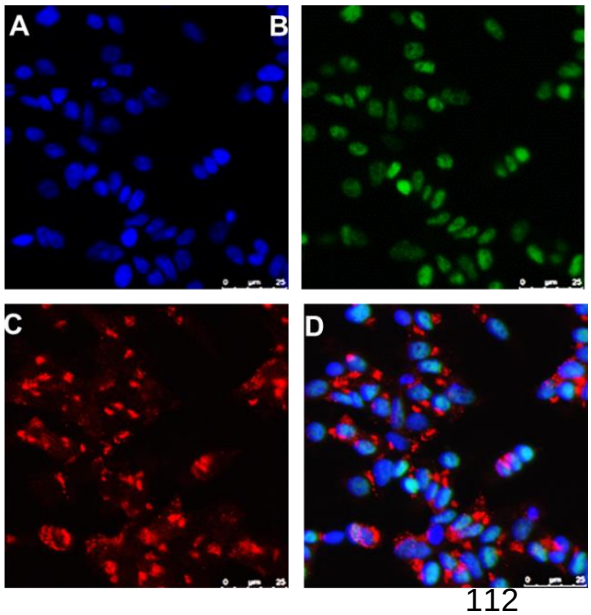

Blue: DAPI Green A-D: NEUROD1 Green E-H: PDX1 Red: Insulin

3 **HUMAN E-H: PDX1**

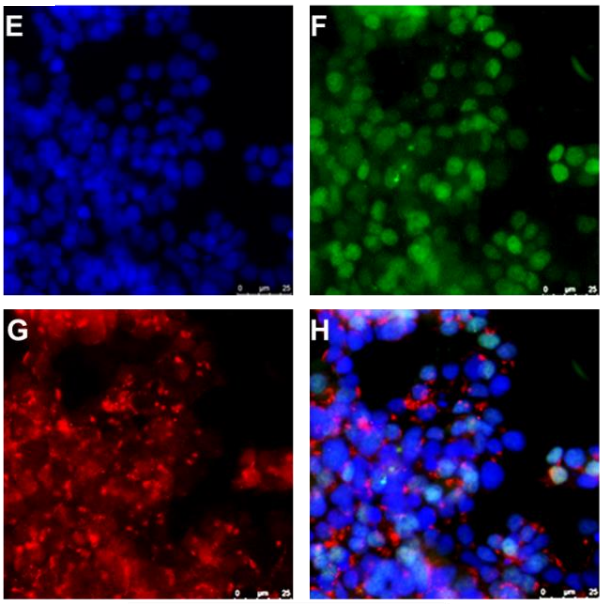

4 **NON-HUMAN E-H: PDX1**

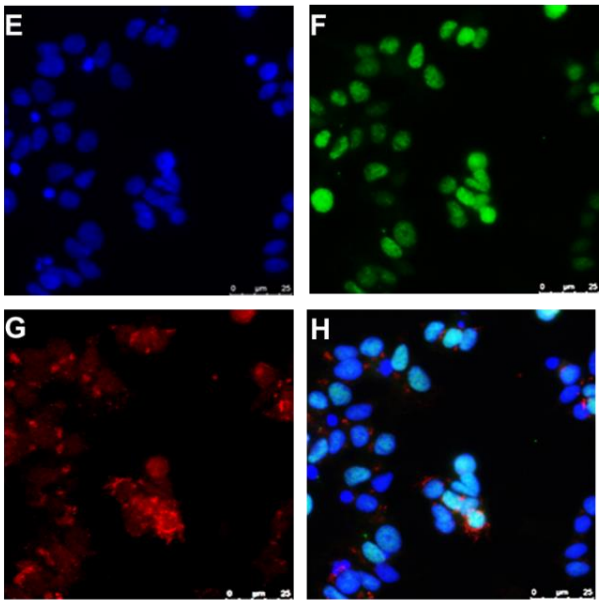

5

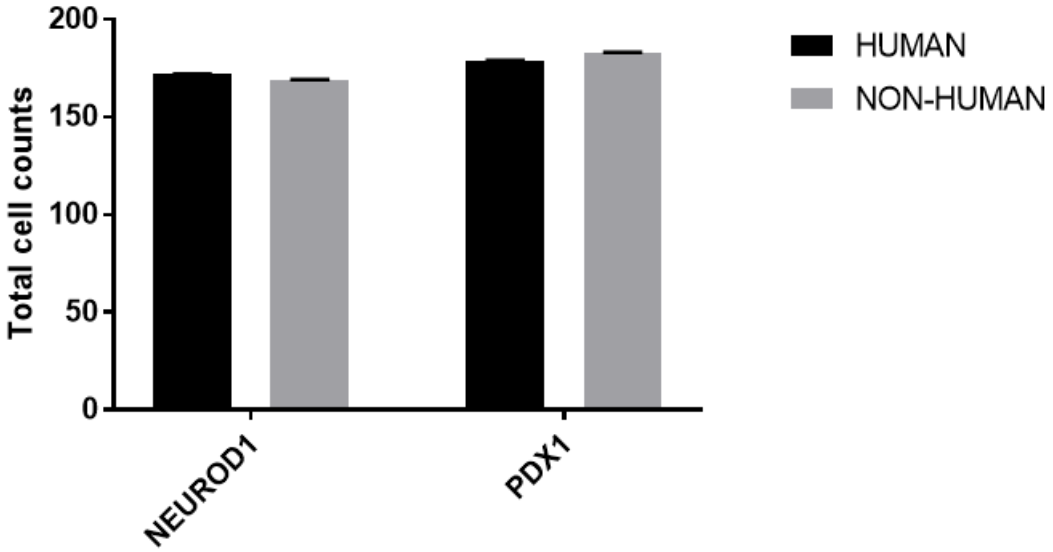

3.3.3 EndoC-βH1 cells cultured in a more human microenvironment exhibit enhanced glucose stimulated insulin secretion (GSIS) compared with those cultured in a non-human microenvironment

We assessed basal insulin release and glucose-stimulated insulin secretion (GSIS) in cells cultured in non-human or human-like microenvironments by ELISA. Cells cultured in a non-human microenvironment stimulated with 20 mM glucose showed a doubling in insulin secretion compared to unstimulated controls which reproduces results found by Anderson et al. (0.13–0.24, n = 10, *p* = 0.047; SD = 0.015; Figure 11A).[19] However, we used a Bonferonni correction to take into account multiple testing and under these conditions (*p* = < 0.016) the cells cultured in a non-human environment did not show a statistically significant increase in insulin secretion following glucose stimulation. In contrast, the cells cultured in a human-like microenvironment showed a much stronger response, demonstrating a 4-fold increase in insulin secretion compared to unstimulated cells following glucose stimulation (0.11–0.47 *p* = 0.006; SD = 0.03; Figure 11A). A significant difference in insulin release in glucose-stimulated cells cultured in a human microenvironment (0.471 mU/ L) was detected compared with those cultured in a non-human microenvironment (0.239 mU/ L; *p* = 0.0003).

Figure 11 (A) Assessment of glucose stimulated insulin secretion and insulin content in EndoC-βH1 cells grown in different species microenvironments. (B) Change in gene expression in EndoC-βH1 cells grown in different species microenvironments.

A

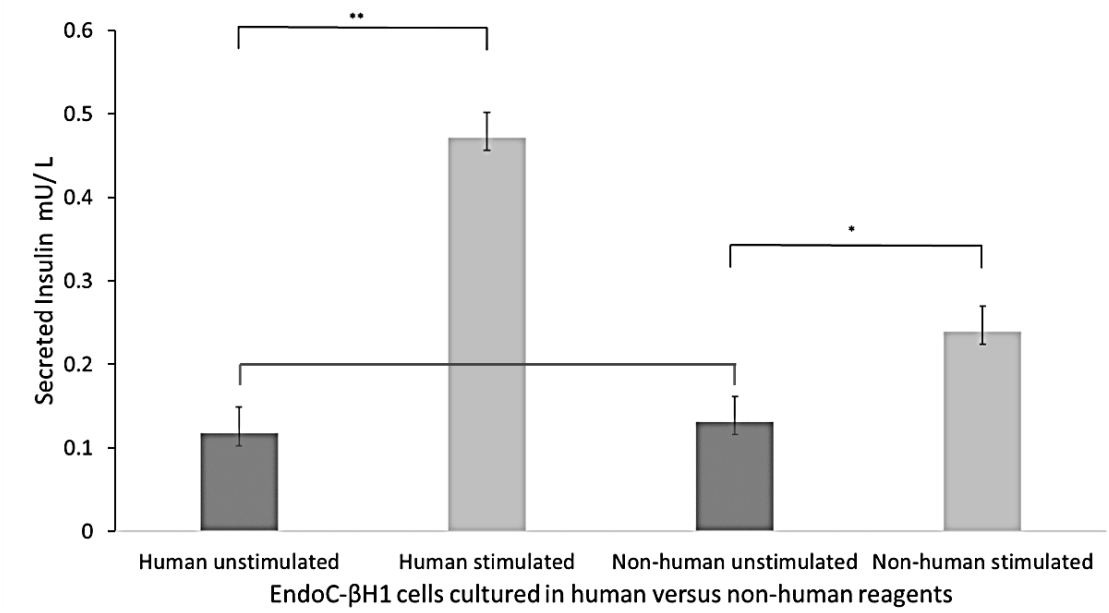

B

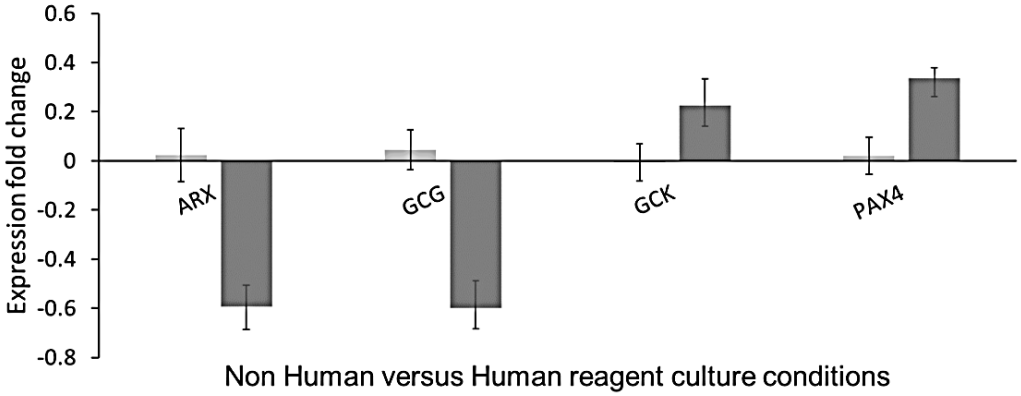

3.3.4 EndoC-βH1 cells cultured in human reagents have an increase in key genes involved in beta cell fate

We compared the expression of a panel of candidate genes involved in beta cell function or maintenance of beta cell differentiation status in EndoC-βH1 cells cultured in a more human microenvironment compared with those cultured in a non-human microenvironment. The genes assessed are described in Table 7. Although overall there was little difference in the gene expression profile between the two different culture methodologies, we did identify some changes in genes relating to alpha cell-like phenotypes. We identified a decrease in the alpha cell marker aristaless related homeobox (*ARX*) in a human-like microenvironment compared with cells cultured in a non-human microenvironment; (mean difference − 0.623, standard error 0.072, p =0.003; Figure 11B). Expression of transcripts encoding glucagon (GCG) showed lower expression in EndoC-βH1 cells cultured in a more human microenvironment compared with cells cultured in a non-human microenvironment (RQ mean difference − 0.577, standard error 0.064, *p*= 0.001; Figure 11B). There was a concomitant increase in PAX4 expression in a human-like microenvironment compared with in cells cultured in a non-human microenvironment (mean difference 0.349, standard error 0.092, *p* = 0.032; Figure 11B). Finally, we noted an increase in the expression of transcripts encoding the pancreatic glucose sensor glucokinase (GCK); mean expression in cells cultured in a human micro- environment when compared with cells cultured in a non-human microenvironment; (mean difference, 0.244, standard error 0.070 *p* = 0.028; Figure 11B).

Table 7 Expression of genes involved in beta cell differentiation, fate or function in EndoC ßH1 cells cultured in human versus non-human microenvironments.

SE = standard error, 95% CI = 95% Confidence Intervals. Genes showing expression differences in cells grown in 'human' or 'non-human' microenvironments are indicated in bold italic type.

t-test for equality of means					
Gene	***p* value**	**Mean diff.**	**SED**	**95% CI**	
				lower	**upper**
ARNT	0.406	0.098	0.104	-0.203	0.399
ARX	**0.003**	**0.624**	**0.072**	**0.400**	**0.847**
DDIT3	0.795	0.031	0.107	-0.358	0.419
FOXO1	0.540	-0.145	0.213	-0.783	0.493
GCG	**0.001**	**0.578**	**0.065**	**0.398**	**0.757**
GCK	**0.028**	**-0.244**	**0.071**	**-0.445**	**-0.043**
HES1	0.192	0.166	0.096	-0.159	0.491
HIF1A	0.241	0.124	0.088	-0.136	0.384
INS	0.107	0.193	0.093	-0.067	0.453
LDHA	0.173	0.134	0.080	-0.093	0.362
MAFA	0.960	-0.011	0.205	-0.580	0.558
MAFB	0.462	-0.124	0.152	-0.554	0.306
MYC	0.930	0.019	0.193	-0.790	0.828
NANOG	0.238	-0.149	0.107	-0.448	0.149
NEUROD1	0.221	-0.190	0.131	-0.555	0.174
NKX2-2	0.575	-0.083	0.135	-0.464	0.298
NKX6-1	0.870	-0.031	0.180	-0.532	0.469
PAX6	0.056	-0.250	0.093	-0.510	0.010
PAX4	**0.032**	**-0.349**	**0.093**	**-0.643**	**-0.055**
PDX1	0.605	-0.089	0.158	-0.533	0.356
POU5F1	0.079	-0.127	0.052	-0.279	0.025
PTPN1	0.244	0.104	0.071	-0.130	0.337
SLC16A1	0.285	0.139	0.109	-0.190	0.468
SLC2A2	0.936	0.010	0.113	-0.338	0.358
SLC2A4	0.385	0.132	0.124	-0.343	0.608
SOX9	0.090	0.346	0.129	-0.111	0.802
SST	0.275	-0.426	0.337	-1.362	0.510
STK11	0.176	-0.060	0.036	-0.163	0.043
SYP	0.339	0.111	0.091	-0.253	0.475

3.4 Discussion

Beta cells are known to interact with their immediate extracellular microenvironment, and cell-cell communication has been shown to be important for regulation of beta cell function and cell identity[249-251]. There are major differences between rodent and human beta cells in relation to cellular signalling, glucose transport and transcriptomic output, which have consequences for beta cell fate and beta cell function[19, 22, 83, 85]. It follows, therefore, that the composition of the cellular microenvironment may influence studies of beta cell biology in human cells *in vitro*. Here, we assess differences in beta cell growth, glucose sensitivity and the expression of genes associated with beta cell function or differentiation in the human beta cell line EndoC-βH1 cultured in human and non-human cellular microenvironments. We demonstrate that EndoC-βH1 cells demonstrate altered cellular morphology and enhanced response to glucose when cultured in a more human microenvironment. However, it is acknowledged that the data presented here represents only measurements of insulin, with first and second phase insulin release combined, and no other functional measurements, such as calcium imaging and electrophysiology, were performed. These features are accompanied by changes in the expression of genes associated with beta cell differentiation or beta cell function consistent with a more consolidated beta cell phenotype.

The cellular microenvironment is known to influence cell fate and differentiation status for many types of cells[256-259]. Fibronectin, in particular, is known to mediate mesodermal cell fate decisions[260]. The extracellular matrix has particular importance in determining the functionality and survival of pancreatic

beta cells[249-251]. Species differences in characteristics of extracellular matrix have previously been reported in relation to extracellular matrix components[261]. Given these observations, it is perhaps unsurprising that cells may behave differently when cultured in cellular microenvironments derived from different species. The increased tendency of the cells to form beta cell only pseudo islet structures when cultured in human derived reagents may improve cell-cell communication and previous studies have shown its importance for insulin secretion in islets[262, 263]. Whilst basal insulin secretion was similar in EndoC-βH1 cells cultured in human and non-human cellular microenvironments, cells maintained in a more human-like microenvironment demonstrated an enhanced response to glucose in terms of combined first and second phase insulin secretion. Human beta cell lines typically exhibit 2–3 fold increases in insulin secretion in response to a glucose stimulus, representing a release of approximately 10% of their insulin content[46, 182, 264] and our results are consistent with this. Since the cells were seeded at the same density and have equivalent PD times, it is not thought that the differences in insulin secretion were caused by differences in cell numbers in culture. Our data suggest that the glucose sensing and secretion machinery remains intact in EndoC-βH1 cells cultured according to our protocols, and that these responses may perhaps be more physiologically representative of primary human beta cells when these cells are cultured in a more human microenvironment. We also assessed the effects of human and non-human cellular microenvironments on the expression of genes involved in beta cell function or beta cell identity in EndoC-βH1 cells. Although we saw little change in expression levels of the majority of genes expressed, changes in markers of alpha cell function (*GCG, ARX,* which were down-regulated) and some genes involved in maintenance of beta cell state (*PAX4*,

which was upregulated) were noted. This finding is consistent with models in the literature which describe a regulatory feedback axis between *ARX* and *PAX4,* where the latter downregulates *ARX* expression to maintain beta cell fate[62, 92, 97, 98]. However, a recent study comparing rodent and human beta cell transcriptomes noted that in the mice, while Pax4 is required for Arx repression, it was undetectable in mature mouse beta cells[265]. Total somatostatin RNA levels were lower in cells cultured in human reagents, but this did not reach statistical significance (Table 7). This is consistent with a more consolidated beta cell phenotype through repression of delta cell characteristics. We also identified an increase in the expression of glucokinase (*GCK*) transcripts in EndoC-βH1 cells cultured in a more human-like microenvironment. Glucokinase is a metabolic sensor which is involved in the regulated secretion of insulin[266], and is also a MODY gene (MODY subtype 2)[267]. The changes in gene expression that we note in our work are probably not confined to the genes we have tested, and emphasise the importance for transcriptomic studies to be carried out using the most physiologically-relevant model systems[41, 42, 72, 85, 90].

The existence of a human cell model such as EndoC-βH1 is a great advantage for characterising disease in humans, but there are inevitably some limitations. EndoC-βH1 cells have been reported to express some disallowed genes[182]. These are genes which are typically not expressed in human beta cells, due their roles in pyruvate and lactate metabolism, as this is imperative to protect against exercise induced insulin secretion. In primary beta cells the lactate dehydrogenase A (*LDHA*) and solute carrier family 15 member 1 (*SLC16A1*) genes are typically expressed at minimal levels[91]. We identified that regardless of the culture microenvironment, EndoC-βH1 cells express the *LDHA* and

SLC16A1 genes at relatively high levels. *LDHA* and *SLC16A1* code for proteins involved with pyruvate metabolism. They are disallowed in beta cells to prevent both inefficient processing of glycolytic products negatively impacting insulin secretion as well as exercise induced insulin release due to inappropriate pyruvate metabolism[91].

The strengths of this study are the creation of a fully human in vitro model system for the study of beta cell biology in the context of human disease. Although islets remain the gold standard for analysis of human disease, EndoC-βH1 represent a good step forward and offer an acceptable, and tractable, substitute, comparable to newly developed Def-PANC IPSC cell lines. Although the findings of this study show that the use of human derived reagents provides a culture environment which is equivalent to the standard culture methodology for EndoC-βH1 cells, there have been some challenges in developing the new protocol. This was particularly relevant for replacing the non-human ECM with a human equivalent and took some time to optimise. Further there are greater cost implications for sourcing human derived reagents. Despite such limitations, it is clear that the novel culture methodology described here can potentially improve the physiological relevance of the cellular microenvironment and provides a more human-like in vitro model system. We have shown that the species origin of the cellular microenvironment has affects and needs to be considered. Furthermore, our findings suggest that for EndoC-βH1 cells, this improves combined first and second phase GSIS response and potentially consolidates mature beta cell status in this cell line. This study also represents the most comprehensive gene expression profile to date for genes involved with beta cell differentiation status

and function, demonstrating the usefulness of this model for studies of islet function in man.

Chapter 4:

Data Chapter.

Cellular stressors may influence the differentiation status of human beta cells by moderation of alternative splicing patterns.

4.1 Introduction

A reduction in beta cell mass occurs during the progression of Type 2 diabetes (T2D) and has been attributed to net enhancement of the rate of beta cell death[76, 268]. It is increasingly apparent, however, that changes in the differentiation status of beta cells may also be a contributory factor[61, 71]. Studies in mice have described a gradual process of trans-differentiation from beta cells to alpha cells in type 2 diabetes models[47, 269], but dedifferentiation to earlier progenitor cell types has also been reported[71, 86]. Indeed, beta cell to delta cell transdifferentiation in response to immunological stimuli with specific relevance to type 1 diabetes, has also been reported by lineage tracing in mouse islets[270]. Data from human pancreas is scarce, but the limited information available suggests that similar changes in differentiation status may also occur in humans[80, 96] .

Maintenance of beta cell identity is determined by a tightly-regulated transcriptional network, consisting of proteins encoded by the Pancreatic and Duodenal Homeobox 1 (*PDX1*), Forkhead Box O1 (*FOXO1*), NK2 Homeobox 2 (*NKX2-2*), MAF BZIP Transcription Factor A (*MAFA*), NK6 Homeobox 1 (*NKX6-1*) and Paired Box 6 (*PAX6*) genes amongst others. Most of these do not display specific expression in beta cells but are also expressed in other pancreatic islet cell types[181, 271] and their role in cell identity definition is likely to involve the relative balance of expression[47, 107, 272]. Among these, the *FOXO1* gene, a downstream effector of AKT signalling in beta cells[273] has been demonstrated to play a specific role in the maintenance of beta cell differentiation status in mice[61]. Indeed, in addition to its role in regulation of beta cell plasticity[104] and

diabetes induced stress responses[274], FOXO1 also regulates alternative splicing[275] a process which occurs in over 95% of human genes[276] and allows for the generation of multiple mRNAs from a single coding unit as a means to provide a powerful interface between cell identity and cell stress[277-279].

The cellular microenvironment created by diabetes is considered to be intensely stressful for beta cells[31] and elevated glucose levels (leading to glucotoxicity) have been linked to reduced expression of nodal genes within the transcriptional network that controls beta cell identity at the level of total gene expression[197]. Changes to beta cell differentiation status also occur in response to chronic hyperglycaemia[82, 86]. In addition, exposure of beta cells to certain lipids (such as the lipotoxic saturated fatty acid, palmitate) or to pro-inflammatory cytokines, has also been shown to induce widespread changes to the beta cell transcriptome[36, 280].

It has been suggested that altered beta cell identity may occur as a protective mechanism in response to a stressful extracellular milieu, with cellular plasticity serving to protect beta cells which might, otherwise, be lost via apoptosis. As such, this reversible plasticity allows for later re-differentiation should the extracellular environment become more conducive[86]. Such effects could be relevant to all beta cells but they may be particularly important for “hub cells” within islets, which are known to be more sensitive to insult than other beta cell subsets, resulting in beta cell failure [79, 281].

We hypothesised that exposure to the cellular stressors that accompany the development of diabetes may cause disrupted regulation of key genes involved

in the maintenance of beta cell identity, leading to changes in beta cell fate. Therefore, we exposed human EndoC-βH1 beta cells in culture to diabetes-related cellular stressors (including elevated glucose and fatty acid levels, hypoxia or pro-inflammatory cytokines) and observed that a small population of cells adopted a delta cell-like phenotype. Elevated numbers of delta cells were also noted in pancreatic sections from individuals with T1D or T2D by immunofluorescence using an antibody to somatostatin, suggesting that such changes may also occur *in vivo*, as has been suggested recently by others[270]. In EndoC βH1 cells, these changes were accompanied by alterations in the expression patterns of several key beta genes involved in the control of cell fate and cell identity. Dysregulation of genes controlling alternative splicing and attendant changes in the splicing patterns of key beta cell genes were also seen. These changes were reversible upon removal of the stressful stimulus suggesting that targeting of the processes controlling alternative splicing patterns may offer a tractable modality for therapeutic intervention to maintain beta cell differentiation in diabetes.

4.2 Research Design and Methods

4.2.1 Culture and treatment of EndoC-βH1 cells

EndoC-βH1 cells at P<25 were seeded in 24-well plates at a density of 6.0 x 10^5 cells/ ml and maintained according to a modified humanised culture protocol as previously described[282] for 72 hrs prior to treatment. For assessment of the effects of altered glycaemia, cells were treated with 2.5 mM and 25 mM D- or L-glucose for 24, 36 or 48 hrs. For assessment of the effects of oxygen levels, cells were grown in 1%, 3% or 21% O_2 for a period of 24, 36 or 48 hrs. For assessment of the effects of altered lipids, cells were treated with 0.5 mM palmitic acid, 0.5mM oleic acid or 0.5mM palmitic acid/0.5mM oleic acid for 12, 24 and 48 hrs, according to concentrations described in the literature[29, 207]. To determine the effects of pro-inflammatory cytokines, cells were treated with TNFα (1000 U/ mL, INFγ (750 U/ mL) and IL1β (75 U/ mL) for 12, 24 and 36 hrs. Cytokines and concentrations selected were based upon those reported in previous studies[39, 205]. For assessment of the effects of ER stress, cells were treated with 0.5 mM Tunicamycin for 24 hrs. Each treatment was carried out in 3 biological replicates, along with vehicle-only controls. Where cells were being used for subsequent immunofluorescence experiments they were cultured on 12 mm diameter coverslips and treated according to the conditions described above before being fixed with 4% paraformaldehyde.

4.2.2 Immunofluorescent characterisation of EndoC-βH1 cells in vitro

The expression of mature beta cell markers, as well as islet cell hormones in EndoC-βH1 cells grown as described above was assessed using co-immunofluorescent microscopy. Briefly, following treatment, cells were fixed with 4% paraformaldehyde for 15 minutes at 4^{o}C. Primary antibodies to PDX-1, PAX-6, SST, GCG and HHEX were diluted in phosphate buffered saline (PBS) with 0.1M Lysine, 10% donor calf serum, 0.02% sodium azide and 0.02% Triton X100 (ADST), to permeabilise the cell membranes and incubated overnight at 4^{o}C. HHEX was selected as a delta cell specific marker as it was not possible to use an antibody against the ghrelin receptor, which would have otherwise been a preferred choice for establishing a delta cell phenotype[283]. Primary antibodies were visualised using species specific highly cross-absorbed secondary antibodies (Invitrogen, Paisley) diluted in ADST at 1/400 and incubated for 1 hr at room temperature. Sequential staining was then performed with an antisera raised against insulin (Supplementary Table S1) diluted in ADST for 1 hr, followed by a goat anti guinea-pig Alexa Fluor 647 along with DAPI (Sigma-Aldrich; 1µg/ml) for 1 hr. Slides were visualised using a Leica AF6000 microscope (Leica, Milton Keynes, UK) and processed using the standard LASX Leica software platform. Ten randomly selected images were taken for each of the three biological replicates. Details of all antibodies are provided in Supplementary table S1.

4.2.3 Immunofluorescent characterisation of human pancreatic tissue sections from patients with Type 1 or Type 2 Diabetes

Immunofluorescence staining was used to determine the expression of islet cell hormones in formalin-fixed paraffin embedded (FFPE) pancreatic sections from individuals with Type 1 diabetes (T1D), Type 2 Diabetes (T2D) and individuals without diabetes from the Exeter Archival Diabetes Biobank (EADB; http://foulis.vub.ac.be/) (Supplementary Table S2). All samples were studied with ethical approval (WoSREC4; 15/WS/0258). Following dewaxing and rehydration, pancreas sections were subjected to heat–induced epitope retrieval (HIER) in 10 mmol/ L citrate buffer (pH 6). The sections were then sequentially probed with antisera to somatostatin, glucagon and insulin (Supplementary Table S1) which were detected using species specific highly cross-absorbed secondary antibodies conjugated with fluorescent dyes (Invitrogen, Paisley, UK; Supplementary Table S1). Cell nuclei were stained with DAPI. Slides were visualised using a Leica AF6000 microscope (Leica, Milton Keynes, UK) and processed using the standard LASX Leica software platform. Quantification of pancreatic endocrine cells types within the islet was achieved by assessing the comparative number of cells as a percentage of total islet area between T1D/ T2D patients and controls. Ten randomly selected images from 7 cases and controls were taken. Areas of somatostatin, insulin and glucagon staining were selected and measured using Image J[(208)].

4.2.4 RNA extraction, reverse transcription and assessment of total gene expression in EndoC-βH1 cells

EndoC-βH1 cells were washed in Dulbecco's phosphate buffered saline (D-PBS) before RNA extraction using TRI® reagent to harvest RNA (Sigma-Aldrich, Steinheim, Germany). RNA concentrations were adjusted to 100 ng/ µL prior to reverse transcription. Synthesis of cDNA was carried out using Superscript® VILO™ cDNA synthesis kit (Thermo Fisher, Foster City USA) according to manufacturer's instructions. Gene expression levels were measured in treated and untreated EndoC-βH1 cells by quantitative real-time PCR. A panel of 30 á priori target genes was selected on the basis that they had known roles in either beta cell fate or function, were markers of cell stress or were markers of other pancreatic endocrine cell types (genes are listed in supplementary table S3). Endogenous control genes (*PPIA, UBC, HPRT1, GUSB, B2M* and *IDH3B*) were empirically selected for stability in response to treatment. qRTPCR reaction mixes included 2.5 µL Taqman® Universal PCR mastermix II (no AmpErase® UNG) (Thermo Fisher, Waltham, MA, USA), 1.75 µL dH2O, 0.5 µL cDNA and 0.25 µL Taqman® gene assay (Thermo Fisher, Foster City USA) in a 5 µL reaction volume. Cycling conditions were: 50°C for 2 min, 95°C for 10 min and 50 cycles of 15 seconds at 95°C for 30 s and 1 minute at 60°C. Reactions were carried out in 3 biological replicates and 3 technical replicates. Assay Identifiers are given in Supplementary table S3. The relative expression of each test transcript was determined by the comparative Ct approach. Expression levels were calculated relative to the geometric mean of the endogenous controls, but also to the global mean of expression across all transcripts tested, (as one would with an array) which was empirically determined not to vary across test conditions

to provide a robust baseline. Expression levels were normalised to the median level of expression seen in untreated EndoC-βH1 cell controls. Differences in gene expression levels between mock-treated and treated EndoC-βH1 cells were compared to the same time point controls for each condition and investigated for statistical significance by student independent t-test carried out using SPSS version 23 (IBM, North Castle, NY, USA). Data were presented as means ± S.E.M.

4.2.5 Determination of Splicing Factor expression in EndoC-βH1 cells

Splice site usage and thus patterns of alternative splicing are determined by the relative balance of serine-arginine rich RNA binding proteins (SRSFs; splice site activators) and heterogeneous nuclear ribonucleoprotein particles (hnRNPs; splice site inhibitors) at each splice site[284]. Splicing factor Assay Ids are given in Supplementary Table S4. Splicing factor expression was quantified in EndoC-βH1 cells using Taqman® Low Density Array (TLDA) on the Quantstudio 12K Flex system. Cycling conditions were 1 cycle each of 50 ^{o}C for 2 minutes, 94.5 ^{o}C for 10 minutes and then 40 cycles of 97 ^{o}C for 30 seconds and 57.9 ^{o}C for 1 minute. The reaction mixes included 50 µL Taqman® Fast Universal PCR Mastermix (Life Technologies, Foster City, USA), 30 µL dH2O and 20 µL cDNA template. The 100 µL reaction mix was dispensed into the TLDA card chamber and centrifuged twice for 1 minute at 1000 rpm to ensure the correct distribution of solution to each well and removal of bubbles. Transcript expression was assessed the by the comparative Ct approach relative to the endogenous control genes *IDH3B, GUSB* and *PPIA* which were selected based upon empirical

evidence for stability in response to treatment and normalised to transcript expression in the untreated cells.

4.2.6 Assessment of alternative splicing in EndoC-βH1 cells

Of the panel of 30 genes selected for total gene expression, 17 were known to exhibit alternative splicing. Of these, 5 were chosen for further analysis in EndoC-βH1 cells according to three criteria: i) unique, isoform-specific exon boundaries, ii) known functional differences between the isoforms, and iii) relevance of isoform differences to beta cell differentiation status or islet function. Isoforms of the *INS*, *PAX6, POU5F1 (OCT4), NANOG* and *PTPN1* genes fulfilled these criteria. Isoform-specific Taqman custom assays (Thermo Fisher, Waltham, MA, USA) were designed across unique splice boundaries that distinguish between the functionally distinct isoforms, please refer to figure 12 . Probe and primer sequences are given in Supplementary Table S5.

To investigate whether the *PAX6(5a)* isoform of the *PAX6* gene was important for changes in beta cell differentiation status during cell stress, a custom select siRNA was designed (assay ID 1THO, Thermo Fisher, Waltham, MA, USA). Effective candidate sequences were selected using siDIRECT2. Cells were cultured in 1 mL penicillin and streptomycin free culture media with 250 µL from a master mix of siRNA containing 300 µL Optim-MEM® (Life Technologies, Foster City, USA) , 9 µL Lipofectamine® (Life Technologies, Foster City, USA) and 3 µL siRNA at 10 µM, made up according to the manufacturer's instructions. Cells were cultured for 72 hrs prior to the administration of siRNA and were then incubated for a further 48 hrs. qPCR was performed to ascertain whether the

PAX6(5a) knock down was successful. Following siRNA validation, cells were cultured in 24 well plates for 72 hours before the addition of the siRNA mastermix at the concentration specified in the manufacturer's protocol. The siRNA was incubated for 48 hrs, before treating relevant wells with 25 mM glucose for 24 hrs. After treatment cells were fixed with 4% paraformaldehyde for 15 minutes at 4 ^{o}C.

Figure 12. Schematic diagram showing regions where isoforms probes were designed.

1) *Insulin gene. Schematic showing exon boundary and region of probe design to distinguish intronic inclusion*
2) *POU5F1. Schematic showing exon boundary to distinguish between OCT4A and OCT4B/B1 variants.*
3) *NANOG. Schematic showing exon boundary to distinguish between long and short variants.*
4) *PTPN1. Schematic showing exon boundary to distinguish between long and short variants and exon inclusion.*
5) *PAX6. Schematic showing exon boundary to distinguish between PAX6(5a) family with exon 5 inclusion and PAX6 canonical family.*

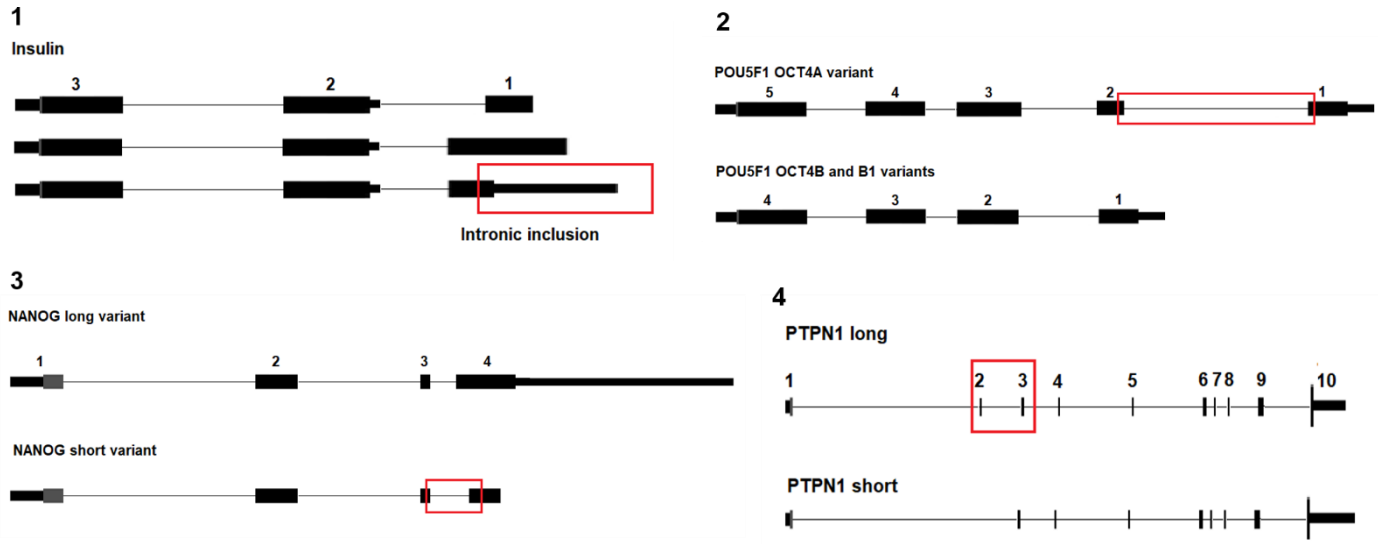

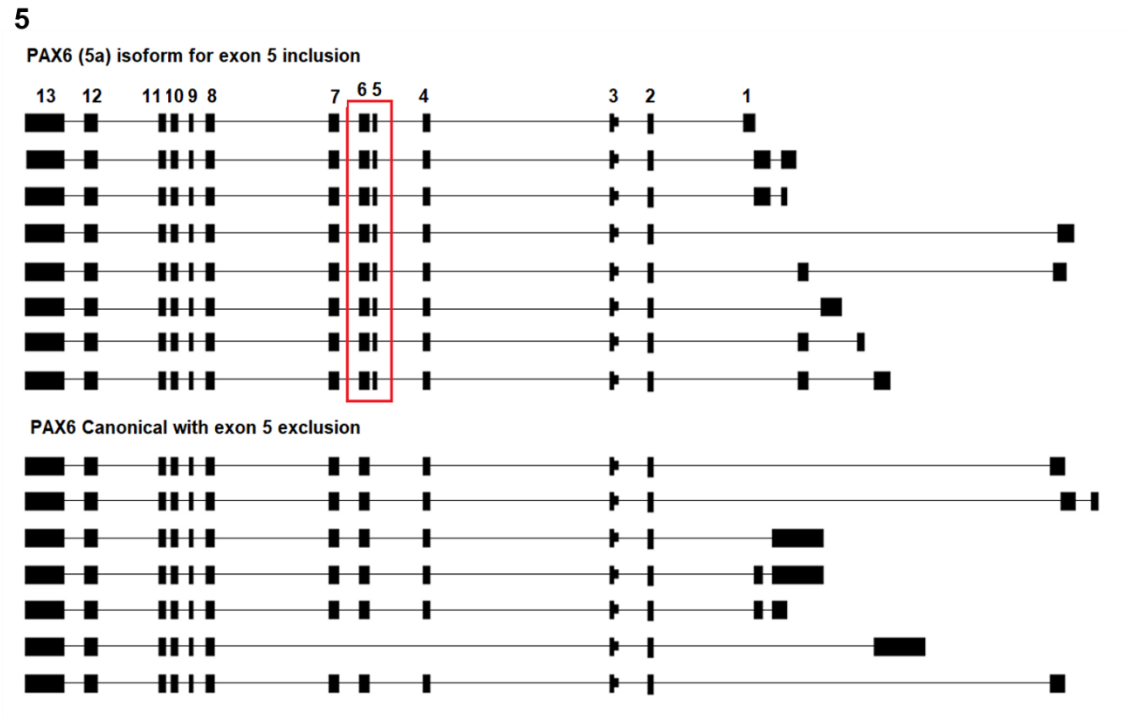

4.2.7 Reversal of delta cell phenotype in EndoC-βH1 cells by restoration of homeostasis

To test for reversibility of effect in our system, cells were first treated with 25 mM glucose or 0.5 mM Tunicamycin for 24 hrs as described above. Immediately following this, cells were restored to normal culture conditions for 72 hrs prior to assessment of cell identity, total gene expression and splicing patterns.

4.2.8 Reversal of delta cell phenotype in EndoC-βH1 cells by restoration of homeostasis or by small molecule inhibition of AKT pathway

Previous reports suggest that changes to beta cell identity can be reversed upon removal of cellular stress[274]. Reports have suggested that the AKT pathway, one of the signalling mechanisms whereby cells can communicate signals from stimuli such as cellular stress stimuli from the exterior of the cell is involved with regulation of splicing decisions and has also been linked with changes in beta

cell plasticity[31, 285, 286]. To test for reversibility of effect in our system, cells were first treated with 25 mM glucose or 0.5 mM Tunicamycin for 24 hrs as described above. Immediately following this, cells were restored to normal culture conditions for 72 hrs prior to assessment of cell identity, total gene expression and splicing patterns. To assess the effect of AKT inhibition on response to hyperglycaemia, cells were treated with 25 mM glucose alone, 1 μM of the AKT inhibitor SH-6 alone, or 25 mM glucose in combination with 1 μM SH-6 for 24 hrs prior to assessment of splicing patterns and cell identity as described above.

4.3 Results

4.3.1 Metabolic and ER stress is associated with beta cell to delta cell-like trans-differentiation in EndoC-βH1 cells

We quantified the effect of treatments designed to mimic the islet milieu in diabetes on cell identity in EndoC-βH1 cells cultured in vitro. A small (~5%) but consistent and statistically robust increase in the number of somatostatin-positive cells was noted in EndoC-βH1 cell cultures in response to incubation with elevated glucose levels (both D- and L-glucose) for 24 hrs. Control cells, incubated in 5.5mM D-glucose showed no evidence of somatostatin immunopositivity (p=9.1 x 10^{-5}, figure 13A). The proportion of somatostatin positive cells remained stable over longer periods of culture and no evidence of increased rates of cell death was seen in cells incubated under hyperglycaemic conditions (figure 13B). An increase in somatostatin positive cells was also noted in response to palmitic acid, hypoxia, pro-inflammatory cytokines, and tunicamycin (p = 5.2 x 10^{-5}, p= 4.2 x 10^{-5}, p=4.0 x 10^{-3}, and p = 5.0 x 10^{-3} respectively; figure 13C). Conversely, no such increase was seen in response to

oleic acid (p=0.343), although cells exposed to both palmitic acid and oleic acids concurrently responded in a similar manner to those treated with palmitate alone (p=0.003). No evidence of increased glucagon expression was noted in control or treated EndoC-βH1 cells at the protein level although a rise in GCG mRNA (and that encoding the transcription factor ARX) was evident in response to some treatment conditions. Despite the increase in somatostatin immunopositivity, we were unable to detect any change in the expression of *HHEX* mRNA transcripts.

Figure 13. The effects of cell stressors on hormone expression.

A) *Immunofluorescence cytochemistry showing gain of somatostatin expression in cells treated with 25 mM high glucose. Cells were treated for 24, 36 and 48 hours and showed gains of somatostatin expression at all time points. There was no increase in the proportion of cells gaining somatostatin expression at later time points. Representative image panels from 36 hour time point. Image 1. 25 mM glucose, DAPI staining. Image2. 25 mM glucose overlay of DAPI, somatostatin (green). Image 3. 25 mM high glucose. DAPI and insulin (red). Image 4. 25 mM high glucose overlay of DAPI, somatostatin (green) and insulin (red).*
B) *Timecourse of somatostatin positivity in cultures of EndoC-βH1cells treated with high glucose (25mM).* ***C)****The number of Somatostatin positive cells in cultures of EndoC-βH1cells treated with high glucose (25mM), Palmitic Acid (PI) 0.5mM, Hypoxia (3% O_2), Cytokines (TNFα [1000 U/ mL], INFγ [750 U/ mL] and IL1β [75 U/ mL]), Tunicamycin (0.5mM) or oleic acid (0.5mM).*

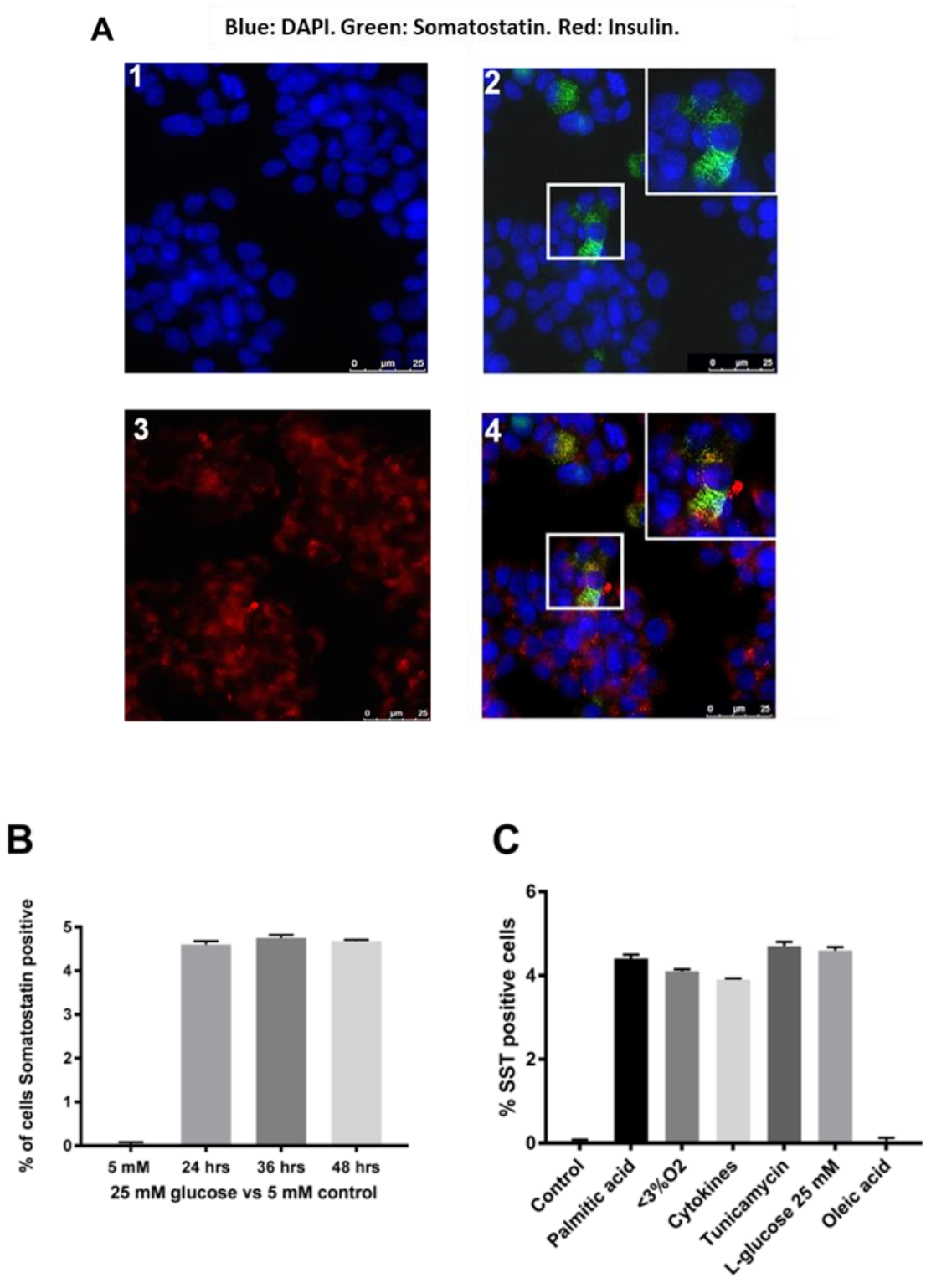

4.3.2 Pancreatic sections from donors with T1D or T2D demonstrate increased numbers of delta cells

To determine if the effects we had noted in EndoC-βH1 cells vitro were also recapitulated in human pancreas, we determined the proportion of different endocrine cell types in islet preparations from donors with T1D or T2D, and in control islets. We identified a significant increase in somatostatin-positive (delta) cell area in tissue sections from patients with either T1D or T2D compared to control islets. The total somatostatin positive area in in situ islets from T1D or T2D donors compared to control islets was 17069.9 μM (3%) v/s 6166.24 μM (1%) for T2D (p= 2.47 x 10^{-9}) and 31713 μM (9.3%) v/s 7360 μM (1% of islet area) for T1D (p= 2.1 x 10^{-6}) (figure 14A and 2B; n=10 images for 5 cases and 5 controls).

Figure 14 Hormone staining patterns of donor islets from controls or individuals with T2D.

A) *Immunofluorescence on human donor pancreatic tissue showing increases in the staining area of delta cells in cases of T1D compared to controls. Representative image panels from cases and controls. Image 1. DAPI and somatostatin (green) staining. Image 2. Overlay of DAPI, somatostatin (green), glucagon (red) and insulin (turquoise). Image 3. DAPI and somatostatin (green) staining. Image 4. Overlay of DAPI, somatostatin (green), glucagon (red), no evidence of insulin (turquoise) in T1D islet.*
B) *Immunofluorescence on human donor pancreatic tissue showing increases in the staining area of delta cells in cases of T2D compared to controls. Representative image panels from cases and controls. Image 5. DAPI and somatostatin (green) staining. Image 6. Overlay of DAPI, somatostatin (green), glucagon (red) and insulin (turquoise). Image 7. DAPI and somatostatin (green) staining. Image 8. Overlay of DAPI, somatostatin (green), glucagon (red) and insulin (turquoise) in T2D islet.*
C) *Graph showing increase in delta cells in T1D and T2D case versus controls.*

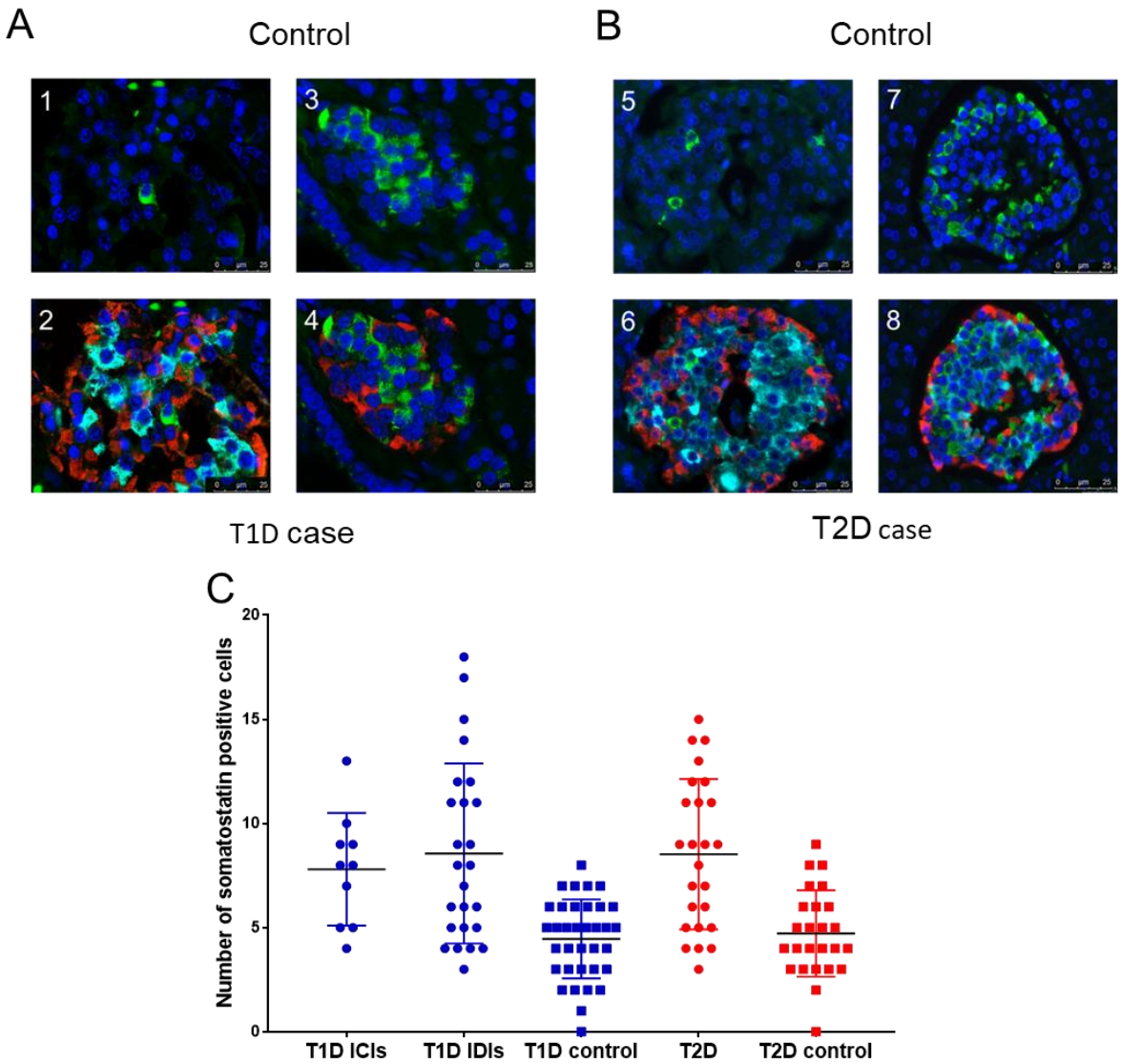

4.3.3 Key beta cell fate and function genes show disrupted expression in response to cell stress stimuli in EndoC-βH1 cells

We tested the total expression levels of 31 genes comprising markers of endocrine cell types, genes with roles in determination of beta cell identity or those acting as markers of cell stress in response to treatments designed to mimic aspects of diabetic pathophysiology. Large scale changes in the expression of the majority of these genes were noted in response to all treatments across all timepoints (supplementary table S6). Representative data for the 24 hr timepoint are given in figure 15. We also noted treatment-responsive differences in the expression of a core set of transcription factors known to be important for maintenance of beta cell fate and function (figure 15; supplementary table S6). Notable amongst these were *MAFA, PAX6, NEUROD1, NKX2-2, PDX1, NKX6-1* and *PAX4* which are known to form an interacting network. All of these were responsive to either 25mM D-glucose or 0.5 mM palmitic acid. *PAX6, NKX2-2, PDX1, NKX6-1* and *PAX4* were similarly responsive to hypoxia. Differences in expression were also evident for *HES1, SOX9, NGN3 NANOG* and *POU5F1* genes which are markers for cellular plasticity (figure 15; supplementary table S6). Markers of cellular stress including *DDIT3, ARNT,* and *MYC* also showed altered expression patterns across all of the assays (figure 15; supplementary table S6).

4.3.4 Changes to the expression of splicing factors and beta cell splicing patterns in response to cell stress stimuli in EndoC-βH1 cells

We assessed the responses of genes encoding splicing factor genes, given their role in mediating the relationships between cell and environment[285, 286]. Several splicing factors, notably the genes encoding *HNRNPA2B1, AKAP17A, PNSIR, SRSF1, SRSF2, SRSF3, SRSF6* and *LSM14A* demonstrated dysregulated expression in response to treatment with cytokines, hypoxia high/low glucose or altered lipids (figure 16; supplementary table S7).

To determine whether these changes had functional significance, we also assessed the splicing patterns of key beta cell genes. Genes were included for analysis where they were known to produce alternatively-spliced isoforms with functionally different roles in beta cell function or differentiation status that we could identify uniquely. 3/5 genes fitting these criteria (*PAX6, PTPN1* and *POU5F1/OCT4)* demonstrated changes in the ratio of alternatively-expressed isoforms in response to treatment (figure 17; supplementary table S8). However, in contrast to what we observed at total gene expression levels, there was only dysregulation of insulin isoforms at the splicing level following exposure to an Hypoxic environment (figure 17, supplementary table S8). Following validation of the siRNA *PAX6(5a)* knockdown, siRNA and 25 mM glucose treated cells showed no change in the proportion of somatostatin positive cells compared to cells treated with 25 mM glucose alone.

Figure 15 Effects of cell stresses on gene expression of genes with roles in beta cell differentiation or function.

Volcano Plot demonstrating the most dysregulated genes in response to 24 hours treatment with cellular stressors associated with a type 2 diabetic microenvironment. Volcano plots are illustrative of the numbers of genes dysregulated by cell stresses, for specific information regarding individual genes at later time points please refer to supplementary data table S6. Y axis shows -log10 of p value. Upper line infers the Bonferroni multiple testing limit. The lower dotted line gives nominal significance.

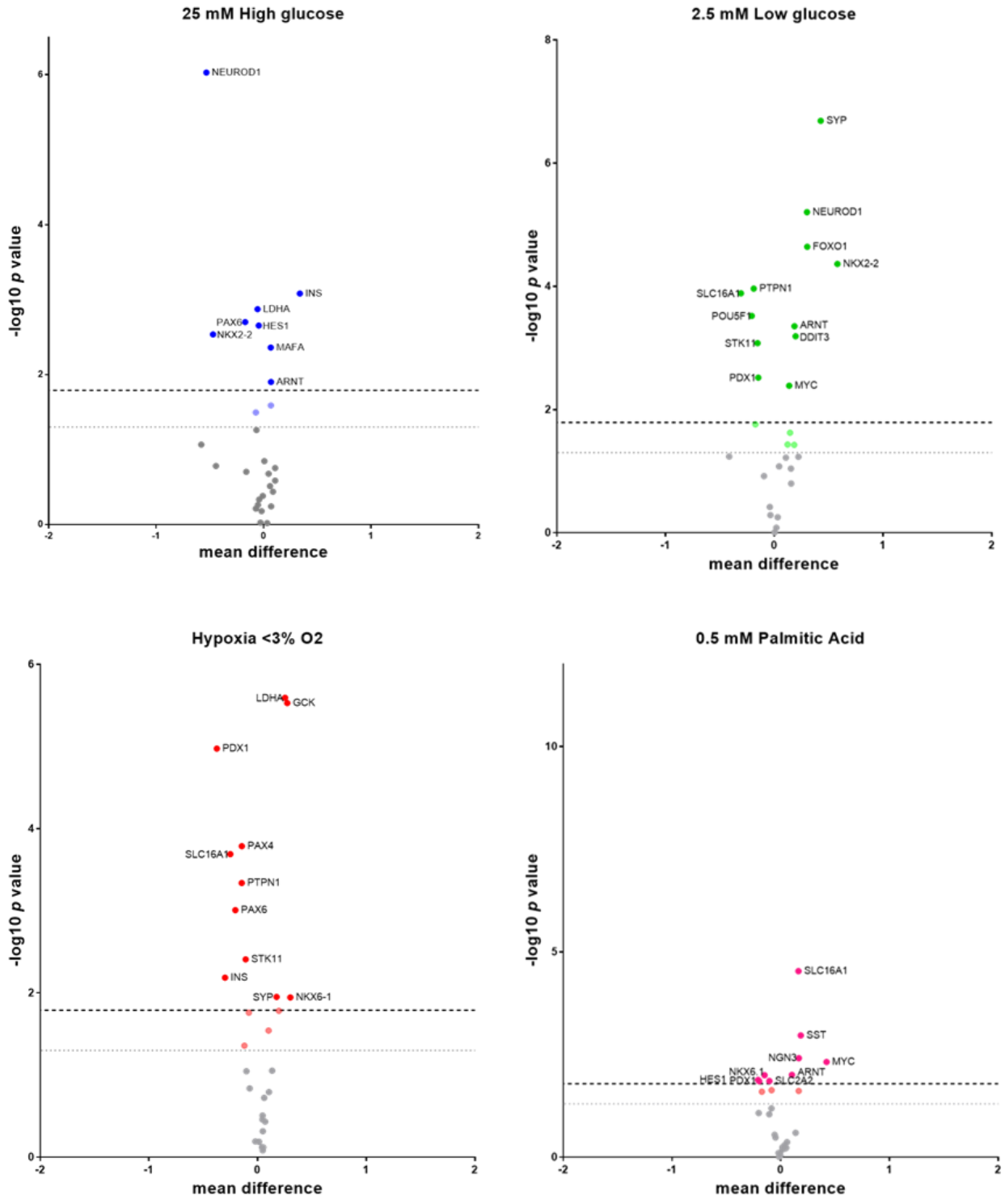

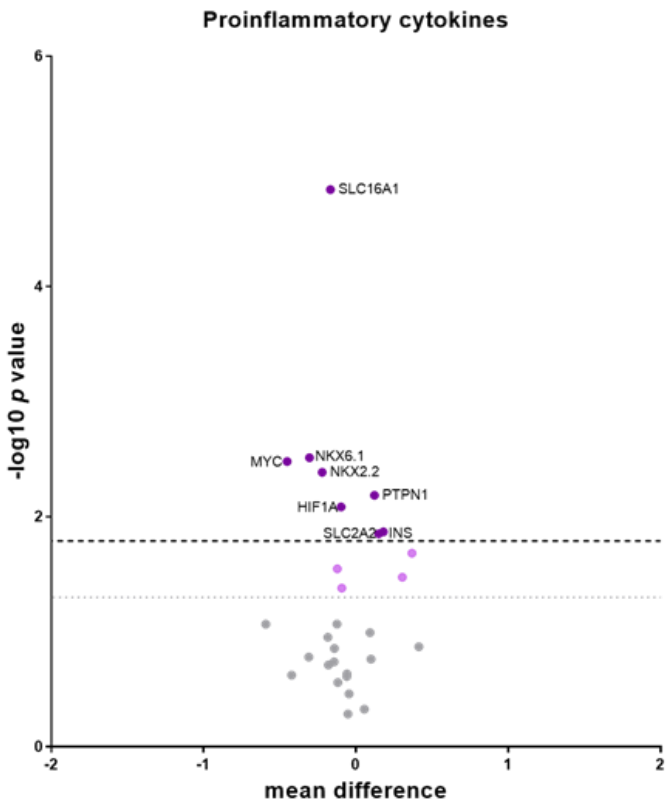
Proinflammatory cytokines
-log10 p value
mean difference
SLC16A1
MYC
NKX6.1
NKX2.2
PTPN1
HIF1A
SLC2A2
INS

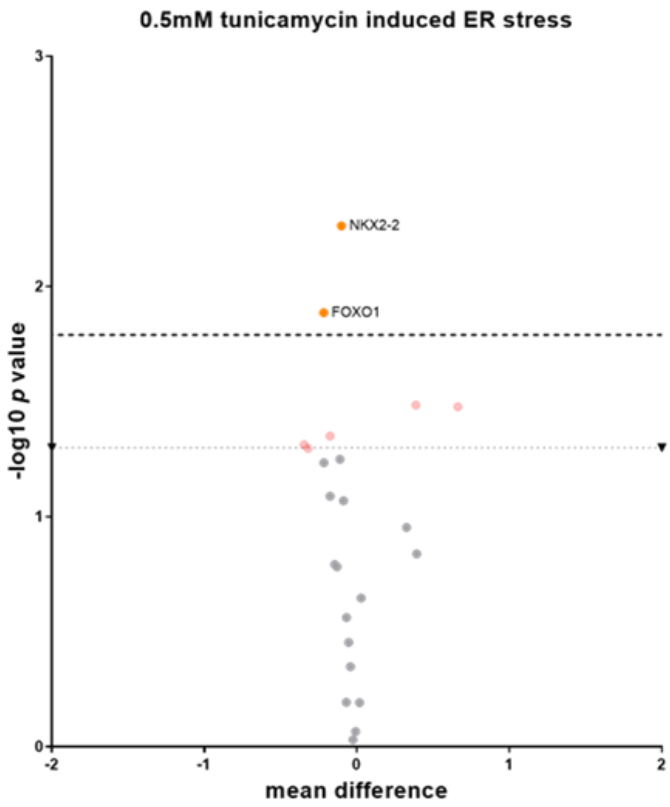
0.5mM tunicamycin induced ER stress
-log10 p value
mean difference
NKX2-2
FOXO1

Figure 16 Effects of cell stresses on splicing factor expression.

Modified Manhattan plot showing the effects of cellular stressors on splicing factor expression. Y axis shows -log10 of p value. Upper line infers the Bonferroni multiple testing limit. The lower dotted line gives nominal significance. Blue circles 25 mM high glucose. Green squares: 2.5mM low glucose. Red diamonds: <3% O2. Purple triangles: 0.5 mM Palmitic Acid. Orange triangles: Cytokines. Upper line infers the Bonferroni multiple testing limit. The lower dotted line gives nominal significance.

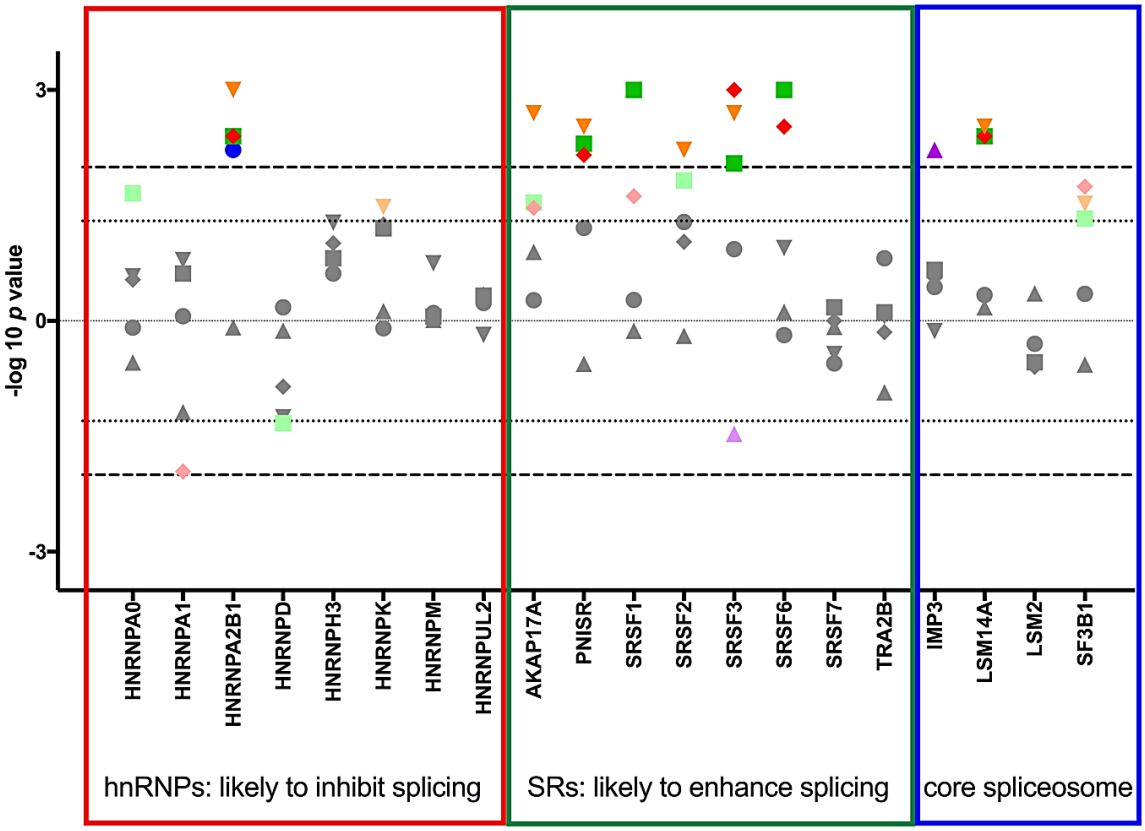

Figure 17 Effects of cell insult treatments on alternatively spliced gene expression.

X axis refs to the ratio of alternatively expressed isoforms at each locus. Isoform variants were divided by canonical variants. Y axis shows -log10 of p value. Upper line infers the Bonferroni multiple testing limit. The lower dotted line gives nominal significance. Blue circles: 25 mM glucose. Green squares: 2.5mM glucose. Red diamonds: <3% O2. Purple triangles: 0.5 mM Palmitic Acid. Pink inverse triangles: Cytokines. Orange hexagons: 0.5 mM.

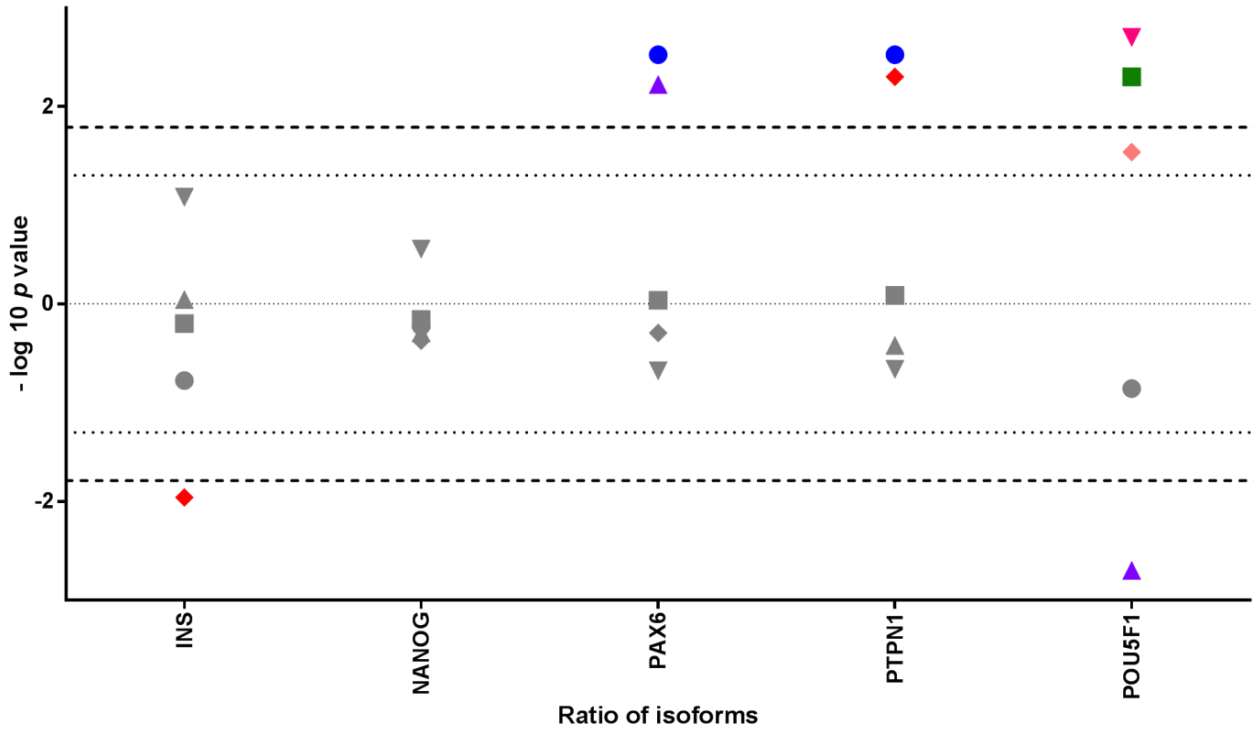

4.3.5 Changes in beta cell identity and beta cell expression patterns are reversible upon restoration of homeostatic conditions in EndoC-βH1 cells

To determine whether the changes in cell identity and gene expression patterns we have observed were permanent or reversible, we exposed EndoC-βH1 cells to cellular stressors for 24 hrs but then returned the cells to control conditions for 72 hrs prior to assessment. Following treatment with either high glucose or tunicamycin, we noted an increase in the number of somatostatin positive cells compared to controls (p=3.69 x 10^{-9} and p=1.3 x 10^{-4}), and dysregulation of splicing ratios of candidate alternatively-spliced genes (figure 18; supplementary table S9). Following return to control conditions, the number of somatostatin positive cells was indistinguishable from zero time point controls, (figure 18a; p=0.568 and p=0.643), and patterns of alternative splicing were restored (figure 18, supplementary table S9) indicating that the treatment induced changes we noted were reversible.

Figure 18 Rescue of phenotype by restoration to normal culture conditions.

Figures show rescue of beta cell phenotype by restoration to 5 mM euglycaemic culture conditions for 72 hrs. ***A).*** *Immunofluorescence image panel. Images 1, 3, 5: DAPI and Somatostatin (green). Images 2, 4, 6: Overlay, DAPI, Somatostatin (green), Insulin (red). Panels* ***1 – 2:*** *representative cells from control. Panels* ***3 – 4****: 25 mM glucose. Panels* ***5 – 6****: 24 hr treatment with 25 mM glucose and restoration to normal culture conditions for 72 hrs.* ***B)****. Graph. Total gene expression 25 mM glucose for 24 hrs versus 25 mM glucose treatment followed by 72 hrs rescue in 5 mM glucose media.* ***C)****. Alternative splicing patterns 25 mM glucose 24 hrs versus 25 mM glucose treatment followed by 72 hrs rescue in 5 mM glucose media.*

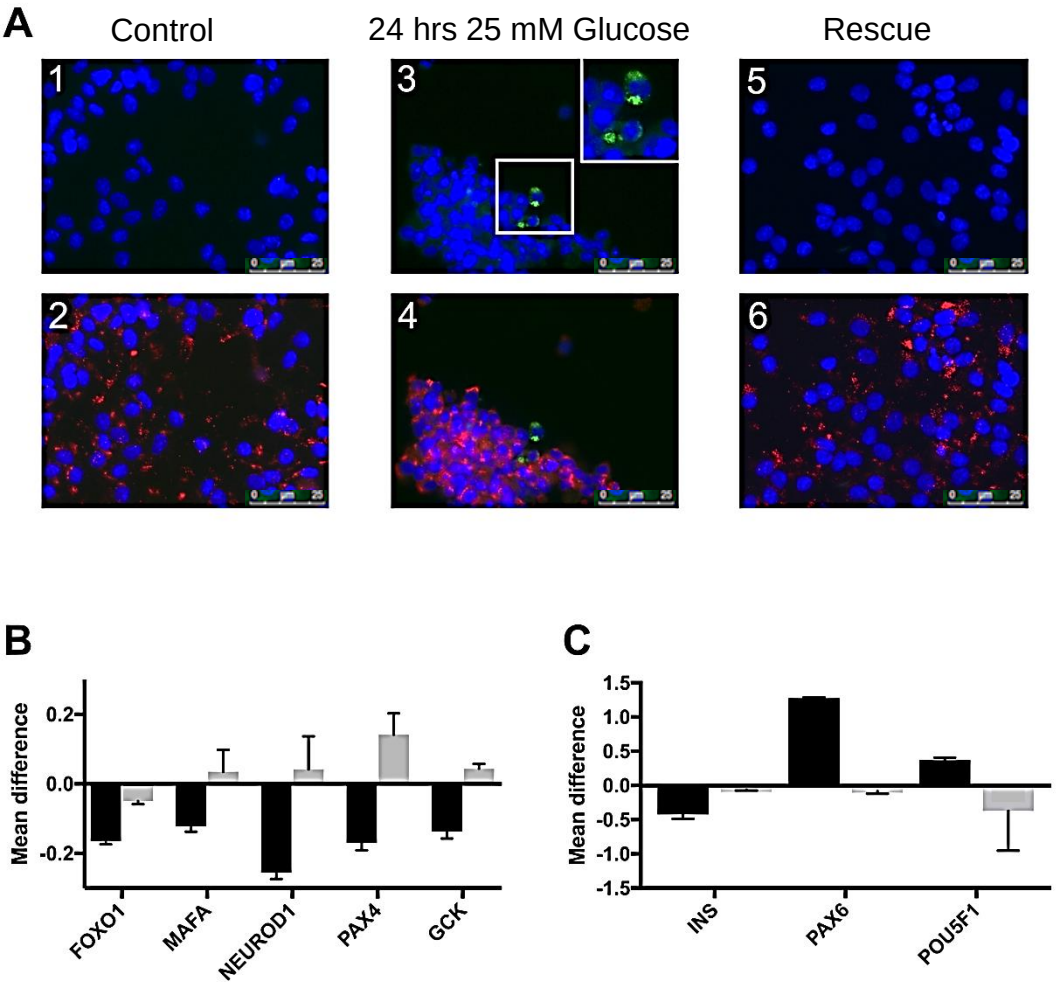

4.3.6 Restoration of splicing patterns and splicing factor activity with the AKT inhibitor SH-6 renders cells immune to transdifferentiation in EndoC-βH1 cells.

The AKT pathway has previously been suggested to have a role in regulation of splicing and splicing factor activity[285]. Treatment with low concentrations of the AKT inhibitor SH-6 alone had no impact on the number of cells staining positively for somatostatin expression, whereas cells treated with 25 mM glucose demonstrated an increase in SST positivity similar to that we observed previously (p = 0.0004). EndoC-βH1 cells treated with SH-6 and subsequently exposed to 25 mM glucose for 24 hrs however showed no increase in the number of somatostatin positive cells compared to controls; figure 19). This effect was also noted at the level of splicing factor expression and alternative splicing (supplementary table S10).

Figure 19 EndoC βH1 cells treated with the AKT pathway inhibitor SH6 and exposed to 25 mM glucose.

Cells showed no increase in the number of somatostatin cells compared with both controls and cells treated with 25 mM glucose alone.

1) *Panels A-D Cells treated with SH6 alone. Panels E-H Cells treated with SH6 and 25 mM high glucose. Panels I-L Control cells no treatment. Panels M-P Cells treated with 25 mM high glucose alone.*

2) *Graph showing the number of somatostatin positive cells counted from 10 separate images.*

1

Blue: DAPI. Green: Somatostatin. Red: Insulin.

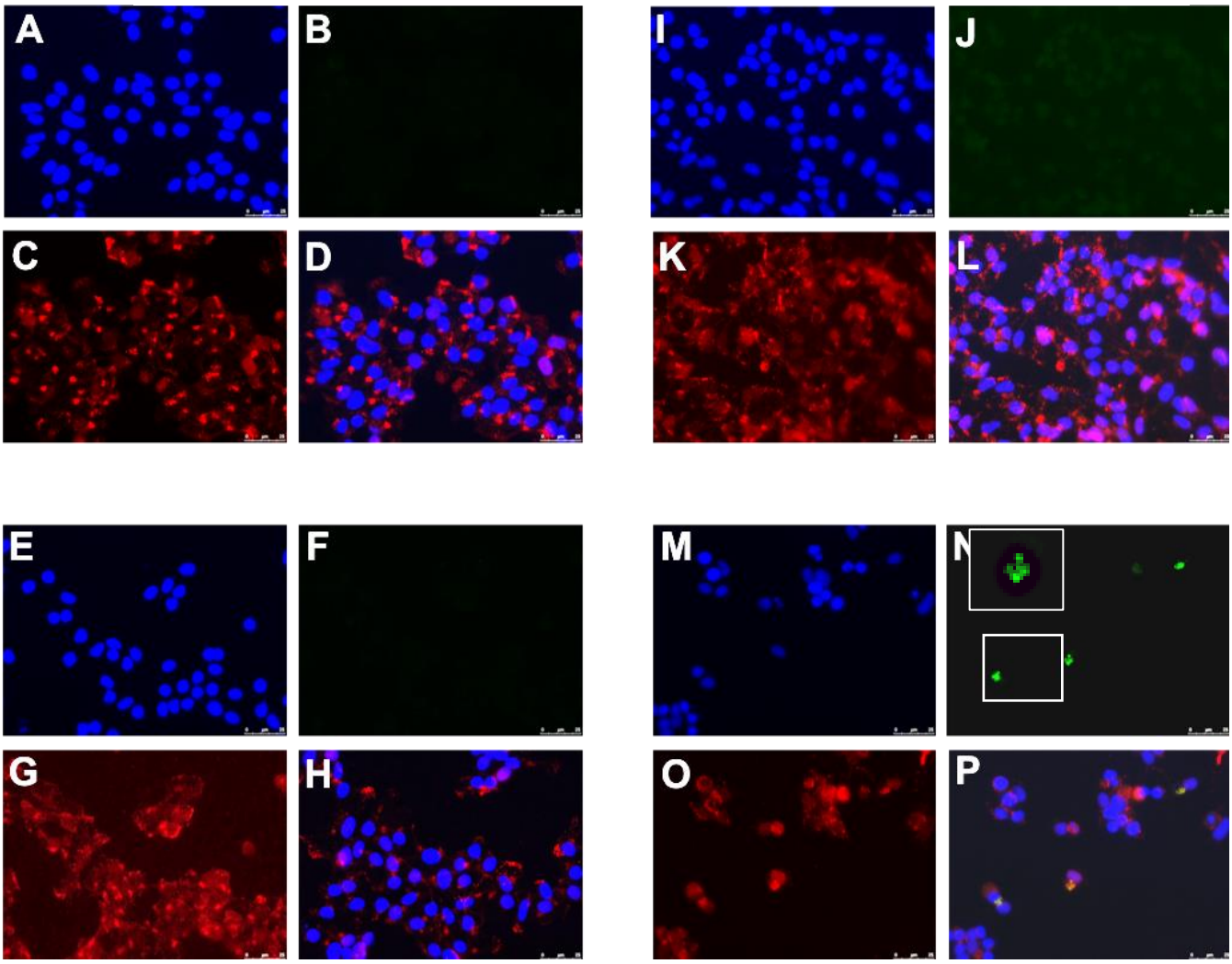

2

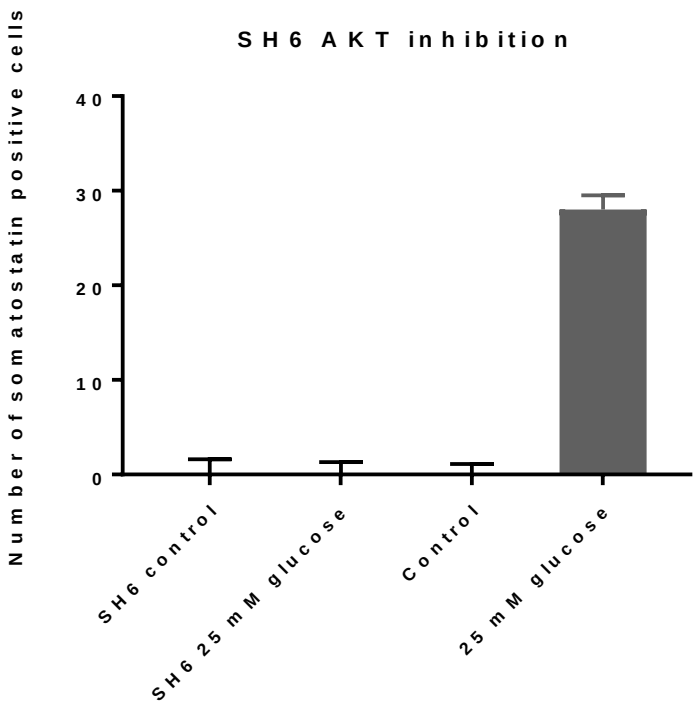

4.4 Discussion

Loss of beta cell mass over the disease course is characteristic of both T1D and T2D. Studies using rodent models have suggested that some of the change may be due to alteration in beta cell differentiation status in response to cellular stresses[57, 96, 113], but this phenomenon has not been explored extensively in humans. In the work described here, we demonstrate that when EndoC-βH1 beta cells are treated with cell stressors designed to mimic aspects of the islet milieu in diabetes (hyperglycaemia, pro-inflammatory cytokines or palmitic acid) or with the ER stress inducer tunicamycin, a small proportion of the cells cease to produce insulin and begin to synthesise somatostatin, suggesting a change in phenotype. Similar effects were also noted when cells were exposed to L-glucose, suggesting that the response may occur in response to an osmotic stress and also that changes to beta cell differentiation status are independent of

metabolism. Conversely, the monounsaturated fatty acid oleate, a fatty acid that is not known to induce metabolic stress in human beta cells[287] elicits no such response. Increased somatostatin positive staining area was also evident in islet preparations from donors with T1D and T2D, suggesting that these changes may also occur in vivo.

The change in differentiation status of EndoC-βH1 cells was accompanied by large-scale alterations in the pattern of expression of key transcription factors involved in the control of beta cell identity, as well as in genes responsible for beta cell identity and function when assessed as an á priori candidate gene set. Beta cell differentiation status is known to be influenced by a transcriptional network of genes including: *PAX6, PDX1, NEUROD1, NKX2-2, NKX6-1, MAFA, PAX4* and *FOXO1*[196, 288] and notably the expression of these genes was significantly disrupted across multiple time points in response to each of the insults employed in the present work. The pattern of expression of serine arginine rich (*SR*) and heterogeneous ribonucleoprotein particle (*HNRNP*) genes, which encode positive and negative regulators of alternative splicing, was also dysregulated, as were patterns of alternative splicing for the majority of functionally-relevant candidate genes tested. However, the knock down of the *PAX6* isoform *PAX6(5a)* did not affect the cells responses to high glucose. We hypothesise that these alterations in splicing patterns may be affected by changes in the expression of *FOXO1* in response to each treatment. *FOXO1* plays a role in the regulation of splicing factors in human primary fibroblasts[275], as well as having well-known roles in cellular stress[289] and in regulation of beta cell plasticity[273]. Alternative splicing of multiple gene targets has been well documented as a response to cellular stress[277]. FOXO1 is a downstream

effector of AKT signalling, and accordingly, inhibition of AKT in our system restored splicing factor expression and patterns of alternative splicing to those seen in euglycaemia and prevented changes to differentiation status. These observations are consistent with previous reports that stress-related changes in beta cell differentiation are modifiable once the noxious stimuli is removed[197, 274].

We noted some interesting differences in the responses measured here compared to those noted previously in other species. For example, studies in murine models of T2D have revealed both beta cell de-differentiation and trans-differentiation, but in these cases the change in phenotype was from beta to alpha cells[47, 269], rather than from beta to delta cells as we observe. Interestingly, we did find an increase in the expression of transcripts encoding both *ARX* and glucagon, which are known alpha cell markers, in EndoC-βH1cells but we did not detect the expression of glucagon at the protein level. The factors underlying apparent species differences may arise because of differences in islet architecture, gene expression and glucose sensing between rodent and human[290], but may also reflect profound differences in mRNA processing between these species since only 30% of splicing events are conserved between mice and humans[291].

We acknowledge that our study has limitations. Firstly, the changes in cell identity were observed in only a small proportion of the total cell population. The reasons for this are unclear but appear to be unrelated to the time of incubation since the response occurred very quickly (within 24 hrs) and was then stable for several days in the continued presence of the stressor. One possibility is that the cultures are heterogeneous and that a small population of cells are more susceptible to

stress-induced plasticity than the majority. It would be interesting to determine whether this putatively 'plastic' cell population shares features with cells such as those identified as 'hubs' in intact islets since these also display a greater degree of plasticity than other beta cell sub populations[79]. However, it may also be that the EndoC βH1 cell line is contaminated with progenitor like cells although the data from the rescue experiments might suggest that this is not the case, given the absence of somatostatin positivity during normal culture conditions.

We also acknowledge that we have not conducted an exhaustive survey of splicing changes in the treated cells. The heterogenous nature of the treated cultures means that only the largest effects would have been revealed by our transcriptome-wide analysis. In particular, we focused on those genes known to be responsible for beta cell identity decisions. Importantly, some of the effects on gene expression had not been detected at the level of total gene expression, highlighting the need to undertake an investigation of splicing changes when considering transcriptomic profiling.

Our data are consistent with a model in which beta cell trans-differentiation, or dedifferentiation to a progenitor like state followed by re-differentiation into a delta cell like state, can occur in response to the imposition of cellular stress and we postulate that this may reflect the dysregulation of splicing factor genes mediated by altered expression of *FOXO1*. This work is, to our knowledge the first demonstration that dedifferentiation and/ or trans-differentiation in human endocrine cells may be specifically associated with changes in the regulation of mRNA splicing. Without lineage tracing experiments, which are not currently possible when using human model systems, it is not possible to infer that these changes are beta to delta cell transdifferentiation.

However, the consequence of the changes we observed may, at the molecular level, result in the altered expression of key genes involved in cell fate decisions. Targeting splicing patterns for therapeutic benefit is now a very real possibility with several approaches already in clinical trials[292]. We have shown that differentiation status in beta cells can be influenced by targeting splicing decisions, and a deeper understanding of the specific points at which such interventions could be focused might confer benefits for diabetes therapy in the future.

Supplementary table S1. Details of antibodies and experimental conditions

Ab	Supplier	Cat #	Lot number	Species	Conc used:
PDX1	Abcam	Ab47267	GR238480-1	Rabbit polyclonal IgG	1/500
NEUROD1	Abcam	Ab60704	GR249997-1	Mouse monoclonal IgG2A	1/400
PAX6	Abcam	Ab195045	GR313146-6	Rabbit monoclonal IgG	1/350
Insulin	DAKO	80564	10088287	Guinea-pig polyclonal	1/363
Glucagon	Abcam	Ab10988	GR260160-1	Mouse monoclonal IgG1	1/2000
Somatostatin	Abcam	Ab30788	GR213035-1	Rat monoclonal IgG2b	1/200
HHEX	LSBIO	LS-B11570	Clone 3F4	Mouse monoclonal IgG2b	1/500

Supplementary table S2. Patient data table.

Disease status	Case ID	Age (years)	Duration (years)
T1D	SC107	18	5
T1D	SC109	20	6
T1D	E557	22	4
T1D	SC112	22	9
T1D	SC116	35	15
T1D	nPOD6038-01PB	37.5	20
T1D	nPOD6086-02PB	78	74
Control	12142	17	-
Control	146/66	18	-
Control	PAN1	22	-
Control	329/72	24	-
Control	447/71	32	-
Control	nPOD6095-06PB	40	-
Control	nPOD6012-4PT	68	-
T2D	38/66	56	0.25
T2D	386/66	unknown	unknown
T2D	184/66	60	unknown
T2D	192/71	65	unknown
T2D	192/69	66	unknown
Control	110/96	58	-
Control	202/75	60	-
Control	224/66	67	-
Control	44/66	60	-
control	244/66	63	-

Supplementary table S3. Assay details of total gene expression

Gene Symbol	Assay ID	Gene Symbol	Assay ID
STK11	Hs00176092_m1	HES1	Hs00172878_m1
FOXO1	Hs01054576_m1	GCG	Hs01031536_m1
PAX6	Hs00240871_m1	PTPN1	Hs00942477_m1
GCK	Hs01564555_m1	POU5F1	Hs04260367_gH
GUSB	Hs00939627_m1	NKX2-2	Hs00159616_m1
SLC16A1	Hs01560299_m1	INS	Hs00355773_m1
MAFA	Hs01651425_s1	HIF1A	Hs00153153_m1
NKX6-1	Hs00232355_m1	NANOG	Hs04399610_g1
ARX	Hs00292465_m1	PAX4	Hs00173014_m1
PPIA	Hs04194521_s1	SST	Hs00356144_m1
LDHA	Hs01378790_g1	ARNT	Hs01121918_m1
NEUROD1	Hs01922995_s1	MYCL	Hs00420495_m1
SOX9	Hs01001343_g1	PDX1	Hs00236830_m1
PTF1A	Hs00603586_g1	SLC2A2	Hs01096908_m1
HPRT1	Hs02800695_m1	DDIT3	Hs00358796_g1
PDGFRA	Hs00998026_m1	MAFB	Hs00271378_s1
SYP	Hs00300531_m1	HHEX	Hs00242160_m1
VIM	Hs00958111_m1	NEUROG3	Hs01875204_s1
ONECUT1	Hs00413554_m1		

Supplementary table S4. Assay Ids for splicing factors quantified in this study.

Gene symbol	Assay ID
AKAP17A	Hs00946624_m1
HNRNPA0	Hs00246543_s1
HNRNPA1	Hs01656228_s1
HNRNPA2B1	Hs00955384_m1
HNRNPD	Hs01086912_m1
HNRNPH3	Hs01032113_g1
HNRNPK	Hs03989611_gH
HNRNPM	Hs00246018_m1
HNRNPUL2	Hs01398726_g1
IMP3	Hs00251000_s1
18s rRNA	Hs99999901_s1
LSM14A	Hs00385941_m1
LSM2	Hs01061967_g1
PNISR	Hs00369090_m1
SF3B1	Hs00961640_g1
SRSF1	Hs00199471_m1
SRSF2	Hs00427515_g1
SRSF3	Hs00751507_s1
SRSF6	Hs00740177_g1
SRSF7	Hs01032695_m1
TRA2B	Hs00190210_m1
IDH3B	Hs00199382_m1
PPIA	Hs04194521_s1
GUSB	Hs00939627_m1

Supplementary table S5. Sequences of isoform specific probes and primers used in this study

Assay Name	Assay IDs	Forward Primer Seq.	Reverse Primer Seq.	Reporter 1 Sequence
INS_EX1	NM_001185097	CCATCAAGCAGGTCTGTTCCAA	GGGCCATGGCAGAAGGA	CCTTTGCGTCAGATCACT
INS_EX1DEL	NM_000207	GGCTTCTTCTACACACCCAAGAC	CCTCCAGGGCCAAGGG	CTGCAGGGCAGCCTG
INS_EX1LNG	NM_001185098	GGACAGGCTGCATCAGAAGAG	GGGCCATGGCAGAAGGA	CCATCAAGCAGATCACTG
PTPN1_EX2DEL	NM_001278618.1	AGTTCGAGCAGATCGACAAGTC	GCGTTGATATAGTCATTATCTTCTTGATGTAGT	CTATGGTCAACTGGTAAATG
NANOG1_EX4LNG	NM_024865.3	TGGCCGAAGAATAGCAATGGT	CATCCCTGGTGGTAGGAAGAGTA	ACGCAGAAGGCCTCAGC
PAX6_EX5DEL	NM_001258462.1 NM_001258463.1 NM_001310158.1 NM_001310160.1 NM_001310161.1 NM_001604.5	CGTGCGACATTTCCCGAATT	GTCTCGTAATACCTGCCCAGAATTT	ATCCGTTGGACACCTGC
NANOG_EX4TRU	NM_001297698	TGGCCGAAGAATAGCAATGGT	GGTTCCCAGTCGGGTTCAC	ACGCAGGGATGCCTG
POU5F1_EX3		GAAGAGGATCACCCTGGGATATACA	TGGCTGAATACCTTCCCAAATAGAAC	CAGGCCGATGTGGCTC

Supplementary table S6: Effects of cell insult treatments on total gene expression.

The p values for statistical significance as determined by independent t-test, Mean difference, Standard errors of measurement (SED) and the 95% confidence intervals are given below. ***Bold italic p<0.016*** *Bonferroni correction for 3 tests: 1st, 2nd and 3rd time-points. Gene list is á priori so no further corrections. Italic underlined p<0.050. No correction for multiple testing. Tunicamycin table* ***Bold italic p=<0.025****. Bonferroni correction for 2 tests: treatment and rescue. Gene list is á priori so no further corrections. Italic underlined p=<0.050. No correction for multiple testing*

Hyperglycaemia 25mM glucose assay Independent t-test p = 0.016																
24 hours						**36 hours**						**48 hours**				
Gene	***P* value**	**Mean Diff.**	**SED**	**95% C I**		**Gene**	***P* value**	**Mean diff.**	**SED**	**95% C I**		**Gene**	***P* value**	**Mean diff.**	**SED**	**95% C I**	
				Lower	**Upper**					**Lower**	**Upper**					**Lower**	**Upper**
INS	***0.001***	***0.338***	***0.072***	***0.178***	***0.498***	*INS*	0.229	0.087	0.07	-0.06	-0.24	*INS*	*0.035*	*-0.223*	*0.09*	0.43	*0.02*
PDX1	0.210	0.047	0.035	-0.031	0.125	*PDX1*	0.732	0.016	0.04	-0.08	-0.11	*PDX1*	0.277	-0.205	0.14	0.79	-0.38
PAX6	***0.002***	***-0.172***	***0.040***	***-0.262***	***-0.081***	*PAX6*	0.496	-0.034	0.05	-0.14	-0.07	*PAX6*	0.168	-0.274	0.13	0.82	-0.27
FOXO1	0.166	-0.444	0.126	-1.860	0.972	*FOXO1*	0.628	-0.292	0.51	-2.5	-1.92	*FOXO1*	0.195	0.292	0.15	0.35	-0.94
NEUROD1	***0.000***	***-0.533***	***0.045***	***-0.635***	***-0.430***	*NEUROD1*	0.639	-0.304	0.56	-2.69	-2.08	*NEUROD1*	0.231	0.216	0.13	0.32	-0.75
NKX2-2	***0.003***	***-0.471***	***0.116***	***-0.734***	***-0.207***	*NKX2-2*	0.487	-0.483	0.57	-2.91	-1.95	*NKX2-2*	0.255	0.387	0.25	0.63	-1.40
MAFA	***0.004***	***0.109***	***0.030***	***0.043***	***0.175***	*MAFA*	***0.007***	***0.120***	***0.04***	**-0.04**	***-0.20***	*MAFA*	0.856	0.014	0.07	0.25	-0.28
MAFB	0.055	-0.056	0.026	-0.114	0.001	*MAFB*	0.619	-0.036	0.06	0.29	-0.22	*MAFB*	0.886	0.015	0.09	0.38	-0.41
GCK	0.573	-0.030	0.051	-0.144	0.084	*GCK*	0.083	-0.085	0.04	0.18	-0.01	*GCK*	0.315	0.049	0.05	0.05	-0.15
SYP	0.086	-0.581	0.091	-1.542	0.380	*SYP*	0.598	-0.334	0.54	2.64	-1.97	*SYP*	0.305	0.303	0.22	0.64	-1.25

Hyperglycaemia 25mM glucose assay Independent t-test p = 0.016																	
24 hours						36 hours						48 hours					
SLC2A2	0.547	0.033	0.053	-0.085	0.150	*SLC2A2*	0.562	0.033	0.06	0.09	-0.16	*SLC2A2*	0.198	0.084	0.06	0.05	-0.22
PTPN1	*0.026*	*-0.072*	*0.028*	*-0.133*	*-0.011*	*PTPN1*	0.943	0.005	0.06	0.22	-0.23	*PTPN1*	0.385	-0.079	0.07	0.37	-0.21
PAX4	0.465	0.068	0.077	-0.235	0.370	*PAX4*	***0.002***	***0.145***	***0.03***	**-0.07**	***-0.22***	*PAX4*	0.243	-0.192	0.12	0.68	-0.30
STK11	0.198	-0.042	0.031	-0.110	0.026	*STK11*	*0.025*	*-0.107*	*0.04*	0.2	*0.02*	*STK11*	0.132	-0.059	0.04	0.14	-0.02
SLC16A1	0.663	-0.019	0.042	-0.112	0.074	*SLC16A1*	0.120	-0.087	0.05	0.2	-0.03	*SLC16A1*	0.308	-0.159	0.12	0.64	-0.32
LDHA	**0.001**	**0.108**	**0.024**	**0.053**	**0.162**	*LDHA*	0.175	0.039	0.03	0.02	-0.10	*LDHA*	***0.003***	***0.125***	***0.03***	-0.05	***-0.20***
GCG	0.307	-0.067	0.062	-0.204	0.071	GCG	0.409	-0.060	0.07	-0.21	0.09	GCG	***0.012***	***0.224***	***0.07***	0.06	***0.39***
SST	0.260	0.060	0.050	-0.052	0.171	SST	0.269	0.060	0.05	-0.05	0.17	SST	***0.004***	***0.211***	***0.06***	0.08	***0.34***
ARX	0.944	0.006	0.088	-0.189	0.202	ARX	0.309	0.091	0.08	-0.1	0.28	ARX	0.480	0.058	0.08	-0.12	0.23
ARNT	**0.013**	**0.107**	**0.033**	**0.030**	**0.184**	ARNT	0.723	0.022	0.06	-0.14	0.18	ARNT	0.144	0.148	0.08	-0.09	0.39
DDIT3	0.142	0.069	0.043	-0.028	0.166	DDIT3	0.386	0.055	0.06	-0.08	0.19	DDIT3	0.062	0.113	0.05	-0.01	0.23
HIF1A	0.416	0.070	0.082	-0.113	0.253	HIF1A	0.701	0.035	0.09	-0.16	0.23	HIF1A	0.051	0.208	0.09	0	0.42
MYC	0.959	-0.008	0.140	-0.590	0.574	MYC	***0.001***	***-0.183***	***0.04***	-0.27	***0.10***	MYC	***0.000***	***0.313***	***0.04***	0.23	***0.40***
SOX9	0.613	-0.053	0.101	-0.277	0.172	SOX9	0.033	0.269	0.11	0.03	0.51	SOX9	***0.001***	***0.277***	***0.06***	0.15	***0.41***
POU5F1	*0.032*	*-0.072*	*0.029*	*-0.137*	*-0.008*	POU5F1	0.215	-0.057	0.04	-0.15	0.04	POU5F1	0.333	-0.096	0.08	-0.4	0.21
NANOG	0.176	0.067	0.046	-0.036	0.169	NANOG	0.194	0.076	0.05	-0.05	0.20	NANOG	***0.008***	***0.165***	***0.05***	0.05	***0.28***
HES1	***0.002***	***-0.161***	***0.040***	***-0.250***	***-0.073***	HES1	***0.000***	***0.243***	***0.05***	0.14	***0.34***	HES1	***0.003***	***-0.149***	***0.04***	-0.24	***-0.06***
NGN3	0.365	-0.045	0.047	-0.151	0.061	NGN3	0.193	-0.062	0.04	-0.16	0.04	NGN3	0.375	-0.052	0.06	-0.18	0.07

Hypoglycaemia 2.5mM glucose assay Independent t-test p=0016																	
24 hours						36 hours						48 hours					
Gene	*P* value	Mean diff.	SED	95% C I		Gene	*P* value	Mean diff	SED	95% C I		Gene	*P* value	Mean diff	SED	95% C I	
				Lower	Upper					Lower	Upper					Lower	Upper
INS	*0.038*	*0.183*	*0.08*	*0.01*	0.35	INS	0.994	0.001	0.06	-0.14	0.14	INS	***0.015***	***-0.284***	***0.10***	***-0.5***	***-0.07***
PDX1	***0.003***	***-0.148***	***0.04***	***-0.23***	***-0.06***	PDX1	***0.000***	***-0.191***	***0.04***	***0.27***	***-0.11***	PDX1	***0.001***	***-0.224***	***0.05***	***-0.33***	***-0.12***
PAX6	0.058	-0.415	0.11	-0.86	0.03	PAX6	***0.000***	***0.269***	***0.04***	***0.35***	***-0.19***	PAX6	***0.000***	***-0.239***	***0.04***	***-0.34***	***-0.14***
FOXO1	***0.000***	***0.303***	***0.04***	***0.21***	***0.39***	FOXO1	***0.000***	***0.372***	***0.04***	***-0.28***	***0.46***	FOXO1	***0.000***	***0.427***	***0.05***	***0.32***	***0.54***
NEUROD1	***0.000***	***0.301***	***0.03***	***0.22***	***0.38***	NEUROD1	***0.000***	***0.348***	***0.04***	***-0.26***	***0.43***	NEUROD1	***0.000***	***0.299***	***0.05***	***0.19***	***0.41***
NKX2-2	***0.000***	***0.580***	***0.08***	***0.39***	***0.77***	NKX2-2	***0.002***	***0.386***	***0.09***	***-0.17***	***0.60***	NKX2-2	***0.001***	***0.409***	***0.09***	***0.21***	***0.61***
MAFA	0.983	0.002	0.07	-0.29	0.3	MAFA	***0.001***	***-0.161***	***0.03***	***0.24***	***-0.08***	MAFA	0.067	-0.292	0.08	-0.63	0.05
MAFB	0.084	0.044	0.02	-0.01	0.1	MAFB	0.816	-0.016	0.06	0.25	0.22	MAFB	0.635	-0.038	0.07	-0.32	0.25
GCK	*0.037*	*0.121*	*0.05*	*0.01*	0.23	GCK	0.063	0.102	0.05	0.01	0.21	GCK	0.857	0.030	0.13	-1.43	1.49
SYP	***0.000***	***0.427***	***0.03***	***0.35***	***0.5***	SYP	***0.000***	***0.420***	***0.04***	***-0.34***	***0.50***	SYP	***0.000***	***0.421***	***0.04***	***0.33***	***0.51***
SLC2A2	***0.024***	***0.145***	***0.05***	***0.02***	***0.27***	SLC2A2	***0.005***	***0.183***	***0.05***	***-0.07***	***0.30***	SLC2A2	0.757	0.019	0.06	-0.12	0.16
PTPN1	***0.000***	***-0.190***	***0.03***	***0.26***	***-0.12***	PTPN1	*0.032*	*-0.082*	*0.03*	-0.16	*-0.01*	PTPN1	***0.001***	***-0.184***	***0.04***	***-0.27***	***-0.09***
PAX4	0.382	-0.042	0.05	0.14	0.06	PAX4	0.063	0.069	0.03	0	0.14	PAX4	***0.000***	***-0.211***	***0.04***	***-0.3***	***-0.12***
STK11	***0.001***	***-0.154***	***0.03***	***0.23***	***-0.08***	STK11	0.312	-0.043	0.04	-0.13	0.05	STK11	***0.000***	***-0.206***	***0.04***	***-0.29***	***-0.12***

Hypoglycaemia 2.5mM glucose assay Independent t-test p=0016																	
24 hours						36 hours							48 hours				
SLC16A1	***0.000***	***-0.307***	***0.05***	***0.42***	***-0.19***	SLC16A1	***0.000***	***-0.301***	***0.04***	***-0.39***	***-0.21***	SLC16A1	***0.000***	***-0.361***	***0.05***	***-0.48***	***-0.24***
LDHA	0.159	0.155	0.07	-0.14	0.45	LDHA	0.485	-0.057	0.07	-0.33	0.22	LDHA	0.249	0.189	0.12	-0.31	0.69
GCG	0.518	-0.036	0.05	-0.16	0.08	GCG	0.468	-0.053	0.07	-0.21	0.10	GCG	***0.001***	***0.311***	***0.07***	***0.16***	***0.46***
SST	0.559	0.030	0.05	-0.08	0.14	SST	0.189	0.078	0.06	-0.05	0.20	SST	***0.000***	***0.259***	***0.05***	***0.15***	***0.36***
ARX	0.831	0.018	0.08	-0.16	0.2	ARX	0.625	0.041	0.08	-0.14	0.22	ARX	*0.020*	*-0.241*	*0.09*	-0.44	*-0.05*
ARNT	***0.000***	***0.185***	***0.04***	***0.11***	***0.26***	ARNT	0.062	0.135	0.06	-0.01	0.28	ARNT	0.311	0.066	0.06	-0.07	0.20
DDIT3	***0.001***	***0.195***	***0.04***	***0.11***	***0.28***	DDIT3	***0.004***	***0.165***	***0.04***	***0.07***	***0.26***	DDIT3	0.269	0.197	0.13	-0.34	0.74
HIF1A	0.091	0.153	0.08	-0.03	0.34	HIF1A	0.355	0.080	0.08	-0.1	0.26	HIF1A	0.501	-0.804	0.99	-5.04	3.43
MYC	***0.004***	***0.136***	***0.04***	***0.05***	0.22	MYC	0.262	0.238	0.16	-0.41	0.89	MYC	0.657	0.019	0.04	-0.08	0.11
SOX9	0.059	0.221	0.10	-0.01	0.45	SOX9	***0.005***	***0.421***	***0.12***	***0.16***	***0.68***	SOX9	***0.015***	***0.371***	***0.12***	***0.09***	***0.65***
POU5F1	***0.000***	***-0.208***	***0.04***	***-0.29***	***-0.12***	POU5F1	***0.001***	***-0.152***	***0.03***	***-0.22***	***-0.08***	POU5F1	***0.001***	***-0.220***	***0.04***	***-0.32***	***-0.12***
NANOG	0.060	0.106	0.05	-0.01	0.22	NANOG	0.186	-0.081	0.06	-0.21	-0.05	NANOG	0.426	0.119	0.12	-0.37	0.61
HES1	0.120	-0.095	0.06	-0.22	0.03	HES1	*0.024*	*0.119*	*0.04*	-0.02	*-0.22*	HES1	0.714	-0.053	0.13	-0.58	0.47

Hypoxia 3% O2 assay Independent t-test p = 0.016																	
4hrs						**12 hrs**						**24hrs**					
Gene	***P* valu e**	**Mean diff.**	**SED**	**95% CI**		**Gene**	***P* value**	**Mean diff.**	**SED**	**95% CI**		**Gene**	***P* value**	**Mean diff.**	**SED**	**95% CI**	
				Lower	**Upper**					**Lower**	**Upper**					**Lower**	**Upper**
NGN3	0.715	-0.024	0.058	-0.255	0.207	NGN3	0.125	-0.137	0.056	-0.360	0.086	NGN3	*0.031*	*0.082*	*0.033*	*0.009*	*0.155*
NANOG	0.819	0.012	0.051	-0.101	0.125	NANOG	0.130	-0.085	0.052	-0.201	0.03	NANOG	0.763	0.013	0.043	-0.082	0.109
POU5F1	0.261	-0.064	0.053	-0.182	0.055	POU5F1	***0.004***	***-0.194***	***0.053***	***-0.312***	***-0.075***	POU5F1	***0.015***	***-0.160***	***0.054***	***-0.280***	***-0.039***
INS	0.561	-0.042	0.071	-0.200	0.115	INS	0.053	-0.154	0.070	-0.309	0.002	INS	***0.002***	***-0.296***	***0.072***	***-0.457***	***-0.135***
PDX1	0.134	-0.303	0.128	-0.821	0.216	PDX1	***0.000***	***-0.332***	***0.047***	***-0.437***	***-0.227***	PDX1	***0.000***	***-0.261***	***0.042***	***-0.354***	***-0.168***
PAX6	*0.037*	*-0.092*	*0.038*	*-0.178*	-0.007	PAX6	***0.000***	***-0.328***	***0.048***	***-0.434***	***-0.222***	PAX6	***0.000***	***-0.379***	***0.040***	***-0.467***	***-0.291***
SLC16A1	***0.000***	***-0.139***	***0.025***	***-0.196***	***-0.083***	SLC16A1	***0.005***	***-0.201***	***0.057***	***-0.328***	***-0.075***	SLC16A1	*0.023*	*-0.114*	*0.042*	*-0.209*	-0.02
FOXO1	0.936	-0.005	0.065	-0.151	0.141	FOXO1	0.281	0.075	0.066	-0.071	0.221	FOXO1	*0.048*	*-0.148*	*0.066*	*-0.294*	-0.002
NEUROD1	0.488	-0.048	0.066	-0.195	0.1	NEUROD1	0.355	0.067	0.069	-0.087	0.221	NEUROD1	0.479	-0.049	0.067	-0.198	0.1
NKX2-2	*0.040*	*0.125*	*0.052*	*0.007*	*0.243*	NKX2-2	***0.015***	***0.165***	***0.055***	***0.040***	***0.29***	NKX2-2	0.192	-0.075	0.053	-0.196	0.045
SYP	0.231	0.065	0.050	-0.049	0.179	SYP	*0.031*	*0.153*	*0.060*	*0.017*	0.29	SYP	*0.036*	*0.122*	*0.050*	*0.010*	0.234
NKX6-1	0.997	0.000	0.100	-0.223	0.222	NKX6-1	***0.004***	***0.446***	***0.118***	***0.183***	***0.708***	NKX6-1	***0.005***	***0.369***	***0.102***	***0.142***	***0.596***
MAFA	0.891	0.007	0.052	-0.123	0.109	MAFA	0.272	0.057	0.049	-0.052	0.166	MAFA	0.801	0.012	0.046	-0.091	0.115
LDHA	***0.000***	***0.163***	***0.026***	***0.104***	***0.222***	LDHA	***0.000***	***0.346***	***0.025***	***0.289***	***0.402***	LDHA	***0.000***	***0.412***	***0.025***	***0.357***	***0.467***

Hypoxia 3% O2 assay Independent t-test p = 0.016																	
4hrs						**12 hrs**						**24hrs**					
MAFB	0.711	0.014	0.037	-0.068	0.096	MAFB	0.959	-0.002	0.037	-0.084	0.08	MAFB	0.373	-0.034	0.037	-0.117	0.048
GCG	0.722	0.076	0.208	-0.387	0.539	GCG	0.098	0.380	0.208	-0.083	0.843	GCG	0.653	-0.096	0.208	-0.559	0.367
SST	***0.000***	***0.096***	***0.018***	***0.056***	***0.137***	SST	0.249	0.025	0.021	-0.021	0.071	SST	***0.000***	***0.139***	***0.018***	***0.099***	***0.178***
ARNT	0.899	0.003	0.021	-0.044	0.049	ARNT	0.246	0.027	0.022	-0.022	0.076	ARNT	0.844	0.004	0.022	-0.044	0.053
DDIT3	0.458	0.029	0.038	-0.055	0.113	DDIT3	0.805	-0.010	0.040	-0.100	0.08	DDIT3	0.248	-0.054	0.044	-0.151	0.044
ARX	0.118	0.057	0.033	-0.017	0.132	ARX	*0.018*	*-0.102*	*0.036*	*-0.183*	-0.022	ARX	0.383	-0.035	0.039	-0.122	0.051
GCK	***0.001***	***0.159***	***0.036***	***0.079***	***0.239***	GCK	***0.000***	***0.360***	***0.019***	***0.316***	***0.405***	GCK	***0.000***	***0.415***	***0.030***	***0.349***	***0.482***
HIF1A	0.245	0.036	0.029	-0.029	0.1	HIF1A	0.314	-0.032	0.030	-0.099	0.035	HIF1A	***0.008***	***-0.108***	***0.032***	***-0.181***	***-0.036***
MYC	***0.004***	***0.170***	***0.044***	***0.071***	***0.268***	MYC	0.689	0.019	0.045	-0.083	0.121	MYC	0.918	0.008	0.077	-0.163	0.18
SLC2A2	***0.002***	***0.088***	***0.022***	***0.040***	***0.137***	SLC2A2	***0.001***	***0.092***	***0.020***	***0.048***	***0.135***	SLC2A2	0.063	-0.159	0.046	-0.338	0.019
SOX9	0.335	0.126	0.125	-0.152	0.404	SOX9	0.453	0.120	0.153	-0.222	0.462	SOX9	***0.000***	***0.659***	***0.123***	***0.386***	***0.933***
PTPN1	*0.049*	*-0.065*	*0.029*	*-0.130*	*0.001*	PTPN1	0.070	-0.203	0.062	-0.442	0.036	PTPN1	0.315	-0.255	0.193	-1.074	0.563
PAX4	***0.001***	***-0.097***	***0.021***	***-0.144***	***-0.05***	PAX4	0.151	-0.106	0.049	-0.297	0.086	PAX4	0.057	-0.196	0.053	-0.407	0.014
STK11	0.145	-0.334	0.144	-0.948	0.28	STK11	0.121	-0.119	0.052	-0.336	0.078	STK11	***0.000***	***-0.341***	***0.021***	***-0.244***	***-0.149***

Hypoxia 1% O2 assay Independent Samples Test p= 0.016																
4hrs						12hrs						24 hours				
Gene	*P* value	Mean diff.	SED	95% CI		Gene	*P* value	Mean diff.	SED	95% CI		Gene	*P* value	Mean diff.	SED	95% CI	
				Lower	Upper					Lower	Upper					Lower	Upper
NGN3	*0.017*	*-0.080*	*0.028*	*-0.143*	-0.017	NGN3	0.555	-0.080	0.653	-2.350	3.268	NGN3	0.566	-0.077	0.096	-1.212	1.058
NANOG	0.145	-0.072	0.046	-0.175	0.03	NANOG	***0.001***	***-0.072***	***0.051***	***-0.343***	***-0.115***	NANOG	0.799	-0.015	0.056	-0.140	0.111
POU5F1	*0.044*	*-0.120*	*0.052*	*-0.237*	-0.004	POU5F1	***0.001***	***-0.120***	***0.066***	***-0.466***	***-0.174***	POU5F1	0.225	-0.083	0.063	-0.226	0.061
INS	***0.007***	***-0.299***	***0.088***	***-0.495***	***-0.104***	INS	0.094	-0.299	0.087	-0.353	0.033	INS	*0.045*	*-0.202*	*0.087*	*-0.400*	-0.005
PDX1	***0.000***	***-0.375***	***0.046***	***-0.479***	***-0.272***	PDX1	***0.000***	***-0.375***	***0.059***	***-0.464***	***-0.201***	PDX1	***0.001***	***-0.271***	***0.051***	***-0.388***	***-0.155***
PAX6	***0.001***	***-0.204***	***0.044***	***-0.303***	***-0.105***	PAX6	***0.000***	***-0.204***	***0.046***	***-0.637***	***-0.434***	PAX6	***0.000***	***-0.371***	***0.050***	***-0.484***	***-0.258***
SLC16A1	***0.000***	***-0.251***	***0.044***	***-0.349***	***-0.152***	SLC16A1	***0.000***	***-0.251***	***0.045***	***-0.611***	***-0.41***	SLC16A1	***0.007***	***-0.178***	***0.052***	***-0.295***	***-0.061***
FOXO1	*0.017*	*0.196*	*0.068*	*0.044*	0.348	FOXO1	0.566	0.196	0.064	-0.181	0.105	FOXO1	*0.041*	*-0.217*	*0.091*	*-0.424*	-0.011
NEUROD1	0.483	0.048	0.066	-0.100	0.196	NEUROD1	0.895	0.048	0.072	-0.170	0.151	NEUROD1	0.111	-0.159	0.090	-0.363	0.044
NKX2-2	0.161	0.105	0.069	-0.050	0.26	NKX2-2	0.502	0.105	0.117	-0.354	0.539	NKX2-2	0.155	-0.114	0.073	-0.282	0.053
SYP	***0.011***	***0.175***	***0.055***	***0.050***	***0.299***	SYP	0.831	0.175	0.077	-0.158	0.191	SYP	0.757	0.020	0.063	-0.165	0.125
NKX6-1	***0.011***	***0.302***	***0.098***	***0.085***	***0.519***	NKX6-1	0.440	0.302	0.113	-0.343	0.161	NKX6-1	0.365	-0.114	0.119	-0.384	0.156
MAFA	0.347	0.045	0.046	-0.057	0.147	MAFA	0.306	0.045	0.453	-1.322	2.557	MAFA	0.453	1.090	0.939	-10.80	12.98
LDHA	***0.000***	***0.253***	***0.027***	***0.193***	***0.312***	LDHA	***0.000***	***0.253***	***0.053***	***0.335***	***0.572***	LDHA	***0.000***	***0.539***	***0.031***	***0.469***	***0.609***
MAFB	0.643	0.021	0.043	-0.117	0.076	MAFB	***0.016***	***0.021***	***0.054***	***-0.275***	***-0.036***	MAFB	0.186	0.069	0.049	-0.180	0.04

Hypoxia 1% O2 assay Independent Samples Test p= 0.016																	
4hrs						**12hrs**							**24 hours**				
GCG	0.827	0.047	0.210	-0.422	0.516	GCG	0.402	0.047	0.209	-0.283	0.648	GCG	0.117	-0.445	0.257	-1.027	0.136
SST	0.088	0.134	0.045	-0.047	0.315	SST	0.928	0.134	0.097	-0.398	0.418	SST	*0.029*	*0.057*	*0.022*	*0.007*	0.108
ARNT	0.649	0.014	0.029	-0.051	0.079	ARNT	0.535	0.014	0.085	-0.414	0.289	ARNT	0.856	0.021	0.093	-1.073	1.116
DDIT3	*0.029*	*0.101*	*0.040*	*0.013*	0.189	DDIT3	***0.000***	***0.101***	***0.052***	***0.240***	***0.47***	DDIT3	*0.026*	*0.122*	*0.046*	*0.018*	0.227
ARX	0.090	-0.102	0.055	-0.225	0.019	ARX	0.099	-0.102	0.081	-0.542	0.095	ARX	***0.000***	***-0.270***	***0.051***	***-0.386***	***-0.155***
GCK	***0.000***	***0.272***	***0.029***	***0.208***	***0.338***	GCK	*0.034*	*0.272*	*0.088*	*0.079*	0.792	GCK	***0.000***	***0.337***	***0.017***	***0.300***	***0.375***
HIF1A	0.311	0.046	0.043	-0.050	0.143	HIF1A	***0.005***	***0.046***	***0.041***	***-0.240***	***-0.057***	HIF1A	***0.000***	***0.301***	***0.037***	***-0.385***	***-0.219***
MYC	0.757	0.051	0.147	-0.518	0.621	MYC	0.185	0.051	0.076	-0.061	0.277	MYC	***0.000***	***0.528***	***0.083***	***0.341***	***0.715***
SLC2A2	0.369	0.069	0.062	-0.181	0.321	SLC2A2	0.244	0.069	0.123	-0.721	0.321	SLC2A2	***0.000***	***-0.232***	***0.025***	***-0.288***	***-0.177***
SOX9	0.757	0.041	0.129	-0.246	0.328	SOX9	***0.002***	***0.041***	***0.147***	***0.324***	***0.987***	SOX9	***0.000***	***1.090***	***0.145***	***0.763***	***1.418***
PTPN1	***0.000***	***-0.146***	***0.029***	***-0.210***	***-0.082***	PTPN1	*0.024*	*-0.146*	*0.084*	*-0.826*	*-0.152*	PTPN1	***0.000***	***-0.289***	***0.037***	***-0.373***	***-0.207***
PAX4	***0.000***	***-0.144***	***0.025***	***-0.200***	***-0.089***	PAX4	*0.050*	*-0.144*	*0.094*	*-0.786*	*-0.001*	PAX4	0.077	-0.665	0.086	-1.673	0.342
STK11	***0.004***	***-0.109***	***0.029***	***-0.174***	***-0.044***	STK11	0.079	-0.109	0.075	-0.556	*0.067*	STK11	***0.000***	***-0.156***	***0.023***	***-0.209***	***-0.104***

Lipotoxicity 0.5 mM Independent Samples Test p = 0.016																	
12hrs						**24hrs**						**48hrs**					
Gene	***P* value**	**Mean diff.**	**SED**	**95% CI**		**Gene**	***P* value**	**Mean diff.**	**SED**	**95% CI**		**Gene**	***P* value**	**Mean. Diff.**	**SED**	**95% CI**	
				Lower	**Upper**					**Lower**	**Upper**					**Lower**	**Upper**
FOXO1	0.909	-0.005	0.049	-0.114	0.103	FOXO1	0.077	-0.104	0.053	-0.222	0.013	FOXO1	0.492	-0.036	0.051	-0.078	0.151
INS	0.591	0.049	0.089	-0.150	0.249	INS	***0.001***	***0.412***	***0.094***	***0.203***	***0.623***	INS	0.531	0.072	0.112	-0.176	0.321
PDX1	***0.014***	***-0.199***	***0.067***	***-0.349***	***-0.050***	PDX1	*0.017*	*0.158*	*0.055*	*0.035*	*0.282*	PDX1	0.464	0.044	0.057	-0.084	0.171
NEUROD 1	0.652	0.016	0.035	-0.061	0.094	NEUROD1	0.583	-0.021	0.037	-0.103	0.061	NEUROD1	***0.000***	***0.357***	***0.032***	***0.285***	***0.429***
SLC16A1	***0.000***	***0.162***	***0.023***	***0.112***	***0.212***	SLC16A1	0.189	-0.040	0.029	-0.104	0.023	SLC16A1	0.08	-0.047	0.024	-0.100	0.007
SYP	0.984	-0.015	0.737	-1.658	1.627	SYP	0.944	0.052	0.738	-1.591	1.696	SYP	*0.047*	*1.668*	*0.738*	*0.024*	*3.313*
GCK	0.285	-0.056	0.050	-0.167	0.055	GCK	***0.007***	***-0.166***	***0.050***	***-0.277***	***-0.056***	GCK	***0.000***	***0.787***	***0.050***	***0.676***	***0.898***
MAFA	0.065	-0.085	0.041	-0.178	0.006	MAFA	0.185	-0.064	0.045	-0.165	0.036	MAFA	***0.000***	***0.636***	***0.039***	***0.550***	***0.724***
NKX2.2	0.090	*-0.106*	0.057	-0.233	0.020	NKX2.2	0.818	0.013	0.057	-0.114	0.141	NKX2.2	***0.003***	***-0.224***	***0.058***	***-0.353***	***-0.096***
LDHA	0.837	-0.008	0.039	-0.095	0.079	LDHA	0.347	0.037	0.038	-0.048	0.123	LDHA	***0.000***	***-0.295***	***0.037***	***-0.378***	***-0.214***
MAFB	0.085	*-0.203*	0.068	-0.470	0.063	MAFB	***0.008***	***-0.096***	***0.029***	***-0.161***	***-0.031***	MAFB	0.225	0.123	0.073	-0.170	0.416
NKX6.1	***0.010***	***-0.149***	***0.047***	***-0.254***	***-0.044***	NKX6.1	*0.044*	*0.108*	*0.047*	*0.004*	*0.214*	NKX6.1	***0.000***	***-0.347***	***0.049***	***-0.455***	***-0.239***
ARNT	***0.010***	***0.102***	***0.032***	***0.031***	***0.175***	ARNT	0.055	-0.071	0.033	-0.144	0.002	ARNT	***0.000***	***-0.165***	***0.032***	***-0.237***	***-0.095***

Lipotoxicity 0.5 mM Independent Samples Test p = 0.016																	
12hrs						24hrs						48hrs					
PAX4	0.431	0.057	0.070	-0.098	0.212	PAX4	0.213	0.099	0.075	-0.067	0.265	PAX4	***0.000***	***1.251***	***0.068***	***1.100***	***1.404***
SST	***0.001***	***0.183***	***0.041***	***0.093***	***0.274***	SST	*0.021*	*0.117*	*0.043*	*0.022*	*0.213*	SST	***0.000***	***-0.500***	***0.046***	***-0.603***	***-0.398***
DDIT3	0.893	-0.004	0.035	-0.083	0.074	DDIT3	***0.000***	***-0.261***	***0.044***	***-0.359***	***-0.164***	DDIT3	***0.000***	***-1.320***	***0.042***	***-1.415***	***-1.226***
GCG	*0.026*	*-0.173*	*0.066*	*-0.321*	*-0.026*	GCG	***0.000***	***-0.503***	***0.065***	***-0.649***	***-0.358***	GCG	***0.000***	***1.209***	***0.067***	***1.061***	***1.359***
PAX6	0.331	-0.049	0.048	-0.156	0.058	PAX6	*0.047*	*-0.108*	*0.048*	*-0.215*	*-0.002*	PAX6	***0.009***	***0.176***	***0.055***	***0.054***	***0.300***
MYC	***0.005***	***0.421***	***0.117***	***0.161***	***0.681***	MYC	0.154	0.156	0.102	-0.070	0.384	MYC	***0.001***	***-0.588***	***0.103***	***-0.739***	***-0.279***
NANOG	0.796	-0.020	0.077	-0.192	0.151	NANOG	0.374	-0.072	0.078	-0.246	0.101	NANOG	***0.000***	***-0.669***	***0.084***	***-0.858***	***-0.482***
SLC2A2	***0.014***	***-0.104***	***0.035***	***-0.183***	***-0.026***	SLC2A2	*0.440*	*0.106*	*0.113*	*-0.353*	*0.566*	SLC2A2	***0.000***	***-0.228***	***0.037***	***-0.311***	***-0.147***
HIF1A	*0.023*	*-0.084*	*0.030*	*-0.154*	*-0.015*	HIF1A	*0.022*	*-0.205*	*0.076*	*-0.374*	*-0.037*	HIF1A	0.301	-0.062	0.057	-0.190	0.065
PTPN1	0.570	0.015	0.027	-0.044	0.075	PTPN1	0.089	-0.047	0.025	-0.104	0.009	PTPN1	***0.004***	***0.111***	***0.030***	***0.045***	***0.177***
STK11	0.509	0.036	0.053	-0.081	0.153	STK11	0.534	-0.038	0.059	-0.170	0.094	STK11	0.211	-0.070	0.053	-0.188	0.047
ARX	0.612	0.043	0.083	-0.142	0.229	ARX	0.053	0.176	0.080	-0.003	0.355	ARX	0.339	-0.075	0.075	-0.242	0.091
SLC2A4	0.382	-0.113	0.124	-0.163	0.389	SLC2A4	0.197	*0.158*	0.115	-0.097	0.414	SLC2A4	0.288	0.136	0.122	-0.135	0.409
SOX9	0.255	0.136	0.113	-0.115	0.387	SOX9	***0.012***	***0.329***	***0.107***	***0.091***	***0.567***	SOX9	***0.000***	***-1.430***	***0.120***	***-1.699***	***-1.162***
HES1	***0.013***	***-0.208***	***0.069***	***-0.363***	***-0.054***	HES1	*0.22*	*0.082*	*0.063*	*-0.058*	*0.223*	HES1	*0.019*	*-1.738*	*0.254*	*-2.801*	*-0.676*
NGN3	***0.004***	***0.165***	***0.044***	***0.067***	***0.264***	NGN3	***0.001***	***0.212***	***0.044***	***0.115***	***0.310***	NGN3	***0.000***	***0.338***	***0.045***	***0.237***	***0.440***
POU5F1	*0.024*	*0.165*	*0.062*	*0.026*	*0.304*	POU5F1	***0.015***	***-0.187***	***0.064***	***-0.331***	***-0.044***	POU5F1	*0.043*	*0.146*	*0.063*	*0.005*	*0.288*

Cytokine assay TNFα INFγ and IL1β Independent Samples Test p = 0.025																	
12 hours						24 hours						36 hours					
Gene	***P* valu e**	**Mean diff.**	**SED.**	**95% CI**		**Gene**	***P* value**	**Mean diff.**	**SED.**	**95% CI**		**Gene**	***P* value**	**Mean diff.**	**SED**	**95% CI**	
				Lower	**Upper**					**Lower**	**Upper**					**Lower**	**Upper**
FOXO1	0.244	-0.060	0.049	-0.168	0.048	FOXO1	*0.021*	*-0.168*	*0.062*	*-0.305*	*-0.031*	FOXO1	***0.000***	***-0.258***	***0.050***	***-0.369***	***-0.146***
INS	***0.014***	***0.149***	***0.050***	***0.037***	***0.262***	INS	0.837	0.009	0.045	-0.090	0.109	INS	0.211	-0.162	0.093	-0.527	0.202
PDX1	0.232	-0.058	0.046	-0.162	0.044	PDX1	*0.045*	*0.109*	*0.048*	*0.003*	*0.217*	PDX1	0.923	0.005	0.048	-0.102	0.112
NEUROD1	0.173	0.099	0.067	-0.051	0.250	NEUROD1	0.697	-0.026	0.067	-0.176	0.123	NEUROD1	0.209	-0.154	0.115	-0.409	0.101
SLC16A1	***0.000***	***-0.166***	***0.021***	***-0.214***	***-0.120***	SLC16A1	***0.000***	***-0.354***	***0.022***	***-0.403***	***-0.305***	SLC16A1	***0.000***	***-0.278***	***0.046***	***-0.380***	***-0.176***
SYP	0.518	-0.051	0.077	-0.224	0.120	SYP	0.68	0.023	0.055	-0.099	0.146	SYP	0.067	0.115	0.056	-0.010	0.241
GCK	*0.034*	*0.304*	*0.124*	*0.029*	*0.580*	GCK	0.62	-0.063	0.124	-0.340	0.213	GCK	0.793	-0.033	0.123	-0.308	0.242
MAFA	0.275	-0.118	0.103	-0.347	0.110	MAFA	0.152	-0.158	0.103	-0.388	0.070	MAFA	0.181	-0.151	0.105	-0.384	0.083
NKX2.2	***0.004***	***-0.221***	***0.060***	***-0.355***	***-0.088***	NKX2.2	0.042	-0.215	0.093	-0.423	-0.009	NKX2.2	0.253	-0.073	0.060	-0.208	0.061
LDHA	*0.028*	*-0.122*	*0.048*	*-0.229*	*-0.016*	LDHA	0.334	0.048	0.047	-0.057	0.154	LDHA	0.994	0.000	0.057	-0.129	0.128
MAFB	*0.042*	*-0.093*	*0.040*	*-0.182*	*-0.004*	MAFB	*0.027*	*-0.105*	*0.041*	*-0.197*	*-0.015*	MAFB	***0.001***	***-0.179***	***0.040***	***-0.268***	***-0.091***
NKX6.1	***0.003***	***-0.304***	***0.079***	***-0.480***	***-0.130***	NKX6.1	0.62	0.041	0.082	-0.140	0.224	NKX6.1	0.714	-0.030	0.078	-0.204	0.145
ARNT	0.086	-0.124	0.065	-0.269	0.021	ARNT	0.311	0.061	0.057	-0.067	0.189	ARNT	0.611	0.036	0.068	-0.116	0.187
PAX4	*0.021*	*0.368*	*0.134*	*0.069*	*0.667*	PAX4	0.316	0.141	0.134	-0.157	0.439	PAX4	0.300	0.147	0.134	-0.152	0.446

Cytokine assay TNFα INFγ and IL1β Independent Samples Test p = 0.025																	
12 hours						24 hours						36 hours					
SST	0.182	-0.143	0.100	-0.366	0.079	SST	0.398	0.086	0.098	-0.132	0.305	SST	0.952	0.006	0.098	-0.212	0.224
DDIT3	0.166	-0.318	0.206	-0.769	0.151	DDIT3	0.956	0.012	0.213	-0.463	0.487	DDIT3	0.219	0.270	0.206	-0.188	0.728
GCG	0.135	0.412	0.254	-0.153	0.979	GCG	0.172	-0.372	0.253	-0.935	0.191	GCG	0.278	-0.291	0.254	-0.856	0.274
PAX6	0.469	0.055	0.074	-0.109	0.220	PAX6	0.625	0.037	0.075	-0.129	0.205	PAX6	0.314	0.078	0.074	-0.086	0.242
MYC	***0.003***	***-0.452***	***0.118***	***-0.715***	***-0.189***	MYC	0.84	0.028	0.136	-0.274	0.330	MYC	0.066	-0.252	0.122	-0.525	0.020
NANOG	0.112	-0.183	0.105	-0.418	0.051	NANOG	0.379	*0.097*	0.106	-0.139	0.335	NANOG	0.372	0.100	0.107	-0.138	0.338
SLC2A2	***0.014***	***0.181***	***0.061***	***0.046***	***0.316***	SLC2A2	0.41	0.061	0.072	-0.098	0.222	SLC2A2	*0.031*	*0.163*	*0.065*	*0.018*	*0.307*
HIF1A	***0.008***	***-0.097***	***0.030***	***-0.164***	***-0.031***	HIF1A	*0.024*	*-0.088*	*0.033*	*-0.162*	*-0.014*	HIF1A	0.104	-0.158	0.060	-0.386	0.071
PTPN1	***0.007***	***0.121***	***0.035***	***0.042***	***0.201***	PTPN1	0.162	0.055	0.037	-0.026	0.137	PTPN1	***0.009***	***0.123***	***0.038***	***0.037***	***0.208***
STK11	0.346	-0.045	0.046	-0.147	0.057	STK11	0.229	*-0.056*	0.044	-0.154	0.042	STK11	0.145	0.066	0.042	-0.027	0.159
ARX	0.194	-0.180	0.099	-0.561	0.199	ARX	***0.001***	***-0.224***	***0.051***	***-0.337***	***-0.111***	ARX	*0.041*	*-0.125*	*0.053*	*-0.244*	*-0.006*
SLC2A4	0.336	0.119	0.118	-0.144	0.384	SLC2A4	0.984	-0.005	0.263	-1.033	1.022	SLC2A4	*0.029*	*-0.369*	*0.144*	*-0.690*	*-0.047*
SOX9	0.086	-0.591	0.310	-1.282	0.100	SOX9	0.233	-0.396	0.312	-1.093	0.299	SOX9	0.974	0.011	0.317	-0.695	0.716
HES1	0.238	-0.422	0.337	-1.173	0.328	HES1	0.611	0.177	0.338	-0.575	0.931	HES1	0.712	0.128	0.338	-0.624	0.880
NGN3	***0.14***	***-0.141***	***0.088***	***-0.338***	***0.055***	NGN3	0.258	0.105	0.088	-0.090	0.301	NGN3	*0.020*	*0.239*	*0.087*	*0.046*	*0.432*
POU5F1	0.102	0.093	0.052	-0.022	0.208	POU5F1	*0.049*	*-0.072*	*0.032*	*-0.146*	*0.000*	POU5F1	***0.010***	***-0.096***	***0.030***	***-0.164***	***-0.029***

Tunicamycin Induced ER stress. Independent Samples Test *p*=0.025					
24 hrs 0.5 mM tunicamycin					
Gene	***P* value**	**Mean diff.**	**SED**		**95% CI**
				Lower	**Upper**
ARNT	0.642	0.017	0.036	-0.081	0.117
ARX	*0.033*	*0.662*	*0.208*	*0.085*	*1.239*
DDIT3	*0.033*	*0.387*	*0.121*	*0.052*	*0.722*
FOXO1	***0.013***	***-0.216***	***0.051***	***-0.357***	***-0.075***
GCG	0.931	-0.025	0.272	-0.781	0.730
GCK	0.081	-0.174	0.075	-0.384	0.035
HHEX	0.115	0.499	0.248	-0.190	1.189
INS	0.448	-0.041	0.05	-0.180	0.096
LDHA	0.226	0.028	0.02	-0.027	0.083
MAFA	*0.050*	*-0.319*	*0.115*	*-0.640*	*0.001*
MAFB	0.085	-0.086	0.038	-0.193	0.019
NANOG	0.274	-0.068	0.054	-0.217	0.081
ND1	0.857	-0.008	0.044	-0.130	0.113
NKX2-2	***0.005***	***0.100***	***0.018***	***0.049***	***0.152***
NKX6-1	0.099	0.174	0.06	-0.080	0.429
PAX4	*0.049*	*-0.345*	*0.123*	*-0.689*	**-0.003**
PAX6	0.161	-0.144	0.084	-0.379	0.089

Tunicamycin Induced ER stress. Independent Samples Test *p*=0.025					
24 hrs 0.5 mM tunicamycin					
PDX1	0.058	-0.216	0.082	-0.444	0.012
POU5F1	0.639	-0.068	0.136	-0.447	0.309
SLC16A1	0.351	-0.053	0.051	-0.195	0.088
SOX9	0.145	0.393	0.218	-0.211	0.998
SST	0.111	0.325	0.16	-0.118	0.770
STK11	0.165	-0.129	0.077	-0.343	0.083
SYP	0.056	-0.110	0.041	-0.226	0.005

Supplementary table S7: Effects of cell insult treatments on splicing factor expression.

The p values for statistical significance as determined by independent t-test, Mean difference, Standard errors of measurement (SED) and the 95% confidence intervals are given below. ***Bold italic p=<0.01 and p=<0.050*** *Bonferroni correction for 5 tests: Control vs high glucose, control vs low glucose, control versus <3% O2, control versus pro-inflammatory cytokines and control versus 'rescue'. Gene list is á priori so no further corrections. A separate control for 0.5 mM Palmitic Acid was used to account for EtOH carrier. p value for this assay was 0.050 as no correction for multiple testing was required. Italic and underlined. P=<0.050 No correction for multiple testing*

25 mM high glucose Independent Samples Test p=0.01					
				95% CI	
	P value	Mean Difference	Std. Error Difference	Lower	Upper
AKAP17A	0.538	0.035	0.052	0.109	-0.179
HNRNPA0	0.816	-0.016	0.063	-0.189	0.158
HNRNPA1	0.872	0.004	0.021	-0.055	0.062
HNRNPA2B1	***0.006***	***0.176***	***0.033***	***0.084***	***0.268***
HNRNPD	0.667	0.083	0.180	-0.416	0.583
HNRNPH3	0.243	0.086	0.063	-0.089	0.262
HNRNPK	0.800	-0.014	0.054	-0.163	0.134
HNRNPM	0.790	0.038	0.135	-0.337	0.414
HNRNPUL2	0.586	0.030	0.050	-0.110	0.170
IMP3	0.364	0.064	0.063	-0.110	0.239
LSM14A	0.461	0.050	0.061	-0.120	0.219
LSM2	0.503	-0.445	0.605	-2.124	1.234
PNISR	0.062	0.114	0.044	-0.009	0.237
SF3B1	0.444	0.069	0.081	-0.156	0.294
SRSF1	0.537	0.025	0.037	-0.078	0.129
SRSF2	0.052	0.142	0.052	-0.002	0.286
SRSF3	0.117	0.090	0.045	-0.035	0.216
SRSF6	0.653	-0.020	0.040	-0.132	0.093
SRSF7	0.280	-0.079	0.063	-0.253	0.096
TRA2B	0.154	0.135	0.077	-0.079	0.348

2.5 mM low glucose Independent Samples Test p=0.01					
				95% CI	
	P value	Mean Difference	Std. Error Difference	Lower	Upper
AKAP17A	*0.029*	*0.159*	*0.048*	*0.026*	*0.291*
HNRNPA0	*0.022*	*0.103*	*0.028*	*0.024*	*0.181*
HNRNPA1	0.242	0.159	0.098	-0.250	0.567
HNRNPA2B1	***0.004***	***0.179***	***0.030***	***0.097***	***0.262***
HNRNPD	*0.047*	*-0.374*	*0.132*	*-0.741*	*-0.007*
HNRNPH3	0.154	0.105	0.060	-0.061	0.271
HNRNPK	0.063	0.069	0.027	-0.006	0.144
HNRNPM	0.879	0.022	0.128	-0.513	0.557
HNRNPUL2	0.471	0.022	0.027	-0.054	0.097
IMP3	0.217	0.028	0.019	-0.025	0.081
LSM14A	***0.004***	***0.109***	***0.019***	***0.057***	***0.160***
LSM2	0.290	-0.712	0.505	-2.812	1.388
PNISR	***0.005***	***0.202***	***0.036***	***0.100***	***0.303***
SF3B1	*0.047*	*0.202*	*0.071*	*0.005*	*0.399*
SRSF1	***0.001***	***0.107***	***0.012***	***0.072***	***0.141***
SRSF2	*0.015*	*0.285*	*0.069*	*0.093*	*0.476*
SRSF3	***0.009***	***0.141***	***0.030***	***0.059***	***0.223***
SRSF6	***0.001***	***0.201***	***0.021***	***0.143***	***0.259***
SRSF7	0.667	0.026	0.055	-0.128	0.179
TRA2B	0.776	0.016	0.052	-0.128	0.159

Hypoxia Independent Samples Test p=0.01					
				95% CI	
	P value	Mean Difference	Std. Error Difference	Lower	Upper
AKAP17A	0.034	0.190	0.060	0.023	0.357
HNRNPA0	0.291	0.029	0.024	-0.038	0.096
HNRNPA1	0.011	-0.098	0.022	-0.158	-0.038
HNRNPA2B1	**0.004**	**0.120**	**0.020**	**0.064**	**0.175**
HNRNPD	0.140	-0.367	0.200	-0.921	0.187
HNRNPH3	0.098	0.126	0.059	-0.037	0.289
HNRNPK	0.056	0.071	0.027	-0.003	0.146
HNRNPM	0.884	0.021	0.132	-0.345	0.386
HNRNPUL2	0.564	0.017	0.027	-0.058	0.092
IMP3	0.274	0.021	0.016	-0.025	0.067
LSM14A	**0.004**	**0.139**	**0.023**	**0.076**	**0.201**
LSM2	0.252	-0.794	0.508	-2.861	1.274
PNISR	**0.007**	**0.234**	**0.046**	**0.107**	**0.362**
SF3B1	0.018	0.201	0.052	0.058	0.345
SRSF1	0.024	0.056	0.016	0.012	0.100
SRSF2	0.094	0.245	0.112	-0.066	0.555
SRSF3	**0.001**	**0.160**	**0.018**	**0.111**	**0.209**
SRSF6	**0.003**	**0.190**	**0.030**	**0.106**	**0.275**
SRSF7	0.994	-0.000	0.054	-0.151	0.150
TRA2B	0.715	-0.020	0.051	-0.162	0.122

Lipotoxicity Independent Samples Test p=0.01					
	P value	Mean Difference	Std. Error Difference	95% CI	
				Lower	Upper
AKAP17A	0.127	0.126	0.066	-0.056	0.309
HNRNPA0	0.288	-0.051	0.042	-0.167	0.065
HNRNPA1	0.065	-0.039	0.016	-0.083	0.004
HNRNPA2B1	0.824	-0.014	0.060	-0.179	0.151
HNRNPD	0.749	-0.074	0.214	-0.669	0.522
HNRNPH3	0.146	0.119	0.066	-0.064	0.302
HNRNPK	0.749	0.011	0.033	-0.081	0.104
HNRNPM	0.967	0.006	0.133	-0.364	0.376
HNRNPUL2	0.453	0.025	0.030	-0.058	0.107
IMP3	**0.006**	**0.084**	**0.016**	**0.039**	**0.128**
LSM14A	0.668	0.012	0.026	-0.060	0.084
LSM2	0.438	0.533	0.620	-1.189	2.256
PNISR	0.277	-0.046	0.037	-0.148	0.056
SF3B1	0.270	-0.088	0.069	-0.279	0.103
SRSF1	0.743	-0.005	0.013	-0.040	0.031
SRSF2	0.639	-0.033	0.064	-0.211	0.146
SRSF3	0.034	-0.096	0.031	-0.181	-0.012
SRSF6	0.762	0.012	0.036	-0.089	0.112
SRSF7	0.837	-0.013	0.059	-0.177	0.151
TRA2B	0.118	-0.106	0.053	-0.254	0.042

Cytokine assay Independent Samples Test *p*=0.01					
	P value	Mean Difference	Std. Error Difference	95% CI	
				Lower	Upper
AKAP17A	**0.002**	**0.240**	**0.032**	**0.151**	**0.329**
HNRNPA0	0.264	0.038	0.030	-0.044	0.120
HNRNPA1	0.162	0.025	0.015	-0.016	0.066
HNRNPA2B1	**0.001**	**0.217**	**0.024**	**0.151**	**0.282**
HNRNPD	0.056	-0.364	0.136	-0.743	0.014
HNRNPH3	0.053	0.143	0.053	-0.003	0.289
HNRNPK	0.033	0.087	0.027	0.012	0.163
HNRNPM	0.179	0.221	0.136	-0.156	0.597
HNRNPUL2	0.656	-0.013	0.027	-0.087	0.061
IMP3	0.736	-0.004	0.011	-0.035	0.027
LSM14A	**0.003**	**0.118**	**0.018**	**0.068**	**0.167**
LSM2	0.253	-0.790	0.508	-2.860	1.281
PNISR	**0.003**	**0.243**	**0.039**	**0.135**	**0.351**
SF3B1	0.030	0.168	0.051	0.026	0.309
SRSF1	**0.000**	**0.117**	**0.009**	**0.093**	**0.141**
SRSF2	**0.006**	**0.274**	**0.051**	**0.134**	**0.414**
SRSF3	**0.002**	**0.185**	**0.027**	**0.110**	**0.260**
SRSF6	0.113	0.058	0.029	-0.021	0.137
SRSF7	0.370	-0.046	0.046	-0.172	0.081
TRA2B	0.867	0.009	0.050	-0.131	0.149

Supplementary table S8: Effects of cell insult treatments on alternatively spliced gene expression.

The p values for statistical significance as determined by independent t-test, Mean difference, Standard errors of measurement (SED) and the 95% confidence intervals are given below. ***Bold italic p=<0.016*** *Bonferroni correction for 3 tests: 1st, 2nd and 3rd time-points. Gene list is á priori so no further corrections. Italic underlined p=<0.050. No correction for multiple testing*

25 mM high glucose Independent Samples Test *p*=0.016																	
	p value	Mean Diff.	SED	95% CI			*p* value	Mean diff	SED	95% CI			*p* value	Mean diff.	SED	95% CI	
				Lower	Upper					Lower	Upper					Lower	Upper
INS	0.619	-.0854	0.149	-0.493	0.664	*INS*	0.184	0.139	0.098	-0.357	0.078	*INS*	0.167	-0.122	0.082	-0.061	0.306
NANOG	0.571	-0.653	0.111	-0.183	0.314	*NANOG*	0.962	0.005	0.107	-0.244	0.234	*NANOG*	0.595	-0.059	0.108	-0.181	0.300
PAX6	***0.007***	***0.494***	***0.147***	***-0.822***	***-0.166***	*PAX6*	***0.002***	***-0.357***	***0.082***	***0.169***	***0.546***	*PAX6*	***0.003***	***1.278***	***0.332***	***-2.018***	***-0.539***
PTPN1	*0.045*	*0.398*	*0.174*	*-0.787*	*-0.011*	*PTPN1*	***0.011***	***-0.417***	***0.125***	***0.126***	***0.708***	*PTPN1*	***0.003***	***0.974***	***0.256***	***-1.545***	***-0.404***
POU5F1	***0.004***	***0.277***	***0.075***	***-0.445***	***-0.111***	*POU5F1*	***0.014***	***-0.173***	***0.058***	***0.044***	***0.303***	*POU5F1*	0.139	-0.090	0.056	-0.035	0.215

2.5 mM low glucose Independent Samples Test *p*=0.016																	
	p value	Mean Diff.	SED	95% CI			*p* value	Mean diff.	SED	95% CI			*p* value	Mean diff.	SED	95% CI	
				Lower	Upper					Lower	Upper					Lower	Upper
INS	0.135	-0.196	0.121	-0.073	0.465	*INS*	0.631	-0.086	0.156	-0.524	0.697	*INS*	0.631	-0.179	0.156	-0.524	0.697
NANOG	0.728	-0.038	0.108	-0.201	0.279	*NANOG*	0.694	0.045	0.111	-0.293	0.203	*NANOG*	0.694	-0.128	0.111	-0.293	0.203
PAX6	0.895	0.027	0.202	-0.477	0.423	*PAX6*	0.920	0.015	0.148	-0.345	0.315	*PAX6*	0.920	2.090	0.148	-0.345	0.315
PTPN1	0.072	0.379	0.189	-0.800	0.041	*PTPN1*	0.821	-0.040	0.173	-0.345	0.426	*PTPN1*	0.821	0.442	0.173	-0.345	0.426
POU5F1	0.304	0.202	0.151	-0.807	0.403	*POU5F1*	***0.005***	***0.238***	***0.066***	***-0.385***	***-0.093***	*POU5F1*	***0.005***	***0.017***	***0.066***	***-0.385***	***-0.093***

<3% O2 Hypoxic conditions Independent Samples Test *p*=0.016																	
	p value	Mean diff.	SED	95% CI			*p* value	Mean diff.	SED	95% CI			P value	Mean diff.	SED	95% CI	
				Lower	Upper					Lower	Upper					Lower	Upper
INS	*0.042*	*-0.117*	*0.052*	*-0.230*	*-0.005*	*INS*	0.624	0.030	0.061	-0.101	0.162	*INS*	***0.011***	***-0.264***	***0.084***	***-0.451***	***-0.077***
NANOG	0.955	-0.004	0.085	-0.187	0.178	*NANOG*	0.538	0.051	0.081	-0.124	0.227	*NANOG*	0.424	-0.094	0.113	-0.346	0.158
PAX6	0.357	0.073	0.077	-0.093	0.241	*PAX6*	0.901	0.010	0.083	-0.169	0.190	*PAX6*	0.510	-0.056	0.083	-0.242	0.128
PTPN1	0.784	0.049	0.174	-0.378	0.477	*PTPN1*	0.582	-0.079	0.141	-0.384	0.225	*PTPN1*	***0.005***	***0.335***	***0.092***	***0.129***	***0.541***
POU5F1	***0.007***	***-0.317***	***0.075***	***-0.504***	***-0.130***	*POU5F1*	0.112	-0.127	0.056	-0.249	-0.006	*POU5F1*	0.029	0.179	0.070	0.023	0.336

0.5 mM Palmitic Acid Independent Samples Test *p*=0.016																	
	p value	Mean diff.	SED	95% CI			*p* *value*	Mean diff	SED	95% CI			*p* value	Mean diff.	SED	95% CI	
				Lower	Upper					Lower	Upper					Lower	Upper
INS	0.036	0.091	0.038	-0.175	-0.007	*INS*	0.840	0.007	0.035	-0.085	0.071	*INS*	0.904	0.015	0.117	-0.498	0.466
NANOG	0.455	-0.244	0.314	-0.456	0.945	*NANOG*	0.313	-0.334	3.147	-0.367	0.103	*NANOG*	0.509	-0.216	0.315	-0.487	0.919
PAX6	***0.015***	***0.344***	***0.118***	***-0.606***	***-0.082***	*PAX6*	0.914	-0.128	0.117	-0.247	0.273	*PAX6*	***0.006***	***0.426***	***0.124***	***-0.702***	***-0.150***
PTPN1	0.614	-0.068	0.131	-0.224	0.362	*PTPN1*	0.308	-0.802	0.773	-0.896	0.225	*PTPN1*	0.380	-0.684	0.738	-0.101	0.238
POU5F1	0.264	0.230	0.195	-0.665	0.204	*POU5F1*	0.168	-0.288	0.194	-0.144	0.720	*POU5F1*	***0.002***	***-0.787***	***0.195***	***0.352***	***1.223***

Pro-inflammatory Cytokines Independent Samples Test *p*=0.016																	
	p value	Mean diff.	SED	95% CI			*p* value	Mean diff.	SED	95% CI			*p* value	Mean diff.	SED	95% CI	
				Lower	Upper					Lower	Upper					Lower	Upper
INS	0.945	-0.003	0.054	-0.117	0.125	*INS*	0.764	0.0143	0.046	-0.118	0.089	*INS*	0.083	0.084	0.044	-0.182	0.013
NANOG	0.138	-0.164	0.102	-0.063	0.391	*NANOG*	0.212	0.138	0.104	-0.371	0.093	*NANOG*	0.279	0.123	0.108	-0.364	0.117
PAX6	0.527	-0.340	0.519	-0.815	1.496	*PAX6*	0.529	-0.347	0.533	-0.841	1.536	*PAX6*	0.211	-0.675	0.505	-0.450	1.800
PTPN1	0.379	-0.356	7.366	-10.125	23.844	*PTPN1*	0.434	0.188	0.231	-0.703	0.326	*PTPN1*	0.218	-0.305	0.232	-0.212	0.824
POU5F1	0.508	-0.242	0.352	-0.543	1.028	*POU5F1*	***0.011***	***1.135***	***0.363***	***-1.943***	***-0.327***	*POU5F1*	***0.002***	***1.426***	***0.354***	***-2.216***	***-0.637***

Supplementary table S9: Effects of rescue from treatment with either 25 mM high glucose or 0.5 mM tunicamycin by 72 hrs restoration to normal culture media on splicing factor, total gene expression and patterns of alternative splicing.

The p values for statistical significance as determined by independent t-test, Standard errors of measurement (SED) and the 95% confidence intervals are given below. Statistically significant results are indicated in ***bold italic*** *typeface p=<0.01. Bonferroni correction for multiple testing, 5 tests. Italic underlined p=0.050 no correction for multiple testing.*

Control vs 24 hrs 25 mM glucose *p*=0.050										
Treatment 24 hrs 25 mM glucose						**Treatment and rescue**				
	P value	Mean diff	SED	95% CI		*P* value	Mean diff	SED	95% CI	
				Lower	Upper				Lower	Upper
ARX	0.620	-0.639	0.119	-0.268	0.396	0.996	-0.0008	0.150	-0.419	0.417
FOXO1	***0.010***	***-0.164***	***0.035***	***-0.262***	***-0.065***	0.157	-0.050	0.288	-0.130	0.029
GCG	0.269	-0.183	0.143	-0.214	0.581	0.832	-0.006	0.026	-0.805	0.068
GCK	***0.006***	***-0.137***	***0.026***	***0.065***	***0.210***	0.418	0.044	0.049	-0.091	0.180
Hhex	0.205	-0.226	0.149	-0.189	0.641	0.611	-0.074	0.134	-0.447	0.299
INS	0.428	-0.071	0.071	-0.235	0.375	0.967	-0.044	0.966	-0.272	0.264
MAFA	***0.020***	***-0.122***	***0.032***	***0.032***	***0.213***	0.257	0.035	0.026	-0.038	0.108
ND1	0.370	-0.255	0.022	-0.069	0.120	0.279	0.042	0.034	-0.052	0.137

Control vs 24 hrs 25 mM glucose *p*=0.050										
Treatment 24 hrs 25 mM glucose					**Treatment and rescue**					
NKX2-2	0.585	0.032	0.055	-0.186	0.121	0.424	0.345	0.247	-0.439	0.506
NKX6-1	0.436	0.050	0.058	-0.211	0.111	0.502	-0.054	0.073	-0.259	0.150
PAX4	***0.021***	***-0.170***	***0.046***	***0.041***	***0.298***	0.448	0.142	0.155	-0.470	0.754
PAX6	0.300	-0.060	0.045	-0.113	0.234	0.481	-0.048	0.062	-0.222	0.125
PDX1	0.236	-0.072	0.052	-0.072	0.216	0.205	-0.055	0.036	-0.157	0.046
SST	0.955	-0.004	0.084	-0.228	0.238	0.715	-0.030	0.078	-0.249	0.188

Control Vs 24hrs 25 mM glucose *p*=0.050										
Treatment 24 hrs 25 mM glucose						**Treatment and rescue**				
	P value	Mean diff	SED	95% CI		*P* value	Mean diff	SED	95% CI	
Gene				Lower	Upper				Lower	Upper
INS	***0.004***	***0.424***	***0.072***	***-0.623***	***-0.226***	0.476	0.058	0.077	-0.124	0.241
NANOG	0.511	0.653	0.923	0.302	0.171	0.983	-0.002	0.107	-0.256	0.251
PAX6	***0.003***	***-1.278***	***0.127***	***0.539***	***0.131***	0.364	-0.082	0.084	-0.255	0.090
PTPN1	0.353	0.959	0.096	0.131	0.323	0.476	0.058	0.077	-0.124	0.241
POU5F1	***0.034***	***0.373***	***0.134***	***0.039***	***0.707***	0.167	-0.373	0.237	-0.954	0.207

Supplementary table S10: Effects of SH6 AKT pathway inhibition and treatment with 25 mM high glucose on splicing factor and patterns of alternative splicing.

The p values for statistical significance as determined by independent t-test, Standard errors of measurement (SED) and the 95% confidence intervals are given below. Statistically significant results are indicated in bold typeface. SH6 small molecule AKT pathway inhibitor S5 splicing factor expression

SH6 and 25 mM glucose Independent Samples Test *p*=0.050				
	p	Std. Error	95% CI	
	value	Difference	Lower	Upper
18S-Hs99999901_s1	0.850	0.094	-0.281	0.243
AKAP17A-Hs00946624_m1	0.621	0.104	-0.232	0.343
GUSB-Hs00939627_m1	0.282	0.042	-0.168	0.064
HNRNPA0-Hs00246543_s1	0.082	0.017	-0.008	0.084
HNRNPA1-Hs01656228_s1	0.466	0.168	-0.331	0.601
HNRNPA2B1-Hs00242600_m1	0.152	0.089	-0.090	0.404
HNRNPD-Hs01086914_g1	0.543	0.038	-0.131	0.080
HNRNPH3-Hs01032113_g1	0.945	0.056	-0.159	0.151
HNRNPK-Hs00829140_s1	0.890	0.055	-0.160	0.144
HNRNPM-Hs00246018_m1	0.638	0.056	-0.185	0.128
HNRNPUL2	0.428	0.062	-0.227	0.117
IDH3B-Hs00199382_m1	0.485	0.022	-0.044	0.078
IMP3-Hs00251000_s1	0.313	0.058	-0.229	0.095
LSM14A-Hs00385941_m1	0.619	0.353	-1.171	0.790
LSM2-Hs01061967_g1	0.385	0.048	-0.179	0.086
PNISR-Hs00369090_m1	0.817	0.087	-0.263	0.220
PPIA-Hs04194521_s1	0.509	0.093	-0.190	0.324
SF3B1-Hs00202782_m1	0.759	0.068	-0.211	0.167
SRSF1-Hs00199471_m1	0.556	0.026	-0.055	0.088
SRSF2-Hs00427515_g1	0.699	0.047	-0.111	0.150
SRSF3-Hs00751507_s1	0.610	0.051	-0.112	0.168
SRSF6-Hs00607200_g1	0.665	0.053	-0.122	0.172

SH6 and 25 mM glucose Independent Samples Test *p*=0.050				
	p value	Std. Error Difference	95% CI	
			Lower	Upper
SRSF7-Hs00196708_m1	0.729	0.084	-0.202	0.265
TRA2B-Hs00907493_m1	0.922	0.044	-0.117	0.126

Independent Samples Test *p*=0.050				
SH6 treated cells exposed to 25 mM high glucose				
	p value	Std. Error Difference	95% CI	
			Lower	Upper
HPRT1	0.599	0.373	-1.250	0.824
IDH3B	0.753	0.419	-1.305	1.023
INS	0.866	0.083	-0.245	0.215
NANOG	0.161	0.112	-0.504	0.119
PAX6	0.179	0.030	-0.035	0.132
POU5F1	0.146	0.104	-0.101	0.477

Chapter 5:

Data Chapter.

Cellular stress responses in the human beta cell line EndoC-βH1 may be co-ordinated by microRNAs.

5.1 Introduction

MicroRNAs (miRNA) are a class of small non-coding RNAs, which regulate gene expression through mRNA degradation and/ or translational repression[156, 164]. This class of RNA regulators have important and defined roles on most cellular processes including development, metabolism, regulation of cell division and regulation of immune function[159, 169, 293]. In accordance with their pivotal role in normal homeostasis[174], dysregulated miRNA expression is also apparent in a wide range of diseases including metabolic disorders[294], cancer[295-297] and neurodegenerative diseases[151]. The biogenesis of miRNAs is thought to be linked to stress responses through stress granule-induced regulation of miRNA expression[176]. Transcription and processing of miRNA genes has also been shown to be regulated by p53 in response to inflammation[176]. These observations suggest that miRNAs may comprise an important component of the molecular stress response.

The diabetic microenvironment is characterised by altered glycaemia, hypoxia, hyperinsulinaemia, dyslipidaemia and heightened inflammation. This yields enormous osmotic and metabolic stresses on beta cells, which adversely affects cell survival, function and differentiation status[31, 176]. Tattikota et al have demonstrated a role for miR-184 targeting Argonaute2 in the regulation of beta cell proliferation during insulin resistance[298]. The miRNA response to stress also includes mir-375[162] and the miR-200[299] family in particular, which have been demonstrated to have involvement in the regulation of apoptosis[160] and responses to inflammatory factors[160, 179]. Well defined roles have also been

described for miRNAs in glucose homeostasis[155], such as miR-124 and miR185, beta cell proliferation, including miR-375 and differentiation, such as miR-7[158, 300] as well as in management of insulin secretion and production [156, 301]. MicroRNAs can directly target components of the insulin secretory machinery[160] in response to hyperglycaemia and their involvement in mediation of the unfolded protein response is also well documented[33]. The cross-regulatory relationship between cellular stress and miRNA expression renders these small non-coding RNA regulators uniquely poised to interface between the cellular microenvironment and beta cell function[176, 179].

Here we hypothesised that exposure to diabetes-related cellular stressors may affect the miRNA repertoire in human beta cells and that this may have functional consequences[151, 164, 179]. We exposed the human EndoCβH1 beta cell line to a variety of diabetes-associated cellular stressors and measured the effects on the miRNA milieu using qRTPCR. We identified 368 miRNAs expressed in EndoCβH1 cells, of which 116 were dysregulated by aspects of the diabetic cellular microenvironment. The 10 most dysregulated miRNAs were validated and targets were predicted using bioinformatics. GSEA gene ontology analysis of dysregulated miRNAs revealed that the FOXO1 and HIPPO pathways, which have been demonstrated to be important in maintenance of beta cell fate and function[47, 302], were enriched in target genes of dysregulated miRNAs. Furthermore, a sub analysis of an *a priori* set of miRNAs predicted to target genes involved in beta cell fate or function revealed that, miR-199a, miR-21 and miR-29a demonstrated dysregulated expression in response to one or more diabetes-associated cellular stressors. These results suggest that the cellular

microenvironment can induce changes in the expression of miRNAs in human beta cells, and that these miRNAs may preferentially target genes involved in beta cell fate or function.

5.2 Research Design and Methods

5.2.1 Culture and treatment of EndoC-βH1 cells

EndoC-βH1 cells at passage <25 were plated in 24-well plates at a density of 6.0 x 10^5 cells/ ml and maintained according to a modified humanised culture protocol[282] for 72 hrs prior to treatment. Cells were then treated with low (2.5 mM) or high glucose (25 mM) for 24, 36 or 48 hrs to mimic disrupted glycaemia, with 0.5 mM palmitic acid/ 0.5 mM oleic acid for 12, 24, and 48 hrs to mimic dyslipidaemia, with TNFα (1000 U/ mL, INFγ (750 U/ mL) and IL1β (75 U/ mL) for 12, 24 and 36 hrs to mimic inflammatory changes or were grown in 1%, 3% or 21% O_2 for a period of 4, 12 or 24 hrs to mimic hypoxia. . Each treatment was carried out in 3 biological replicates, along with vehicle-only controls.

5.2.2 RNA extraction and reverse transcription

Treated EndoC-βH1 cells were washed in Dulbecco's phosphate buffered saline (D-PBS) before RNA extraction using TRI® reagent to harvest both the small (<200bp) and long RNA fractions (Sigma-Aldrich, Steinheim, Germany). RNA concentrations were adjusted to 100 ng/ µL prior to reverse transcription. For miRNA assessment, cDNA synthesis was carried out in 20 µL reactions using the Taqman® Advanced miRNA Assay kit (Thermo Fisher, Waltham, MA USA)

according to the manufacturer's instructions. For assessment of mRNA target levels, cDNA synthesis was carried out using EvoScript Universal cDNA master (Roche life science, Burgess Hill, UK). Samples were normalised to 100 ng/ µL RNA prior to reverse transcription.

5.2.3 Large-scale miRNA screen

The miRNA milieu of treated and endogenous control cells was assessed using Taqman® Advanced miRNA (miR) open arrays on the Thermo Fisher 12K OpenArray Flex platform (Thermo Fisher, Waltham, MA USA). These arrays contain unique probes to 757 miR targets as detailed in supplementary table S11. Data was analysed using Thermo Fisher Connect your lab software (Thermo Fisher Connect™, Thermo Fisher, Waltham, MA USA, available at https://www.thermofisher.com). Target microRNAs were selected by choosing those with the largest fold changes in cells exposed to the cellular stressors compared to the endogenous controls, table 8 and supplementary table S11 for assay IDs.

5.2.4 Validation of dysregulated miRNAs

The 10 most dysregulated miRNAs were then validated using a separate probe set. In a sub analysis, we also validated a panel of 10 candidate miRNAs predicted by miRTarBase[303] to target an *á priori* panel of genes selected on the basis of known roles in relation to beta cell fate, function or cellular stress. Genes associated with other pancreatic islet cell types were also included in the target

panel, see table 4 and supplemental table S12. MicroRNAs were validated using Taqman® advanced miR assays (Thermo Fisher, Waltham, MA USA). The three most stable miRNAs (miR 106b-3p, miR-191-3p and miR103-3p) were selected for use as endogenous controls. qRTPCR reaction mixes included 2.5 µL Taqman® Universal PCR mastermix II (no AmpErase® UNG) (Thermo Fisher, Waltham, MA, USA), 1.75 µL dH_2O, 0.5 µL cDNA and 0.25 µL Taqman® gene assay (Thermo Fisher, Foster City USA) in a 5 µL reaction volume. Cycling conditions were: 50 °C for 2 min, 95 °C for 10 min and 50 cycles of 15 s at 95 °C for 30 s and 1 minute at 60 °C. Reactions were carried out in 3 biological replicates and 3 technical replicates. MicroRNA assay identifiers are given in supplementary table S13. The relative expression of each was determined by the comparative Ct approach and were calculated relative to the geometric mean of the endogenous controls. We also carried out an analysis relative to the global mean of expression across all transcripts tested. Expression levels were then normalised to the median level of expression seen in untreated EndoC-βH1 cells. Differences in gene expression levels between mock-treated and treated EndoC-βH1 cells were compared to the same time point controls for each condition and investigated for statistical significance by student independent t-test carried out using SPSS version 23 (IBM, North Castle, NY, USA). Data were presented as means ± S.E.M.

5.2.5 miRNA pathway enrichment analysis

To assess pathway and gene targets for miRNAs dysregulated in response to the cellular stress assays, we used the DNA intelligent analysis (DIANA) miRPath v3.0 and the DIANA-microT-CDS v 5.0 algorithm[246, 247]. The DIANA mirPath

database focuses on the identification of miRNA targeted cell pathways, the algorithm performs gene set enrichment analysis (GSEA) using a Fisher's exact test to determine the statistical significance of microRNA gene targets in KEGG pathways. Identified pathways were fed into the DIANA microT-CDS database entries to determine pathway target genes predicted by this pattern of altered miRNA expression. Genes have a microRNA target (MITG) score which predicts the probability of the microRNA targeting that gene[248]. A score of 0 means there is zero probability, a score of 1 means a very high probability of targeting the gene. Here, we used this platform to carry out GSEA using miRNAs differentially regulated across several treatment regimes to determine whether any were overrepresented in gene ontology or functional category pathways derived from KEGG. The *p* value was set to 0.05 and the MicroT threshold to 0.8, see table 8.

5.2.6 Validation of miRNA target gene mRNA levels

Target genes for validation were based on the MITG scores from the DIANA-microT-CDS v5.0 algorithm[246], supplementary table S14. The MITG score is the predictive score, where the higher the score the higher the probability that the gene in question is a target of the miRNA on the basis of complementarity[248]. A panel of 10 mRNAs were selected on the basis of highest MITG score, most statistically significant *p* value, number of genes predicted and number of miRNAs targeting the top 5 pathways; Lysine degradation, FOXO signalling pathway, HIPPO signalling pathway, TGFβ - estrogen signalling and Pathways in Cancer.

The expression levels of predicted target genes was then measured using IDT mini primetime™ gene expression assays (Integrated DNA Technologies, Skokie, Illinois, USA) as detailed in supplementary table S15. Reactions were run in triplicate on 384 well plates, using one assay per plate containing all samples. Each reaction included 2.5 µL Taqman® Universal PCR mastermix II (no AmpErase® UNG) (Thermo Fisher, Waltham, MA, USA), 1.75 µL dH_2O, 0.5 µL cDNA and 0.25 µL using IDT mini primetime™ gene expression assays (Integrated DNA Technologies, Skokie, Illinois, USA) in a 5 µL reaction volume. Cycling conditions were: 50 °C for 2 min, 95 °C for 10 min and 50 cycles of 15 s at 95 °C for 30 s and 1 min at 60 °C. Associations between miRNA and mRNA target expression were assessed using independent t-tests carried out using SPSS v23 (IBM, North Castle, NY, USA). We identified correlations by integrating miR expression data with mRNA expression to assess expression changes that occurred in response to the same cellular stresses. This method was used to assess relationships between the miRNA and mRNA, particularly where the predicted miRNA target gene expression was contrary to that of the miRNA[304, 305].

5.3 Results

5.3.1 Large scale dysregulation of miRNAs in response to the diabetic milieu

368 out of 757 miRNAs tested were expressed in untreated EndoC-βH1 human beta cells. 116 miRNAs demonstrated evidence of dysregulation upon treatment with altered glycaemia, dyslipidaemia, hypoxia or cytokines, (supplementary table S16). Independent validation of the miRNAs demonstrating the largest fold

change in the initial analysis showed that 5 miRNAs survived independent validation, as shown in figure 20 and supplemental table S17. miRNA miR-136-5p was altered in response to 25 mM high glucose, palmitic acid and inflammatory factors (p=0.008, mean diff 0.782, p=0.01, mean diff 1.047 and p=0.002, mean diff -0.634 respectively). miR-299-5p showed altered expression in response to changes in glycaemia and <3% O_2 (p=0.002, mean diff -0.619 and 0.01 mean diff -0.685 respectively). miR-454-5p responded to 2.5 mM low glucose (p=0.012, mean diff 4.145). Both miR-152 and miR-185 responded to 25 mM high glucose (p=0.005 mean diff 0.536 and p=0.024 mean diff -2.221 respectively).

Table 8 Large scale microRNA screen.

High throughout global microRNA screen results showing the most altered microRNAs for pathways analysis. Table shows microRNAs shown to have large fold changes from the near global screen that were also validated in studies in islets[159, 175]. Possible switch refers to cases where a very large fold change might indicate the presence of an on/ off switch mechanism in response to specific stressors.

miR name	Cell assay Altered in top 50.	Validated in islets[175]	Possible switch: on/ off	In top 20 most up/ down regulated
Mir_hsa-185-3p	3 assays	YES	NO	In 3 assays
Mir_hsa-885-5p	All assays	YES	YES	In 3 assays
miR_hsa-576-5p	All assays	YES	NO	In 3 assays
miR_hsa-27b-3p	All assays	YES	NO	In 3 assays
miR_hsa-124-3p	All assays	NO	NO	In 3 assays
miR_hsa-136-5p	All assays	NO	NO	In 3 assays
miR_hsa-152-3p	4 assays	NO	NO	In 3 assays
miR_hsa-299-5p	All assays	NO	NO	In 2 assays
miR_hsa-93-5p	All assays	NO	NO	In 2 assays
Mir_hsa-454-5p	All assays	YES	YES in 1 assay	In 1 assay

Table 9 Large scale micro RNA screen.

High throughput global microRNA screen results showing the most altered microRNAs validated for genes in beta cell target panel. Table shows those microRNAs identified by miRTarBase as experimentally validated to target genes in a panel of beta cell relevant genes with known roles in beta cell fate and function. miRTarBase defines strong validation as experimentally characterised and weak validation as those identified from NGS studies. Possible switch refers to cases where a very large fold change might indicate the presence of an on/ off switch mechanism in response to specific stressors.

Micro-RNA	**Genes in target panel**	**Cell Assay**	**Empirically validated[303]**	**NGS validated**	**Possible switch: on/off**
miR-202-5p	SOX9	Glycaemia Hypoxia Cytokine	YES	YES	YES – 3 assays
miR-92b-5p	GCK	All assays	YES		
miR-9-5p	FOXO1	All assays	YES	YES	YES
miR-34a-5p	NANOG, MYC, LDHA	Low glucose Hypoxia Palmitic acid	YES	YES	YES
miR-21-3p	FOXO1, SOX9	All assays	YES	YES	NO
miR-101-3p	SOX9	All assays	YES	YES	NO
miR-376a-3p	SLC16A1	All assays	YES	YES	NO
miR-199a-3p	STK11	All assays	YES	YES	YES
miR-374b-3p	SLC16A1	All assays	NO	YES	YES
miR-29a-3p	FOXO1	All assays	YES	YES	NO

Figure 20 Targeted microRNA expression of most altered miRNAs from large scale miRNA screen.

Larger dotted line shows significance p=<0.016. Bonferroni multiple testing correction for 3 tests. Coloured shapes denote significance. Smaller dotted line shows significance p -<0.050 no correction for multiple testing. Circles: 25 mM high glucose. Squares: 2.5 mM low glucose. Diamonds: <3% O2. Triangles: 0.5 mM palmitic acid. Stars pro-inflammatory factors.

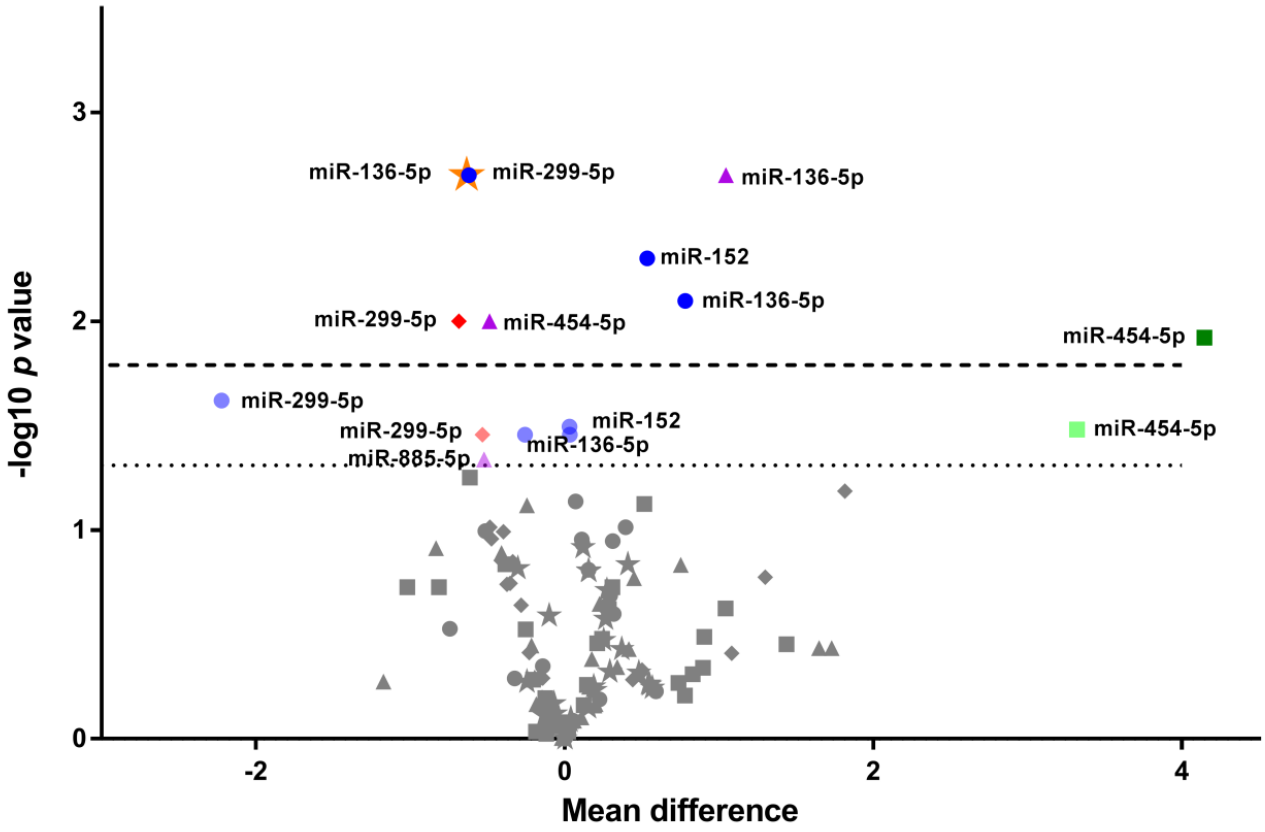

5.3.3 The Lysine degradation, HIPPO and FOXO pathways are enriched in genes targeted by dysregulated miRNAs

We then determined the gene ontology pathways enriched for genes targeted by the 5 responsive miRNAs. The top 5 pathways targeted by these miRNAs included: Lysine degradation 12 genes (p=3.0x10^{-3}), HIPPO signalling pathway 17 genes (p=5.84x10^{-5}), FOXO signalling pathway 18 genes (p=0.02), TGFβ - oestrogen 15 genes (p=0.02) and Pathways in Central Cancer 9 genes (p=3.0x10^{-3}), supplementary table S14.

5.3.4 Correlation of miRNA and mRNA target expression

Target genes of the dysregulated miRNAs were identified from the pathways analysis. We therefore correlated the mRNA expression level of the target genes in question with its respective miRNA as previously described[304, 305]. We found that changes in the expression of 3 of the miRNAs, miR-136-5p, miR299-5p and miR-454-5P negatively correlated with expression changes in response to the cellular stressors in their respective target genes, *MAPK1/ DLG2*, *PDK1* and *MAPK1,* see supplementary tables S17 and S18, figure 21. A positive correlation between miRNA and mRNA was also noted for miR-185 and MAPK1 in response to 25 mM high glucose.

Figure 21 mRNA expression of predicted target genes from DIANA pathways analysis.

Smaller dotted line shows significance p -<0.050 no requirement of correction for multiple testing. Circles: 25 mM high glucose, dark blue p=0.050 Squares: 2.5 mM low glucose, dark green p=0.050. Diamonds: <3% O2, dark red p=0.050. Triangles: 0.5 mM palmitic acid, dark purple p=0.050. Inverse triangles: inflammatory factors, dark purple p=0.050. Inverse triangles: proinflammatory factors, dark pink p=0.050.

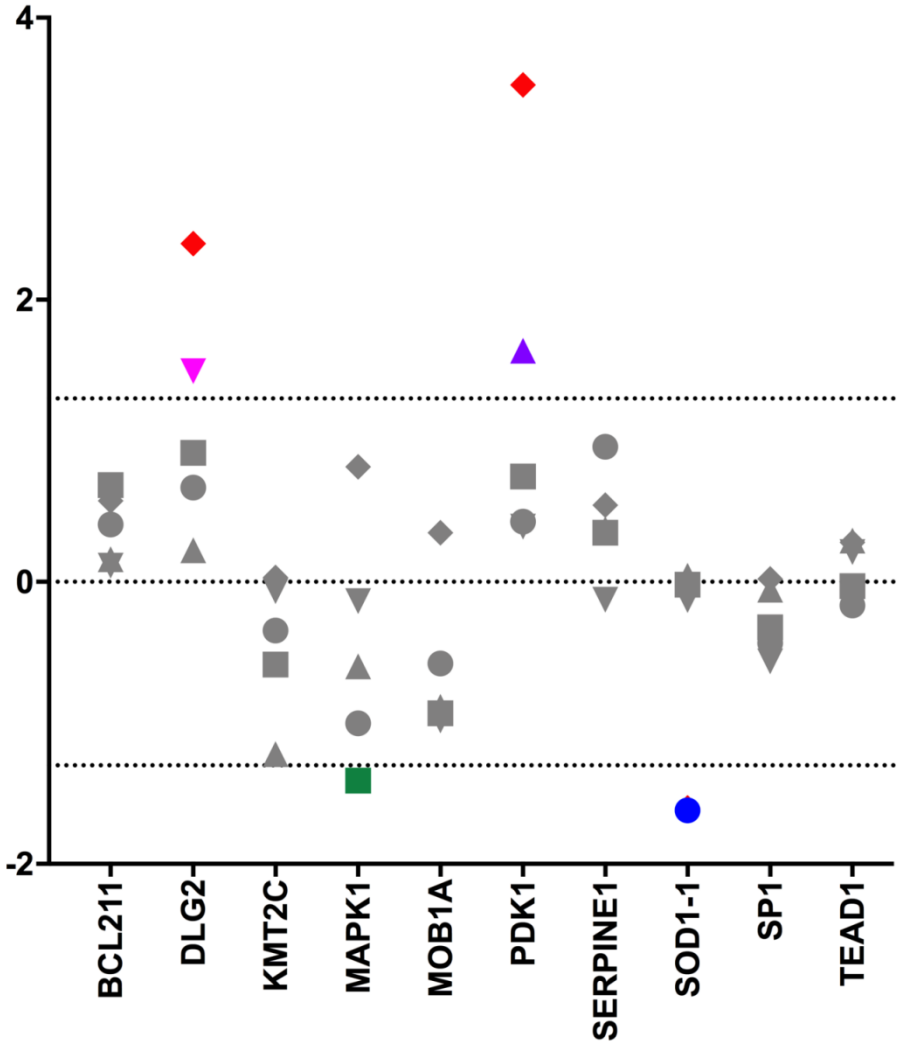

5.3.5 STK11, SOX9 and FOXO1 mRNA expression demonstrates negative associations with miR199a, miR-21 and miR-29a following diabetes-related cellular stresses.

Three of ten miRNAs selected on the basis of miRTarBase[303] evidence of roles in the regulation of a beta cell-specific target panel also demonstrated expression changes in treated cells, supplementary table S19. We integrated miR expression with mRNA expression to identify expression changes, (either positive or negative correlations), that occurred in response to the same cellular stresses. Changes in the expression of miR-199a, miR-21 and miR-29a negatively correlated with expression changes in their gene targets (*STK11, SOX9* and *FOXO1* respectively) in response to 25 mM high glucose and inflammatory factors, see supplementary tables S19 and S20, figure 22. Altered expression levels were also apparent for miR-199a, miR-21 and miR-29a (p=0.001 mean diff 4.438, p=0.016 mean diff -0.663 and p=0.001 mean diff 1.477) in response to either high glucose or inflammatory factors.

Figure 22 Targeted expression of microRNAs strongly validated to beta cell genes.

Larger dotted line shows significance p=<0.016. Bonferroni multiple testing correction for 3 tests. Smaller dotted line shows significance p -<0.050 no correction for multiple testing. Circles: 25 mM high glucose, dark blue p=0.016, light blue p=0.050. Squares: 2.5 mM low glucose, light green p=0.050. Diamonds: <3% O2. Triangles: 0.5 mM palmitic acid. Inverse triangles: inflammatory factors, dark pink p=0.016, light pink p=0.050

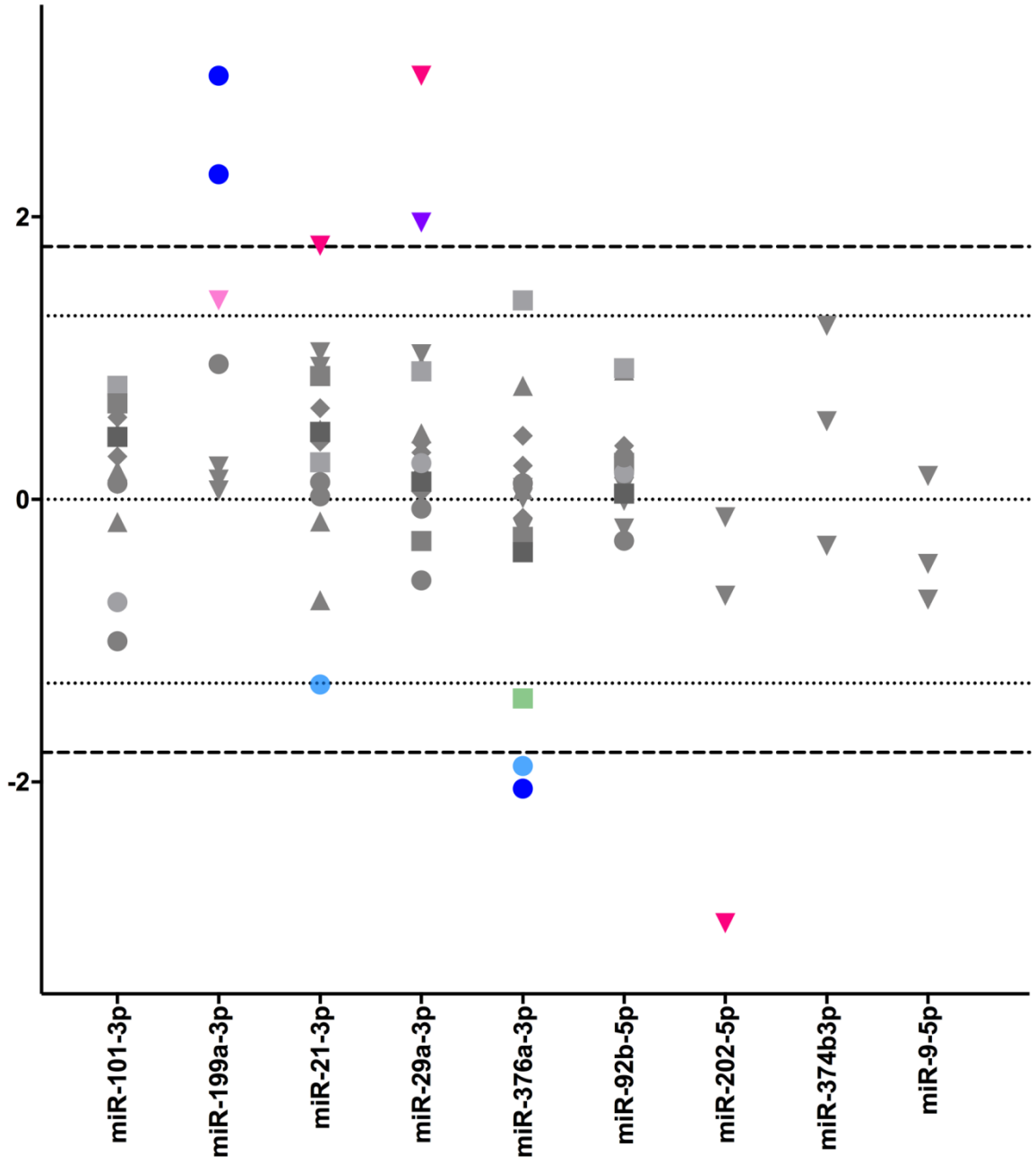

5.4 Discussion

A number of studies have reported the importance of miRNA regulation on gene expression relating to cellular stress responses in beta cells[151, 179]. High throughput miRNA profiling in rodent models and human islets have identified a number of miRNAs that are associated with beta cell dysfunction[174, 175]. MicroRNAs have been previously implicated in beta cell stress responses[30, 151, 176, 177, 179, 306]. Here, we found that cellular stresses associated with a T2D microenvironment caused dysregulation of miRNA expression for 5 miRNAs, miR136-5p, miR-299-5p, miR-454-5p, mir-152 and miR-185. Gene set enrichment analysis identified 3 KEGG pathways, lysine degradation, HIPPO and FOXO as predicted targets for these miRNAs. Subsequent gene target validation showed negative correlations for 3 miRNAs and their respective target genes, miR-136-5p and *MAPK1/ DLG2*, miR299-5p and *PDK1* and miR454-5p and its predicted target *MAPK1.* Validation of miRNAs previously predicted to target beta cell genes also showed negative correlation for 3 miRNAs and their predicted targets, miR-199a and *STK11,* miR-21 and *SOX9* and miR-29a and *FOXO1.*

miRNAs have been shown to have various functions in mediating beta cell responses to stresses including regulation of beta cell proliferation, insulin secretion and glucose homeostasis, beta cell differentiation and apoptosis. MicroRNA miR-375 is known to regulate beta cell proliferation in response to chronic metabolic stresses and miR-21, miR-29a, along with the miR-200 family, are associated with regulation of apoptosis[162, 299, 307]. Increased expression of miR-21 and miR-29a are associated with increased beta cell proliferation but also rates of apoptosis in the presence of cytokines[293, 307]. Our data also show

elevated levels of miR-21 and miR-29a in response to inflammatory factors, supporting the hypothesis that microRNAs coordinate stress response in a manner which creates an intimate relationship between beta cell function and survival.

Changes in glucose concentration in the cellular microenvironment have been shown to increase the expression of miR-124, which is known to negatively regulate insulin secretion. miRNAs miR-185, miR-152 and miR-21 have all be previously identified in relation to the regulation of glucose homeostasis via altered insulin secretion, signalling, glucose sensitivity and cell survival[151, 158, 307]. [157-159]. Increased levels of miR-185 have recently been shown to enhance insulin secretion[158]. Here we found reduced levels of miR-185 after exposure to 25 mM glucose, suggesting, in line with the literature, that insulin secretion may be impaired under high glucose stresses. In contrast, elevated levels of miR-21 and miR-152 have been seen in patients with T2D[157, 170, 307] and have been shown to negatively impact glucose sensitive insulin secretion (GSIS)[157, 307]. Our data show very marked increases in the levels of miR-152 in EndoC-βH1 cells exposed to 25 mM high glucose and miR-21 in response to inflammatory factors, which again may suggest impaired insulin secretion as a result of altered miRNA expression. These data suggest a clear association between altered miRNA expression in response to cell stress and impaired insulin secretion and may implicate miRNAs in the coordination of beta cell stress response and pathogenesis of T2D.

Correlation analysis is a recognised technique for identifying potential roles for miRNA in gene regulation, with negative correlations being the most commonly

observed phenomenon[304, 305]. Investigation of miRNAs known to target genes with known beta cell and pancreatic endocrine functions show negative correlations for miR-199a and its validated target *STK11 (LKB1)*, miR-21 and its validated target *SOX9* and miR-29a and its validated target *FOXO1. Here, STK11 (LKB1)* is significantly down regulated in response to high glucose with increased expression of miR-199-a. Increased levels of miR-199a are known to reduce *STK11* expression[308]. Importantly, STK11 (*LKB1*) has been shown to maintain beta cell identity[171] as well as increased beta cell size and polarity[309]. A recent study has also shown that *TCF7L2,* a previously identified T2D GWAS hit[310], mediates a signalling mechanism that acts via *STK11 (LKB1)* to negatively regulate insulin secretion[311]. This suggests that cellular stressors associated with T2D may contribute to increased cellular plasticity through dysregulation of miRNA expression. *SOX9* is also a marker for beta cell plasticity and our data show significantly increased expression in response to glycaemia, hypoxia and dyslipidaemia along with reduced miR-21 expression. This again implies a role for miRNA dysregulation in changes to mature beta cell differentiation status in T2D. Finally, *FOXO1* has been described as the master regulator for beta cell identity[43] and here we saw decreased expression in response to inflammatory factors with increased expression of miR-29a. Taken together, these data suggest that miRNA dysregulation is an important feature of the increased beta cell plasticity reported in T2D[159].

Validation of miR targets identified from pathways analysis showed negative correlations for miR-454-5p and its predicted target *MAPK1*, miR-136-5p and its predicted target *DLG2* and miR-299-5p and its predicted target *PDK1*. What is striking from these data is the number correlations for genes with known roles in

beta cell dysfunction and survival, which is likely due to their tight regulation during periods of cell stress. *MAPK1* signalling in particular, occurs in response to microenvironmental changes affecting cellular metabolism and is implicated in the pathogenesis of metabolic syndrome[312]. Both *DLG2* and *PDK1* have also been shown to have roles in beta cell stress response in relation to insulin signalling, survival and apoptosis[287, 313]. Here, low glycaemia showed marked increases in expression of miR454-5p, compared to negligible levels in controls, along with significantly decreased expression of *MAPK1*. Downregulation of *MAPK1* leads to increased apoptosis and so it may be possible that miR-454-5p is influencing rates of apoptosis during cellular stress. miR-299 showed significantly reduced expression in response to both high glucose and hypoxia, however, PDK1 only showed increased expression following exposure to <3%O2. Inflammatory factors resulted in lower levels of miR-136-5p with concomitant increases in its predicted target *DLG2*. Taken together, all these data may suggest that cellular stresses activate miRNA regulation of beta cell survival pathways that regulate rates of apoptosis.

The increased expression of miR-21 and miR-29 we found in response to inflammatory factors is known to be associated with increased rates of apoptosis, implying that cytokine exposure negatively impacts beta cell survival[293, 307]. Similarly, negative correlations between miR-454-5p, miR-136-5p and miR-299-5p with their respective target genes *MAPK1, DLG2* and *PDK1* are also implicated in the negative regulation of beta cell survival in response to cell stress. Studies have indicated that miRNAs may also influence beta cell stress responses via changes in mature beta cell differentiation status[314, 315]. miR-7 has been identified in association with beta cell differentiation in response to

metabolic stresses[179]. Here, validation of miRNAs predicted to target beta cell genes showed negative correlations between miR-199a, miR-21, miR-29a and their target genes, *STK11, SOX9* and *FOXO1*. The pattern of altered gene expression we identified may suggest increased beta cell plasticity in response to cell stress. We also found a pattern of dysregulated expression for miR-185, miR-21 and miR-152 that can potentially be explained by cellular stresses causing impaired insulin secretion in a manner that may be coordinated by microRNAs. Taking these data together, this could support a model where the cellular stress response is, at least in part, coordinated by miRNAs and affects beta cell survival, function and differentiation status.

We acknowledge that our results are based upon an *in* vitro model and are not supported by data from *in vivo* or *ex vivo* islet comparisons. However, looking at these data as a whole, it supports a hypothesis where altered miRNA expression following exposure to the types of cellular stress seen in patients with T2D, can potentially influence genes with roles in both beta cell fate and survival. This would be consistent with recent reports in the literature which show that the beta cell mass loss seen in T2D are caused by both loss of mature beta cell identity as well as cell death[61, 86, 113]. However, it may be that the miRNA expression changes we observed may be a secondary response to the cellular stressors rather than mediating phenotypic changes; miRNAs responding to cellular stressor rather than driving the beta cell stress response itself. To investigate this further, and experimentally validate these findings, studies employing either miRNA upregulation or miRNA loss of function techniques such as genetic knockouts, antisense oligonucleotide inhibitors[316, 317] and miRNA sponges[318]

would be advised to elucidate causality and better characterise the relationship between beta cell stress, miRNAs and their target genes.

Within the literature there is considerable heterogeneity between studies, possibly the result of differences in islet handling and cell culture techniques[175]. It is also notable that there are important distinctions between rodent and human datasets[169]. However, perhaps surprisingly, given the levels of heterogeneity between studies, it is a strength of our study that these data confirm results that have been seen in a number of other studies relating to miR-185, miR-152, miR-199a, miR-21, miR-29a, miR-376a and miR-136-5p.

We have shown evidence that three miRNAs, miR-454-5p, miR136-5p and miR-299-5p, correlate with expression changes in target genes which are associated with the cellular pathways FOXO and MAPK. These pathways are likely to regulate beta cell survival in response to cell stress. We also present evidence that three miRNAs, miR-199a, miR-21 and miR-29, correlate with altered expression in their respective beta cell target genes, *STK11, SOX9 and FOXO1.* These miRNA/ mRNA interactions may have implications for maintenance of beta cell identity following exposure to cell stress. Taken together, these data suggest that the beta cell stress response may be coordinated by microRNAs and their dysregulated expression is an important feature of T2D.

Supplementary table 11. Large scale microRNA screen assay IDs.

Assay ID	Target name	Assay ID	Target name	Assay ID	Target name
478872	hsa-miR-409-5p	477906	hsa-miR-139-3p	478658	hsa-miR-1252-5p
478092	hsa-miR-424-5p	479485	hsa-miR-517a-3p	478660	hsa-miR-1254
478007	hsa-miR-30b-5p	478989	hsa-miR-520a-3p	478662	hsa-miR-1255b-5p
478587	hsa-miR-29a-3p	478231	hsa-miR-199a-5p	477929	hsa-miR-15b-3p
478125	hsa-miR-485-3p	478997	hsa-miR-526b-5p	478641	hsa-miR-1226-5p
478308	hsa-miR-484	478585	hsa-miR-196b-5p	477880	hsa-miR-124-5p
477854	hsa-miR-380-3p	479340	hsa-miR-519e-3p	477875	hsa-miR-1225-3p
478826	hsa-miR-323b-5p	478995	hsa-miR-525-3p	478644	hsa-miR-1228-5p
478126	hsa-miR-485-5p	478984	hsa-miR-518f-3p	478657	hsa-miR-1251-5p
478293	cel-miR-39-3p	478153	hsa-miR-542-3p	477874	hsa-miR-122-3p
478561	hsa-miR-449a	479393	hsa-miR-518d-3p	478730	hsa-miR-1825
478591	hsa-miR-302b-3p	478112	hsa-miR-455-3p	479120	hsa-miR-641
478086	hsa-miR-411-5p	478685	hsa-miR-1283	479176	hsa-miR-767-5p
478024	hsa-miR-324-5p	478165	hsa-miR-576-5p	478661	hsa-miR-1255a
478008	hsa-miR-30c-5p	478351	hsa-miR-200c-3p	479128	hsa-miR-649
477816	hsa-miR-381-3p	479396	hsa-miR-525-5p	478638	hsa-miR-1224-3p
478860	hsa-miR-376b-3p	479285	hsa-miR-524-5p	478340	hsa-miR-631
478790	hsa-miR-296-3p	478210	hsa-miR-93-5p	478637	hsa-miR-1208
478087	hsa-miR-412-3p	478991	hsa-miR-520g-3p	478161	hsa-miR-564
477849	hsa-miR-429	479408	hsa-miR-518e-3p	479063	hsa-miR-581
478106	hsa-miR-450a-5p	479343	hsa-miR-520f-3p	479040	hsa-miR-555
478113	hsa-miR-455-5p	477825	hsa-miR-301b-3p	477973	hsa-miR-21-3p
478509	hsa-miR-302c-3p	478498	hsa-miR-520e	478631	hsa-miR-1200
478491	hsa-miR-204-5p	478914	hsa-miR-450b-5p	478788	hsa-miR-26a-2-3p
478411	ath-miR159a	479053	hsa-miR-570-3p	479058	hsa-miR-578
477916	hsa-miR-145-5p	478672	hsa-miR-1267	477862	hsa-let-7i-3p
477925	hsa-miR-154-5p	478156	hsa-miR-544a	477850	hsa-let-7g-3p

Assay ID	Target name	Assay ID	Target name	Assay ID	Target name
477900	hsa-miR-132-3p	479501	hsa-miR-548a-5p	477869	hsa-miR-1180-3p
477908	hsa-miR-140-3p	477833	hsa-miR-548d-3p	478341	hsa-miR-7-5p
478789	hsa-miR-27b-5p	478418	hsa-miR-26b-5p	478221	hsa-let-7b-3p
477858	hsa-miR-15a-5p	478544	hsa-miR-129-2-3p	478787	hsa-miR-26a-1-3p
478399	hsa-miR-146a-5p	477835	hsa-miR-487b-3p	477984	hsa-miR-223-5p
477824	hsa-miR-148b-3p	478132	hsa-miR-491-5p	478784	hsa-miR-24-1-5p
477889	hsa-miR-127-3p	478139	hsa-miR-499a-5p	478630	hsa-miR-1197
477857	hsa-miR-181a-5p	478744	hsa-miR-195-3p	478755	hsa-miR-202-5p
478312	hsa-miR-139-5p	478049	hsa-miR-34b-3p	478774	hsa-miR-218-1-3p
477911	hsa-miR-142-5p	478035	hsa-miR-337-3p	478745	hsa-miR-196a-3p
477891	hsa-miR-127-5p	479057	hsa-miR-577	478625	hsa-miR-1178-3p
477840	hsa-miR-130b-3p	478831	hsa-miR-33a-3p	478713	hsa-miR-143-5p
477935	hsa-miR-182-5p	478188	hsa-miR-645	478846	hsa-miR-367-5p
477918	hsa-miR-150-5p	478840	hsa-miR-363-5p	479115	hsa-miR-633
477896	hsa-miR-129-5p	478317	hsa-miR-20a-3p	479125	hsa-miR-646
478624	hsa-miR-10a-3p	478750	hsa-miR-19a-5p	479150	hsa-miR-665
478584	hsa-miR-18b-5p	478710	hsa-miR-135b-3p	479139	hsa-miR-657
478313	hsa-miR-15b-5p	477915	hsa-miR-145-3p	479116	hsa-miR-634
477938	hsa-miR-184	477895	hsa-miR-1290	477899	hsa-miR-130b-5p
478551	hsa-miR-18a-5p	478055	hsa-miR-361-3p	479140	hsa-miR-658
479537	hsa-miR-548c-3p	479451	hsa-miR-1296-5p	479127	hsa-miR-648
478166	hsa-miR-582-5p	477951	hsa-miR-191-3p	479151	hsa-miR-668-3p
478164	hsa-miR-576-3p	478725	hsa-miR-154-3p	479146	hsa-miR-663b
480870	hsa-miR-548d-5p	478505	hsa-miR-151a-5p	477958	hsa-miR-196b-3p
477860	hsa-miR-16-5p	478051	hsa-miR-34c-3p	478342	hsa-miR-766-3p
478792	hsa-miR-299-3p	477919	hsa-miR-151a-3p	479119	hsa-miR-640
478000	hsa-miR-28-5p	478671	hsa-miR-1265	479204	hsa-miR-924
478594	hsa-miR-320a	479478	hsa-miR-181a-2-3p	479206	hsa-miR-92a-2-5p
478459	hsa-miR-376c-3p	478729	hsa-miR-182-3p	479210	hsa-miR-935

Assay ID	Target name	Assay ID	Target name	Assay ID	Target name
478090	hsa-miR-423-5p	479181	hsa-miR-802	479452	hsa-miR-1298-5p
478481	hsa-miR-422a	479205	hsa-miR-92a-1-5p	479220	hsa-miR-944
478075	hsa-miR-377-3p	479175	hsa-miR-767-3p	479214	hsa-miR-938
478793	hsa-miR-299-5p	478681	hsa-miR-1278	479198	hsa-miR-892b
477974	hsa-miR-214-3p	479191	hsa-miR-888-3p	479048	hsa-miR-563
478133	hsa-miR-492	478650	hsa-miR-1243	479065	hsa-miR-583
478432	hsa-miR-483-5p	478209	hsa-miR-93-3p	479055	hsa-miR-573
478578	hsa-let-7f-5p	479217	hsa-miR-941	479039	hsa-miR-554
478579	hsa-let-7e-5p	479071	hsa-miR-588	477836	hsa-miR-296-5p
478131	hsa-miR-490-3p	479349	hsa-miR-513c-5p	477820	hsa-miR-1-3p
477980	hsa-miR-219a-5p	479084	hsa-miR-603	479456	hsa-miR-216b-5p
478602	hsa-miR-23b-3p	479212	hsa-miR-937-3p	477983	hsa-miR-223-3p
479235	hsa-miR-30e-5p	479100	hsa-miR-617	478029	hsa-miR-329-3p
478447	hsa-miR-17-5p	479117	hsa-miR-635	477992	hsa-miR-24-3p
478580	hsa-let-7g-5p	479098	hsa-miR-614	477863	hsa-miR-101-3p
477976	hsa-miR-216a-5p	479113	hsa-miR-630	477977	hsa-miR-218-5p
477978	hsa-miR-219a-1-3p	479069	hsa-miR-586	477994	hsa-miR-25-3p
478375	hsa-let-7i-5p	478168	hsa-miR-590-3p	478225	hsa-miR-106a-5p
477940	hsa-miR-186-5p	479085	hsa-miR-604	478384	hsa-miR-27a-3p
479189	hsa-miR-887-3p	477868	hsa-miR-10b-3p	477961	hsa-miR-199a-3p
478200	hsa-miR-744-5p	478980	hsa-miR-517-5p	479544	hsa-miR-186-3p
477883	hsa-miR-125a-3p	479075	hsa-miR-592	478363	hsa-miR-373-3p
479134	hsa-miR-653-5p	479097	hsa-miR-613	478490	hsa-miR-200a-3p
477987	hsa-miR-22-5p	479043	hsa-miR-557	478238	hsa-miR-374a-5p
479196	hsa-miR-891a-5p	479025	hsa-miR-548p	478070	hsa-miR-371a-3p
479121	hsa-miR-642a-5p	478173	hsa-miR-601	478025	hsa-miR-325
478191	hsa-miR-655-3p	479038	hsa-miR-553	478059	hsa-miR-362-5p
478519	hsa-miR-99a-5p	478727	hsa-miR-16-1-3p	478979	hsa-miR-516b-5p
478343	hsa-miR-99b-5p	478711	hsa-miR-138-2-3p	478264	hsa-miR-19b-3p

Assay ID	Target name	Assay ID	Target name	Assay ID	Target name
479131	hsa-miR-651-5p	478719	hsa-miR-148b-5p	478323	hsa-miR-331-3p
478207	hsa-miR-885-5p	479051	hsa-miR-569	478134	hsa-miR-493-3p
478185	hsa-miR-636	477914	hsa-miR-144-5p	478350	hsa-miR-501-3p
479197	hsa-miR-891b	478758	hsa-miR-203b-5p	478972	hsa-miR-512-5p
479184	hsa-miR-875-3p	478680	hsa-miR-1276	478960	hsa-miR-507
479371	hsa-miR-892a	477943	hsa-miR-188-5p	478145	hsa-miR-505-3p
478513	hsa-miR-146b-5p	478699	hsa-miR-1304-5p	479089	hsa-miR-608
478785	hsa-miR-24-2-5p	477811	hsa-miR-151b	478982	hsa-miR-518c-3p
478205	hsa-miR-874-3p	478147	hsa-miR-515-5p	478142	hsa-miR-501-5p
479186	hsa-miR-876-3p	477890	hsa-miR-1275	479530	hsa-miR-518d-5p
479517	hsa-miR-181d-5p	477936	hsa-miR-183-3p	478958	hsa-miR-506-3p
478036	hsa-miR-337-5p	478673	hsa-miR-1270	478309	hsa-miR-500a-5p
478027	hsa-miR-326	478647	hsa-miR-1236-3p	478971	hsa-miR-512-3p
477806	hsa-miR-208b-3p	477933	hsa-miR-181c-3p	479101	hsa-miR-618
478389	hsa-miR-374b-5p	479078	hsa-miR-595	478088	hsa-miR-421
478590	hsa-miR-98-5p	477944	hsa-miR-18a-3p	478968	hsa-miR-510-5p
478076	hsa-miR-378a-5p	479091	hsa-miR-609	478367	hsa-miR-590-5p
478855	hsa-miR-374a-3p	479104	hsa-miR-620	479073	hsa-miR-589-5p
478091	hsa-miR-424-3p	479067	hsa-miR-585-3p	479469	hsa-miR-625-5p
478084	hsa-miR-409-3p	478691	hsa-miR-1292-5p	478977	hsa-miR-516a-3p
478002	hsa-miR-29a-5p	478362	hsa-miR-548e-3p	478177	hsa-miR-616-3p
479362	hsa-miR-30d-3p	479024	hsa-miR-548n	478215	hsa-miR-96-5p
478388	hsa-miR-30e-3p	479512	hsa-miR-623	478427	hsa-miR-627-5p
479448	hsa-miR-30a-5p	479532	hsa-miR-518f-5p	478348	hsa-miR-502-3p
478859	hsa-miR-376a-5p	478349	hsa-miR-378a-3p	479064	hsa-miR-582-3p
478799	hsa-miR-302b-5p	479338	hsa-miR-524-3p	478077	hsa-miR-379-5p
478237	hsa-miR-302d-3p	479110	hsa-miR-626	477879	hsa-miR-124-3p
479401	hsa-miR-30c-2-3p	479020	hsa-miR-548g-3p	478532	hsa-miR-23a-3p
478012	hsa-miR-31-3p	479297	hsa-miR-513b-5p	478586	hsa-miR-20a-5p

Assay ID	Target name	Assay ID	Target name	Assay ID	Target name
478888	hsa-miR-431-3p	479082	hsa-miR-600	477904	hsa-miR-137
478800	hsa-miR-302c-5p	480874	hsa-miR-548i	478136	hsa-miR-495-3p
478775	hsa-miR-218-2-3p	479391	hsa-miR-548l	478060	hsa-miR-363-3p
478101	hsa-miR-432-5p	477852	hsa-miR-550a-5p	477814	hsa-miR-148a-3p
478311	hsa-miR-138-1-3p	478990	hsa-miR-520d-3p	478030	hsa-miR-330-3p
478801	hsa-miR-302d-5p	478951	hsa-miR-500a-3p	478066	hsa-miR-367-3p
479281	hsa-let-7e-3p	478988	hsa-miR-519e-5p	478324	hsa-miR-335-5p
478939	hsa-miR-488-5p	479054	hsa-miR-571	478325	hsa-miR-339-3p
478782	hsa-miR-23a-5p	477848	hsa-let-7d-3p	478052	hsa-miR-34c-5p
478476	hsa-miR-1260a	479491	hsa-miR-518e-5p	477957	hsa-miR-195-5p
477948	hsa-miR-190b	478198	hsa-miR-7-1-3p	478071	hsa-miR-372-3p
478642	hsa-miR-1227-3p	477887	hsa-miR-126-3p	477917	hsa-miR-149-5p
478663	hsa-miR-1256	478102	hsa-miR-433-3p	477954	hsa-miR-193a-5p
478655	hsa-miR-1250-5p	478109	hsa-miR-452-5p	478307	hsa-miR-136-5p
477998	hsa-miR-27a-5p	478094	hsa-miR-425-5p	478058	hsa-miR-362-3p
478634	hsa-miR-1205	478006	hsa-miR-302a-3p	478040	hsa-miR-339-5p
477877	hsa-miR-1233-3p	478074	hsa-miR-375	478830	hsa-miR-330-5p
478633	hsa-miR-1204	477853	hsa-miR-323a-3p	478986	hsa-miR-519d-3p
477888	hsa-miR-126-5p	478105	hsa-miR-448	479228	hsa-miR-19a-3p
477882	hsa-miR-1247-5p	478240	hsa-miR-376a-3p	478306	hsa-miR-193a-3p
478669	hsa-miR-1263	478889	hsa-miR-431-5p	477956	hsa-miR-194-5p
478654	hsa-miR-1249-3p	478369	hsa-miR-29b-3p	478970	hsa-miR-511-5p
478635	hsa-miR-1206	478329	hsa-miR-454-3p	479249	hsa-miR-518a-5p
478666	hsa-miR-125b-2-3p	478015	hsa-miR-31-5p	478616	hsa-miR-520d-5p
478652	hsa-miR-1245a	478128	hsa-miR-486-5p	477927	hsa-miR-155-5p
478186	hsa-miR-637	479483	hsa-miR-513a-5p	478999	hsa-miR-541-3p
478651	hsa-miR-1244	478078	hsa-miR-382-5p	479003	hsa-miR-545-5p
478047	hsa-miR-34a-3p	479528	hsa-miR-449b-5p	478994	hsa-miR-523-3p
478668	hsa-miR-1262	478501	hsa-miR-141-3p	478152	hsa-miR-539-5p

Assay ID	Target name	Assay ID	Target name	Assay ID	Target name
479035	hsa-miR-551b-5p	478026	hsa-miR-32-5p	478336	hsa-miR-532-3p
478649	hsa-miR-1238-3p	478430	hsa-miR-298	479495	hsa-miR-519c-3p
479137	hsa-miR-656-3p	478422	hsa-miR-486-3p	479002	hsa-miR-545-3p
479045	hsa-miR-559	479229	hsa-miR-29c-3p	479509	hsa-miR-520b
478167	hsa-miR-584-5p	478581	hsa-miR-135a-5p	479534	hsa-miR-519a-3p
478273	hsa-miR-30a-3p	478715	hsa-miR-146b-3p	478993	hsa-miR-522-3p
478704	hsa-miR-1324	478717	hsa-miR-147b	479404	hsa-miR-520a-5p
477843	hsa-let-7f-2-3p	477892	hsa-miR-128-3p	478149	hsa-miR-521
477866	hsa-miR-106b-3p	477851	hsa-miR-130a-3p	478163	hsa-miR-574-3p
477991	hsa-miR-23b-5p	478779	hsa-miR-222-5p	478151	hsa-miR-532-5p
478778	hsa-miR-221-5p	477912	hsa-miR-143-3p	479503	hsa-miR-548h-5p
478626	hsa-miR-1179	477910	hsa-miR-142-3p	479018	hsa-miR-548b-3p
478619	hsa-miR-100-3p	477905	hsa-miR-138-5p	480872	hsa-miR-548am-5p
479405	hsa-miR-181a-3p	478670	hsa-miR-1264	479041	hsa-miR-556-3p
478628	hsa-miR-1182	478589	hsa-miR-548b-5p	478157	hsa-miR-548a-3p
477861	hsa-let-7a-3p	478514	hsa-miR-147a	478107	hsa-miR-451a
478742	hsa-miR-193b-5p	478582	hsa-miR-135b-5p	478214	hsa-miR-9-5p
478622	hsa-miR-105-3p	477937	hsa-miR-183-5p	478175	hsa-miR-615-3p
477996	hsa-miR-26b-3p	477942	hsa-miR-188-3p	477901	hsa-miR-134-5p
478620	hsa-miR-101-5p	478511	hsa-miR-133a-3p	478752	hsa-miR-200a-5p
477962	hsa-miR-19b-1-5p	477921	hsa-miR-152-3p	478753	hsa-miR-200b-5p
477870	hsa-miR-1183	478159	hsa-miR-551b-3p	479032	hsa-miR-550a-3p
479162	hsa-miR-708-3p	478721	hsa-miR-150-3p	478741	hsa-miR-192-3p
479165	hsa-miR-744-3p	477939	hsa-miR-185-5p	478754	hsa-miR-200c-5p
478187	hsa-miR-638	477952	hsa-miR-191-5p	478764	hsa-miR-20b-3p
479144	hsa-miR-661	480871	hsa-miR-133b	478193	hsa-miR-664a-3p
479129	hsa-miR-650	478358	hsa-miR-190a-5p	477902	hsa-miR-136-3p
478199	hsa-miR-7-2-3p	478575	hsa-let-7a-5p	478712	hsa-miR-141-5p
479126	hsa-miR-647	478507	hsa-miR-211-5p	478743	hsa-miR-194-3p

Assay ID	Target name	Assay ID	Target name	Assay ID	Target name
478033	hsa-miR-335-3p	479059	hsa-miR-579-3p	477968	hsa-miR-206
479145	hsa-miR-662	479042	hsa-miR-556-5p	479036	hsa-miR-552-3p
479141	hsa-miR-659-3p	478085	hsa-miR-410-3p	478041	hsa-miR-340-3p
478196	hsa-miR-675-5p	477826	hsa-miR-487a-3p	478347	hsa-miR-33a-5p
479209	hsa-miR-934	477999	hsa-miR-28-3p	477913	hsa-miR-144-3p
478211	hsa-miR-9-3p	478079	hsa-miR-383-5p	478720	hsa-miR-149-3p
479124	hsa-miR-644a	478254	hsa-miR-107	478693	hsa-miR-1294
479203	hsa-miR-922	478080	hsa-miR-384	478718	hsa-miR-148a-5p
479118	hsa-miR-639	478913	hsa-miR-450b-3p	478212	hsa-miR-942-5p
478245	hsa-miR-939-5p	477995	hsa-miR-26a-5p	478697	hsa-miR-1302
479030	hsa-miR-549a	478327	hsa-miR-423-3p	478690	hsa-miR-1291
479207	hsa-miR-92b-5p	479241	hsa-miR-10a-5p	477931	hsa-miR-16-2-3p
479044	hsa-miR-558	478130	hsa-miR-489-3p	479202	hsa-miR-921
479061	hsa-miR-580-3p	477982	hsa-miR-222-3p	479208	hsa-miR-933
478702	hsa-miR-130a-5p	477865	hsa-miR-105-5p	478686	hsa-miR-1284
478224	hsa-miR-100-5p	477981	hsa-miR-221-3p	479526	hsa-miR-411-3p
478439	hsa-let-7d-5p	477884	hsa-miR-125a-5p	479201	hsa-miR-920
477970	hsa-miR-210-3p	478494	hsa-miR-10b-5p	479173	hsa-miR-765
478773	hsa-miR-217	477815	hsa-miR-301a-3p	479211	hsa-miR-936
477985	hsa-miR-22-3p	477934	hsa-miR-181c-5p	478946	hsa-miR-497-3p
478253	hsa-miR-103a-3p	478942	hsa-miR-491-3p	479076	hsa-miR-593-3p
478065	hsa-miR-365a-3p	477979	hsa-miR-219a-2-3p	478050	hsa-miR-34b-5p
477971	hsa-miR-2110	478516	hsa-miR-215-5p	479088	hsa-miR-607
477986	hsa-miR-224-5p	478270	hsa-miR-27b-3p	479087	hsa-miR-606
478056	hsa-miR-361-5p	478368	hsa-miR-654-5p	479106	hsa-miR-622
478318	hsa-miR-212-3p	478412	hsa-miR-106b-5p	478983	hsa-miR-518c-5p
478262	hsa-miR-192-5p	477864	hsa-miR-103a-2-5p	478181	hsa-miR-628-3p
478577	hsa-let-7c-5p	477885	hsa-miR-125b-5p	479070	hsa-miR-587
478044	hsa-miR-342-5p	478192	hsa-miR-660-5p	479072	hsa-miR-589-3p

Assay ID	Target name	Assay ID	Target name	Assay ID	Target name
478046	hsa-miR-346	478038	hsa-miR-338-5p	479077	hsa-miR-593-5p
478042	hsa-miR-340-5p	478197	hsa-miR-708-5p	479177	hsa-miR-769-3p
478366	hsa-miR-345-5p	478194	hsa-miR-671-3p	477893	hsa-miR-1286
478965	hsa-miR-509-5p	477922	hsa-miR-153-3p	478338	hsa-miR-596
478749	hsa-miR-198	477975	hsa-miR-21-5p	479105	hsa-miR-621
478316	hsa-miR-203a-3p	479135	hsa-miR-654-3p	478174	hsa-miR-605-5p
477963	hsa-miR-200b-3p	478048	hsa-miR-34a-5p	479047	hsa-miR-562
478417	hsa-miR-202-3p	479192	hsa-miR-888-5p	478158	hsa-miR-551a
478576	hsa-let-7b-5p	478189	hsa-miR-652-3p	478162	hsa-miR-572
478948	hsa-miR-499a-3p	477823	hsa-miR-92b-3p	479373	hsa-miR-566
478135	hsa-miR-494-3p	479188	hsa-miR-885-3p	478216	hsa-miR-99b-3p
478144	hsa-miR-504-5p	478204	hsa-miR-873-5p	477932	hsa-miR-17-3p
478976	hsa-miR-515-3p	477855	hsa-miR-122-5p	478688	hsa-miR-1288-3p
478203	hsa-miR-769-5p	479123	hsa-miR-643	478674	hsa-miR-1271-5p
479487	hsa-miR-517c-3p	479187	hsa-miR-876-5p	479522	hsa-miR-1269a
478129	hsa-miR-488-3p	478583	hsa-miR-181b-5p	480873	hsa-miR-129-1-3p
478148	hsa-miR-518b	478208	hsa-miR-889-3p	477897	hsa-miR-1301-3p
478143	hsa-miR-503-5p	477827	hsa-miR-92a-3p	478732	hsa-miR-185-3p
477909	hsa-miR-140-5p	479166	hsa-miR-758-3p	478675	hsa-miR-1272
478963	hsa-miR-509-3-5p	479194	hsa-miR-890	478714	hsa-miR-146a-3p
478954	hsa-miR-502-5p	477967	hsa-miR-205-5p	478230	hsa-miR-196a-5p
478978	hsa-miR-516a-5p	477941	hsa-miR-187-3p	478687	hsa-miR-1285-3p
478961	hsa-miR-508-3p	479421	hsa-miR-374b-3p	478692	hsa-miR-1293
478981	hsa-miR-518a-3p	478863	hsa-miR-377-5p	477928	hsa-miR-15a-3p
478183	hsa-miR-629-5p	478917	hsa-miR-452-3p	478689	hsa-miR-1289
478172	hsa-miR-598-3p	479049	hsa-miR-567	478659	hsa-miR-1253
479219	hsa-miR-943	478798	hsa-miR-302a-5p	478698	hsa-miR-1303
478339	hsa-miR-597-5p	478804	hsa-miR-30b-3p	478310	hsa-miR-1203
478176	hsa-miR-615-5p	478093	hsa-miR-425-3p	478683	hsa-miR-1282

Assay ID	Target name	Assay ID	Target name	Assay ID	Target name
479108	hsa-miR-624-3p	479178	hsa-miR-770-5p	478664	hsa-miR-1257
479112	hsa-miR-628-5p	478003	hsa-miR-29b-2-5p	479099	hsa-miR-616-5p
478160	hsa-miR-561-3p	479412	hsa-miR-30c-1-3p	478178	hsa-miR-624-5p
478023	hsa-miR-324-3p	478892	hsa-miR-432-3p	479074	hsa-miR-591
478213	hsa-miR-95-3p	478827	hsa-miR-32-3p	478182	hsa-miR-629-3p
478335	hsa-miR-496	478919	hsa-miR-454-5p	479081	hsa-miR-599
478326	hsa-miR-370-3p	478606	hsa-miR-30d-5p	478179	hsa-miR-625-3p
478028	hsa-miR-328-3p	478865	hsa-miR-380-5p	479499	hsa-miR-520h
477959	hsa-miR-197-3p	478786	hsa-miR-25-5p	478138	hsa-miR-497-5p
478037	hsa-miR-338-3p	478588	hsa-miR-320b	478155	hsa-miR-543
478043	hsa-miR-342-3p	478623	hsa-miR-106a-3p	478957	hsa-miR-505-5p
478314	hsa-miR-193b-3p	478794	hsa-miR-29b-1-5p	479022	hsa-miR-548j-5p
478486	hsa-miR-199b-5p	478768	hsa-miR-214-5p	479023	hsa-miR-548m
477804	hsa-miR-20b-5p	478629	hsa-miR-1184	479000	hsa-miR-541-5p
478032	hsa-miR-331-5p	477801	hsa-let-7f-1-3p	479536	hsa-miR-520c-3p
478479	hsa-miR-33b-5p	478122	hsa-miR-483-3p	478705	hsa-miR-132-5p
478067	hsa-miR-369-3p	478734	hsa-miR-18b-3p	479333	hsa-miR-519b-3p
478068	hsa-miR-369-5p	478665	hsa-miR-125b-1-3p	479374	hsa-miR-548k
477819	hsa-miR-208a-3p	478653	hsa-miR-1248	479056	hsa-miR-575
478337	hsa-miR-542-5p	477926	hsa-miR-155-3p	479222	hsa-miR-96-3p
478962	hsa-miR-508-5p	479185	hsa-miR-875-5p	479224	hsa-miR-99a-3p
478005	hsa-miR-29c-5p				

Supplementary table S12. Genes with known roles in beta cell fate, function, markers of cell stress or other pancreatic endocrine cell type.

Gene Symbol	**Assay ID**	**Role in beta cells**
GUSB	Hs00939627_m1	Housekeeper
PPIA	Hs04194521_s1	Housekeeper
HPRT1	Hs02800695_m1	Housekeeper
STK11	Hs00176092_m1	Beta cell function
FOXO1	Hs01054576_m1	Beta cell differentiation and beta cell function
PAX6	Hs00240871_m1	Beta cell differentiation and beta cell function
GCK	Hs01564555_m1	Beta cell function
MAFA	Hs01651425_s1	Beta cell function
NKX6-1	Hs00232355_m1	Beta cell differentiation and beta cell function
NEUROD1	Hs01922995_s1	Beta cell differentiation and beta cell function
NKX2-2	Hs00159616_m1	Beta cell differentiation and beta cell function
INS	Hs00355773_m1	Beta cell function
PDX1	Hs00236830_m1	Beta cell differentiation and beta cell function
PTPN1	Hs00942477_m1	Beta cell function
SLC16A1	Hs01560299_m1	Lactate/ pyruvate solute carrier – disallowed in beta cells
SYP	Hs00300531_m1	Beta cell function
LDHA	Hs01378790_g1	Lactate/ pyruvate solute carrier – disallowed in beta cells
PAX4	Hs00173014_m1	Beta cell differentiation and beta cell function
MAFB	Hs00271378_s1	Beta cell function
SLC2A2	Hs01096908_m1	Beta cell function
ARX	Hs00292465_m1	Alpha cell differentiation and function
GCG	Hs01031536_m1	Alpha cell function
SST	Hs00356144_m1	Delta cell function

Gene Symbol	Assay ID	Role in beta cells
HHEX	Hs00242160_m1	Delta cell marker
SOX9	Hs01001343_g1	Beta cell progenitor marker
NEUROG3	Hs01875204_s1	Beta cell progenitor marker
HES1	Hs00172878_m1	Beta cell progenitor marker
POU5F1	Hs04260367_gH	Beta cell progenitor marker
NANOG	Hs04399610_g1	Beta cell progenitor marker
HIF1A	Hs00153153_m1	Hypoxia marker
ARNT	Hs01121918_m1	Cellular stress and hypoxia marker
MYCL	Hs00420495_m1	Cellular stress and proliferation marker
DDIT3	Hs00358796_g1	Cellular stress and apoptosis marker

Supplementary table S13. Selected microRNA assay IDs

Assay name	Assay ID	Assay name	Assay ID
hsa-miR-576-5p	478165_mir	hsa-miR-885-5p	478207_mir
hsa-miR-376a-3p	478240_mir	hsa-miR-374b-3p	479421_mir
hsa-miR-9-5p	478214_mir	hsa-miR-148b-5p	478719_mir
hsa-miR-101-3p	477863_mir	hsa-miR-454-5p	478919_mir
hsa-miR-365a-3p	478065_mir	hsa-miR-30c-2-3p	479401_mir
hsa-miR-202-5p	478755_mir	hsa-miR-27b-3p	478270_mir
hsa-miR-34a-5p	478048_mir	hsa-miR-186-3p	479544_mir
hsa-miR-93-5p	478210_mir	hsa-miR-34a-5p	478048_mir
hsa-miR-23a-3p	478532_mir	hsa-miR-195-3p	478744_mir
hsa-miR-34b-3p	478049_mir	hsa-miR-593-5p	479077_mir
hsa-miR-34c-5p	478052_mir	hsa-miR-106b-3p	477866_mir
hsa-miR-30c-1-3p	479412_mir	hsa-miR-577	479057_mir
hsa-miR-27a-3p	478384_mir	hsa-miR-299-5p	478793_mir
hsa-miR-92b-5p	479207_mir	hsa-miR-199a-3p	477961_mir
hsa-miR-30a-5p	479448_mir	hsa-miR-99a-3p	479224_mir
hsa-miR-185-3p	478732_mir	hsa-miR-124-3p	477879_mir
hsa-miR-152-3p	477921_mir	hsa-miR-29a-3p	478587_mir
hsa-miR-21-3p	477973_mir	hsa-miR-136-5p	478307_mir

Supplementary table S14. Targets from DIANA pathways analysis

GENE	**Pathway**	**Pathway *p*-value**	**MITG score(s)**	**ASSAYS**
KMT2C	Lysine degradation	3.00×10^{-3}	0.97/0.92/0.80	All assays
BCL2L11	FOXO	0.02	0.99/ 0.89	Glycaemia and Palmitic acid
DLG2	Hippo	5.84×10^{-5}	0.92/0.81	Glycaemia, Palmitic acid and pro-inflammatory cytokines
SP1	TGFβ and Estrogen	0.02	0.99	Glycaemia and Hypoxia
SOD	FOXO	0.02	0.98	Glycaemia and Palmitic acid
MAPK1	FOXO	0.02	0.9	Glycaemia and Palmitic acid
TEAD1	Hippo	5.84×10^{-5}	0.85	Glycaemia and Hypoxia
SERPINE1	Hippo	5.84×10^{-5}	0.82	Glycaemia
MOB1A	Hippo	5.84×10^{-5}	0.82	Glycaemia
PDK1	Central carbon cancer	3.00×10^{-3}	0.82	Glycaemia and Hypoxia

Supplementary table S15. Assay IDs for predicted mRNA targets.

Gene	Assay ID	RefSeq
PPIA	Hs.PT.58v.38887593.g	NM_021130
HPRT1	Hs.PT.58.2145446	NM_000194
IDH3B	Hs.PT.19660618	NM_174855
MOB1A	Hs.PT.58.1530191	NM_018221
PDK1	Hs.PT.58.19794808	NM_002610
SOD1	Hs.PT.58.20593019	NM_000454
SP1	Hs.PT.58.19745651	NM_138473
KMT2C	Hs.PT.19586130	NM_170606
DLG2	Hs.PT.58.28262784	NM_001142702
BCL2L1	Hs.PT.56a.39595693.g	NM_138578
MAPK1	Hs.PT.58.39782850	NM_138957
SERPINE1	Hs.PT.58.3938488.g	NM_000602
TEAD1	Hs.PT.58.22785339	NM_021961

Supplementary table S16. miRNAs showing dysregulation following treatment with cellular stresses associated with T2D.

Assay ID	miRNA	Assay ID	miRNA	Assay ID	miRNA
478591	hsa-miR-302b-3p	478163	hsa-miR-574-3p	478183	hsa-miR-629-5p
478719	hsa-miR-148b-5p	478270	hsa-miR-27b-3p	479177	hsa-miR-769-3p
477962	hsa-miR-19b-1-5p	478131	hsa-miR-490-3p	478826	hsa-miR-323b-5p
479224	hsa-miR-99a-3p	478193	hsa-miR-664a-3p	478785	hsa-miR-24-2-5p
479064	hsa-miR-582-3p	477952	hsa-miR-191-5p	477833	hsa-miR-548d-3p
478732	hsa-miR-185-3p	478439	hsa-let-7d-5p	478318	hsa-miR-212-3p
477913	hsa-miR-144-3p	478831	hsa-miR-33a-3p	478065	hsa-miR-365a-3p
478687	hsa-miR-1285-3p	478165	hsa-miR-576-5p	478629	hsa-miR-1184
478914	hsa-miR-450b-5p	479217	hsa-miR-941	478273	hsa-miR-30a-3p
479003	hsa-miR-545-5p	478329	hsa-miR-454-3p	478411	ath-miR159a
478168	hsa-miR-590-3p	478660	hsa-miR-1254	477936	hsa-miR-183-3p
478175	hsa-miR-615-3p	477934	hsa-miR-181c-5p	477895	hsa-miR-1290
478177	hsa-miR-616-3p	479067	hsa-miR-585-3p	479087	hsa-miR-606

Assay ID	miRNA	Assay ID	miRNA	Assay ID	miRNA
478786	hsa-miR-25-5p	478913	hsa-miR-450b-3p	478514	hsa-miR-147a
478917	hsa-miR-452-3p	478293	cel-miR-39-3p	478238	hsa-miR-374a-5p
478979	hsa-miR-516b-5p	477863	hsa-miR-101-3p	478048	hsa-miR-34a-5p
478307	hsa-miR-136-5p	478179	hsa-miR-625-3p	477933	hsa-miR-181c-3p
478827	hsa-miR-32-3p	477963	hsa-miR-200b-3p	478532	hsa-miR-23a-3p
478012	hsa-miR-31-3p	478620	hsa-miR-101-5p	478513	hsa-miR-146b-5p
477921	hsa-miR-152-3p	478432	hsa-miR-483-5p	479530	hsa-miR-518d-5p
478491	hsa-miR-204-5p	478793	hsa-miR-299-5p	478623	hsa-miR-106a-3p
478742	hsa-miR-193b-5p	478384	hsa-miR-27a-3p	477896	hsa-miR-129-5p
479059	hsa-miR-579-3p	478691	hsa-miR-1292-5p	477912	hsa-miR-143-3p
479041	hsa-miR-556-3p	478753	hsa-miR-200b-5p	477942	hsa-miR-188-3p
477991	hsa-miR-23b-5p	477998	hsa-miR-27a-5p	477961	hsa-miR-199a-3p
478003	hsa-miR-29b-2-5p	478755	hsa-miR-202-5p	478589	hsa-miR-548b-5p
478032	hsa-miR-331-5p	478790	hsa-miR-296-3p	478622	hsa-miR-105-3p
478044	hsa-miR-342-5p	479024	hsa-miR-548n	478655	hsa-miR-1250-5p

Assay ID	miRNA	Assay ID	miRNA	Assay ID	miRNA
478105	hsa-miR-448	479178	hsa-miR-770-5p	478662	hsa-miR-1255b-5p
478130	hsa-miR-489-3p	479374	hsa-miR-548k	478717	hsa-miR-147b
478157	hsa-miR-548a-3p	479391	hsa-miR-548l	478919	hsa-mir-454-5p
478174	hsa-miR-605-5p	479412	hsa-miR-30c-1-3p	479401	hsa-mir-30c-2-3p
478182	hsa-miR-629-3p	480870	hsa-miR-548d-5p	479544	hsa-mir-186-3p
478185	hsa-miR-636	478240	hsa-miR-376a-3p	478744	hsa-mir-195-3p
478207	hsa-miR-885-5p	478210	hsa-miR-93-5p	478754	hsa-miR-200c-5p
478214	hsa-miR-9-5p	478049	hsa-mir-34b-3p	478399	hsa-miR-146a-5p
478337	hsa-miR-542-5p	478052	hsa-mir-34c-5p	478561	hsa-miR-449a
478342	hsa-miR-766-3p	479207	hsa-mir-92b-5p	479448	hsa-mir-30a-5p
479421	hsa-mir-374b-3p				

Supplementary table S17 Targeted expression of most altered microRNAs high throughput global microRNA screen.
The p values for statistical significance as determined by independent t-test, Mean difference, Standard errors of measurement (SED) and the 95% confidence intervals are given below. ***Bold italic p<0.016*** *Bonferroni correction for 3 tests: 1st, 2nd and 3rd time-points. Gene list is á priori so no further corrections. Italic underlined p<0.050. No correction for multiple testing.*

25 mM glucose Independent Samples Test- t- test p = 0.016																	
24 hrs						36 hrs						48 hrs					
	p value	Mean diff.	SED	95% CI			*p* value	Mean diff.	SED	95% CI			*p* value	Mean diff.	SED	95% CI	
				Lower	Upper					Lower	Upper					Lower	Upper
miR-185-3p	0.297	-0.743	0.675	-2.247	0.762	miR-185-3p	*0.024*	*-2.221*	*0.820*	*-4.076*	*-0.366*	miR-185-3p	*0.035*	*-1.629*	*0.667*	*-3.116*	*-0.142*
miR-885-5p	0.646	0.226	0.470	-0.886	1.338	miR-885-5p	0.98	0.007	0.272	-0.609	0.624	miR-885-5p	0.575	0.226	0.387	-0.665	1.118
miR-27b-3p	0.999	0.000	0.184	-0.411	0.411	miR-27b-3p	0.113	0.312	0.179	-0.088	0.711	miR-27b-3p	0.116	0.312	0.181	-0.091	0.715
miR-124-3p	0.206	0.296	0.219	-0.192	0.783	miR-124-3p	0.819	0.053	0.226	-0.450	0.556	miR-124-3p	0.592	-0.120	0.216	-0.601	0.362
miR-136-5p	0.252	0.318	0.262	-0.266	0.902	miR-136-5p	***0.008***	***0.782***	***0.236***	***0.257***	***1.306***	miR-136-5p	0.571	0.143	0.244	-0.400	0.685
miR-152-3p	0.448	-0.141	0.179	-0.539	0.257	miR-152-3p	***0.005***	***0.536***	***0.148***	***0.206***	***0.866***	miR-152-3p	0.111	0.288	0.165	-0.079	0.655
miR-299-5p	***0.002***	***-0.619***	***0.139***	***-0.933***	***-0.304***	miR-299-5p	*0.035*	*-0.255*	*0.103*	*-0.487*	*-0.023*	miR-299-5p	0.155	0.164	0.106	-0.075	0.404
miR-576-5p	0.514	-0.322	0.464	-1.456	0.813	miR-576-5p	0.101	-0.514	0.266	-1.164	0.136	miR-576-5p	*0.032*	*-0.683*	*0.224*	*-1.275*	*-0.091*
miR-93-5p	0.232	0.263	0.207	-0.197	0.724	miR-93-5p	0.097	0.395	0.216	-0.086	0.876	miR-93-5p	0.073	0.446	0.223	-0.050	0.942

2.5 mM glucose Independent Samples Test- t- test p = 0.016																
24 hrs						36 hrs						48 hrs				
	p value	Mean diff.	SED	95% CI			*p* value	Mean diff.	SED	95% CI			*p* value	Mean diff.	SED	95% CI	
miR-185-3p	0.188	-1.019	0.721	-2.626	0.587	miR-185-3p	0.146	-3.828	1.737	-10.675	3.019	miR-185-3p	0.108	-5.380	2.020	-13.523	2.763
miR-885-5p	0.188	-2.368	1.677	-6.105	1.368	miR-885-5p	0.325	0.905	0.862	-1.082	2.892	miR-885-5p	0.924	-0.184	1.876	-4.365	3.997
miR-454-5p	0.62	0.781	1.529	-2.625	4.187	miR-454-5p	*0.033*	*3.320*	*1.346*	*0.321*	*6.318*	miR-454-5p	***0.012***	***4.145***	***1.350***	***1.138***	***7.153***
miR-27b-3p	0.188	0.311	0.220	-0.179	0.801	miR-27b-3p	0.922	0.024	0.239	-0.508	0.556	miR-27b-3p	0.349	0.211	0.215	-0.267	0.690
miR-124-3p	0.689	-0.122	0.296	-0.782	0.538	miR-124-3p	0.056	-0.614	0.284	-1.247	0.020	miR-124-3p	0.521	-0.203	0.305	-0.882	0.476
miR-136-5p	0.075	0.518	0.260	-0.062	1.097	miR-136-5p	0.84	-0.056	0.269	-0.656	0.544	miR-136-5p	0.69	0.124	0.301	-0.548	0.795
miR-152-3p	0.637	-0.125	0.257	-0.697	0.447	miR-152-3p	0.299	-0.251	0.229	-0.762	0.260	miR-152-3p	0.239	0.288	0.230	-0.225	0.800
miR-299-5p	*0.49*	*0.831*	*1.159*	*-1.752*	*3.414*	miR-299-5p	0.457	0.897	1.160	-1.687	3.482	miR-299-5p	0.539	0.739	1.161	-1.848	3.326
miR-576-5p	0.352	1.439	1.475	-1.846	4.725	miR-576-5p	0.237	1.044	0.818	-0.839	2.928	miR-576-5p	0.946	-0.117	1.676	-3.852	3.618
miR-93-5p	0.332	0.244	0.239	-0.289	0.778	miR-93-5p	0.873	-0.042	0.257	-0.614	0.530	miR-93-5p	0.551	0.145	0.235	-0.378	0.668

<3% O2 Independent Samples Test- t- test p = 0.016																	
4 hrs						12 hrs						24 hrs					
	p value	Mean diff.	SED	95% CI			*p* value	Mean diff.	SED	95% CI			*p* value	Mean diff.	SED	95% CI	
				Lower	Upper					Lower	Upper					Lower	Upper
miR-27b-3p	0.14	-0.411	0.262	-0.977	0.155	miR-27b-3p	0.387	-0.229	0.256	-0.781	0.323	miR-27b-3p	0.18	-0.353	0.249	-0.891	0.185
miR-124-3p	0.065	1.816	0.852	-0.139	3.770	miR-124-3p	0.168	1.301	0.866	-0.665	3.268	miR-124-3p	0.389	1.083	1.215	-1.542	3.708
miR-136-5p	0.52	0.441	0.668	-1.001	1.884	miR-136-5p	0.468	0.502	0.672	-0.949	1.953	miR-136-5p	0.486	0.493	0.686	-0.990	1.975
miR-152-3p	0.142	-0.336	0.209	-0.807	0.135	miR-152-3p	0.511	-0.141	0.205	-0.607	0.326	miR-152-3p	0.11	-0.472	0.276	-1.068	0.123
miR-299-5p	***0.01***	***-0.685***	***0.220***	***-1.171***	***-0.200***	miR-299-5p	*0.035*	*-0.532*	*0.221*	*-1.020*	*-0.045*	miR-299-5p	0.182	-0.373	0.265	-0.945	0.199
miR-93-5p	0.102	-0.396	0.217	-0.889	0.097	miR-93-5p	0.229	-0.282	0.218	-0.777	0.213	miR-93-5p	0.097	-0.483	0.270	-1.067	0.101
miR-21-3p	0.238	0.826	0.650	-0.660	2.311	miR-21-3p	0.171	0.976	0.652	-0.512	2.464	miR-21-3p	0.265	0.771	0.645	-0.710	2.253

0.5 mM Palmitic acid Independent Samples Test- t- test p = 0.016																	
12 hrs						24 hrs						48 hrs					
	p value	Mean diff.	SED	95% CI			*p* value	Mean diff.	SED	95% CI			*p* value	Mean diff.	SED	95% CI	
				Lower	Upper					Lower	Upper					Lower	Upper
miR-185-3p	0.147	2.754	1.749	-1.144	6.651	miR-185-3p	0.992	-0.017	1.772	-3.966	3.931	miR-185-3p	0.368	1.731	1.835	-2.357	5.820
miR-885-5p	0.819	0.062	0.266	-0.531	0.656	miR-885-5p	0.634	-0.146	0.297	-0.809	0.516	miR-885-5p	*0.046*	*-0.522*	*0.230*	*-1.034*	*-0.010*
miR-27b-3p	0.682	-0.184	0.435	-1.152	0.785	miR-27b-3p	0.693	0.194	0.478	-0.872	1.260	miR-27b-3p	0.454	0.341	0.438	-0.635	1.318
miR-124-3p	0.814	-0.053	0.218	-0.540	0.434	miR-124-3p	0.651	-0.103	0.220	-0.594	0.388	miR-124-3p	0.226	0.228	0.169	-0.186	0.641
miR-136-5p	0.803	-0.060	0.235	-0.583	0.463	miR-136-5p	0.79	0.110	0.401	-0.783	1.002	miR-136-5p	***0.002***	***1.047***	***0.259***	***0.469***	***1.624***
miR-152-3p	0.357	-0.213	0.221	-0.705	0.279	miR-152-3p	0.563	0.160	0.268	-0.437	0.757	miR-152-3p	0.17	0.450	0.305	-0.229	1.129
miR-299-5p	0.076	-0.242	0.122	-0.515	0.030	miR-299-5p	0.86	-0.055	0.305	-0.736	0.625	miR-299-5p	0.415	0.178	0.209	-0.287	0.642
miR-576-5p	0.508	-0.192	0.280	-0.816	0.432	miR-576-5p	0.368	1.650	1.440	-4.412	7.712	miR-576-5p	0.129	-0.408	0.230	-0.978	0.163
miR-93-5p	0.794	-0.112	0.417	-1.042	0.818	miR-93-5p	0.683	0.201	0.479	-0.867	1.269	miR-93-5p	0.371	0.416	0.444	-0.574	1.406

proinflammatory cytokines Independent Samples Test- t- test p = 0.016																	
12 hrs						24 hrs						36 hrs					
	p value	Mean diff.	SED	95% CI			*p* value	Mean diff.	SED	95% CI			*p* value	Mean diff.	SED	95% CI	
				Lower	Upper					Lower	Upper					Lower	Upper
miR-885-5p	0.993	0.004	0.380	-0.857	0.864	miR-885-5p	0.773	-0.130	0.436	-1.116	0.856	miR-885-5p	0.121	0.667	0.389	-0.214	1.547
miR-454-5p	0.583	0.198	0.342	-0.638	1.034	miR-454-5p	0.702	-0.107	0.265	-0.755	0.542	miR-454-5p	0.57	-0.166	0.278	-0.823	0.492
miR-27b-3p	0.477	0.294	0.398	-0.593	1.180	miR-27b-3p	0.706	0.155	0.400	-0.737	1.048	miR-27b-3p	0.481	0.291	0.398	-0.595	1.178
miR-124-3p	0.146	0.411	0.261	-0.170	0.992	miR-124-3p	0.336	0.254	0.251	-0.305	0.813	miR-124-3p	0.55	0.148	0.240	-0.385	0.682
miR-136-5p	***0.002***	***-0.634***	***0.156***	***-0.982***	***-0.286***	miR-136-5p	0.562	0.190	0.282	-0.890	1.269	miR-136-5p	0.266	-0.547	0.368	-2.020	0.926
miR-152-3p	0.674	-0.069	0.158	-0.422	0.284	miR-152-3p	0.756	-0.060	0.188	-0.480	0.360	miR-152-3p	0.544	-0.251	0.353	-1.633	1.131
miR-299-5p	0.822	0.036	0.154	-0.308	0.379	miR-299-5p	0.152	-0.302	0.194	-0.735	0.132	miR-299-5p	0.371	0.128	0.137	-0.177	0.433
miR-576-5p	0.798	0.040	0.154	-0.302	0.383	miR-576-5p	0.194	0.276	0.198	-0.165	0.717	miR-576-5p	0.157	0.269	0.176	-0.123	0.660
miR-93-5p	0.257	-0.098	0.082	-0.281	0.084	miR-93-5p	0.533	-0.243	0.328	-1.605	1.118	miR-93-5p	0.156	-0.199	0.130	-0.489	0.090

Supplementary table S18 Validated of gene targets identified from DIANA pathways analysis.

The p values for statistical significance as determined by independent t-test, Mean difference, Standard errors of measurement (SED) and the 95% confidence intervals are given below. ***Bold italic p<0.050*** *Gene list is á priori and single test applied so no correction for multiple testing.*

25 mM high glucose Independent Samples Test *p* = 0.050					
Gene	*p* value	Mean Diff.	SED	95% CI	
				Lower	Upper
BCL211	0.392	0.060	0.066	-0.096	0.217
DLG2	0.215	0.184	0.135	-0.135	0.504
KMT2C	0.451	-0.069	0.087	-0.275	0.136
MAPK1	0.099	-0.048	0.025	-0.107	0.012
MOB1A	0.263	-0.075	0.061	-0.219	0.070
PDK1	0.373	0.094	0.099	-0.140	0.328
SERPINE1	0.11	0.085	0.046	-0.025	0.194
SOD1-1	***0.024***	***-0.085***	***0.030***	***-0.155***	***-0.015***
SP1	0.367	-0.064	0.067	-0.222	0.093
TEAD1	0.682	-0.033	0.077	-0.216	0.150

2.5 mM low glucose Independent Samples Test *p* = 0.050					
Gene	*p* value	Mean Diff.	SED	95% CI	
				Lower	Upper
BCL211	0.206	0.083	0.060	-0.058	0.225
DLG2	0.122	0.234	0.133	-0.080	0.549
KMT2C	0.259	-0.054	0.044	-0.158	0.050
MAPK1	***0.039***	***-0.117***	***0.046***	***-0.226***	***-0.007***
MOB1A	0.117	-0.103	0.057	-0.238	0.033

2.5 mM low glucose Independent Samples Test *p* = 0.050					
Gene	*p* value	Mean Diff.	SED	95% CI	
				Lower	Upper
PDK1	0.179	0.151	0.101	-0.088	0.391
SERPINE1	0.448	0.037	0.046	-0.071	0.145
SOD1-1	0.957	-0.002	0.037	-0.090	0.086
SP1	0.475	-0.052	0.069	-0.216	0.111
TEAD1	0.931	-0.007	0.077	-0.190	0.176

Hypoxia Independent Samples Test *p*=0.050					
Gene	*p* value	Mean Diff.	SED	95% CI	
				Lower	Upper
BCL211	0.266	-0.088	0.072	-0.264	0.088
DLG2	***0.004***	***-0.457***	***0.091***	***-0.689***	***-0.225***
KMT2C	0.934	0.005	0.057	-0.135	0.145
MAPK1	0.153	0.054	0.033	-0.027	0.134
MOB1A	0.449	-0.058	0.072	-0.233	0.117
PDK1	***0.0003***	***0.873***	***0.121***	***0.577***	***1.170***
SERPINE1	0.285	-0.082	0.070	-0.254	0.089
SOD1-1	0.025	-0.077	0.025	-0.140	-0.013
SP1	0.95	0.005	0.083	-0.197	0.208
TEAD1	0.525	0.071	0.105	-0.186	0.328

0.5 mM Palmitic Acid Independent Samples Test *p*=0.050					
Gene	*p* value	Mean Diff.	SED	95% CI	
				Lower	Upper
BCL211	0.692	0.023	0.057	-0.110	0.157
DLG2	0.598	0.073	0.133	-0.240	0.387
KMT2C	0.06	-0.138	0.061	-0.283	0.007
MAPK1	0.252	-0.031	0.025	-0.090	0.028
MOB1A	0.13	-0.099	0.057	-0.234	0.037
PDK1	***0.023***	***0.281***	***0.097***	***0.053***	***0.510***
SERPINE1	0.423	0.043	0.050	-0.076	0.161
SOD1-1	0.905	0.005	0.040	-0.090	0.099
SP1	0.882	-0.010	0.068	-0.171	0.150
TEAD1	0.51	0.054	0.078	-0.130	0.237

Pro-inflammatory cytokines Independent Samples Test *p*=0.050					
Gene	*p* value	Mean Diff.	SED	95% CI	
				Lower	Upper
BCL211	0.766	0.015	0.049	-0.101	0.132
DLG2	***0.032***	***0.267***	***0.095***	***0.032***	***0.502***
KMT2C	0.861	-0.014	0.076	-0.193	0.165
MAPK1	0.729	-0.012	0.034	-0.094	0.069
MOB1A	0.104	-0.104	0.056	-0.236	0.028
PDK1	0.407	0.086	0.097	-0.144	0.315

Pro-inflammatory cytokines Independent Samples Test *p*=0.050					
SERPINE1	0.746	-0.017	0.051	-0.138	0.104
SOD1-1	0.741	-0.014	0.040	-0.110	0.082
SP1	0.273	-0.102	0.085	-0.304	0.100
TEAD1	0.615	0.045	0.085	-0.156	0.246

Supplementary table S19 Targeted expression of microRNAs strongly validated to target panel of genes with known roles in beta cells

The p values for statistical significance as determined by independent t-test, Mean difference, Standard errors of measurement (SED) and the 95% confidence intervals are given below. ***Bold italic p<0.016*** *Bonferroni correction for 3 tests: 1st, 2nd and 3rd time-points. Gene list is á priori so no further corrections.Italic underlined p<0.050. No correction for multiple testing*

25 mM High glucose Independent Samples Test *p*=0.016																	
MiRNA	*p* value	Mean diff.	SED	95% CI		miRNA	*p* value	Mean diff.	SED	95% CI		miRNA	*p* value	Mean diff.	SED	95% CI	
				Lower	Upper					Lower	Upper					Lower	Upper
miR-101-3p	0.099	-0.435	0.239	-0.968	0.098	miR-101-3p	0.773	0.093	0.315	-0.609	0.796	miR-101-3p	0.187	-0.312	0.221	-0.804	0.179
miR-199a-3p	***0.001***	***4.438***	***0.917***	***2.395***	***6.482***	miR-199a-3p	0.11	2.021	1.151	-0.544	4.587	miR-199a-3p	***0.005***	***3.436***	***0.944***	***1.332***	***5.539***
miR-21-3p	0.755	0.080	0.251	-0.478	0.639	miR-21-3p	0.952	0.019	0.301	-0.652	0.689	miR-21-3p	*0.049*	*-0.532*	*0.238*	*-1.063*	*-0.002*
miR-29a-3p	0.267	-2.144	1.432	-8.023	3.734	miR-29a-3p	0.861	-0.077	0.428	-1.030	0.876	miR-29a-3p	0.555	-0.249	0.407	-1.157	0.659
miR-376a-3p	***0.013***	***-1.208***	***0.399***	***-2.099***	***-0.317***	miR-376a-3p	0.769	-0.225	0.744	-1.882	1.433	miR-376a-3p	***0.009***	***-1.252***	***0.374***	***-2.108***	***-0.397***
miR-92b-5p	0.504	0.911	1.315	-2.019	3.841	miR-92b-5p	0.51	-1.046	1.529	-4.453	2.361	miR-92b-5p	0.651	0.607	1.304	-2.299	3.514

2.5 mM Low glucose Independent Samples Test *p*=0.016																	
	p value	Mean diff.	SED	95% CI			*p* value	Mean diff.	SED	95% CI			*p* value	Mean diff.	SED	95% CI	
				Lower	Upper					Lower	Upper					Lower	Upper
miR-101-3p	0.361	0.226	0.235	-0.305	0.757	miR-101-3p	0.209	0.322	0.238	-0.217	0.860	miR-101-3p	0.157	0.361	0.234	-0.168	0.891
miR-21-3p	0.333	0.197	0.194	-0.235	0.628	miR-21-3p	0.134	0.309	0.189	-0.113	0.731	miR-21-3p	0.546	0.122	0.195	-0.313	0.557
miR-29a-3p	0.746	0.116	0.347	-0.658	0.890	miR-29a-3p	0.507	-0.257	0.374	-1.089	0.575	miR-29a-3p	0.124	0.579	0.344	-0.188	1.345
miR-376a-3p	0.423	-0.477	0.571	-1.751	0.796	miR-376a-3p	0.545	-0.353	0.564	-1.609	0.903	miR-376a-3p	*0.039*	*-1.345*	*0.565*	*-2.603*	*-0.087*
miR-92b-5p	0.907	0.031	0.261	-0.560	0.622	miR-92b-5p	0.551	0.13321	0.215	-0.3532	0.619	miR-92b-5p	0.118	0.454	0.259	-0.144	1.052

<3% O2 Hypoxia Independent Samples Test *p*=0.016																	
	p value	Mean diff.	SED	95% CI			*p* value	Mean diff.	SED	95% CI			*p* value	Mean diff.	SED	95% CI	
				Lower	Upper					Lower	Upper					Lower	Upper
miR-101-3p	0.495	0.097	0.138	-0.202	0.396	miR-101-3p	0.263	0.178	0.152	-0.151	0.507	miR-101-3p	0.78	0.061	0.213	-0.403	0.524
miR-21-3p	0.782	0.038	0.133	-0.256	0.331	miR-21-3p	0.391	-0.159	0.177	-0.549	0.232	miR-21-3p	0.226	-0.172	0.134	-0.470	0.125
miR-29a-3p	0.466	0.227	0.303	-0.427	0.881	miR-29a-3p	0.879	-0.053	0.343	-0.795	0.688	miR-29a-3p	0.393	0.329	0.371	-0.480	1.138
miR-376a-3p	0.74	-0.146	0.430	-1.076	0.784	miR-376a-3p	0.576	0.217	0.378	-0.600	1.034	miR-376a-3p	0.355	0.464	0.483	-0.588	1.516
miR-92b-5p	0.852	0.058	0.302	-0.600	0.715	miR-92b-5p	0.858	0.06112	0.333	-0.6814	0.803	miR-92b-5p	0.418	-0.342	0.405	-1.244	0.560

0.5 mM Palmitic Acid Independent Samples Test *p*=0.016																	
	p value	Mean diff.	SED	95% CI			*p* value	Mean diff.	SED	95% CI			*p* value	Mean diff.	SED	95% CI	
				Lower	Upper					Lower	Upper					Lower	Upper
miR-101-3p	0.625	0.064	0.127	-0.219	0.346	miR-101-3p	0.692	-0.066	0.162	-0.428	0.295	miR-101-3p	0.338	-0.190	0.188	-0.616	0.235
miR-21-3p	0.193	-0.316	0.227	-0.821	0.189	miR-21-3p	0.697	-0.091	0.227	-0.597	0.415	miR-21-3p	0.321	-0.276	0.265	-0.866	0.314
miR-29a-3p	0.34	0.144	0.144	-0.177	0.465	miR-29a-3p	0.114	0.260	0.150	-0.074	0.594	miR-29a-3p	0.587	0.109	0.194	-0.323	0.541
miR-376a-3p	0.157	0.275	0.180	-0.126	0.676	miR-376a-3p	0.847	0.040	0.204	-0.415	0.496	miR-376a-3p	0.705	-0.221	0.569	-1.488	1.045
miR-92b-5p	0.732	0.106	0.296	-0.594	0.805	miR-92b-5p	0.601	0.15959	0.291	-0.5292	0.848	miR-92b-5p	0.122	0.705	0.401	-0.244	1.653

Pro-inflammatory cytokines Independent Samples Test *p*=0.016																	
	p value	Mean diff.	SED	95% CI			*p* value	Mean diff.	SED	95% CI			*p* value	Mean diff.	SED	95% CI	
				Lower	Upper					Lower	Upper					Lower	Upper
miR-101-3p	0.776	-0.151	0.516	-1.319	1.017	miR-101-3p	0.724	0.184	0.506	-0.961	1.330	miR-101-3p	0.862	0.091	0.508	-1.058	1.240
miR-199a-3p	0.585	0.192	0.336	-0.603	0.987	miR-199a-3p	*0.039*	*0.576*	*0.219*	*0.040*	*1.112*	miR-199a-3p	0.966	-0.021	0.469	-1.131	1.089
miR-202-5p	0.749	-0.493	1.502	-3.840	2.853	miR-202-5p	***0.001***	***-3.623***	***0.758***	***-5.355***	***-1.890***	miR-202-5p	0.208	-2.071	1.538	-5.498	1.356
miR-21-3p	0.115	0.404	0.234	-0.117	0.925	miR-21-3p	***0.016***	***-0.663***	***0.229***	***0.152***	***1.174***	miR-21-3p	0.091	0.448	0.239	-0.085	0.982
miR-29a-3p	0.094	0.824	0.434	-0.177	1.825	miR-29a-3p	***0.001***	***1.477***	***0.263***	***0.857***	***2.097***	miR-29a-3p	***0.011***	***0.930***	***0.281***	***0.281***	***1.580***
miR-374b3p	0.471	-0.343	0.439	-1.473	0.787	miR-374b3p	0.279	0.372	0.317	-0.378	1.123	miR-374b3p	0.059	0.618	0.274	-0.030	1.266
miR-376a-3p	0.829	0.116	0.522	-1.047	1.278	miR-376a-3p	0.982	0.012	0.525	-1.158	1.182	miR-376a-3p	0.623	-0.301	0.593	-1.622	1.020
miR-9-5p	0.195	-0.541	0.371	-1.448	0.366	miR-9-5p	0.35	-0.292	0.288	-0.998	0.414	miR-9-5p	0.683	0.140	0.327	-0.660	0.940
miR-92b-5p	0.624	-0.2902	0.57225	-1.5847	1.00436	miR-92b-5p	0.98	-0.012	0.439	-0.990	0.967	miR-92b-5p	0.817	0.112	0.470	-0.935	1.159

Supplementary table S20: Effects of cell insult treatments on total gene expression of significant miRNA target genes from beta cell specific target panel.

The p values for statistical significance as determined by independent t-test, Mean difference, Standard errors of measurement (SED) and the 95% confidence intervals are given below. ***Bold italic p<0.016*** *Bonferroni correction for 3 tests: 1st, 2nd and 3rd time-points. Gene list is á priori so no further corrections.*

Gene	Associated miRNA	*p* value	Mean diff.	SED	95% C I	
					Lower	Upper
STK11	miR-199a	0.002	-0.107	0.04	0.2	0.02
SOX9	miR-21	0.005	0.421	0.12	0.16	0.68
FOXO1	miR-29a	0.000	-0.258	0.050	-0.369	-0.146

Chapter 6:

Discussion

Summary of thesis

Type 2 Diabetes (T2D) is characterised by cell stressors associated with the diabetic physiology including: poor glucose homeostasis, dyslipidaemia, hypoxia and pro-inflammatory cytokines. Studies in rodent models have shown that exposure to these cellular stresses elicits a change in beta cell differentiation status, which contributes to the beta cell mass loss that is seen in the disease. I have investigated this phenomenon using the EndoC-βH1 human beta cell line, along with human islets from cases with Type 2 Diabetes and long duration Type 1 Diabetes. To characterise the importance of the cellular microenvironment on the EndoC βH1 cell modeI, I investigated the importance of the species origin on markers of beta cell fate and function, which allowed optimisation of an entirely human culture protocol. I found that using human culture reagents improved glucose sensitive insulin secretion and improved the physiological relevance of the model for assessing cellular stress response. Having optimised the cell model, I assessed changes in response to diabetes related cell stresses to the targeted transcriptomic profile, splicing changes, altered microRNA expression and changes in protein expression, in both cells and islets from cases with either T2D or T1D. I found that changes to beta cell differentiation status occur in response to these cellular stressors via altered expression of genes known to influence beta cell fate and altered splicing factor expression, leading to changes in the patterns of alternative splicing and altered microRNA expression. This altered transcriptomic profile causes a beta to delta phenotypic shift in a proportion of cells and this is also seen in the islets of patients with T2D and long duration type 1 Diabetes.

Summary of data chapters

Chapter 3. The species origin of the cellular microenvironment influences markers of beta cell fate and function in EndoC-βH1 cells

Summary

In chapter 3, I investigated the effects of species origin on the cellular microenvironment on markers of beta cell fate and function in EndoC-βH1 cells. I compared the responses of the cells to non-human and human derived culture reagents and assessed these in relation to growth, morphology, gene expression and glucose simulated insulin secretion (GSIS). I found that EndoC-βH1 cells cultured in entirely human derived culture reagents demonstrated a greater tendency to form cell clusters and exhibited reduced alpha cell markers at the mRNA level, for *ARX* and *GCG* genes respectively. No differences were noted in the protein expression of mature beta cell markers, such as *PDX1* and *NEUROD1*, in EndoC-βH1 cells cultured in a human microenvironment but the cells were more sensitive to glucose, showing a 4.3-fold increase in insulin secretion following glucose challenge compared with a 1.9-fold increase in cells grown in a non-human microenvironment.

Importance of findings

Our data suggest that the tissue origin of the cellular microenvironment has effects on the function of EndoC-βH1 cells in vitro, and the use of a more human-

like culture microenvironment may bring benefits in terms of increased physiological relevance.

Future work

It would be beneficial for understanding the importance of reagent species origin in tissue culture for these findings to be replicated in other human cell lines, to evaluate if this should be considered when assessing the effect of microenvironment on gene expression. It would also be of interest to investigate genome wide effects. Creating a 3D culture microenvironment to investigate whether formation of beta-cell only pseudo islets affect responses to cellular stresses may provide greater insights into how beta cells interact with their immediate microenvironment as well as their proliferation. This has been shown to improve beta cell survival and insulin secretion in rodent cell lines and so it would be important for these results to be validated in human models[319]. However, these considerations have not been investigated further here, as they lay outside the remit of this project.

Chapter 4. Cellular stressors may influence transdifferentiation in human beta cells by moderation of alternative splicing patterns.

Summary

In Chapter 4, I investigated changes in beta cell differentiation status via assessing total gene expression for a target gene panel, alternative splicing patterns, splicing factor expression, protein expression in both EndoC-βH1 cells and pancreatic sections from cases with either T2D or T1D (compared to individuals without diabetes) and the effects of small molecule inhibition of the AKT pathway. The *in vitro* work involved exposing the EndoC-βH1 human beta cell line to relevant cellular stresses associated with a T2D physiology in order to assess their effects. Assessment of total gene expression was carried out by analysis of a target panel of 35 genes, chosen for their roles in either beta cell fate and function, or as markers of plasticity, cellular stress or other pancreatic islet cell type. Data from each of the cell treatment assays showed dysregulation of the majority of these genes, including a network known to be important to the maintenance of beta cell fate. Altered splicing patterns were assessed by analysing ratio changes in genes within the target panel, with functionally relevant isoform changes, and where it was possible to design probes to distinguish between the isoforms. These data showed significant dysregulation at the level of splicing. Splicing factor expression was also investigated and again showed widespread dysregulation in expression levels, indicating the importance of altered splicing in changes to beta cell differentiation status.

Immunofluorescence was used to investigate changes to hormone expression in both treated EndoC-βH1cells, as well as pancreatic sections islets from cases with either T2D or long duration (>5 y) T1D. The *in vitro* data showed a statistically significant shift from a beta to delta cell phenotype in a proportion of treated cells, with loss of insulin and gain of somatostatin expression in these altered cells. Immunofluorescent staining of pancreatic sections from cases with either T2D or T1D also showed statistically significant increases in the number of delta cells within diabetic islets.

Our group had previously identified *FOXO1* as a regulator of splicing factor expression via the AKT pathway and, given the altered splicing patterns and splicing factor expression seen in response to cellular stresses, I used small molecule inhibition of the AKT pathway to determine effects on splicing and protein expression. I found that inhibition of the AKT pathway, via the small molecule SH6, prevented the beta to delta phenotypic shifts following exposure to 25 mM high glucose.

Importance of findings

This is, to my knowledge, the first demonstration using human models that changes in beta cell differentiation status, following exposure to cellular stresses relevant to T2D physiology, occur due to altered splicing as a result of dysregulated splicing factor expression via dysregulation of *FOXO1*. These data offer the possibility of targeting splicing patterns for therapeutic benefit in the management of diabetes.

Future work

It would be of benefit to characterise the specific splicing regulatory changes that occur following exposure to cellular stresses associated with the diabetic physiology. This would potentially allow identification of targets for small molecule and antisense oligonucleotide interventions to restore mature beta cell identity. This could be achieved by sorting those cells that appear to have transdifferentiated, following cell stress treatment, to identify the regulators that are responsible for splicing decisions. It may then be possible to restore splicing patterns in the transdifferentiated cells using small molecules to target individual splice sites using antisense oligonucleotides. Assessing the subcellular location of FOXO1, possibly using sub-cellular fractionation would also be an important next step. Investigating the effect of these changes on beta cell function would also be beneficial. Dynamic studies investigating the effect of these cellular stressors on insulin release via the use of insulin reporters would be a useful technique, along with calcium imaging and electrophysiology[320].

Chapter 5. Cellular stress responses in the human beta cell line EndoC-βH1 may be co-ordinated by microRNAs.

Summary

In Chapter 5, I investigated the effects of T2D related cellular stresses on MicroRNA expression. A global high throughout miRNA screen was used to identify miRs expressed in the EndoC-βH1 cell line, and those with the greatest fold change in response to cellular stresses were used for pathways analysis. Validation of target genes from pathway analysis was also investigated. I found negative correlations for miR-454-5p and its predicted target *MAPK1*, miR-136-5p and its predicted target *DLG2* and miR-299-5p and its predicted target *PDK1*. Each of these genes is known to influence beta cell dysfunction and survival. This may suggest miRNA regulation of rates of beta cell apoptosis in response to these cellular stressors.

miRNAs that were strongly validated against targets in an *á priori* target panel of genes with roles in beta cell fate and function, marker for cellular stress, and markers for other pancreatic endocrine cell types, were assessed for altered levels of expression. Target panel genes were also assessed for altered expression in response to these cellular stressors. I found that there were negative correlations for miR-199a and its validated target *STK11 (LKB1)*, miR-21 and its validated target *SOX9* and miR-29a and its validated target *FOXO1.* These findings are interesting because both *STK11* and *FOXO1* are associated with maintenance of mature beta cell differentiation status. *SOX9* is a beta cell

marker and the increased expression that is observed in response to T2D relevant cellular stresses may suggest increased cellular plasticity.

Importance of findings

Taking all these data together, this may suggest that beta cell responses to these cellular stressors involves altered miRNA regulation of genes with roles in both beta cell fate and beta cell survival.

Future work

These findings support recent studies which have shown that microRNAs are an intrinsic part of the cell's adaptive response to cellular stresses. This is of particular importance in relation to maintenance of mature beta cell differentiation status and survival. Assessment of miRNA regulation of beta cell stress responses offers the potential for targeting specific miRNAs as a possible therapeutic intervention. However, the exact mechanism of how miRNAs are dysregulated in response to diabetes related cell stresses remains to be elucidated[157]. This would be an important area for future research. In relation to miRNA regulation of beta cell de-differentitaion, it would also be important to evaluate whether restoring those miRNAs which are dysregulated in response to cell stress promote beta cell redifferentitaion. In this work, we identified changes in differentiation status in only a proportion of the culture and hypothesized that these cells might form a subset within the culture. Assessing whether there are miRs which specifically target different beta cell subsets, or promote beta cell diversity within islets would also be a critical next step.

Discussion of thesis

This thesis discusses the effects of cell stresses, associated with T2D, on beta cell differentiation status. To do this, I first optimised the EndoC βH1 cell model to develop a physiologically relevant system for studying the effects of cell stress. I then went on to consider the effects of these cell stresses on gene expression, splicing patterns, splicing factor expression, microRNA expression and hormone expression. I have provided key insights into changes in beta cell fate and have identified, for the first time, that dysregulation of alternative splicing, associated with changes in splicing factor expression via dysregulation of *FOXO1,* causes a beta to delta shift in a proportion of EndoCβH1 cells. I have also found that this shift in phenotype from beta to delta is seen in islets from cases with either T2D or long duration T1D. To complete this targeted transcriptomic profile, I also investigated the effects of diabetes related cellular stresses on microRNA expression and used gene enrichment analysis to identify the pathways implicated by altered microRNA expression. This work identified that cellular stresses do cause changes in microRNA expression, which may increase cellular plasticity via miRNA regulation of genes known to be important for maintenance of beta cell fate. It also showed changes in the expression of microRNAs associated with beta cell survival, with changes in the expression of miRNAs targeting genes with known roles in rates of apoptosis. Taking the findings from each of these studies together, it may suggest that cell stress affects beta cell plasticity and may influence beta cell differentiation status.

The development of the EndoC βH1 cell line has allowed, for the first time, a reliable model for studying human disease. Previous human beta cell lines have

been derived from ductal cells, such as the fusion cell line 1.1B4, and so assessing differentiation using cells of this type is problematic[264]. Improving the physiological validity of the cell model for studying human disease was an important first step in this project. To study the effects of changes in beta cell differentiation status in response to a diabetic physiology in humans, I first investigated the importance of the species origin of culture reagents on the EndoC-βH1 cell model. It is known that cellular microenvironment is particularly important to beta cells as they interact intimately with their environment to sense changes in glucose and react to other pancreatic islet cell hormones[70, 249, 321]. Communication between beta cells is intrinsic to their function and beta cell subsets exist within islets, including beta cell hubs, which regulate insulin secretion across the islet[79, 281]. Beta cell hubs show increased plasticity and are particularly vulnerable to cellular stressors in the islet microenvironment[79]. It has been shown that beta cell mass loss alone can drive changes in beta cell differentiation, underlining the importance of close cell-cell communication, not only for function, but also maintenance of beta cell fate[69, 70]. Considering how important cellular microenvironment is to beta cell fate and function, assessing the impact of species origin of culture reagents was an important first step in assessing the effects of T2D related cellular stresses on beta cell differentiation status.

The effect of the species origin on the EndoC-βH1 human beta cell model was assessed by analysing changes in total gene expression, hormone expression and GSIS between non-human and human culture reagents. I have demonstrated that cells cultured using human reagents showed reduced expression of alpha cell markers and improved GSIS compared to those cultured

using animal derived reagents. This suggests that species origin should be considered when investigating the effects of changes in the cellular microenvironment to avoid potentially confounding results. It also optimised the cell model to a fully human system for investigating human disease.

Having optimised the cell model in this way, I investigated the effects of the diabetic physiology (changes in glucose homeostasis, dyslipidaemia, hypoxia and proinflammatory cytokines) on total gene expression for genes in the previously described target panel. Across each of the assays there were changes to a number of genes in a network that is known to influence beta cell fate. The network, comprising: *PAX6, PDX1, NEUROD1, NKX2-2, NKX6-1, PAX4* and *FOXO1* regulate insulin synthesis, maintenance of beta cell function during cell stress and maintenance of beta cell fate. Reduced expression of genes within this network has been associated with a loss of mature beta cell status and transdifferentiation to an alpha cell phenotype in murine models, please refer to figure 23[96, 197]. *PAX6* is vital for beta cell function and is known to directly bind and activate the *INS*, *PDX1*, and *MAFA* gene promotor regions[79, 196]. It also interacts with the beta cell specific transcription factors *PDX1, NEUROD1, NKX2-2 and NKX6-1,* of which NKX2-2 activates *PAX6*[288]. It has been shown to regulate beta cell identity by promoting the expression of glucose sensing genes and by inhibition of the disallowed beta cell gene *SLC16A1*[288]. In conjunction with *PDX1, PAX6* is known to bind the somatostatin gene promoter and studies using *PAX6* knockouts have shown reduced expression of insulin, glucagon and somatostatin[271, 322].

Figure 23. Schematic representation of transcriptional network and model of FOXO1 inhibition of splicing factor expression.

The tight regulation of the genes within this network are important to establishing and maintaining mature beta cell status. The schematic shows gene interactions and indicates the importance of nodal genes within the network.

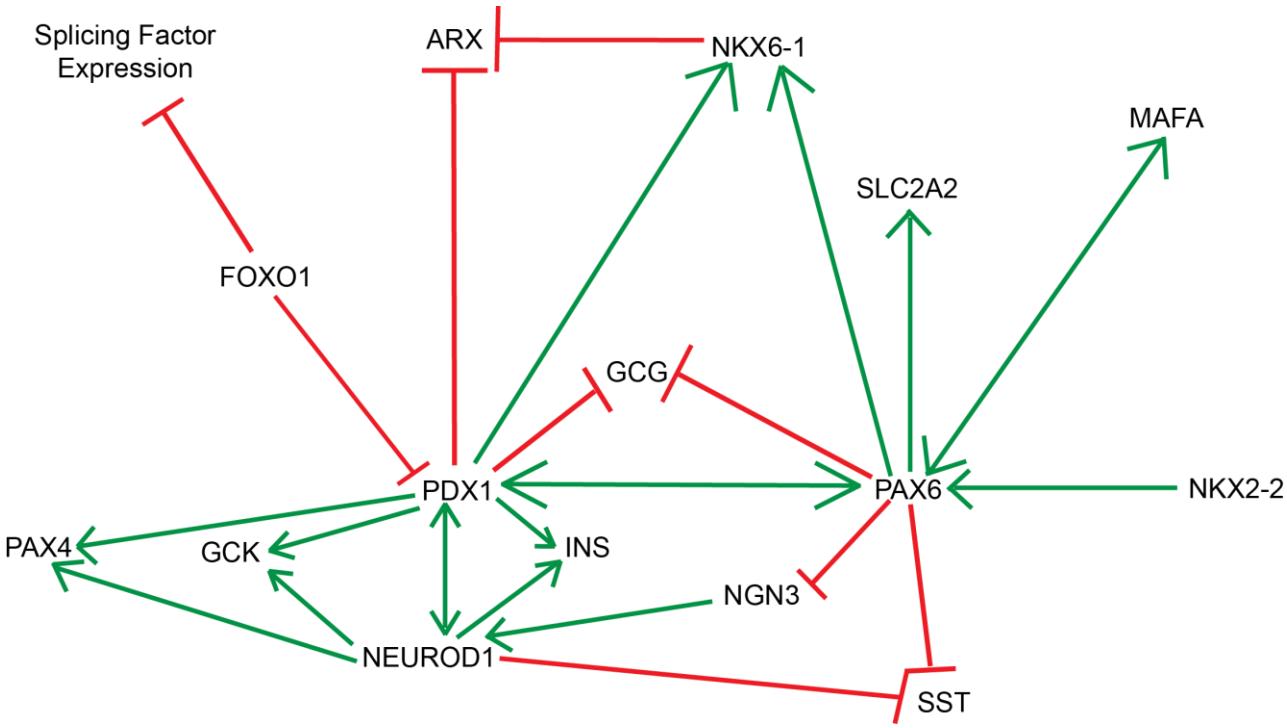

Loss of *PDX1* expression has been shown to result in the loss of mature beta cells status[269]. It also has roles in the maintenance of beta cell function, proliferation during cell stress and ageing via beta cell neogenesis. As a transcription factor, it forms a nucleoprotein complex with *NEUROD1* on the *INS* gene to allow interactions with transcription factors and transcriptional machinery[323]. *PDX1* also maintains beta cell differentiation status via inhibition of the alpha cell genes *ARX* and *GCG*[57, 323]. Similarly to *PDX1, NKX2-2, NKX6-1* and *PAX4* also maintain mature beta cell status via repression of the alpha cell gene *ARX*[107]. *NKX2-2* and *PAX4* are known to form an axis with *ARX*, whereby *NKX2-2* and *PAX4* repress *ARX* to favour a beta cell phenotype, but in alpha

cells, increased *ARX* expression suppresses them in turn to maintain mature alpha cell status[119]. Together, *PAX6, PDX1, NEUROD1, NKX2-2, NKX6-1* and *PAX4* form interactions which maintain beta cell function and beta cell fate, as shown in figure 23[84, 107, 324]. However, the majority of these genes are also expressed in the other islet cell types and so it is the tight regulation of expression levels which confers each cell types differentiation status[57]. Importantly, changes in the expression levels of genes within this network disrupt maintenance of the mature beta cell fate[71].

FOXO1 is also known to have key roles in beta cell fate and function. It has been shown in rodent models to be important for beta cell compensation for insulin resistance via augmentation of glucose sensing and management of oxidative stress[289]. In euglycaemic states, FOXO1 is located in the cytoplasm of beta cells in response to insulin production which activates AKT, leading to phosphorylation of serine and threonine sites in FOXO1[274]. During oxidative stress FOXO1 is acetylated, which both protects it from ubiquitination and targets it to the nucleus[47, 274]. ER stress also induces FOXO1 to translocate to the nucleus but acts via MAPK activation[103, 273, 274]. There is controversy over its role in beta cell replication, Kitamura et al, using Foxo1-ADA, suggest Foxo1 inhibits the proliferative activities of Pdx1[47], however, Zhang et al used a wtFoxo1 in their study[289], arguing that Foxo1 improves beta cell responses to hyperglycaemia via increasing beta cell mass, glucose sensing and anti-oxidative function[289]. There is also disagreement over its interaction with *PDX1*, with Kawamori et al[325] and Kitamura et al[47] suggesting *FOXO1* inhibits the activity and expression of *PDX1*, while Zhang et al[289] and Al-Masri et al[273] argue that it acts in parallel with *PDX1*. Our group have recently discovered a potential role for dysregulated

FOXO1 in the regulation of splicing factor expression and alternative splicing patterns, as a downstream activator of AKT, as shown in figure 23. Here, *FOXO1* expression is dysregulated in response to a number of the cellular stresses. Cells also showed increased expression of markers for cellular stress that are known to occur in response to hyperglycaemia, ER stress and oxidative stress. These conditions are known to alter the subcellular location of FOXO1, thereby affecting its activity[103, 274, 325]. This led to a hypothesis where dysregulated *FOXO1* expression and activity may result in dysregulation of splicing via altered splicing factor expression, resulting in changes to mature beta cell differentiation status.

As alternative splicing is well known to respond to cellular stresses[277], I investigated whether dysregulation of the pathways which regulate splicing may affect beta cell differentiation status, by assessing their effect on splicing factor expression and alternative splicing for specific genes in the target panel. Importantly, expression of splicing factor, serine arginine rich (SR) and heterogenous ribonucleoprotein particle (HnRNP) genes, which encode positive and negative regulators of alternative splicing, were also dysregulated by exposure to the cell stresses. Assessment of the alternative splicing patterns for genes selected from the target panel, showed significant differences in *PAX6, PTPN1* and *POU5F1* isoform expression.

Changes in the ratio of isoforms are important as this may result in change of function[326]. In the case of *PAX6,* switches in isoform ratio are known to affect DNA binding of downstream targets[224, 227]. The *PAX6* exon 5 insertion isoform (PAX6-5a) lacks the DNA binding ability of the N-terminal subdomain and unmasks the DNA binding ability of the C-terminal subdomain[224, 227]. This

change in DNA binding activity is thought to function as a molecular switch that specifies target genes[228, 288]. *POU5F1* isoform differences are known to confer differences in response to cellular stress and increased plasticity[327], with the *OCT4B* and *B1* variants believed to shuttle to the cytoplasm in response to cell stress[230]. I found ratio changes in the expression of *OCT4* isoforms in response to all of the cellular stressors tested. Protein tyrosine phosphatase *PTPN1 (PTP1B)* is known to negatively regulate insulin and leptin signalling via dephosphorylation of the activating phosphorotyrosines on the insulin receptor[144, 212, 235]. There are two variants resulting from alternative splicing: a long transcript which includes intron 9 and a shorter form where intron 9 is excised[235]. Studies have shown that the long isoform is associated with body fat percentage and fasting insulin scores and has been suggested as a biomarker for hyperinsulinaemia in Diabetes[235]. Taken together, the dysregulation of splicing factor expression and patterns of alternative splicing in response to cellular stresses support the hypothesis that this may be a mechanism for the loss of mature beta cell status in T2D.

To investigate the effects of the T2D relevant cellular stressors on hormone expression, I assessed insulin, glucagon and somatostatin expression in EndoC-βH1 cells using immunofluorescence microscopy. I found that in treated cells a small, but statistically significant, proportion of the cells lost insulin expression and gained somatostatin expression following exposure to the noxious stimuli. There was no evidence of glucagon expression in any of the treated cells. To test whether these effects related to non-specific stresses, I also treated the cells with oleic acid, a fatty acid that is not known to induce metabolic stress in human beta cells and has been reported to confer protection from beta cell apoptosis to cells

co-treated with palmitic acid[28, 207]. Here, oleate did not cause an increase in somatostatin positivity, but it also conferred no protective effect against palmitate. This indicates that the shift from a beta to delta phenotype was not indiscriminate and occurs through different mechanisms to those involved in oleate-mediated protection from palmitate-induced apoptosis.

As these findings may have been purely a characteristic of EndoC-βH1 cell responses, I also assessed changes in hormone expression in islets from donors with long duration T1D and T2D using immunofluorescence microscopy. This showed statistically significant increases in somatostatin staining in both T1D and T2D islets. In T2D islets the increase in somatostatin staining was not associated with a significant loss in total islet area. The increase in somatostatin staining in T1D islets was particularly striking, although this was also associated with a loss in total islet area due to the depletion of beta cells. These findings support the idea that there may be a change in the differentiation status of islets cells in response to stresses associated with diabetes. Importantly, it also suggests that transdifferentiation in humans appears to be from beta to delta, rather than from beta to alpha, in the manner that has been seen in rodent models[61].

To investigate the idea that ER stress may contribute to changes in beta cell differentiation via altered splicing, as a result of altered *FOXO1* activity and expression, EndoC-βH1 cells were treated with the ER stress inducer tunicamycin. I found that tunicamycin treatment also caused a statistically significant loss of insulin and gain of somatostatin expression in a proportion of the cells. ER stress has been shown to regulate transcriptional and translational responses in T2D, particularly because high demand for insulin makes beta cells

extremely sensitive to ER stress[11, 38]. It has been proposed that ER stress leads to beta cell dysfunction and cell death as a result of impaired insulin secretion and increased sensitivity to glucotoxicity[11, 33, 38]. Here, levels of *FOXO1* transcript expression were reduced following exposure to tunicamycin. Zhang et al have suggested that FOXO1 activity is vital for the enhancement of beta cell function during oxidative and ER stress[289], under which conditions it is known to translocate from the cytoplasm to the nucleus, where it acts as a transcription factor[325]. These findings support the idea that cellular stresses disrupt mature beta cell status and again imply a role for dysregulation of *FOXO1* in this process.

While it is acknowledged that only a small, but significant, proportion of cells shifted from a beta to delta-like phenotype, it is known there are at least 4 subsets of beta cells and it may be possible these subsets respond differently to cellular stresses[281, 328]. Beta cell hubs in particular are considered to be more susceptible to changes in their cellular microenvironment and are known to have increased plasticity[79]. It may be that the proportion of cells in the culture which respond to cellular stresses, by a shift from a beta to delta phenotype, do so because they are more sensitive to stresses than other cells in the culture. This is a feature of the EndoC-βH1 model that should be investigated in the future, as it will better characterise their use as a model system as well as potentially providing insight into the effects of cell stress on beta cell subsets. To determine whether there was evidence for full transdifferentiation from beta to delta, gene and protein expression levels for *HHEX* were also carried out. *HHEX* is known to be exclusively associated with delta cells in the endocrine pancreas and its absence may indicate that the cells were probably not fully transdifferentiated[329].

To determine whether the effects of cellular stresses caused permanent changes to beta cell differentiation status, I investigated whether removal of the cellular stress and restoration under standard culture conditions could rescue a mature beta cell phenotype in the EndoC-βH1 cells. As in the previous assays, I found that cells that had been treated with high glucose for 24 hours showed a loss of insulin expression and gain of somatostatin expression using immunofluorescence microscopy, indicating a shift from beta to delta-like phenotype. However, when treated cells were restored to standard culture conditions for 72 hours there was no longer any evidence of somatostatin staining, indicating that it is possible to rescue the cells to a mature beta cell status. This finding may offer an explanation for anecdotal evidence from patients with T2D who report remission of their disease following a strict diet and exercise regime.

Taking all these data together in the context of the model which describes changes to beta cell differentiation status occurring due to dysregulation of splicing, possibly caused by altered FOXO1 activity, I investigated the potential role of the AKT pathway. I assessed the effects of AKT pathway inhibition via the small molecule inhibitor of AKT, SH6, to determine whether this affected the beta to delta cell like shift in phenotype. EndoC-βH1 cells treated with SH6, showed no increase in somatostatin hormone expression following treatment with 25 mM high glucose. Importantly, there was also no evidence for dysregulation of splicing factor expression or patterns of alternative splicing. This may suggest that disruption of the AKT pathway, in particular *FOXO1*, is important for transdifferentiation from a mature beta cell status to a delta cell like phenotype to occur. This would fit a model where cellular stressors relevant to T2D cause

dysregulation of the activity and expression of *FOXO1*, which in turn disrupts splicing factor expression and patterns of alternative splicing in genes with known roles in the maintenance of beta cell fate and function.

Since microRNA (miRNA) expression is also known to be significantly altered by exposure to cellular stresses and a number of miRNAs have been linked to T2D[300, 301, 330], I performed a large scale miRNA screen to identify the most altered miRNAs for further investigation. I selected 10 miRNAs that are known to be empirically strongly validated to targets in the panel of genes with relevance to beta cell fate and function and found negative correlations for 3 miRNAs and their target genes. miR-199a and its validated target *STK11 (LKB1)*, a gene that has been shown to maintain beta cell identity[171], responded to 25mM high glucose, with *STK11(LKB1)* significantly decreased in expression. miR-29a has *FOXO1* as one of its targets and here levels were increased, in contrast to reduced *FOXO1* expression in response to inflammatory factors. Importantly, STK11 (LKB1) is required for AKT mediated phosphorylation and activation of *FOXO1*[331]. Following treatment with low glucose, hypoxia and palmitic acid, miR-21 showed reduced expression while there was increased expression of its target *SOX9,* a gene associated with increased cellular plasticity[213]. Taking these findings together, a model can be hypothesized whereby cellular stresses cause dysregulation of miRNA expression for miRNAs that are known to target genes important for the maintenance of beta cell fate and function.

Along with assessment of miRNA expression of miRNAs strongly validated to the target panel, 10 miRNAs were selected that had the highest fold change across all of the cell treatment assays. These were assessed for their response to the

cellular stresses and the list of significant mRNAs were taken into pathways analysis. This identified a number of pathways which were ranked according to *p* value, MITG score and number of genes affected[248]. Genes from the top ranked pathways were selected for further validation. Notably, one of the pathways selected included FOXO, with genes from the other pathways that were selected also known to interact with *FOXO1*, in particular *MAPK1*. From validation of the genes identified by the pathways analysis, 3 negative correlations were detected: miR-454-5p and its predicted target *MAPK1*, miR-136-5p and its predicted target *DLG2* and miR-299-5p and its predicted target *PDK1*. These genes all have roles in pathways that are important for beta cell survival and which also interact with the FOXO pathway. Here, each of the negative correlations favoured pro-apoptotic responses, with increases in *PDK1* and *DLG2* expression, with concomitant decreases in the expression of the miRs known to target them. Increased expression of these genes favours activation of proapoptotic pathways[287, 297, 313, 332]. There was increased expression of miR454-5p with decreased expression of its predicted target *MAPK1*, which is also known to increase rates of apoptosis.

It is acknowledged that there are limitations with the work described in this thesis. There is a strong emphasis on the transcriptomic profile of beta cell responses to T2D related cellular stressors and future work elucidating functional responses, including electrophysiology, will be important. It will also be critical to extend the transcriptomic profile to genome wide, as this study was restricted to investigating changes in a target panel of specific beta cell relevant genes. The EndoC βH1 cell model, while an important recent development in the study of diabetes, does have a number of issues that needs to be taken into account when interpreting

results. The cell line is derived from foetal pancreatic buds and may be more prone to changes in differentiation status. These cells are also known to express genes that have been previously described as 'disallowed' in beta cells, although these were derived from murine studies. For this reason, this study also utilised *ex vivo* human islets to characterise possible changes in differentiation status. It is also acknowledged that the work on altered miRNA expression in the final chapter will benefit from replication in human islets and that validation of the results to determine causality will be an important next step.

Conclusion

T2D has strong associations with obesity and a sedentary lifestyle, with well documented increases in the levels of physiological stresses in the islet microenvironment. These stresses are known to lead to beta cell mass loss resulting from apoptosis. However, recent studies in mice show changes to beta cell differentiation status in response to cellular stresses. These findings require corroboration using human models and elucidation of the mechanisms underpinning changes in differentiation status are important for understanding human disease. Characterisation of these mechanisms also presents an opportunity for identifying future treatment targets. The results of this study show, for the first time, that exposure to cellular stresses causes a shift from a beta to delta cell phenotype in a proportion of beta cells. These changes are associated with dysregulation of key genes with roles in beta cell fate, including *FOXO1,* as well as disruption of alternative splicing and splicing factor expression. This supports a model where disruption to the activity and expression of *FOXO1* affects splicing factor expression and alternative splicing. Inhibition of the AKT

pathway, which activates FOXO1, prevented changes in differentiation status in cells exposed to high glucose. Assessment of miRNA expression showed dysregulation of miRs strongly validated to target genes important for beta cell fate, including *FOXO1* and genes known to be important for FOXO1 activation. Pathways analysis of miRs most altered following exposure to the cell stresses also implicated FOXO related pathways and cell survival.

These findings provide a new insight into the response of human beta cells to cellular stresses associated with T2D. They show that, in human disease, changes in beta cell differentiation status are an important feature of T2D but that changes in phenotype are from beta to delta cell. This contrasts with findings from studies in mice which suggest transdifferentiation occurs from a beta to alpha cell phenotype. These data may suggest that dysregulation of *FOXO1* activity and expression leads to dysregulation of splicing factor expression and alternative splicing which in turn increases beta cell plasticity allowing for changes in mature beta cell differentiation status. The data also show that beta cell stress responses may be co-ordinated by microRNAs and again imply a role for *FOXO1* in this process in relation to both maintenance of beta cell fate and survival.

References

1. Chang-Chen KJ, Mullur R, Bernal-Mizrachi E. Beta-cell failure as a complication of diabetes. Reviews in endocrine & metabolic disorders. 2008;9(4):329-43.
2. Nordmann TM, Dror E, Schulze F, Traub S, Berishvili E, Barbieux C, et al. The Role of Inflammation in β-cell Dedifferentiation. Scientific Reports. 2017;7(1):6285.
3. Donath MY, Shoelson SE. Type 2 diabetes as an inflammatory disease. Nature Reviews Immunology. 2011;11:98.
4. Thiruvoipati T, Kielhorn CE, Armstrong EJ. Peripheral artery disease in patients with diabetes: Epidemiology, mechanisms, and outcomes. World Journal of Diabetes. 2015;6(7):961-9.
5. Rask-Madsen C, King George L. Vascular Complications of Diabetes: Mechanisms of Injury and Protective Factors. Cell Metabolism. 2013;17(1):20-33.
6. Hex N, Bartlett C, Wright D, Taylor M, Varley D. Estimating the current and future costs of Type 1 and Type 2 diabetes in the UK, including direct health costs and indirect societal and productivity costs. Diabetic medicine : a journal of the British Diabetic Association. 2012;29(7):855-62.
7. Briggs ADM, Scarborough P, Wolstenholme J. Estimating comparable English healthcare costs for multiple diseases and unrelated future costs for use in health and public health economic modelling. PLOS ONE. 2018;13(5):e0197257.
8. Roberts S, Craig D, Adler A, McPherson K, Greenhalgh T. Economic evaluation of type 2 diabetes prevention programmes: Markov model of low- and high-intensity lifestyle programmes and metformin in participants with different categories of intermediate hyperglycaemia. BMC Medicine. 2018;16(1):16.
9. Worldwide trends in diabetes since 1980: a pooled analysis of 751 population-based studies with 4·4 million participants. The Lancet. 2016;387(10027):1513-30.
10. Bommer C, Sagalova V, Heesemann E, Manne-Goehler J, Atun R, Bärnighausen T, et al. Global Economic Burden of Diabetes in Adults: Projections From 2015 to 2030. Diabetes Care. 2018:dc171962.
11. Fonseca SG, Gromada J, Urano F. Endoplasmic reticulum stress and pancreatic beta cell death. Trends in endocrinology and metabolism: TEM. 2011;22(7):266-74.
12. Fu Z, Gilbert ER, Liu D. Regulation of Insulin Synthesis and Secretion and Pancreatic Beta-Cell Dysfunction in Diabetes. Current diabetes reviews. 2013;9(1):25-53.
13. Leibiger IB, Leibiger B, Berggren P-O. Insulin Signaling in the Pancreatic β-Cell. Annual review of nutrition. 2008;28(1):233-51.
14. Navale AM, Paranjape AN. Glucose transporters: physiological and pathological roles. Biophysical reviews. 2016;8(1):5-9.
15. Thorens B, Mueckler M. Glucose transporters in the 21st Century. American journal of physiology Endocrinology and metabolism. 2010;298(2):E141-5.
16. De Vos A, Heimberg H, Quartier E, Huypens P, Bouwens L, Pipeleers D, et al. Human and rat beta cells differ in glucose transporter but not in glucokinase gene expression. Journal of Clinical Investigation. 1995;96(5):2489-95.
17. Matschinsky F, Liang Y, Kesavan P, Wang L, Froguel P, Velho G, et al. Glucokinase as pancreatic beta cell glucose sensor and diabetes gene. The Journal of clinical investigation. 1993;92(5):2092-8.
18. Efrat S, Leiser M, Wu YJ, Fusco-DeMane D, Emran OA, Surana M, et al. Ribozyme-mediated attenuation of pancreatic beta-cell glucokinase expression in transgenic mice results in impaired glucose-induced insulin secretion. Proc Natl Acad Sci U S A. 1994;91(6):2051-5.
19. Dolensek J, Rupnik MS, Stozer A. Structural similarities and differences between the human and the mouse pancreas. Islets. 2015;7(1):e1024405.
20. Levetan CS, Pierce SM. Distinctions between the islets of mice and men: implications for new therapies for type 1 and 2 diabetes. Endocrine practice : official journal of the American College of Endocrinology and the American Association of Clinical Endocrinologists. 2013;19(2):301-12.
21. Brereton H, Carvell MJ, Persaud SJ, Jones PM. Islet alpha-cells do not influence insulin secretion from beta-cells through cell-cell contact. Endocrine. 2007;31.
22. Steiner DJ, Kim A, Miller K, Hara M. Pancreatic islet plasticity: interspecies comparison of islet architecture and composition. Islets. 2010;2(3):135-45.
23. Benner C, van der Meulen T, Caceres E, Tigyi K, Donaldson CJ, Huising MO. The transcriptional landscape of mouse beta cells compared to human beta cells reveals notable species differences in long non-coding RNA and protein-coding gene expression. BMC Genomics. 2014;15:620.
24. Samuel VT, Shulman GI. Integrating Mechanisms for Insulin Resistance: Common Threads and Missing Links. Cell. 2012;148(5):852-71.
25. Dresner A, Laurent D, Marcucci M, Griffin ME, Dufour S, Cline GW, et al. Effects of free fatty acids on glucose transport and IRS-1-associated phosphatidylinositol 3-kinase activity. J Clin Invest. 1999;103(2):253-9.
26. Itani SI, Ruderman NB, Schmieder F, Boden G. Lipid-induced insulin resistance in human muscle is associated with changes in diacylglycerol, protein kinase C, and IkappaB-alpha. Diabetes. 2002;51(7):2005-11.
27. Fabbrini E, Magkos F, Mohammed BS, Pietka T, Abumrad NA, Patterson BW, et al. Intrahepatic fat, not visceral fat, is linked with metabolic complications of obesity. Proc Natl Acad Sci U S A. 2009;106(36):15430-5.
28. Welters HJ, Tadayyon M, Scarpello JH, Smith SA, Morgan NG. Mono-unsaturated fatty acids protect against beta-cell apoptosis induced by saturated fatty acids, serum withdrawal or cytokine exposure. FEBS letters. 2004;560(1-3):103-8.
29. Vasu S, McClenaghan NH, McCluskey JT, Flatt PR. Effects of lipotoxicity on a novel insulin-secreting human pancreatic beta-cell line, 1.1B4. Biological chemistry. 2013;394(7):909-18.
30. Berry C, Lal M, Binukumar BK. Crosstalk Between the Unfolded Protein Response, MicroRNAs, and Insulin Signaling Pathways: In Search of Biomarkers for the Diagnosis and Treatment of Type 2 Diabetes. Frontiers in Endocrinology. 2018;9:210.
31. Li N, Frigerio F, Maechler P. The sensitivity of pancreatic beta-cells to mitochondrial injuries triggered by lipotoxicity and oxidative stress. Biochem Soc Trans. 2008;36(Pt 5):930-4.

32. Oslowski CM, Urano F. Measuring ER stress and the unfolded protein response using mammalian tissue culture system. Methods in enzymology. 2011;490:71-92.
33. Özcan U, Cao Q, Yilmaz E, Lee A-H, Iwakoshi NN, Özdelen E, et al. Endoplasmic Reticulum Stress Links Obesity, Insulin Action, and Type 2 Diabetes. Science. 2004;306(5695):457-61.
34. Han J, Kaufman RJ. The role of ER stress in lipid metabolism and lipotoxicity. Journal of lipid research. 2016;57(8):1329-38.
35. Rehman K, Akash MSH. Mechanisms of inflammatory responses and development of insulin resistance: how are they interlinked? Journal of Biomedical Science. 2016;23(1):87.
36. Ortis F, Naamane N, Flamez D, Ladrière L, Moore F, Cunha DA, et al. Cytokines Interleukin-1β and Tumor Necrosis Factor-α Regulate Different Transcriptional and Alternative Splicing Networks in Primary β-Cells. Diabetes. 2010;59(2):358-74.
37. Shoelson SE, Lee J, Goldfine AB. Inflammation and insulin resistance. Journal of Clinical Investigation. 2006;116(7):1793-801.
38. Brozzi F, Eizirik DL. ER stress and the decline and fall of pancreatic beta cells in type 1 diabetes. Upsala Journal of Medical Sciences. 2016;121(2):133-9.
39. Brozzi F, Nardelli T, Lopes M, Millard I, Barthson J, Igoillo-Esteve M, et al. Cytokines induce endoplasmic reticulum stress in human, rat and mouse beta cells via different mechanisms. Diabetologia. 2015;58(10):2307-16.
40. Eizirik DL, Sammeth M, Bouckenooghe T, Bottu G, Sisino G, Igoillo-Esteve M, et al. The human pancreatic islet transcriptome: expression of candidate genes for type 1 diabetes and the impact of pro-inflammatory cytokines. PLoS Genet. 2012;8.
41. Bonnavion R, Jaafar R, Kerr-Conte J, Assade F, van Stralen E, Leteurtre E, et al. Both PAX4 and MAFA Are Expressed in a Substantial Proportion of Normal Human Pancreatic Alpha Cells and Deregulated in Patients with Type 2 Diabetes. PLoS ONE. 2013;8(8):e72194.
42. Guo S, Dai C, Guo M, Taylor B, Harmon JS, Sander M, et al. Inactivation of specific β cell transcription factors in type 2 diabetes. The Journal of clinical investigation. 2013;123(8):3305-16.
43. Kobayashi M, Kikuchi O, Sasaki T, Kim H-J, Yokota-Hashimoto H, Lee Y-S, et al. FoxO1 as a double-edged sword in the pancreas: analysis of pancreas- and β-cell-specific FoxO1 knockout mice. American Journal of Physiology - Endocrinology and Metabolism. 2012;302(5):E603-E13.
44. Fiori JL, Shin Y-K, Kim W, Krzysik-Walker SM, González-Mariscal I, Carlson OD, et al. Resveratrol Prevents β-Cell Dedifferentiation in Nonhuman Primates Given a High-Fat/High-Sugar Diet. Diabetes. 2013;62(10):3500-13.
45. Sato Y, Inoue M, Yoshizawa T, Yamagata K. Moderate Hypoxia Induces β-Cell Dysfunction with HIF-1–Independent Gene Expression Changes. PLoS ONE. 2014;9(12):e114868.
46. Vasu S, McClenaghan NH, McCluskey JT, Flatt PR. Cellular responses of novel human pancreatic beta-cell line, 1.1B4 to hyperglycemia. Islets. 2013;5(4):170-7.
47. Kitamura T. The role of FOXO1 in [beta]-cell failure and type 2 diabetes mellitus. Nat Rev Endocrinol. 2013;9(10):615-23.
48. Weaver JR, Holman TR, Imai Y, Jadhav A, Kenyon V, Maloney DJ, et al. Integration of pro-inflammatory cytokines, 12-lipoxygenase and NOX-1 in pancreatic islet beta cell dysfunction. Mol Cell Endocrinol. 2012;358(1):88-95.
49. Morrison F, Johnstone K, Murray A, Locke J, Harries LW. Oxidative Metabolism Genes Are Not Responsive to Oxidative Stress in Rodent Beta Cell Lines. Experimental Diabetes Research. 2012;2012:793783.
50. Xin Y, Dominguez Gutierrez G, Okamoto H, Kim J, Lee A-H, Adler C, et al. Pseudotime Ordering of Single Human β-Cells Reveals States of Insulin Production and Unfolded Protein Response. Diabetes. 2018;67(9):1783-94.
51. Zheng X, Wang X, Ma Z, Gupta Sunkari V, Botusan I, Takeda T, et al. Acute hypoxia induces apoptosis of pancreatic beta-cell by activation of the unfolded protein response and upregulation of CHOP. Cell death & disease. 2012;3:e322.
52. Gerber PA, Rutter GA. The Role of Oxidative Stress and Hypoxia in Pancreatic Beta-Cell Dysfunction in Diabetes Mellitus. Antioxidants & Redox Signaling. 2017;26(10):501-18.
53. Norouzirad R, González-Muniesa P, Ghasemi A. Hypoxia in Obesity and Diabetes: Potential Therapeutic Effects of Hyperoxia and Nitrate. Oxidative Medicine and Cellular Longevity. 2017;2017:5350267.
54. Sharma RB, Alonso LC. Lipotoxicity in the Pancreatic Beta Cell: Not Just Survival and Function, but Proliferation as Well? Current diabetes reports. 2014;14(6):492-.
55. Pappan KL, Pan Z, Kwon G, Marshall CA, Coleman T, Goldberg IJ, et al. Pancreatic β-Cell Lipoprotein Lipase Independently Regulates Islet Glucose Metabolism and Normal Insulin Secretion. Journal of Biological Chemistry. 2005;280(10):9023-9.
56. Collier JJ, Burke SJ, Eisenhauer ME, Lu D, Sapp RC, Frydman CJ, et al. Pancreatic β-Cell Death in Response to Pro-Inflammatory Cytokines Is Distinct from Genuine Apoptosis. PLOS ONE. 2011;6(7):e22485.
57. Fujimoto K, Polonsky KS. Pdx1 and other factors that regulate pancreatic beta-cell survival. Diabetes, obesity & metabolism. 2009;11 Suppl 4:30-7.
58. Gao T, McKenna B, Li C, Reichert M, Nguyen J, Singh T, et al. Pdx1 maintains β-cell identity and function by repressing an α-cell program. Cell Metab. 2014;19.
59. Avrahami D, Li C, Zhang J, Schug J, Avrahami R, Rao S, et al. Aging-Dependent Demethylation of Regulatory Elements Correlates with Chromatin State and Improved β Cell Function. Cell Metabolism.
60. Wang Yue J, Golson Maria L, Schug J, Traum D, Liu C, Vivek K, et al. Single-Cell Mass Cytometry Analysis of the Human Endocrine Pancreas. Cell Metabolism. 2016;24(4):616-26.
61. Talchai C, Xuan S, Lin HV, Sussel L, Accili D. Pancreatic β-Cell Dedifferentiation As Mechanism Of Diabetic β-Cell Failure. Cell. 2012;150(6):1223-34.
62. Dhawan S, Georgia S, Tschen S-i, Fan G, Bhushan A. Pancreatic β Cell Identity Is Maintained by DNA Methylation-Mediated Repression of Arx. Developmental cell. 2011;20(4):419-29.
63. Chera S, Baronnier D, Ghila L, Cigliola V, Jensen JN, Gu G, et al. Diabetes recovery by age-dependent conversion of pancreatic δ-cells into insulin producers. Nature. 2014;514.
64. Zhang X, Yalcin S, Lee D-F, Yeh T-YJ, Lee S-M, Su J, et al. FOXO1 is an essential regulator of pluripotency in human embryonic stem cells. Nat Cell Biol. 2011;13(9):1092-9.
65. Thorel F, Nepote V, Avril I, Kohno K, Desgraz R, Chera S, et al. Conversion of adult pancreatic alpha-cells to beta-cells after extreme beta-cell loss. Nature. 2010;464(7292):1149-54.
66. Dietrich C, Scherwat J, Faust D, Oesch F. Subcellular Localization of β-Catenin Is Regulated by Cell Density. Biochemical and Biophysical Research Communications. 2002;292(1):195-9.

67. Zhang C, Lu L, Li Y, Wang X, Zhou J, Liu Y, et al. IGF binding protein-6 expression in vascular endothelial cells is induced by hypoxia and plays a negative role in tumor angiogenesis. International Journal of Cancer Journal International du Cancer. 2012;130(9):2003-12.
68. Gage BK, Webber TD, Kieffer TJ. Initial Cell Seeding Density Influences Pancreatic Endocrine Development During <italic>in vitro</italic> Differentiation of Human Embryonic Stem Cells. PLoS ONE. 2013;8(12):e82076.
69. Kulkarni RN, Mizrachi EB, Ocana AG, Stewart AF. Human beta-cell proliferation and intracellular signaling: driving in the dark without a road map. Diabetes. 2012;61(9):2205-13.
70. Back Wd, Zimm R, Brusch L. Transdifferentiation of pancreatic cells by loss of contact-mediated signaling. BMC Systems Biology. 2013;7(1):77.
71. van der Meulen T, Huising MO. The role of transcription factors in the transdifferentiation of pancreatic islet cells. Journal of molecular endocrinology. 2015;54(2):R103-R17.
72. Brissova M, Aamodt K, Brahmachary P, Prasad N, Hong J-Y, Dai C, et al. Islet Microenvironment, Modulated by Vascular Endothelial Growth Factor-A Signaling, Promotes β Cell Regeneration. Cell Metabolism. 2014;19(3):498-511.
73. Butler AE, Janson J, Bonner-Weir S, Ritzel R, Rizza RA, Butler PC. Beta-cell deficit and increased beta-cell apoptosis in humans with type 2 diabetes. Diabetes. 2003;52(1):102-10.
74. Kloppel G, Lohr M, Habich K, Oberholzer M, Heitz PU. Islet pathology and the pathogenesis of type 1 and type 2 diabetes mellitus revisited. Survey and synthesis of pathology research. 1985;4(2):110-25.
75. Meier JJ, Bonadonna RC. Role of Reduced β-Cell Mass Versus Impaired β-Cell Function in the Pathogenesis of Type 2 Diabetes. Diabetes Care. 2013;36(Suppl 2):S113-S9.
76. Marchetti P, Del Guerra S, Marselli L, Lupi R, Masini M, Pollera M, et al. Pancreatic islets from type 2 diabetic patients have functional defects and increased apoptosis that are ameliorated by metformin. The Journal of clinical endocrinology and metabolism. 2004;89(11):5535-41.
77. Hattersley AT, Tooke JE. The fetal insulin hypothesis: an alternative explanation of the association of low birthweight with diabetes and vascular disease. Lancet (London, England). 1999;353(9166):1789-92.
78. Ashcroft Frances M, Rorsman P. Diabetes Mellitus and the β Cell: The Last Ten Years. Cell. 2012;148(6):1160-71.
79. Johnston Natalie R, Mitchell Ryan K, Haythorne E, Pessoa Maria P, Semplici F, Ferrer J, et al. Beta Cell Hubs Dictate Pancreatic Islet Responses to Glucose. Cell Metabolism.24(3):389-401.
80. White MG, Marshall HL, Rigby R, Huang GC, Amer A, Booth T, et al. Expression of Mesenchymal and α-Cell Phenotypic Markers in Islet β-Cells in Recently Diagnosed Diabetes. Diabetes Care. 2013;36(11):3818-20.
81. Chakravarthy H, Gu X, Enge M, Dai X, Wang Y, Damond N, et al. Converting Adult Pancreatic Islet α Cells into β Cells by Targeting Both Dnmt1 and Arx. Cell Metabolism. 2017;25(3):622-34.
82. Brereton MF, Iberl M, Shimomura K, Zhang Q, Adriaenssens AE, Proks P, et al. Reversible changes in pancreatic islet structure and function produced by elevated blood glucose. Nature Communications. 2014;5:4639.
83. Kim A, Miller K, Jo J, Kilimnik G, Wojcik P, Hara M. Islet architecture: A comparative study. Islets. 2009;1(2):129-36.
84. Wang J, Elghazi L, Parker SE, Kizilocak H, Asano M, Sussel L, et al. The concerted activities of Pax4 and Nkx2.2 are essential to initiate pancreatic β-cell differentiation. Developmental biology. 2004;266(1):178-89.
85. Dai C, Brissova M, Hang Y, Thompson C, Poffenberger G, Shostak A, et al. Islet-enriched gene expression and glucose-induced insulin secretion in human and mouse islets. Diabetologia. 2012;55(3):707-18.
86. Puri S, Hebrok M. Diabetic β Cells: To Be or Not To Be? Cell. 2012;150(6):1103-4.
87. White P, May CL, Lamounier RN, Brestelli JE, Kaestner KH. Defining pancreatic endocrine precursors and their descendants. Diabetes. 2008;57(3):654-68.
88. Murtaugh LC. Pancreas and beta-cell development: from the actual to the possible. Development. 2007;134.
89. Chakrabarti SK, Mirmira RG. Transcription factors direct the development and function of pancreatic beta cells. Trends in endocrinology and metabolism: TEM. 2003;14(2):78-84.
90. Bernardo AS, Hay CW, Docherty K. Pancreatic transcription factors and their role in the birth, life and survival of the pancreatic β cell. Molecular and Cellular Endocrinology. 2008;294(1–2):1-9.
91. Pullen TJ, Khan AM, Barton G, Butcher SA, Sun G, Rutter GA. Identification of genes selectively disallowed in the pancreatic islet. Islets. 2010;2(2):89-95.
92. Collombat P, Mansouri A, Hecksher-Sørensen J, Serup P, Krull J, Gradwohl G, et al. Opposing actions of Arx and Pax4 in endocrine pancreas development. Genes & Development. 2003;17(20):2591-603.
93. Collombat P, Xu X, Ravassard P, Sosa-Pineda B, Dussaud S, Billestrup N, et al. The ectopic expression of Pax4 in the mouse pancreas converts progenitor cells into alpha and subsequently beta cells. Cell. 2009;138(3):449-62.
94. Yang YP, Thorel F, Boyer DF, Herrera PL, Wright CV. Context-specific alpha- to-beta-cell reprogramming by forced Pdx1 expression. Genes Dev. 2011;25(16):1680-5.
95. McKenna B, Guo M, Reynolds A, Hara M, Stein R. Dynamic recruitment of functionally distinct Swi/Snf chromatin remodeling complexes modulates Pdx1 activity in islet beta cells. Cell reports. 2015;10(12):2032-42.
96. Spijker HS, Ravelli RBG, Mommaas-Kienhuis AM, Apeldoorn AA, Engelse MA, Zaldumbide A, et al. Conversion of mature human β-cells into glucagon-producing α-cells. Diabetes. 2013;62.
97. Papizan JB, Singer RA, Tschen S-I, Dhawan S, Friel JM, Hipkens SB, et al. Nkx2.2 repressor complex regulates islet β-cell specification and prevents β-to-α-cell reprogramming. Genes & Development. 2011;25(21):2291-305.
98. Wilcox CL, Terry NA, Walp ER, Lee RA, May CL. Pancreatic α-Cell Specific Deletion of Mouse Arx Leads to α-Cell Identity Loss. PLOS ONE. 2013;8(6):e66214.
99. Collombat P, Hecksher-Sorensen J, Krull J, Berger J, Riedel D, Herrera PL, et al. Embryonic endocrine pancreas and mature beta cells acquire alpha and PP cell phenotypes upon Arx misexpression. The Journal of clinical investigation. 2007;117(4):961-70.
100. Conrad E, Dai C, Spaeth J, Guo M, Cyphert HA, Scoville D, et al. The MAFB transcription factor impacts islet alpha-cell function in rodents and represents a unique signature of primate islet beta-cells. American journal of physiology Endocrinology and metabolism. 2016;310(1):E91-e102.
101. Bramswig NC, Everett LJ, Schug J, Dorrell C, Liu C, Luo Y, et al. Epigenomic plasticity enables human pancreatic alpha to beta cell reprogramming. The Journal of clinical investigation. 2013;123(3):1275-84.

102. Klotz L-O, Sánchez-Ramos C, Prieto-Arroyo I, Urbánek P, Steinbrenner H, Monsalve M. Redox regulation of FoxO transcription factors. Redox Biology. 2015;6:51-72.
103. Yamagata K, Daitoku H, Takahashi Y, Namiki K, Hisatake K, Kako K, et al. Arginine Methylation of FOXO Transcription Factors Inhibits Their Phosphorylation by Akt. Molecular Cell. 2008;32(2):221-31.
104. Elghazi L, Weiss AJ, Barker DJ, Callaghan J, Staloch L, Sandgren EP, et al. Regulation of Pancreas Plasticity and Malignant Transformation by Akt Signaling. Gastroenterology. 2009;136(3):1091-103.e8.
105. Binot A-C, Manfroid I, Flasse L, Winandy M, Motte P, Martial JA, et al. Nkx6.1 and nkx6.2 regulate α- and β-cell formation in zebrafish by acting on pancreatic endocrine progenitor cells. Developmental biology. 2010;340.
106. Taylor BL, Liu F-F, Sander M. Nkx6.1 is essential for maintaining the functional state of pancreatic beta cells. Cell reports. 2013;4(6):1262-75.
107. Schaffer AE, Taylor BL, Benthuysen JR, Liu J, Thorel F, Yuan W, et al. Nkx6.1 controls a gene regulatory network required for establishing and maintaining pancreatic Beta cell identity. PLoS genetics. 2013;9(1):e1003274.
108. Schaffer AE, Freude KK, Nelson SB, Sander M. Nkx6 transcription factors and Ptf1a function as antagonistic lineage determinants in multipotent pancreatic progenitors. Developmental cell. 2010;18(6):1022-9.
109. Riedel MJ, Asadi A, Wang R, Ao Z, Warnock GL, Kieffer TJ. Immunohistochemical characterisation of cells co-producing insulin and glucagon in the developing human pancreas. Diabetologia. 2012;55(2):372-81.
110. Nelson SB, Schaffer AE, Sander M. The transcription factors Nkx6.1 and Nkx6.2 possess equivalent activities in promoting beta-cell fate specification in Pdx1+ pancreatic progenitor cells. Development (Cambridge, England). 2007;134.
111. Oliver-Krasinski JM, Stoffers DA. On the origin of the beta cell. Genes Dev. 2008;22(15):1998-2021.
112. Gu G, Dubauskaite J, Melton DA. Direct evidence for the pancreatic lineage: NGN3+ cells are islet progenitors and are distinct from duct progenitors. Development (Cambridge, England). 2002;129(10):2447-57.
113. Wang Z, York NW, Nichols CG, Remedi MS. Pancreatic beta cell dedifferentiation in diabetes and redifferentiation following insulin therapy. Cell Metab. 2014;19(5):872-82.
114. Wang S, Jensen JN, Seymour PA, Hsu W, Dor Y, Sander M, et al. Sustained Neurog3 expression in hormone-expressing islet cells is required for endocrine maturation and function. Proceedings of the National Academy of Sciences. 2009;106(24):9715-20.
115. Szabat M, Lynn FC, Hoffman BG, Kieffer TJ, Allan DW, Johnson JD. Maintenance of β-Cell Maturity and Plasticity in the Adult Pancreas. Developmental Biology Concepts in Adult Physiology. 2012;61(6):1365-71.
116. Gomez DL, O'Driscoll M, Sheets TP, Hruban RH, Oberholzer J, McGarrigle JJ, et al. Neurogenin 3 Expressing Cells in the Human Exocrine Pancreas Have the Capacity for Endocrine Cell Fate. PLOS ONE. 2015;10(8):e0133862.
117. Jorgensen MC, Ahnfelt-Ronne J, Hald J, Madsen OD, Serup P, Hecksher-Sorensen J. An illustrated review of early pancreas development in the mouse. Endocrine reviews. 2007;28(6):685-705.
118. Kordowich S, Collombat P, Mansouri A, Serup P. Arx and Nkx2.2 compound deficiency redirects pancreatic alpha- and beta-cell differentiation to a somatostatin/ghrelin co-expressing cell lineage. BMC developmental biology. 2011;11:52.
119. Doyle MJ, Loomis ZL, Sussel L. Nkx2.2-repressor activity is sufficient to specify α-cells and a small number of β-cells in the pancreatic islet. Development (Cambridge, England). 2007;134(3):515-23.
120. Doyle MJ, Sussel L. Nkx2.2 regulates beta-cell function in the mature islet. Diabetes. 2007;56(8):1999-2007.
121. Luger K, Mader AW, Richmond RK, Sargent DF, Richmond TJ. Crystal structure of the nucleosome core particle at 2.8 A resolution. Nature. 1997;389(6648):251-60.
122. McGinty RK, Tan S. Nucleosome Structure and Function. Chemical Reviews. 2015;115(6):2255-73.
123. Struhl K, Segal E. Determinants of nucleosome positioning. Nature structural & molecular biology. 2013;20(3):267-73.
124. Gaffney DJ, McVicker G, Pai AA, Fondufe-Mittendorf YN, Lewellen N, Michelini K, et al. Controls of Nucleosome Positioning in the Human Genome. PLOS Genetics. 2012;8(11):e1003036.
125. Handy DE, Castro R, Loscalzo J. Epigenetic Modifications: Basic Mechanisms and Role in Cardiovascular Disease. Circulation. 2011;123(19):2145-56.
126. Portela A, Esteller M. Epigenetic modifications and human disease. Nature Biotechnology. 2010;28:1057.
127. Moore MJ, Proudfoot NJ. Pre-mRNA Processing Reaches Back toTranscription and Ahead to Translation. Cell. 2009;136(4):688-700.
128. Catalanotto C, Cogoni C, Zardo G. MicroRNA in Control of Gene Expression: An Overview of Nuclear Functions. International Journal of Molecular Sciences. 2016;17(10):1712.
129. Gulyaeva LF, Kushlinskiy NE. Regulatory mechanisms of microRNA expression. Journal of translational medicine. 2016;14(1):143.
130. Mann M, Jensen ON. Proteomic analysis of post-translational modifications. Nature Biotechnology. 2003;21:255.
131. Matera AG, Wang Z. A day in the life of the spliceosome. Nature reviews Molecular cell biology. 2014;15(2):108-21.
132. Will CL, Lührmann R. Spliceosome Structure and Function. Cold Spring Harbor Perspectives in Biology. 2011;3(7):a003707.
133. Poulos MG, Batra R, Charizanis K, Swanson MS. Developments in RNA Splicing and Disease. Cold Spring Harbor Perspectives in Biology. 2011;3(1):a000778.
134. Kalsotra A, Cooper TA. Functional consequences of developmentally regulated alternative splicing. Nature reviews Genetics. 2011;12(10):715-29.
135. Tazi J, Bakkour N, Stamm S. Alternative splicing and disease. Biochimica et Biophysica Acta (BBA) - Molecular Basis of Disease. 2009;1792(1):14-26.
136. Harries LW. Messenger RNA processing and its role in diabetes. Diabetic medicine : a journal of the British Diabetic Association. 2011;28(9):1010-7.
137. Wang ET, Sandberg R, Luo S, Khrebtukova I, Zhang L, Mayr C, et al. Alternative isoform regulation in human tissue transcriptomes. Nature. 2008;456:470.
138. Lewis BP, Green RE, Brenner SE. Evidence for the widespread coupling of alternative splicing and nonsense-mediated mRNA decay in humans. Proceedings of the National Academy of Sciences. 2003;100(1):189-92.
139. McGlincy NJ, Smith CWJ. Alternative splicing resulting in nonsense-mediated mRNA decay: what is the meaning of nonsense? Trends in Biochemical Sciences. 2008;33(8):385-93.

140. Harries LW, Ellard S, Stride A, Morgan NG, Hattersley AT. Isomers of the TCF1 gene encoding hepatocyte nuclear factor-1 alpha show differential expression in the pancreas and define the relationship between mutation position and clinical phenotype in monogenic diabetes. Human molecular genetics. 2006;15(14):2216-24.
141. Harries LW, Locke JM, Shields B, Hanley NA, Hanley KP, Steele A, et al. The Diabetic Phenotype in HNF4A Mutation Carriers Is Moderated By the Expression of HNF4A Isoforms From the P1 Promoter During Fetal Development. Diabetes. 2008;57(6):1745-52.
142. Shalev A, Blair PJ, Hoffmann SC, Hirshberg B, Peculis BA, Harlan DM. A Proinsulin Gene Splice Variant with Increased Translation Efficiency Is Expressed in Human Pancreatic Islets. Endocrinology. 2002;143(7):2541-7.
143. Huang Z, Bodkin NL, Ortmeyer HK, Hansen BC, Shuldiner AR. Hyperinsulinemia is associated with altered insulin receptor mRNA splicing in muscle of the spontaneously obese diabetic rhesus monkey. The Journal of clinical investigation. 1994;94(3):1289-96.
144. Fernandez-Ruiz R, Vieira E, Garcia-Roves PM, Gomis R. Protein Tyrosine Phosphatase-1B Modulates Pancreatic β-cell Mass. PLoS ONE. 2014;9(2):e90344.
145. Ukkola O, Santaniemi M. Protein tyrosine phosphatase 1B: a new target for the treatment of obesity and associated co-morbidities. Journal of internal medicine. 2002;251(6):467-75.
146. Sen S, Talukdar I, Webster NJ. SRp20 and CUG-BP1 modulate insulin receptor exon 11 alternative splicing. Molecular and cellular biology. 2009;29(3):871-80.
147. Sesti G, Tullio AN, Marini MA, Manera E, Borboni P, Accili D, et al. Role of the exon 11 of the insulin receptor gene on insulin binding identified by anti-peptide antibodies. Molecular and cellular endocrinology. 1994;101(1-2):121-7.
148. Bates DO, Morris JC, Oltean S, Donaldson LF. Pharmacology of Modulators of Alternative Splicing. Pharmacological reviews. 2017;69(1):63-79.
149. Wahid F, Shehzad A, Khan T, Kim YY. MicroRNAs: Synthesis, mechanism, function, and recent clinical trials. Biochimica et Biophysica Acta (BBA) - Molecular Cell Research. 2010;1803(11):1231-43.
150. Leung AKL, Sharp PA. MicroRNA Functions in Stress Responses. Molecular cell. 2010;40(2):205-15.
151. Emde A, Hornstein E. miRNAs at the interface of cellular stress and disease. The EMBO journal. 2014;33(13):1428-37.
152. Shivdasani RA. MicroRNAs: regulators of gene expression and cell differentiation. Blood. 2006;108(12):3646-53.
153. Gulyaeva LF, Kushlinskiy NE. Regulatory mechanisms of microRNA expression. Journal of Translational Medicine. 2016;14:143.
154. Bossé GD, Simard MJ. A new twist in the microRNA pathway: Not Dicer but Argonaute is required for a microRNA production. Cell research. 2010;20:735.
155. van de Bunt M, Gaulton KJ, Parts L, Moran I, Johnson PR, Lindgren CM, et al. The miRNA Profile of Human Pancreatic Islets and Beta-Cells and Relationship to Type 2 Diabetes Pathogenesis. PloS one. 2013;8(1):e55272.
156. Locke JM, da Silva Xavier G, Dawe HR, Rutter GA, Harries LW. Increased expression of miR-187 in human islets from individuals with type 2 diabetes is associated with reduced glucose-stimulated insulin secretion. Diabetologia. 2014;57(1):122-8.
157. Ofori JK, Salunkhe VA, Bagge A, Vishnu N, Nagao M, Mulder H, et al. Elevated miR-130a/miR130b/miR-152 expression reduces intracellular ATP levels in the pancreatic beta cell. Scientific Reports. 2017;7:44986.
158. Bao L, Fu X, Si M, Wang Y, Ma R, Ren X, et al. MicroRNA-185 Targets SOCS3 to Inhibit Beta-Cell Dysfunction in Diabetes. PloS one. 2015;10(2):e0116067.
159. Esguerra JL, Bolmeson C, Cilio CM, Eliasson L. Differential glucose-regulation of microRNAs in pancreatic islets of non-obese type 2 diabetes model Goto-Kakizaki rat. PloS one. 2011;6(4):e18613.
160. Filios SR, Shalev A. β-Cell MicroRNAs: Small but Powerful. Diabetes. 2015;64(11):3631-44.
161. Rodriguez-Comas J, Moreno-Asso A, Moreno-Vedia J, Martin M, Castano C, Marza-Florensa A, et al. Stress-Induced MicroRNA-708 Impairs beta-Cell Function and Growth. Diabetes. 2017;66(12):3029-40.
162. Song I, Roels S, Martens GA, Bouwens L. Circulating microRNA-375 as biomarker of pancreatic beta cell death and protection of beta cell mass by cytoprotective compounds. PLoS One. 2017;12(10):e0186480.
163. Li X. miR-375, a microRNA related to diabetes. Gene. 2014;533(1):1-4.
164. Martinez-Sanchez A, Rutter GA, Latreille M. MiRNAs in β-Cell Development, Identity, and Disease. Frontiers in Genetics. 2016;7:226.
165. Keller DM, McWeeney S, Arsenlis A, Drouin J, Wright CVE, Wang H, et al. Characterization of Pancreatic Transcription Factor Pdx-1 Binding Sites Using Promoter Microarray and Serial Analysis of Chromatin Occupancy. Journal of Biological Chemistry. 2007;282(44):32084-92.
166. Lynn FC, Skewes-Cox P, Kosaka Y, McManus MT, Harfe BD, German MS. MicroRNA Expression Is Required for Pancreatic Islet Cell Genesis in the Mouse. Diabetes. 2007;56(12):2938-45.
167. Pan FC, Brissova M. Pancreas development in humans. Current opinion in endocrinology, diabetes, and obesity. 2014;21(2):77-82.
168. Kanji MS, Martin MG, Bhushan A. Dicer1 is required to repress neuronal fate during endocrine cell maturation. Diabetes. 2013;62(5):1602-11.
169. Joglekar MV, Joglekar VM, Hardikar AA. Expression of islet-specific microRNAs during human pancreatic development. Gene Expr Patterns. 2009;9(2):109-13.
170. Larsen L, Rosenstierne MW, Gaarn LW, Bagge A, Pedersen L, Dahmcke CM, et al. Expression and Localization of microRNAs in Perinatal Rat Pancreas: Role of miR-21 in Regulation of Cholesterol Metabolism. PLOS ONE. 2011;6(10):e25997.
171. Kone M, Pullen TJ, Sun G, Ibberson M, Martinez-Sanchez A, Sayers S, et al. LKB1 and AMPK differentially regulate pancreatic β-cell identity. The FASEB Journal. 2014;28(11):4972-85.
172. Butler AE, Dhawan S, Hoang J, Cory M, Zeng K, Fritsch H, et al. beta-Cell Deficit in Obese Type 2 Diabetes, a Minor Role of beta-Cell Dedifferentiation and Degranulation. The Journal of clinical endocrinology and metabolism. 2016;101(2):523-32.
173. Rutter Guy A, Pullen Timothy J, Hodson David J, Martinez-Sanchez A. Pancreatic β-cell identity, glucose sensing and the control of insulin secretion. Biochemical Journal. 2015;466(2):203-18.
174. Tattikota SG, Rathjen T, Hausser J, Khedkar A, Kabra UD, Pandey V, et al. miR-184 Regulates Pancreatic β-Cell Function According to Glucose Metabolism. Journal of Biological Chemistry. 2015;290(33):20284-94.
175. Locke JM, Harries LW. MicroRNA expression profiling of human islets from individuals with and without type 2 diabetes: promises and pitfalls. Biochemical Society transactions. 2012;40(4):800-3.

176. Leung AK, Sharp PA. MicroRNA functions in stress responses. Molecular cell. 2010;40(2):205-15.
177. Mori MA, Raghavan P, Thomou T, Boucher J, Robida-Stubbs S, Macotela Y, et al. Role of microRNA processing in adipose tissue in stress defense and longevity. Cell Metab. 2012;16(3):336-47.
178. Anderson RM. A role for dicer in aging and stress survival. Cell metabolism. 2012;16(3):285-6.
179. LaPierre MP, Stoffel M. MicroRNAs as stress regulators in pancreatic beta cells and diabetes. Molecular Metabolism. 2017;6(9):1010-23.
180. Baeyens L, Lemper M, Leuckx G, De Groef S, Bonfanti P, Stange G, et al. Transient cytokine treatment induces acinar cell reprogramming and regenerates functional beta cell mass in diabetic mice. Nature biotechnology. 2014;32(1):76-83.
181. Bramswig NC, Kaestner KH. Transcriptional regulation of alpha-cell differentiation. Diabetes, obesity & metabolism. 2011;13 Suppl 1:13-20.
182. Andersson LE, Valtat B, Bagge A, Sharoyko VV, Nicholls DG, Ravassard P, et al. Characterization of stimulus-secretion coupling in the human pancreatic EndoC-betaH1 beta cell line. PLoS One. 2015;10(3):e0120879.
183. Ravassard P, Hazhouz Y, Pechberty S, xE, verine, Bricout-Neveu E, et al. A genetically engineered human pancreatic β cell line exhibiting glucose-inducible insulin secretion. The Journal of clinical investigation. 2011;121(9):3589-97.
184. Weir GC, Bonner-Weir S. Finally! A human pancreatic β cell line. The Journal of clinical investigation. 2011;121(9):3395-7.
185. Gurgul-Convey E, Kaminski MT, Lenzen S. Physiological characterization of the human EndoC-betaH1 beta-cell line. Biochem Biophys Res Commun. 2015;464(1):13-9.
186. Hastoy B, Godazgar M, Clark A, Nylander V, Spiliotis I, van de Bunt M, et al. Electrophysiological properties of human beta-cell lines EndoC-βH1 and -βH2 conform with human beta-cells. Scientific reports. 2018;8(1):16994-.
187. Kaddis JS, Olack BJ, Sowinski J, Cravens J, Contreras JL, Niland JC. Human Pancreatic Islets and Diabetes Research. JAMA : the journal of the American Medical Association. 2009;301(15):1580-7.
188. Pisania A, Weir GC, O'Neil JJ, Omer A, Tchipashvili V, Lei J, et al. Quantitative analysis of cell composition and purity of human pancreatic islet preparations. Laboratory investigation; a journal of technical methods and pathology. 2010;90(11):1661-75.
189. Quiskamp N, E. Bruin J, J. Kieffer T. Differentiation of Human Pluripotent Stem Cells into β-cells: Potential and Challenges2015.
190. Hrvatin S, O'Donnell CW, Deng F, Millman JR, Pagliuca FW, Dilorio P, et al. Differentiated human stem cells resemble fetal, not adult, β cells. Proceedings of the National Academy of Sciences. 2014;111(8):3038-43.
191. Pagliuca Felicia W, Millman Jeffrey R, Gürtler M, Segel M, Van Dervort A, Ryu Jennifer H, et al. Generation of Functional Human Pancreatic β Cells In Vitro. Cell. 2014;159(2):428-39.
192. Zhou Q, Brown J, Kanarek A, Rajagopal J, Melton DA. In vivo reprogramming of adult pancreatic exocrine cells to [bgr]-cells. Nature. 2008;455(7213):627-32.
193. Kroon E, Martinson LA, Kadoya K, Bang AG, Kelly OG, Eliazer S, et al. Pancreatic endoderm derived from human embryonic stem cells generates glucose-responsive insulin-secreting cells in vivo. Nature biotechnology. 2008;26(4):443-52.
194. Zhang D, Jiang W, Liu M, Sui X, Yin X, Chen S, et al. Highly efficient differentiation of human ES cells and iPS cells into mature pancreatic insulin-producing cells. Cell research. 2009;19(4):429-38.
195. Ahlqvist E, Turrini F, Lang ST, Taneera J, Zhou Y, Almgren P, et al. A common variant upstream of the PAX6 gene influences islet function in man. Diabetologia. 2012;55(1):94-104.
196. Gosmain Y, Katz LS, Masson MH, Cheyssac C, Poisson C, Philippe J. Pax6 Is Crucial for β-Cell Function, Insulin Biosynthesis, and Glucose-Induced Insulin Secretion. Molecular Endocrinology. 2012;26(4):696-709.
197. Swisa A, Avrahami D, Eden N, Zhang J, Feleke E, Dahan T, et al. PAX6 maintains β cell identity by repressing genes of alternative islet cell types. The Journal of clinical investigation. 2017;127(1):230-43.
198. Latorre E, Birar VC, Sheerin AN, Jeynes JCC, Hooper A, Dawe HR, et al. Small molecule modulation of splicing factor expression is associated with rescue from cellular senescence. BMC Cell Biology. 2017;18:31.
199. Scharfmann R, xEb, Pechberty S, Hazhouz Y, von B, xFc, et al. Development of a conditionally immortalized human pancreatic β cell line. The Journal of clinical investigation. 2014;124(5):2087-98.
200. Andersen L, Dinesen B, Jørgensen PN, Poulsen F, Røder ME. Enzyme immunoassay for intact human insulin in serum or plasma. Clinical Chemistry. 1993;39(4):578-82.
201. Brereton MF, Rohm M, Shimomura K, Holland C, Tornovsky-Babeay S, Dadon D, et al. Hyperglycaemia induces metabolic dysfunction and glycogen accumulation in pancreatic β-cells. Nature Communications. 2016;7:13496.
202. Wu D, Yotnda P. Induction and Testing of Hypoxia in Cell Culture. Journal of Visualized Experiments : JoVE. 2011(54):2899.
203. Wenger RH, Kurtcuoglu V, Scholz CC, Marti HH, Hoogewijs D. Frequently asked questions in hypoxia research. Hypoxia. 2015;3:35-43.
204. Oh YS. Mechanistic insights into pancreatic beta-cell mass regulation by glucose and free fatty acids. Anatomy & Cell Biology. 2015;48(1):16-24.
205. Oleson BJ, McGraw JA, Broniowska KA, Annamalai M, Chen J, Bushkofsky JR, et al. Distinct differences in the responses of the human pancreatic β-cell line EndoC-βH1 and human islets to proinflammatory cytokines. American Journal of Physiology-Regulatory, Integrative and Comparative Physiology. 2015;309(5):R525-R34.
206. Nami B, Donmez H, Kocak N. Tunicamycin-induced endoplasmic reticulum stress reduces in vitro subpopulation and invasion of CD44+/CD24- phenotype breast cancer stem cells. Experimental and toxicologic pathology : official journal of the Gesellschaft fur Toxikologische Pathologie. 2016;68(7):419-26.
207. Sommerweiss D, Gorski T, Richter S, Garten A, Kiess W. Oleate rescues INS-1E β-cells from palmitate-induced apoptosis by preventing activation of the unfolded protein response. Biochemical and Biophysical Research Communications. 2013;441(4):770-6.
208. Schindelin J, Arganda-Carreras I, Frise E, Kaynig V, Longair M, Pietzsch T, et al. Fiji: an open-source platform for biological-image analysis. Nature methods. 2012;9(7):676-82.
209. Hu C, Zhang R, Wang C, Yu W, Lu J, Ma X, et al. Effects of GCK, GCKR, G6PC2 and MTNR1B Variants on Glucose Metabolism and Insulin Secretion. PLOS ONE. 2010;5(7):e11761.
210. Hang Y, Stein R. MafA and MafB activity in pancreatic β cells. Trends in endocrinology and metabolism: TEM. 2011;22(9):364-73.

211. Marselli L, Thorne J, Dahiya S, Sgroi DC, Sharma A, Bonner-Weir S, et al. Gene Expression Profiles of Beta-Cell Enriched Tissue Obtained by Laser Capture Microdissection from Subjects with Type 2 Diabetes. PLoS ONE. 2010;5(7):e11499.
212. Bettaieb A, Liu S, Xi Y, Nagata N, Matsuo K, Matsuo I, et al. Differential Regulation of Endoplasmic Reticulum Stress by Protein Tyrosine Phosphatase 1B and T Cell Protein Tyrosine Phosphatase. Journal of Biological Chemistry. 2011;286(11):9225-35.
213. Puri S, Folias Alexandra E, Hebrok M. Plasticity and Dedifferentiation within the Pancreas: Development, Homeostasis, and Disease. Cell Stem Cell. 2015;16(1):18-31.
214. Bar Y, Russ HA, Knoller S, Ouziel-Yahalom L, Efrat S. HES-1 Is Involved in Adaptation of Adult Human β-Cells to Proliferation In Vitro. Diabetes. 2008;57(9):2413-20.
215. Weinberg N, Ouziel-Yahalom L, Knoller S, Efrat S, Dor Y. Lineage Tracing Evidence for In Vitro Dedifferentiation but Rare Proliferation of Mouse Pancreatic β-Cells. Diabetes. 2007;56(5):1299-304.
216. Schuit F, Van Lommel L, Granvik M, Goyvaerts L, de Faudeur G, Schraenen A, et al. β-Cell–Specific Gene Repression: A Mechanism to Protect Against Inappropriate or Maladjusted Insulin Secretion? Diabetes. 2012;61(5):969-75.
217. Pullen TJ, Rutter GA. When less is more: the forbidden fruits of gene repression in the adult β-cell. Diabetes, Obesity and Metabolism. 2013;15(6):503-12.
218. Marhfour I, Lopez XM, Lefkaditis D, Salmon I, Allagnat F, Richardson SJ, et al. Expression of endoplasmic reticulum stress markers in the islets of patients with type 1 diabetes. Diabetologia. 2012;55(9):2417-20.
219. Mirmira RG, Sims EK, Syed F, Evans-Molina C. Biomarkers of β-Cell Stress and Death in Type 1 Diabetes. Current diabetes reports. 2016;16(10):95-.
220. Courtney M, Gjernes E, Druelle N, Ravaud C, Vieira A, Ben-Othman N, et al. The inactivation of Arx in pancreatic α-cells triggers their neogenesis and conversion into functional β-like cells. PLoS Genet. 2013;9.
221. DiGruccio MR, Mawla AM, Donaldson CJ, Noguchi GM, Vaughan J, Cowing-Zitron C, et al. Comprehensive alpha, beta and delta cell transcriptomes reveal that ghrelin selectively activates delta cells and promotes somatostatin release from pancreatic islets. Molecular Metabolism. 2016;5(7):449-58.
222. Minn AH, Lan H, Rabaglia ME, Harlan DM, Peculis BA, Attie AD, et al. Increased Insulin Translation from an Insulin Splice-Variant Overexpressed in Diabetes, Obesity, and Insulin Resistance. Molecular Endocrinology. 2005;19(3):794-803.
223. Sasamoto Y, Hayashi R, Park S-J, Saito-Adachi M, Suzuki Y, Kawasaki S, et al. PAX6 Isoforms, along with Reprogramming Factors, Differentially Regulate the Induction of Cornea-specific Genes. Scientific Reports. 2016;6:20807.
224. Kozmik Z, Czerny T, Busslinger M. Alternatively spliced insertions in the paired domain restrict the DNA sequence specificity of Pax6 and Pax8. The EMBO journal. 1997;16(22):6793-803.
225. Walther C, Gruss P. Pax-6, a murine paired box gene, is expressed in the developing CNS. Development (Cambridge, England). 1991;113(4):1435-49.
226. Jeffery N, Harries LW. beta-cell differentiation status in type 2 diabetes. Diabetes, obesity & metabolism. 2016;18(12):1167-75.
227. Epstein JA, Glaser T, Cai J, Jepeal L, Walton DS, Maas RL. Two independent and interactive DNA-binding subdomains of the Pax6 paired domain are regulated by alternative splicing. Genes Dev. 1994;8(17):2022-34.
228. Azuma N, Yamaguchi Y, Handa H, Hayakawa M, Kanai A, Yamada M. Missense mutation in the alternative splice region of the PAX6 gene in eye anomalies. American Journal of Human Genetics. 1999;65(3):656-63.
229. Chauhan BK, Reed NA, Zhang W, Duncan MK, Kilimann MW, Cvekl A. Identification of Genes Downstream of Pax6 in the Mouse Lens Using cDNA Microarrays. Journal of Biological Chemistry. 2002;277(13):11539-48.
230. Wang X, Dai J. Concise Review: Isoforms of OCT4 Contribute to the Confusing Diversity in Stem Cell Biology. Stem Cells (Dayton, Ohio). 2010;28(5):885-93.
231. Lee J, Kim HK, Rho JY, Han YM, Kim J. The human OCT-4 isoforms differ in their ability to confer self-renewal. The Journal of biological chemistry. 2006;281(44):33554-65.
232. Das S, Jena S, Levasseur DN. Alternative Splicing Produces Nanog Protein Variants with Different Capacities for Self-renewal and Pluripotency in Embryonic Stem Cells. The Journal of biological chemistry. 2011;286(49):42690-703.
233. Wang J, Levasseur DN, Orkin SH. Requirement of Nanog dimerization for stem cell self-renewal and pluripotency. Proc Natl Acad Sci U S A. 2008;105(17):6326-31.
234. Kim JS, Kim J, Kim BS, Chung HY, Lee YY, Park CS, et al. Identification and functional characterization of an alternative splice variant within the fourth exon of human nanog. Experimental & molecular medicine. 2005;37(6):601-7.
235. Sell SM, Reese D. Insulin-inducible changes in the relative ratio of PTP1B splice variants. Molecular genetics and metabolism. 1999;66(3):189-92.
236. Hummon AB, Lim SR, Difilippantonio MJ, Ried T. Isolation and solubilization of proteins after TRIzol(®) extraction of RNA and DNA from patient material following prolonged storage. BioTechniques. 2007;42(4):467-72.
237. Pena-Llopis S, Brugarolas J. Simultaneous isolation of high-quality DNA, RNA, miRNA and proteins from tissues for genomic applications. Nature protocols. 2013;8(11):2240-55.
238. Vorreiter F, Richter S, Peter M, Baumann S, von Bergen M, Tomm JM. Comparison and optimization of methods for the simultaneous extraction of DNA, RNA, proteins, and metabolites. Analytical biochemistry. 2016;508:25-33.
239. Kim YK, Yeo J, Kim B, Ha M, Kim VN. Short structured RNAs with low GC content are selectively lost during extraction from a small number of cells. Mol Cell. 2012;46(6):893-5.
240. Schmittgen TD, Livak KJ. Analyzing real-time PCR data by the comparative CT method. Nature protocols. 2008;3:1101.
241. Livak KJ, Schmittgen TD. Analysis of relative gene expression data using real-time quantitative PCR and the 2(-Delta Delta C(T)) Method. Methods (San Diego, Calif). 2001;25(4):402-8.
242. Pfaffl MW. A new mathematical model for relative quantification in real-time RT–PCR. Nucleic Acids Research. 2001;29(9):e45-e.
243. Rutledge RG. Sigmoidal curve-fitting redefines quantitative real-time PCR with the prospective of developing automated high-throughput applications. Nucleic Acids Research. 2004;32(22):e178-e.
244. Swillens S, Dessars B, Housni HE. Revisiting the sigmoidal curve fitting applied to quantitative real-time PCR data. Analytical biochemistry. 2008;373(2):370-6.

245. Ghasemi A, Zahediasl S. Normality tests for statistical analysis: a guide for non-statisticians. International journal of endocrinology and metabolism. 2012;10(2):486-9.
246. Paraskevopoulou MD, Georgakilas G, Kostoulas N, Vlachos IS, Vergoulis T, Reczko M, et al. DIANA-microT web server v5.0: service integration into miRNA functional analysis workflows. Nucleic Acids Res. 2013;41(Web Server issue):W169-73.
247. Vlachos IS, Zagganas K, Paraskevopoulou MD, Georgakilas G, Karagkouni D, Vergoulis T, et al. DIANA-miRPath v3.0: deciphering microRNA function with experimental support. Nucleic Acids Research. 2015;43(Web Server issue):W460-W6.
248. Maragkakis M, Reczko M, Simossis VA, Alexiou P, Papadopoulos GL, Dalamagas T, et al. DIANA-microT web server: elucidating microRNA functions through target prediction. Nucleic Acids Research. 2009;37(Web Server issue):W273-W6.
249. Maillard E, Sencier MC, Langlois A, Bietiger W, Krafft M, Pinget M, et al. Extracellular matrix proteins involved in pseudoislets formation. Islets. 2009;1(3):232-41.
250. Stendahl JC, Kaufman DB, Stupp SI. Extracellular Matrix in Pancreatic Islets: Relevance to Scaffold Design and Transplantation. Cell transplantation. 2009;18(1):1-12.
251. Kilkenny DM, Rocheleau JV. Fibroblast growth factor receptor-1 signaling in pancreatic islet beta-cells is modulated by the extracellular matrix. Mol Endocrinol. 2008;22(1):196-205.
252. Newby BN, Terada N, Mathews CE. In search of a surrogate: engineering human beta cell lines for therapy. Trends in Endocrinology & Metabolism. 2014;25(8):378-80.
253. Lightfoot YL, Chen J, Mathews CE. Immune-mediated β-cell death in type 1 diabetes: lessons from human β-cell lines. European journal of clinical investigation. 2012;42(11):1244-51.
254. Webster M, Witkin KL, Cohen-Fix O. Sizing up the nucleus: nuclear shape, size and nuclear-envelope assembly. Journal of cell science. 2009;122(Pt 10):1477-86.
255. Futcher B. Cyclins and the wiring of the yeast cell cycle. Yeast (Chichester, England). 1996;12(16):1635-46.
256. Dzobo K, Vogelsang M, Parker MI. Wnt/beta-Catenin and MEK-ERK Signaling are Required for Fibroblast-Derived Extracellular Matrix-Mediated Endoderm Differentiation of Embryonic Stem Cells. Stem Cell Rev. 2015;11(5):761-73.
257. Calle EA, Mendez JJ, Ghaedi M, Leiby KL, Bove PF, Herzog EL, et al. Fate of distal lung epithelium cultured in a decellularized lung extracellular matrix. Tissue Eng Part A. 2015;21(11-12):1916-28.
258. Mercier F. Fractones: extracellular matrix niche controlling stem cell fate and growth factor activity in the brain in health and disease. Cell Mol Life Sci. 2016;73(24):4661-74.
259. Bi Y, Stuelten CH, Kilts T, Wadhwa S, Iozzo RV, Robey PG, et al. Extracellular matrix proteoglycans control the fate of bone marrow stromal cells. J Biol Chem. 2005;280(34):30481-9.
260. Cheng P, Andersen P, Hassel D, Kaynak BL, Limphong P, Juergensen L, et al. Fibronectin mediates mesendodermal cell fate decisions. Development. 2013;140(12):2587-96.
261. Dobaczewski M, Bujak M, Zymek P, Ren G, Entman ML, Frangogiannis NG. Extracellular matrix remodeling in canine and mouse myocardial infarcts. Cell Tissue Res. 2006;324(3):475-88.
262. Bavamian S, Klee P, Britan A, Populaire C, Caille D, Cancela J, et al. Islet-cell-to-cell communication as basis for normal insulin secretion. Diabetes, Obesity and Metabolism. 2007;9:118-32.
263. Konstantinova I, Nikolova G, Ohara-Imaizumi M, Meda P, Kučera T, Zarbalis K, et al. EphA-Ephrin-A-Mediated β Cell Communication Regulates Insulin Secretion from Pancreatic Islets. Cell. 2007;129(2):359-70.
264. McCluskey JT, Hamid M, Guo-Parke H, McClenaghan NH, Gomis R, Flatt PR. Development and functional characterization of insulin-releasing human pancreatic beta cell lines produced by electrofusion. The Journal of biological chemistry. 2011;286(25):21982-92.
265. Benner C, Meulen T, Cacéres E, Tigyi K, Donaldson CJ, Huising MO, et al. The transcriptional landscape of mouse beta cells compared to human beta cells reveals notable species differences in long non-coding RNA and protein-coding gene expression. BMC Genomics. 2014;15.
266. Johnson D, Shepherd RM, Gill D, Gorman T, Smith DM, Dunne MJ. Glucose-Dependent Modulation of Insulin Secretion and Intracellular Calcium Ions by GKA50, a Glucokinase Activator. Diabetes. 2007;56(6):1694-702.
267. Ajjan RA, Owen KR. Glucokinase MODY and implications for treatment goals of common forms of diabetes. Curr Diab Rep. 2014;14(12):559.
268. Butler PC, Meier JJ, Butler AE, Bhushan A. The replication of [beta] cells in normal physiology, in disease and for therapy. Nat Clin Pract End Met. 2007;3(11):758-68.
269. Gao T, McKenna B, Li C, Reichert M, Nguyen J, Singh T, et al. Pdx1 Maintains β Cell Identity and Function by Repressing an α Cell Program. Cell Metabolism. 2014;19(2):259-71.
270. Piran R, Lee SH, Li CR, Charbono A, Bradley LM, Levine F. Pharmacological induction of pancreatic islet cell transdifferentiation: relevance to type I diabetes. Cell death & disease. 2014;5:e1357.
271. Hart AW, Mella S, Mendrychowski J, van Heyningen V, Kleinjan DA. The Developmental Regulator Pax6 Is Essential for Maintenance of Islet Cell Function in the Adult Mouse Pancreas. PLoS ONE. 2013;8(1):e54173.
272. Guo S, Dai C, Guo M, Taylor B, Harmon JS, Sander M, et al. Inactivation of specific beta cell transcription factors in type 2 diabetes. The Journal of clinical investigation. 2013;123(8):3305-16.
273. Al-Masri M, Krishnamurthy M, Li J, Fellows GF, Dong HH, Goodyer CG, et al. Effect of forkhead box O1 (FOXO1) on beta cell development in the human fetal pancreas. Diabetologia. 2010;53(4):699-711.
274. Ponugoti B, Dong G, Graves DT. Role of forkhead transcription factors in diabetes-induced oxidative stress. Experimental diabetes research. 2012;2012:939751.
275. Latorre E, Ostler EL, Faragher RGA, Harries LW. FOXO1 and ETV6 genes may represent novel regulators of splicing factor expression in cellular senescence. FASEB journal : official publication of the Federation of American Societies for Experimental Biology. 2018:fj201801154R.
276. Pan Q, Shai O, Lee LJ, Frey BJ, Blencowe BJ. Deep surveying of alternative splicing complexity in the human transcriptome by high-throughput sequencing. Nature Genetics. 2008;40:1413.
277. Mastrangelo AM, Marone D, Laido G, De Leonardis AM, De Vita P. Alternative splicing: enhancing ability to cope with stress via transcriptome plasticity. Plant science : an international journal of experimental plant biology. 2012;185-186:40-9.
278. Pagliarini V, Naro C, Sette C. Splicing Regulation: A Molecular Device to Enhance Cancer Cell Adaptation. BioMed research international. 2015;2015:543067.

279. Marden JH. Quantitative and evolutionary biology of alternative splicing: how changing the mix of alternative transcripts affects phenotypic plasticity and reaction norms. Heredity. 2008;100(2):111-20.
280. Cnop M, Abdulkarim B, Bottu G, Cunha DA, Igoillo-Esteve M, Masini M, et al. RNA sequencing identifies dysregulation of the human pancreatic islet transcriptome by the saturated fatty acid palmitate. Diabetes. 2014;63(6):1978-93.
281. Dorrell C, Schug J, Canaday PS, Russ HA, Tarlow BD, Grompe MT, et al. Human islets contain four distinct subtypes of β cells. Nature Communications. 2016;7:11756.
282. Jeffery N, Richardson S, Beall C, Harries LW. The species origin of the cellular microenvironment influences markers of beta cell fate and function in EndoC-betaH1 cells. Exp Cell Res. 2017;361(2):284-91.
283. DiGruccio MR, Mawla AM, Donaldson CJ, Noguchi GM, Vaughan J, Cowing-Zitron C, et al. Comprehensive alpha, beta and delta cell transcriptomes reveal that ghrelin selectively activates delta cells and promotes somatostatin release from pancreatic islets. Mol Metab. 2016;5.
284. Cartegni L, Chew SL, Krainer AR. Listening to silence and understanding nonsense: exonic mutations that affect splicing. Nature reviews Genetics. 2002;3(4):285-98.
285. Long Jennifer C, Caceres Javier F. The SR protein family of splicing factors: master regulators of gene expression. Biochemical Journal. 2009;417(1):15-27.
286. Biamonti G, Caceres JF. Cellular stress and RNA splicing. Trends Biochem Sci. 2009;34(3):146-53.
287. Hashimoto N, Kido Y, Uchida T, Asahara S-i, Shigeyama Y, Matsuda T, et al. Ablation of PDK1 in pancreatic β cells induces diabetes as a result of loss of β cell mass. Nature Genetics. 2006;38:589.
288. Mitchell RK, Nguyen-Tu M-S, Chabosseau P, Callingham RM, Pullen TJ, Cheung R, et al. The transcription factor Pax6 is required for pancreatic β cell identity, glucose-regulated ATP synthesis, and Ca2+ dynamics in adult mice. Journal of Biological Chemistry. 2017;292(21):8892-906.
289. Zhang T, Kim DH, Xiao X, Lee S, Gong Z, Muzumdar R, et al. FoxO1 Plays an Important Role in Regulating β-Cell Compensation for Insulin Resistance in Male Mice. Endocrinology. 2016;157(3):1055-70.
290. Benner C, van der Meulen T, Cacéres E, Tigyi K, Donaldson CJ, Huising MO. The transcriptional landscape of mouse beta cells compared to human beta cells reveals notable species differences in long non-coding RNA and protein-coding gene expression. BMC Genomics. 2014;15(1):620.
291. Barbosa-Morais NL, Irimia M, Pan Q, Xiong HY, Gueroussov S, Lee LJ, et al. The evolutionary landscape of alternative splicing in vertebrate species. Science (New York, NY). 2012;338(6114):1587-93.
292. Havens MA, Duelli DM, Hastings ML. Targeting RNA splicing for disease therapy. Wiley interdisciplinary reviews RNA. 2013;4(3):247-66.
293. Roggli E, Britan A, Gattesco S, Lin-Marq N, Abderrahmani A, Meda P, et al. Involvement of MicroRNAs in the Cytotoxic Effects Exerted by Proinflammatory Cytokines on Pancreatic β-Cells. Diabetes. 2010;59(4):978-86.
294. Rottiers V, Näär AM. MicroRNAs in Metabolism and Metabolic Disorders. Nature reviews Molecular cell biology. 2012;13(4):239-50.
295. Kaur S, Krishn SR, Rachagani S, Batra SK. Significance of microRNA-based biomarkers for pancreatic cancer. Annals of Translational Medicine. 2015;3(18):277.
296. Schickel R, Park SM, Murmann AE, Peter ME. miR-200c regulates induction of apoptosis through CD95 by targeting FAP-1. Mol Cell. 2010;38(6):908-15.
297. Wang X, Liu B, Wen F, Song Y. MicroRNA-454 inhibits the malignant biological behaviours of gastric cancer cells by directly targeting mitogen-activated protein kinase 1. Oncol Rep. 2018;39(3):1494-504.
298. Tattikota Sudhir G, Rathjen T, McAnulty Sarah J, Wessels H-H, Akerman I, van de Bunt M, et al. Argonaute2 Mediates Compensatory Expansion of the Pancreatic β Cell. Cell Metabolism. 2014;19(1):122-34.
299. Belgardt BF, Ahmed K, Spranger M, Latreille M, Denzler R, Kondratiuk N, et al. The microRNA-200 family regulates pancreatic beta cell survival in type 2 diabetes. Nature medicine. 2015;21(6):619-27.
300. Roggli E, Gattesco S, Caille D, Briet C, Boitard C, Meda P, et al. Changes in MicroRNA Expression Contribute to Pancreatic β-Cell Dysfunction in Prediabetic NOD Mice. Diabetes. 2012;61(7):1742-51.
301. Kalis M, Bolmeson C, Esguerra JL, Gupta S, Edlund A, Tormo-Badia N, et al. Beta-cell specific deletion of Dicer1 leads to defective insulin secretion and diabetes mellitus. PloS one. 2011;6(12):e29166.
302. Ardestani A, Maedler K. The Hippo Signaling Pathway in Pancreatic beta-Cells: Functions and Regulations. Endocrine reviews. 2018;39(1):21-35.
303. Hsu S-D, Lin F-M, Wu W-Y, Liang C, Huang W-C, Chan W-L, et al. miRTarBase: a database curates experimentally validated microRNA–target interactions. Nucleic Acids Research. 2011;39(Database issue):D163-D9.
304. Ye B, Wang R, Wang J. Correlation analysis of the mRNA and miRNA expression profiles in the nascent synthetic allotetraploid Raphanobrassica. Scientific Reports. 2016;6:37416.
305. Ruike Y, Ichimura A, Tsuchiya S, Shimizu K, Kunimoto R, Okuno Y, et al. Global correlation analysis for micro-RNA and mRNA expression profiles in human cell lines. J Hum Genet. 2008;53(6):515-23.
306. Dotta F, Ventriglia G, Snowhite IV, Pugliese A. MicroRNAs: markers of beta-cell stress and autoimmunity. Current opinion in endocrinology, diabetes, and obesity. 2018;25(4):237-45.
307. Backe MB, Novotny GW, Christensen DP, Grunnet LG, Mandrup-Poulsen T. Altering beta-cell number through stable alteration of miR-21 and miR-34a expression. Islets. 2014;6(1):e27754.
308. Lee CG, Kim YW, Kim EH, Meng Z, Huang W, Hwang SJ, et al. Farnesoid X Receptor Protects Hepatocytes From Injury by Repressing miR-199a-3p, Which Increases Levels of LKB1. Gastroenterology. 2012;142(5):1206-17.e7.
309. Granot Z, Swisa A, Magenheim J, Stolovich-Rain M, Fujimoto W, Manduchi E, et al. LKB1 regulates pancreatic beta cell size, polarity, and function. Cell metabolism. 2009;10(4):296-308.
310. Facchinello N, Tarifeño-Saldivia E, Grisan E, Schiavone M, Peron M, Mongera A, et al. Tcf7l2 plays pleiotropic roles in the control of glucose homeostasis, pancreas morphology, vascularization and regeneration. Scientific Reports. 2017;7(1):9605.
311. Nguyen-Tu M-S, da Silva Xavier G, Leclerc I, Rutter GA. Transcription factor-7-like 2 (TCF7L2) gene acts downstream of the Lkb1/Stk11 kinase to control mTOR signaling, β cell growth, and insulin secretion. Journal of Biological Chemistry. 2018.
312. Gehart H, Kumpf S, Ittner A, Ricci R. MAPK signalling in cellular metabolism: stress or wellness? EMBO Reports. 2010;11(11):834-40.

313. Aoyagi K, Ohara-Imaizumi M, Nishiwaki C, Nakamichi Y, Ueki K, Kadowaki T, et al. Acute Inhibition of PI3K-PDK1-Akt Pathway Potentiates Insulin Secretion through Upregulation of Newcomer Granule Fusions in Pancreatic β-Cells. PloS one. 2012;7(10):e47381.
314. Martinez-Sanchez A, Rutter GA, Latreille M. MiRNAs in β-Cell Development, Identity, and Disease. Frontiers in Genetics. 2017;7(226).
315. Wang Y, Liu J, Liu C, Naji A, Stoffers DA. MicroRNA-7 Regulates the mTOR Pathway and Proliferation in Adult Pancreatic β-Cells. Diabetes. 2013;62(3):887-95.
316. Meister G, Landthaler M, Dorsett Y, Tuschl T. Sequence-specific inhibition of microRNA- and siRNA-induced RNA silencing. RNA (New York, NY). 2004;10(3):544-50.
317. Krutzfeldt J, Rajewsky N, Braich R, Rajeev KG, Tuschl T, Manoharan M, et al. Silencing of microRNAs in vivo with 'antagomirs'. Nature. 2005;438(7068):685-9.
318. Ebert MS, Neilson JR, Sharp PA. MicroRNA sponges: competitive inhibitors of small RNAs in mammalian cells. Nature methods. 2007;4(9):721-6.
319. Weber LM, Hayda KN, Anseth KS. Cell–Matrix Interactions Improve β-Cell Survival and Insulin Secretion in Three-Dimensional Culture. Tissue Engineering Part A. 2008;14(12):1959-68.
320. Johnston NR, Mitchell RK, Haythorne E, Pessoa MP, Semplici F, Ferrer J, et al. Beta Cell Hubs Dictate Pancreatic Islet Responses to Glucose. Cell metabolism. 2016;24(3):389-401.
321. Bernal-Mizrachi E, Kulkarni RN, Scott DK, Mauvais-Jarvis F, Stewart AF, Garcia-Ocana A. Human beta-cell proliferation and intracellular signaling part 2: still driving in the dark without a road map. Diabetes. 2014;63(3):819-31.
322. Andersen FG, Jensen J, Heller RS, Petersen HV, Larsson LI, Madsen OD, et al. Pax6 and Pdx1 form a functional complex on the rat somatostatin gene upstream enhancer. FEBS letters. 1999;445(2-3):315-20.
323. Babu DA, Chakrabarti SK, Garmey JC, Mirmira RG. Pdx1 and BETA2/NeuroD1 Participate in a Transcriptional Complex That Mediates Short-range DNA Looping at the Insulin Gene. The Journal of biological chemistry. 2008;283(13):8164-72.
324. Gauthier BR, Gosmain Y, Mamin A, Philippe J. The beta-cell specific transcription factor Nkx6.1 inhibits glucagon gene transcription by interfering with Pax6. The Biochemical journal. 2007;403(3):593-601.
325. Kawamori D, Kaneto H, Nakatani Y, Matsuoka TA, Matsuhisa M, Hori M, et al. The forkhead transcription factor Foxo1 bridges the JNK pathway and the transcription factor PDX-1 through its intracellular translocation. The Journal of biological chemistry. 2006;281(2):1091-8.
326. Dlamini Z, Mokoena F, Hull R. Abnormalities in alternative splicing in diabetes: therapeutic targets. Journal of molecular endocrinology. 2017;59(2):R93-r107.
327. Cauffman G, Liebaers I, Van Steirteghem A, Van de Velde H. POU5F1 Isoforms Show Different Expression Patterns in Human Embryonic Stem Cells and Preimplantation Embryos. STEM CELLS. 2006;24(12):2685-91.
328. Dorrell C, Schug J, Lin CF, Canaday PS, Fox AJ, Smirnova O, et al. Transcriptomes of the major human pancreatic cell types. Diabetologia. 2011;54.
329. Zhang J, McKenna LB, Bogue CW, Kaestner KH. The diabetes gene Hhex maintains delta-cell differentiation and islet function. Genes Dev. 2014;28(8):829-34.
330. He Y, Ding Y, Liang B, Lin J, Kim T-K, Yu H, et al. A Systematic Study of Dysregulated MicroRNA in Type 2 Diabetes Mellitus. International Journal of Molecular Sciences. 2017;18(3):456.
331. Zhong D, Liu X, Khuri FR, Sun S-Y, Vertino PM, Zhou W. LKB1 is Necessary for Akt-mediated Phosphorylation of Pro-apoptotic Proteins. Cancer research. 2008;68(18):7270-7.
332. Westmoreland JJ, Wang Q, Bouzaffour M, Baker SJ, Sosa-Pineda B. Pdk1 activity controls proliferation, survival, and growth of developing pancreatic cells. Developmental biology. 2009;334(1):285-98.

Appendix